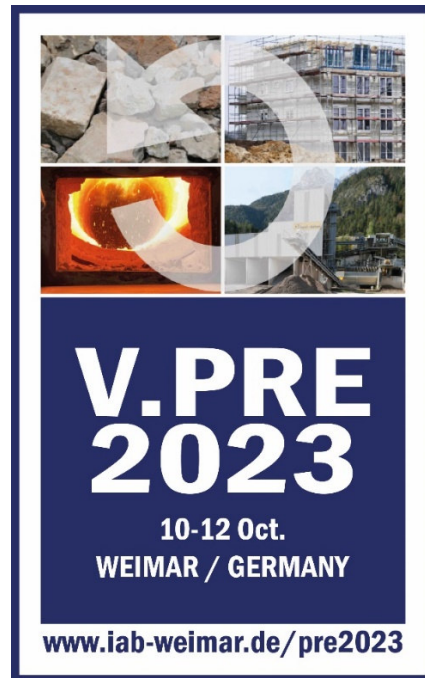# Proceedings of the V International Conference Progress of Recycling in the Built Environment

Edited by Ines Döring, Yury Villagrán Zaccardi, Anette Müller

V International Conference Progress of Recycling in the Built Environment

RILEM, The International Union of Laboratories and Experts in Construction Materials, Systems and Structures, is a non profit-making, non-governmental technical association whose vocation is to contribute to progress in the construction sciences, techniques and industries, essentially by means of the communication it fosters between research and practice. RILEM's activity therefore aims at developing the knowledge of properties of materials and performance of structures, at defining the means for their assessment in laboratory and service conditions and at unifying measurement and testing methods used with this objective.
RILEM was founded in 1947, and has a membership of over 2600 in some 90 countries. It forms an institutional framework for co-operation by experts to:
(optimise and harmonise test methods for measuring properties and performance of building and civil engineering materials and structures under laboratory and service environments,
(prepare technical recommendations for testing methods,
(prepare state-of-the-art reports to identify further research needs,
(collaborate with national or international associations in realising these objectives.

RILEM members include the leading building research and testing laboratories around the world, industrial research, manufacturing and contracting interests, as well as a significant number of individual members from industry and universities. RILEM's focus is on construction materials and their use in building and civil engineering structures, covering all phases of the building process from manufacture to use and recycling of materials.

RILEM meets these objectives through the work of its technical committees. Symposia, workshops and seminars are organised to facilitate the exchange of information and dissemination of knowledge. RILEM's primary output consists of technical recommendations. RILEM also publishes the journal *Materials and Structures* which provides a further avenue for reporting the work of its committees. Many other publications, in the form of reports, monographs, symposia and workshop proceedings are produced.

V International Conference Progress of Recycling in the Built Environment

10-12 October 2023
Weimar, Germany

Edited by
Ines Döring, Yury Villagrán Zaccardi, Anette Müller

RILEM Publications

The following list is presenting the global offer of RILEM Publications, sorted by series. Each publication is available in printed version and/or in online version.

RILEM PROCEEDINGS (PRO)

PRO 1: Durability of High Performance Concrete (ISBN: 2-912143-03-9; e-ISBN: 2-351580-12-5; e-ISBN: 2351580125); *Ed. H. Sommer*

PRO 2: Chloride Penetration into Concrete (ISBN: 2-912143-00-04; e-ISBN: 2912143454); *Eds. L.-O. Nilsson and J.-P. Ollivier*

PRO 3: Evaluation and Strengthening of Existing Masonry Structures (ISBN: 2-912143-02-0; e-ISBN: 2351580141); *Eds. L. Binda and C. Modena*

PRO 4: Concrete: From Material to Structure (ISBN: 2-912143-04-7; e-ISBN: 2351580206); *Eds. J.-P. Bournazel and Y. Malier*

PRO 5: The Role of Admixtures in High Performance Concrete (ISBN: 2-912143-05-5; e-ISBN: 2351580214); *Eds. J. G. Cabrera and R. Rivera-Villarreal*

PRO 6: High Performance Fiber Reinforced Cement Composites - HPFRCC 3 (ISBN: 2-912143-06-3; e-ISBN: 2351580222); *Eds. H. W. Reinhardt and A. E. Naaman*

PRO 7: 1st International RILEM Symposium on Self-Compacting Concrete (ISBN: 2-912143-09-8; e-ISBN: 2912143721); *Eds. Å. Skarendahl and Ö. Petersson*

PRO 8: International RILEM Symposium on Timber Engineering (ISBN: 2-912143-10-1; e-ISBN: 2351580230); *Ed. L. Boström*

PRO 9: 2nd International RILEM Symposium on Adhesion between Polymers and Concrete ISAP '99 (ISBN: 2-912143-11-X; e-ISBN: 2351580249); *Eds. Y. Ohama and M. Puterman*

PRO 10: 3rd International RILEM Symposium on Durability of Building and Construction Sealants (ISBN: 2-912143-13-6; e-ISBN: 2351580257); *Eds. A. T. Wolf*

PRO 11: 4th International RILEM Conference on Reflective Cracking in Pavements (ISBN: 2-912143-14-4; e-ISBN: 2351580265); *Eds. A. O. Abd El Halim, D. A. Taylor and El H. H. Mohamed*

PRO 12: International RILEM Workshop on Historic Mortars: Characteristics and Tests (ISBN: 2-912143-15-2; e-ISBN: 2351580273); *Eds. P. Bartos, C. Groot and J. J. Hughes*

PRO 13: 2nd International RILEM Symposium on Hydration and Setting (ISBN: 2-912143-16-0; e-ISBN: 2351580281); *Ed. A. Nonat*

PRO 14: Integrated Life-Cycle Design of Materials and Structures - ILCDES 2000 (ISBN: 951-758-408-3; e-ISBN: 235158029X); (ISSN: 0356-9403); *Ed. S. Sarja*

PRO 15: Fifth RILEM Symposium on Fibre-Reinforced Concretes (FRC) - BEFIB'2000 (ISBN: 2-912143-18-7; e-ISBN: 291214373X); *Eds. P. Rossi and G. Chanvillard*

PRO 16: Life Prediction and Management of Concrete Structures (ISBN: 2-912143-19-5; e-ISBN: 2351580303); *Ed. D. Naus*

PRO 17: Shrinkage of Concrete – Shrinkage 2000 (ISBN: 2-912143-20-9; e-ISBN: 2351580311); *Eds. V. Baroghel-Bouny and P.-C. Aïtcin*

PRO 18: Measurement and Interpretation of the On-Site Corrosion Rate (ISBN: 2-912143-21-7; e-ISBN: 235158032X); *Eds. C. Andrade, C. Alonso, J. Fullea, J. Polimon and J. Rodriguez*

PRO 19: Testing and Modelling the Chloride Ingress into Concrete (ISBN: 2-912143-22-5; e-ISBN: 2351580338); *Eds. C. Andrade and J. Kropp*

PRO 20: 1st International RILEM Workshop on Microbial Impacts on Building Materials (CD 02) (e-ISBN 978-2-35158-013-4); *Ed. M. Ribas Silva*

PRO 21: International RILEM Symposium on Connections between Steel and Concrete (ISBN: 2-912143-25-X; e-ISBN: 2351580346); *Ed. R. Eligehausen*

PRO 22: International RILEM Symposium on Joints in Timber Structures (ISBN: 2-912143-28-4; e-ISBN: 2351580354); *Eds. S. Aicher and H.-W. Reinhardt*

PRO 23: International RILEM Conference on Early Age Cracking in Cementitious Systems (ISBN: 2-912143-29-2; e-ISBN: 2351580362); *Eds. K. Kovler and A. Bentur*

PRO 24: 2nd International RILEM Workshop on Frost Resistance of Concrete (ISBN: 2-912143-30-6; e-ISBN: 2351580370); *Eds. M. J. Setzer, R. Auberg and H.-J. Keck*

PRO 25: International RILEM Workshop on Frost Damage in Concrete (ISBN: 2-912143-31-4; e-ISBN: 2351580389); *Eds. D. J. Janssen, M. J. Setzer and M. B. Snyder*

PRO 26: International RILEM Workshop on On-Site Control and Evaluation of Masonry Structures (ISBN: 2-912143-34-9; e-ISBN: 2351580141); *Eds. L. Binda and R. C. de Vekey*

PRO 27: International RILEM Symposium on Building Joint Sealants (CD03; e-ISBN: 235158015X); *Ed. A. T. Wolf*

PRO 28: 6th International RILEM Symposium on Performance Testing and Evaluation of Bituminous Materials - PTEBM'03 (ISBN: 2-912143-35-7; e-ISBN: 978-2-912143-77-8); *Ed. M. N. Partl*

PRO 29: 2nd International RILEM Workshop on Life Prediction and Ageing Management of Concrete Structures (ISBN: 2-912143-36-5; e-ISBN: 2912143780); *Ed. D. J. Naus*

PRO 30: 4th International RILEM Workshop on High Performance Fiber Reinforced Cement Composites - HPFRCC 4 (ISBN: 2-912143-37-3; e-ISBN: 2912143799); *Eds. A. E. Naaman and H. W. Reinhardt*

PRO 31: International RILEM Workshop on Test and Design Methods for Steel Fibre Reinforced Concrete: Background and Experiences (ISBN: 2-912143-38-1; e-ISBN: 2351580168); *Eds. B. Schnütgen and L. Vandewalle*

PRO 32: International Conference on Advances in Concrete and Structures 2 vol. (ISBN (set): 2-912143-41-1; e-ISBN: 2351580176); *Eds. Ying-shu Yuan, Surendra P. Shah and Heng-lin Lü*

PRO 33: 3rd International Symposium on Self-Compacting Concrete (ISBN: 2-912143-42-X; e-ISBN: 2912143713); *Eds. Ó. Wallevik and I. Níelsson*

PRO 34: International RILEM Conference on Microbial Impact on Building Materials (ISBN: 2-912143-43-8; e-ISBN: 2351580184); *Ed. M. Ribas Silva*

PRO 35: International RILEM TC 186-ISA on Internal Sulfate Attack and Delayed Ettringite Formation (ISBN: 2-912143-44-6; e-ISBN: 2912143802); *Eds. K. Scrivener and J. Skalny*

PRO 36: International RILEM Symposium on Concrete Science and Engineering – A Tribute to Arnon Bentur (ISBN: 2-912143-46-2; e-ISBN: 2912143586); *Eds. K. Kovler, J. Marchand, S. Mindess and J. Weiss*

PRO 37: 5th International RILEM Conference on Cracking in Pavements – Mitigation, Risk Assessment and Prevention (ISBN: 2-912143-47-0; e-ISBN: 2912143764); *Eds. C. Petit, I. Al-Qadi and A. Millien*

PRO 38: 3rd International RILEM Workshop on Testing and Modelling the Chloride Ingress into Concrete (ISBN: 2-912143-48-9; e-ISBN: 2912143578); *Eds. C. Andrade and J. Kropp*

PRO 39: 6th International RILEM Symposium on Fibre-Reinforced Concretes - BEFIB 2004 (ISBN: 2-912143-51-9; e-ISBN: 2912143748); *Eds. M. Di Prisco, R. Felicetti and G. A. Plizzari*

PRO 40: International RILEM Conference on the Use of Recycled Materials in Buildings and Structures (ISBN: 2-912143-52-7; e-ISBN: 2912143756); *Eds. E. Vázquez, Ch. F. Hendriks and G. M. T. Janssen*

PRO 41: RILEM International Symposium on Environment-Conscious Materials and Systems for Sustainable Development (ISBN: 2-912143-55-1; e-ISBN: 2912143640); *Eds. N. Kashino and Y. Ohama*

PRO 42: SCC'2005 - China: 1st International Symposium on Design, Performance and Use of Self-Consolidating Concrete (ISBN: 2-912143-61-6; e-ISBN: 2912143624); *Eds. Zhiwu Yu, Caijun Shi, Kamal Henri Khayat and Youjun Xie*

PRO 43: International RILEM Workshop on Bonded Concrete Overlays (e-ISBN: 2-912143-83-7); *Eds. J. L. Granju and J. Silfwerbrand*

PRO 44: 2nd International RILEM Workshop on Microbial Impacts on Building Materials (CD11) (e-ISBN: 2-912143-84-5); *Ed. M. Ribas Silva*

PRO 45: 2nd International Symposium on Nanotechnology in Construction, Bilbao (ISBN: 2-912143-87-X; e-ISBN: 2912143888); *Eds. Peter J. M. Bartos, Yolanda de Miguel and Antonio Porro*

PRO 46: ConcreteLife'06 - International RILEM-JCI Seminar on Concrete Durability and Service Life Planning: Curing, Crack Control, Performance in Harsh Environments (ISBN: 2-912143-89-6; e-ISBN: 291214390X); *Ed. K. Kovler*

PRO 47: International RILEM Workshop on Performance Based Evaluation and Indicators for Concrete Durability (ISBN: 978-2-912143-95-2; e-ISBN: 9782912143969); *Eds. V. Baroghel-Bouny, C. Andrade, R. Torrent and K. Scrivener*

PRO 48: 1st International RILEM Symposium on Advances in Concrete through Science and Engineering (e-ISBN: 2-912143-92-6); *Eds. J. Weiss, K. Kovler, J. Marchand, and S. Mindess*

PRO 49: International RILEM Workshop on High Performance Fiber Reinforced Cementitious Composites in Structural Applications (ISBN: 2-912143-93-4; e-ISBN: 2912143942); *Eds. G. Fischer and V.C. Li*

PRO 50: 1st International RILEM Symposium on Textile Reinforced Concrete (ISBN: 2-912143-97-7; e-ISBN: 2351580087); *Eds. Josef Hegger, Wolfgang Brameshuber and Norbert Will*

PRO 51: 2nd International Symposium on Advances in Concrete through Science and Engineering (ISBN: 2-35158-003-6; e-ISBN: 2-35158-002-8); *Eds. J. Marchand, B. Bissonnette, R. Gagné, M. Jolin and F. Paradis*

PRO 52: Volume Changes of Hardening Concrete: Testing and Mitigation (ISBN: 2-35158-004-4; e-ISBN: 2-35158-005-2); *Eds. O. M. Jensen, P. Lura and K. Kovler*

PRO 53: High Performance Fiber Reinforced Cement Composites - HPFRCC5
(ISBN: 978-2-35158-046-2; e-ISBN: 978-2-35158-089-9); *Eds. H. W. Reinhardt and A. E. Naaman*

PRO 54: 5th International RILEM Symposium on Self-Compacting Concrete
(ISBN: 978-2-35158-047-9; e-ISBN: 978-2-35158-088-2); *Eds. G. De Schutter and V. Boel*

PRO 55: International RILEM Symposium Photocatalysis, Environment and Construction Materials (ISBN: 978-2-35158-056-1; e-ISBN: 978-2-35158-057-8); *Eds. P. Baglioni and L. Cassar*

PRO 56: International RILEM Workshop on Integral Service Life Modelling of Concrete Structures (ISBN 978-2-35158-058-5; e-ISBN: 978-2-35158-090-5); *Eds. R. M. Ferreira, J. Gulikers and C. Andrade*

PRO 57: RILEM Workshop on Performance of cement-based materials in aggressive aqueous environments (e-ISBN: 978-2-35158-059-2); *Ed. N. De Belie*

PRO 58: International RILEM Symposium on Concrete Modelling - CONMOD'08
(ISBN: 978-2-35158-060-8; e-ISBN: 978-2-35158-076-9); *Eds. E. Schlangen and G. De Schutter*

PRO 59: International RILEM Conference on On Site Assessment of Concrete, Masonry and Timber Structures - SACoMaTiS 2008 (ISBN set: 978-2-35158-061-5; e-ISBN: 978-2-35158-075-2); *Eds. L. Binda, M. di Prisco and R. Felicetti*

PRO 60: Seventh RILEM International Symposium on Fibre Reinforced Concrete: Design and Applications - BEFIB 2008 (ISBN: 978-2-35158-064-6; e-ISBN: 978-2-35158-086-8); *Ed. R. Gettu*

PRO 61: 1st International Conference on Microstructure Related Durability of Cementitious Composites 2 vol., (ISBN: 978-2-35158-065-3; e-ISBN: 978-2-35158-084-4); *Eds. W. Sun, K. van Breugel, C. Miao, G. Ye and H. Chen*

PRO 62: NSF/ RILEM Workshop: In-situ Evaluation of Historic Wood and Masonry Structures (e-ISBN: 978-2-35158-068-4); *Eds. B. Kasal, R. Anthony and M. Drdácký*

PRO 63: Concrete in Aggressive Aqueous Environments: Performance, Testing and Modelling, 2 vol., (ISBN: 978-2-35158-071-4; e-ISBN: 978-2-35158-082-0); *Eds. M. G. Alexander and A. Bertron*

PRO 64: Long Term Performance of Cementitious Barriers and Reinforced Concrete in Nuclear Power Plants and Waste Management - NUCPERF 2009 (ISBN: 978-2-35158-072-1; e-ISBN: 978-2-35158-087-5); *Eds. V. L'Hostis, R. Gens, C. Gallé*

PRO 65: Design Performance and Use of Self-consolidating Concrete - SCC'2009
(ISBN: 978-2-35158-073-8; e-ISBN: 978-2-35158-093-6); *Eds. C. Shi, Z. Yu, K. H. Khayat and P. Yan*

PRO 66: 2nd International RILEM Workshop on Concrete Durability and Service Life Planning - ConcreteLife'09 (ISBN: 978-2-35158-074-5; ISBN: 978-2-35158-074-5); *Ed. K. Kovler*

PRO 67: Repairs Mortars for Historic Masonry (e-ISBN: 978-2-35158-083-7); *Ed. C. Groot*

PRO 68: Proceedings of the 3rd International RILEM Symposium on 'Rheology of Cement Suspensions such as Fresh Concrete (ISBN 978-2-35158-091-2; e-ISBN: 978-2-35158-092-9); *Eds. O. H. Wallevik, S. Kubens and S. Oesterheld*

PRO 69: 3rd International PhD Student Workshop on 'Modelling the Durability of Reinforced Concrete (ISBN: 978-2-35158-095-0); *Eds. R. M. Ferreira, J. Gulikers and C. Andrade*

PRO 70: 2nd International Conference on 'Service Life Design for Infrastructure' (ISBN set: 978-2-35158-096-7, e-ISBN: 978-2-35158-097-4); *Ed. K. van Breugel, G. Ye and Y. Yuan*

PRO 71: Advances in Civil Engineering Materials - The 50-year Teaching Anniversary of Prof. Sun Wei' (ISBN: 978-2-35158-098-1; e-ISBN: 978-2-35158-099-8); *Eds. C. Miao, G. Ye, and H. Chen*

PRO 72: First International Conference on 'Advances in Chemically-Activated Materials – CAM'2010' (2010), 264 pp, ISBN: 978-2-35158-101-8; e-ISBN: 978-2-35158-115-5, *Eds. Caijun Shi and Xiaodong Shen*

PRO 73: 2nd International Conference on 'Waste Engineering and Management - ICWEM 2010' (2010), 894 pp, ISBN: 978-2-35158-102-5; e-ISBN: 978-2-35158-103-2, *Eds. J. Zh. Xiao, Y. Zhang, M. S. Cheung and R. Chu*

PRO 74: International RILEM Conference on 'Use of Superabsorsorbent Polymers and Other New Addditives in Concrete' (2010) 374 pp., ISBN: 978-2-35158-104-9; e-ISBN: 978-2-35158-105-6;
Eds. O.M. Jensen, M.T. Hasholt, and S. Laustsen

PRO 75: International Conference on 'Material Science - 2nd ICTRC - Textile Reinforced Concrete - Theme 1' (2010) 436 pp., ISBN: 978-2-35158-106-3; e-ISBN: 978-2-35158-107-0; *Ed. W. Brameshuber*

PRO 76: International Conference on 'Material Science - HetMat - Modelling of Heterogeneous Materials - Theme 2' (2010) 255 pp., ISBN: 978-2-35158-108-7; e-ISBN: 978-2-35158-109-4; *Ed. W. Brameshuber*

PRO 77: International Conference on 'Material Science - AdIPoC - Additions Improving Properties of Concrete - Theme 3' (2010) 459 pp., ISBN: 978-2-35158-110-0; e-ISBN: 978-2-35158-111-7; *Ed. W. Brameshuber*

PRO 78: 2nd Historic Mortars Conference and RILEM TC 203-RHM Final Workshop – HMC2010 (2010) 1416 pp., e-ISBN: 978-2-35158-112-4; *Eds J. Válek, C. Groot, and J. J. Hughes*

PRO 79: International RILEM Conference on Advances in Construction Materials Through Science and Engineering (2011) 213 pp., ISBN: 978-2-35158-116-2, e-ISBN: 978-2-35158-117-9; *Eds Christopher Leung and K.T. Wan*

PRO 80: 2nd International RILEM Conference on Concrete Spalling due to Fire Exposure (2011) 453 pp., ISBN: 978-2-35158-118-6, e-ISBN: 978-2-35158-119-3; *Eds E.A.B. Koenders and F. Dehn*

PRO 81: 2nd International RILEM Conference on Strain Hardening Cementitious Composites (SHCC2-Rio) (2011) 451 pp., ISBN: 978-2-35158-120-9, e-ISBN: 978-2-35158-121-6; *Eds R.D. Toledo Filho, F.A. Silva, E.A.B. Koenders and E.M.R. Fairbairn*

PRO 82: 2nd International RILEM Conference on Progress of Recycling in the Built Environment (2011) 507 pp., e-ISBN: 978-2-35158-122-3; *Eds V.M. John, E. Vazquez, S.C. Angulo and C. Ulsen*

PRO 83: 2nd International Conference on Microstructural-related Durability of Cementitious Composites (2012) 250 pp., ISBN: 978-2-35158-129-2; e-ISBN: 978-2-35158-123-0; *Eds G. Ye, K. van Breugel, W. Sun and C. Miao*

PRO 84: CONSEC13 - Seventh International Conference on Concrete under Severe Conditions – Environment and Loading (2013) 1930 pp., ISBN: 978-2-35158-124-7; e-ISBN: 978-2- 35158-134-6; *Eds Z.J. Li, W. Sun, C.W. Miao, K. Sakai, O.E. Gjorv & N. Banthia*

PRO 85: RILEM-JCI International Workshop on Crack Control of Mass Concrete and Related issues concerning Early-Age of Concrete Structures – ConCrack 3 – Control of Cracking in Concrete Structures 3 (2012) 237 pp., ISBN: 978-2-35158-125-4; e-ISBN: 978-2-35158-126-1; *Eds F. Toutlemonde and J.-M. Torrenti*

PRO 86: International Symposium on Life Cycle Assessment and Construction (2012) 414 pp., ISBN: 978-2-35158-127-8, e-ISBN: 978-2-35158-128-5; *Eds A. Ventura and C. de la Roche*

PRO 87: UHPFRC 2013 – RILEM-fib-AFGC International Symposium on Ultra-High Performance Fibre-Reinforced Concrete (2013), ISBN: 978-2-35158-130-8, e-ISBN: 978-2-35158-131-5; *Eds F. Toutlemonde*

PRO 88: 8th RILEM International Symposium on Fibre Reinforced Concrete (2012) 344 pp., ISBN: 978-2-35158-132-2, e-ISBN: 978-2-35158-133-9; *Eds Joaquim A.O. Barros*

PRO 89: RILEM International workshop on performance-based specification and control of concrete durability (2014) 678 pp, ISBN: 978-2-35158-135-3, e-ISBN: 978-2-35158-136-0; *Eds. D. Bjegović, H. Beushausen and M. Serdar*

PRO 90: 7th RILEM International Conference on Self-Compacting Concrete and of the 1st RILEM International Conference on Rheology and Processing of Construction Materials (2013) 396 pp, ISBN: 978-2-35158-137-7, e-ISBN: 978-2-35158-138-4; *Eds. Nicolas Roussel and Hela Bessaies-Bey*

PRO 91: CONMOD 2014 - RILEM International Symposium on Concrete Modelling (2014), ISBN: 978-2-35158-139-1; e-ISBN: 978-2-35158-140-7; *Eds. Kefei Li, Peiyu Yan and Rongwei Yang*

PRO 92: CAM 2014 - 2nd International Conference on advances in chemically-activated materials (2014) 392 pp., ISBN: 978-2-35158-141-4; e-ISBN: 978-2-35158-142-1; *Eds. Caijun Shi and Xiadong Shen*

PRO 93: SCC 2014 - 3rd International Symposium on Design, Performance and Use of Self-Consolidating Concrete (2014) 438 pp., ISBN: 978-2-35158-143-8; e-ISBN: 978-2-35158-144-5; *Eds. Caijun Shi, Zhihua Ou, Kamal H. Khayat*

PRO 94 (online version): HPFRCC-7 - 7th RILEM conference on High performance fiber reinforced cement composites (2015), e-ISBN: 978-2-35158-146-9; *Eds. H.W. Reinhardt, G.J. Parra-Montesinos, H. Garrecht*

PRO 95: International RILEM Conference on Application of superabsorbent polymers and other new admixtures in concrete construction (2014), ISBN: 978-2-35158-147-6; e-ISBN: 978-2-35158-148-3; *Eds. Viktor Mechtcherine, Christof Schroefl*

PRO 96 (online version): XIII DBMC: XIII International Conference on Durability of Building Materials and Components(2015), e-ISBN: 978-2-35158-149-0; *Eds. M. Quattrone, V.M. John*

PRO 97: SHCC3 – 3rd International RILEM Conference on Strain Hardening Cementitious Composites (2014), ISBN: 978-2-35158-150-6; e-ISBN: 978-2-35158-151-3; *Eds. E. Schlangen, M.G. Sierra Beltran, M. Lukovic, G. Ye*

PRO 98: FERRO-11 – 11th International Symposium on Ferrocement and 3rd ICTRC - International Conference on Textile Reinforced Concrete (2015), ISBN: 978-2-35158-152-0; e-ISBN: 978-2-35158-153-7; *Ed. W. Brameshuber*

PRO 99 (online version): ICBBM 2015 - 1st International Conference on Bio-Based Building Materials (2015), e-ISBN: 978-2-35158-154-4; *Eds. S. Amziane, M. Sonebi*

PRO 100: SCC16 - RILEM Self-Consolidating Concrete Conference (2016), ISBN: 978-2-35158-156-8; e-ISBN: 978-2-35158-157-5; *Ed. Kamal H. Kayat*

PRO 101 (online version): III Progress of Recycling in the Built Environment (2015), e-ISBN: 978-2-35158-158-2; *Eds I. Martins, C. Ulsen and S. C. Angulo*

PRO 102 (online version): RILEM Conference on Microorganisms-Cementitious Materials Interactions (2016), e-ISBN: 978-2-35158-160-5; *Eds. Alexandra Bertron, Henk Jonkers, Virginie Wiktor*

PRO 103 (online version): ACESC'16 - Advances in Civil Engineering and Sustainable Construction (2016), e-ISBN: 978-2-35158-161-2; *Eds. T.Ch. Madhavi, G. Prabhakar, Santhosh Ram and P.M. Rameshwaran*

PRO 104 (online version): SSCS'2015 - Numerical Modeling - Strategies for Sustainable Concrete Structures (2015), e-ISBN: 978-2-35158-162-9

PRO 105: 1st International Conference on UHPC Materials and Structures (2016), ISBN: 978-2-35158-164-3, e-ISBN: 978-2-35158-165-0

PRO 106: AFGC-ACI-fib-RILEM International Conference on Ultra-High-Performance Fibre-Reinforced Concrete – UHPFRC 2017 (2017), ISBN: 978-2-35158-166-7, e-ISBN: 978-2-35158-167-4; *Eds. François Toutlemonde & Jacques Resplendino*

PRO 107 (online version): XIV DBMC – 14th International Conference on Durability of Building Materials and Components (2017), e-ISBN: 978-2-35158-159-9; *Eds. Geert De Schutter, Nele De Belie, Arnold Janssens, Nathan Van Den Bossche*

PRO 108: MSSCE 2016 - Innovation of Teaching in Materials and Structures (2016), ISBN: 978-2-35158-178-0, e-ISBN: 978-2-35158-179-7; *Ed. Per Goltermann*

PRO 109 (2 volumes): MSSCE 2016 - Service Life of Cement-Based Materials and Structures (2016), ISBN Vol. 1: 978-2-35158-170-4, Vol. 2: 978-2-35158-171-4, Set Vol. 1&2: 978-2-35158-172-8, e-ISBN : 978-2-35158-173-5; *Eds. Miguel Azenha, Ivan Gabrijel, Dirk Schlicke, Terje Kanstad and Ole Mejlhede Jensen*

PRO 110: MSSCE 2016 - Historical Masonry (2016), ISBN: 978-2-35158-178-0, e-ISBN: 978-2-35158-179-7; *Eds. Inge Rörig-Dalgaard and Ioannis Ioannou*

PRO 111: MSSCE 2016 - Electrochemistry in Civil Engineering (2016), ISBN: 978-2-35158-176-6, e-ISBN: 978-2-35158-177-3; *Ed. Lisbeth M. Ottosen*

PRO 112: MSSCE 2016 - Moisture in Materials and Structures (2016), ISBN: 978-2-35158-178-0, e-ISBN: 978-2-35158-179-7; *Eds. Kurt Kielsgaard Hansen, Carsten Rode and Lars-Olof Nilsson*

PRO 113: MSSCE 2016 - Concrete with Supplementary Cementitious Materials (2016), ISBN: 978-2-35158-178-0, e-ISBN: 978-2-35158-179-7; *Eds. Ole Mejlhede Jensen, Konstantin Kovler and Nele De Belie*

PRO 114: MSSCE 2016 - Frost Action in Concrete (2016), ISBN: 978-2-35158-182-7, e-ISBN: 978-2-35158-183-4; *Eds. Marianne Tange Hasholt, Katja Fridh and R. Doug Hooton*

PRO 115: MSSCE 2016 - Fresh Concrete (2016), ISBN: 978-2-35158-184-1, e-ISBN: 978-2-35158-185-8; *Eds. Lars N. Thrane, Claus Pade, Oldrich Svec and Nicolas Roussel*

PRO 116: BEFIB 2016 – 9th RILEM International Symposium on Fiber Reinforced Concrete (2016), ISBN: 978-2-35158-187-2, e-ISBN: 978-2-35158-186-5; *Eds. N. Banthia, M. di Prisco and S. Soleimani-Dashtaki*

PRO 117: 3rd International RILEM Conference on Microstructure Related Durability of Cementitious Composites (2016), ISBN: 978-2-35158-188-9, e-ISBN: 978-2-35158-189-6; *Eds. Changwen Miao, Wei Sun, Jiaping Liu, Huisu Chen, Guang Ye and Klaas van Breugel*

PRO 118 (4 volumes): International Conference on Advances in Construction Materials and Systems (2017), ISBN Set: 978-2-35158-190-2, Vol. 1: 978-2-35158-193-3, Vol. 2: 978-2-35158-194-0, Vol. 3: ISBN:978-2-35158-195-7, Vol. 4: ISBN:978-2-35158-196-4, e-ISBN: 978-2-35158-191-9; *Eds. Manu Santhanam, Ravindra Gettu, Radhakrishna G. Pillai and Sunitha K. Nayar*

PRO 119 (online version): ICBBM 2017 - Second International RILEM Conference on Bio-based Building Materials, (2017), e-ISBN: 978-2-35158-192-6; *Ed. Sofiane Amziane*

PRO 120 (2 volumes): EAC-02 - 2nd International RILEM/COST Conference on Early Age Cracking and Serviceability in Cement-based Materials and Structures, (2017), Vol. 1: 978-2-35158-199-5, Vol. 2: 978-2-35158-200-8, Set: 978-2-35158-197-1, e-ISBN: 978-2-35158-198-8; *Eds. Stéphanie Staquet and Dimitrios Aggelis*

PRO 121 (2 volumes): SynerCrete18: Interdisciplinary Approaches for Cement-based Materials and Structural Concrete: Synergizing Expertise and Bridging Scales of Space and Time, (2018), Set: 978-2-35158-202-2, Vol.1: 978-2-35158-211-4, Vol.2: 978-2-35158-212-1, e-ISBN: 978-2-35158-203-9; *Eds. Miguel Azenha, Dirk Schlicke, Farid Benboudjema, Agnieszka Knoppik*

PRO 122: SCC'2018 China - Fourth International Symposium on Design, Performance and Use of Self-Consolidating Concrete, (2018), ISBN: 978-2-35158-204-6, e-ISBN: 978-2-35158-205-3; *Eds. C. Shi, Z. Zhang, K. H. Khayat*

PRO 123: Final Conference of RILEM TC 253-MCI: Microorganisms-Cementitious Materials Interactions (2018), Set: 978-2-35158-207-7, Vol.1: 978-2-35158-209-1, Vol.2: 978-2-35158-210-7, e-ISBN: 978-2-35158-206-0; *Ed. Alexandra Bertron*

PRO 124 (online version): Fourth International Conference Progress of Recycling in the Built Environment (2018), e-ISBN: 978-2-35158-208-4; *Eds. Isabel M. Martins, Carina Ulsen, Yury Villagran*

PRO 125 (online version): SLD4 - 4th International Conference on Service Life Design for Infrastructures (2018), e-ISBN: 978-2-35158-213-8; *Eds. Guang Ye, Yong Yuan, Claudia Romero Rodriguez, Hongzhi Zhang, Branko Savija*

PRO 126: Workshop on Concrete Modelling and Material Behaviour in honor of Professor Klaas van Breugel (2018), ISBN: 978-2-35158-214-5, e-ISBN: 978-2-35158-215-2; *Ed. Guang Ye*

PRO 127 (online version): CONMOD2018 - Symposium on Concrete Modelling (2018), e-ISBN: 978-2-35158-216-9; *Eds. Erik Schlangen, Geert de Schutter, Branko Savija, Hongzhi Zhang, Claudia Romero Rodriguez*

PRO 128: SMSS2019 - International Conference on Sustainable Materials, Systems and Structures (2019), ISBN: 978-2-35158-217-6, e-ISBN: 978-2-35158-218-3

PRO 129: 2nd International Conference on UHPC Materials and Structures (UHPC2018-China), ISBN: 978-2-35158-219-0, e-ISBN: 978-2-35158-220-6;

PRO 130: 5th Historic Mortars Conference (2019), ISBN: 978-2-35158-221-3, e-ISBN: 978-2-35158-222-0; *Eds. José Ignacio Álvarez, José María Fernández, Íñigo Navarro, Adrián Durán, Rafael Sirera*

PRO 131 (online version): 3rd International Conference on Bio-Based Building Materials - ICBBM2019, e-ISBN: 978-2-35158-229-9; *Eds. Mohammed Sonebi, Sofiane Amziane, Jonathan Page*

PRO 132: IRWRMC'18 - International RILEM Workshop on Rheological Measurements of Cement-based Materials (2018), ISBN: 978-2-35158-230-5, e-ISBN: 978-2-35158-231-2; *Eds. Chafika Djelal, Yannick Vanhove*

PRO 133 (online version): CO2STO2019 - International Workshop CO2 Storage in Concrete, e-ISBN: 978-2-35158-232-9; *Eds. Assia Djerbi, Othman Omikrine-Metalssi, Teddy Fen-Chong*

PRO 134: 3rd ACF/HNU International Conference on UHPC Materials and Structures, UHPC'2020 (2020), ISBN: 978-2-35158-233-6, e-ISBN: 978-2-35158-234-3; *Eds. Caijun Shi & Jiaping Liu*

PRO 135: Fourth International Conference on Chemically Activated Materials (CAM2021), ISBN: 978-2-35158-235-0, e-ISBN: 978-2-35158-236-7; *Eds. Caijun Shi & Xiang Hu*

RILEM REPORTS (REP)

Report 19: Considerations for Use in Managing the Aging of Nuclear Power Plant Concrete Structures (ISBN: 2-912143-07-1); *Ed. D. J. Naus*

Report 20: Engineering and Transport Properties of the Interfacial Transition Zone in Cementitious Composites (ISBN: 2-912143-08-X); *Eds. M. G. Alexander, G. Arliguie, G. Ballivy, A. Bentur and J. Marchand*

Report 21: Durability of Building Sealants (ISBN: 2-912143-12-8); *Ed. A. T. Wolf*

Report 22: Sustainable Raw Materials - Construction and Demolition Waste (ISBN: 2-912143-17-9); *Eds. C. F. Hendriks and H. S. Pietersen*

Report 23: Self-Compacting Concrete state-of-the-art report (ISBN: 2-912143-23-3); *Eds. Å. Skarendahl and Ö. Petersson*

Report 24: Workability and Rheology of Fresh Concrete: Compendium of Tests (ISBN: 2-912143-32-2); *Eds. P. J. M. Bartos, M. Sonebi and A. K. Tamimi*

Report 25: Early Age Cracking in Cementitious Systems (ISBN: 2-912143-33-0); *Ed. A. Bentur*

Report 26: Towards Sustainable Roofing (Joint Committee CIB/RILEM) (CD 07) (e-ISBN 978-2-912143-65-5); *Eds. Thomas W. Hutchinson and Keith Roberts*

Report 27: Condition Assessment of Roofs (Joint Committee CIB/RILEM) (CD 08) (e-ISBN 978-2-912143-66-2); *Ed. CIB W 83/RILEM TC166-RMS*

Report 28: Final report of RILEM TC 167-COM 'Characterisation of Old Mortars with Respect to Their Repair (ISBN: 978-2-912143-56-3); *Eds. C. Groot, G. Ashall and J. Hughes*

Report 29: Pavement Performance Prediction and Evaluation (PPPE): Interlaboratory Tests (e-ISBN: 2-912143-68-3); *Eds. M. Partl and H. Piber*

Report 30: Final Report of RILEM TC 198-URM 'Use of Recycled Materials' (ISBN: 2-912143-82-9; e-ISBN: 2-912143-69-1); *Eds. Ch. F. Hendriks, G. M. T. Janssen and E. Vázquez*

Report 31: Final Report of RILEM TC 185-ATC 'Advanced testing of cement-based materials during setting and hardening' (ISBN: 2-912143-81-0; e-ISBN: 2-912143-70-5); *Eds. H. W. Reinhardt and C. U. Grosse*

Report 32: Probabilistic Assessment of Existing Structures. A JCSS publication (ISBN 2-912143-24-1); *Ed. D. Diamantidis*

Report 33: State-of-the-Art Report of RILEM Technical Committee TC 184-IFE 'Industrial Floors' (ISBN 2-35158-006-0); *Ed. P. Seidler*

Report 34: Report of RILEM Technical Committee TC 147-FMB 'Fracture mechanics applications to anchorage and bond' Tension of Reinforced Concrete Prisms – Round Robin Analysis and Tests on Bond (e-ISBN 2-912143-91-8); *Eds. L. Elfgren and K. Noghabai*

Report 35: Final Report of RILEM Technical Committee TC 188-CSC 'Casting of Self Compacting Concrete' (ISBN 2-35158-001-X; e-ISBN: 2-912143-98-5); *Eds. Å. Skarendahl and P. Billberg*

Report 36: State-of-the-Art Report of RILEM Technical Committee TC 201-TRC 'Textile Reinforced Concrete' (ISBN 2-912143-99-3); *Ed. W. Brameshuber*

Report 37: State-of-the-Art Report of RILEM Technical Committee TC 192-ECM 'Environment-conscious construction materials and systems' (ISBN: 978-2-35158-053-0);
Eds. N. Kashino, D. Van Gemert and K. Imamoto

Report 38: State-of-the-Art Report of RILEM Technical Committee TC 205-DSC 'Durability of Self-Compacting Concrete' (ISBN: 978-2-35158-048-6); *Eds. G. De Schutter and K. Audenaert*

Report 39: Final Report of RILEM Technical Committee TC 187-SOC 'Experimental determination of the stress-crack opening curve for concrete in tension' (ISBN 978-2-35158-049-3); *Ed. J. Planas*

Report 40: State-of-the-Art Report of RILEM Technical Committee TC 189-NEC 'Non-Destructive Evaluation of the Penetrability and Thickness of the Concrete Cover' (ISBN 978-2-35158-054-7); *Eds. R. Torrent and L. Fernández Luco*

Report 41: State-of-the-Art Report of RILEM Technical Committee TC 196-ICC 'Internal Curing of Concrete' (ISBN 978-2-35158-009-7); *Eds. K. Kovler and O. M. Jensen*

Report 42: 'Acoustic Emission and Related Non-destructive Evaluation Techniques for Crack Detection and Damage Evaluation in Concrete' - Final Report of RILEM Technical Committee 212-ACD (e-ISBN: 978-2-35158-100-1); *Ed. M. Ohtsu*

Report 45: Repair Mortars for Historic Masonry - State-of-the-Art Report of RILEM Technical Committee TC 203-RHM (e-ISBN: 978-2-35158-163-6); *Eds. Paul Maurenbrecher and Caspar Groot*

Report 46: *S*urface delamination of concrete industrial floors and other durability related aspects guide - Report of RILEM Technical Committee TC 268-SIF (e-ISBN: 978-2-35158-201-5); *Ed. Valerie Pollet*

Honorary Chairs

Prof. Enric Vázquez Ramonich (UPC – Spain)

Dr.-Ing. Ulrich Palzer (IAB Weimar gGmbH – Germany)

Conference Chair

Prof. Anette Müller (IAB Weimar gGmbH – Germany)

Prof. Carina Ulsen (USP-Brazil)

Dr. Isabel Martins (LNEC, Portugal)

Dr. Yury Villagrán Zaccardi (VITO – Belgium)

Members Organizing Committee

Dipl.-Ing. Mirko Landmann (IAB Weimar gGmbH – Germany)

Dr.-Ing. Barbara Leydolph (IAB Weimar gGmbH – Germany)

Prof. Sérgio Cirelli Angulo (USP – Brazil)
Prof. Vanderley Moacyr John (USP – Brazil)

Scientific Committee

Co-Chairs

Prof. Sergio Cirelli Angulo (USP – Brazil)

Dipl.-Ing. Mirko Landmann (IAB Weimar gGmbH – Germany)

Members

Dr. Ana Cristina Freire (LNEC – Portugal)

Prof. Anette Müller (IAB Weimar gGmbH – Germany)

Dr. António Roque (LNEC – Portugal)

Prof. Enric Vázquez Ramonich (UPC – Spain)

Prof. Carina Ulsen (USP – Brazil)

Dr. Yury Villagrán Zaccardi (VITO – Belgium)

Dr. Isabel Martins (LNEC – Portugal)

Dr. Maria do Rosário Veiga (LNEC – Portugal)

Dr. Manuel Gomes Vieira (LNEC – Portugal)

Prof. Jorge De Brito (IST – Portugal)

Prof. Sérgio Cirelli Angulo (USP – Brazil)

Prof. Vanderley Moacyr John (USP – Brazil)

Prof. Dr. rer. nat. Dietmar Stephan (TU Berlin – Germany)

Prof. Dr. Adriane Ruff (Hochschule Nordhausen – Germany)

Prof. Luc Courard (University of Liège – Belgium)

Prof. Jiabin Li (KULeuven – Belgium)

Prof. Jean-Michel Torrenti (University Gustave Eiffel – France)

Dr. Claudio Zega (LEMIT – Argentina)

Prof. Francesca Tittarelli (Marche Polytechnic University – Italy)

Prof. Zengfeng Zhao (Tongji University – China)

Prof. Tung-Chai Ling (Hunan University – China)

Prof. Jianzhuang Xiao (Tongji University – China)

Dr. Maria Eva Sosa (National University of Technology – Argentina)

Prof. Miren Etxeberría (BarcelonaTech – Spain)

Prof. Carlos Thomas (University of Cantabria – Spain)

Prof. César Medina (University of Extremadura – Spain)

Prof. Francesco di Maio (Delft University of Technology – Netherlands)

Prof. Takafumi Noguchi (The University of Tokyo – Japan)

Dr. Julien Hubert (University of Liège – Belgium)

Ir. Jeroen Vrijders (Buildwise – Belgium)

Preface

Recycling materials has a long tradition in human history. In the Palaeolithic, for example, the reuse of discarded stone artefacts was likely a common strategy for obtaining raw materials. Later, "scrap metal" became an important material source for remanufacturing. Recycling also played a role in the Dark Ages, with the collection and recycling of materials such as scrap metal, rags, clothing, paper, bones, and ashes being widespread. Technological progress and the initially seemingly limitless transportation possibilities reduce the demand for recycling with the advancements in the industrial era. However, it has become relevant again due to signs of a shortage of resources such as primary construction raw materials such as sand, gypsum, and natural rocks. Simultaneously, avoiding the landfill of valuable secondary resources is a must nowadays, as a strong push towards the circular economy.

There is still significant progress to be made in building materials research to achieve balanced solutions in terms of performance and circularity of building materials. This conference aimed at address these issues by enhancing our understanding of secondary resources as challenging raw materials and by exploring their impacts when used in advanced product developments and processing technologies. Innovative approaches such as energy savings and reduced CO_2 emissions through new recycling solutions are part of these new developments.

The V.PRE Conference is part of a series started in 2009 by the RILEM Committee TC-217 "Progress of Recycling in the Built Environment." The 2023 edition was particularly significant, marking a long-awaited gathering after the hiatus forced by the COVID-19 crisis that forced the suspension of many such international events, with the PRE series being no exception. THE V.PRE edition brought a renewed enthusiasm among participants and organizers alike. The highly appreciated face-to-face interactions fostered collaboration and innovation in the field, making this edition all the more momentous. Throughout the conference, there were debates and discussions on recent developments in the characterization, processing, and application of secondary construction materials to enhance their production, build confidence in their use, and consequently boost their demand. This was done also with the goal of increasing stakeholder participation and raising awareness about the importance of recycling construction and demolition waste as a key resource.

These Proceedings detail the high-level scientific sessions that addressed pressing issues in recycling in the built environment. They intend to serve as a valuable resource for improving resource efficiency in the construction sector, offering insights into material reuse and recycling, low carbon products, and preservation of natural resources.

This 2023 edition was hosted by the Weimar Institute of Applied Construction Research – IAB gGmbH and fundamentally supported by several esteemed organizations. These are RILEM: International Union of Laboratories and Experts in Construction Materials, Systems and Structures, LNEC: Laboratório Nacional de Engenharia Civil (Portugal), VITO: The Flemish Institute for Technological Research (Belgium), USP: University of São Paulo (Brazil), and the European Demolition Association. We deeply appreciate their contributions, which were essential for the event to achieve its objectives.

The V.PRE featured contributions on • New and enhanced processing techniques for CDW; • Innovative solutions for products based on CDW; • Performance and durability of products with/from recycled material; • Contributions of CDW recycling against the shortage of raw materials; • Contributions of recycling against CO_2 emission; • Quality and confidence, and • Case studies. These diverse topics fostered comprehensive discussions among participants. We thank all contributors to V.PRE for their valuable participation.

The debate was notably enhanced by insights from Keynote Speakers: Prof. Takafumi Noguchi, Dr. Maciej Zajac, Prof. Luc Courard, and Prof. Anette Müller. Their varied backgrounds provided a rich perspective on the theme of the event, offering the audience fresh perspectives. Special thanks also go to the Honorary Chairs of this Event: Prof. Enric Vázquez, a pioneer in the research and application of construction and demolition waste, and Dr.-Ing. Ulrich Palzer, who facilitated structural support from IAB.

We believe these Proceedings are a valuable resource for those interested in secondary resources in the built environment, including the recycling of construction and demolition waste.

The Chairs of the Organising Committee of the IV PRE
Dr. Isabel Martins (LNEC, Portugal)
Dr. Yury Villagrán Zaccardi (VITO, Belgium)
Prof. Carina Ulsen (USP, Brazil)
Prof. Anette Müller (IAB Weimar, Germany)

Contents

Progresses and Challenges in Recycling of Construction and Demolition Waste

Anette Müller[(1)]

(1) Weimar Institute of Applied Construction Research, Germany

Abstract

The need to establish material cycles in the building industry is undisputed. Knowledge on this topic is available in many places. In this paper the state of the arte of processing and developments for the sorting of Construction and Demolition Waste (CDW) are described. The main fields of application of the processed material are road construction and increasingly the production of concrete. For the latter, the development of the applicable standards is discussed. Examples of applications are presented. Certain types of construction waste must be excluded from the above-mentioned areas of application due to their chemical components or physical characteristics. Heterogeneity can be a further exclusion criterion. Special technologies that are available or under development for these materials are introduced.

1 Raw material consumption and waste generation of the construction industry in the European Union

The EU's material footprint amounted to 13.7 tons per capita in 2020. The largest share of around 7.1 tons per capita is accounted by non-metallic minerals, which are mainly used in the construction industry. Since 2012, there is no significant trend toward a decrease. The total amount of waste generated is 4.8 tons per capita. The largest amount is caused by the construction industry with 1.8 tons per capita respectively 37.5 % (Figure 1). Mining and quarrying waste that can also be a source for building material manufacture occurs in an amount of 1.1 tons per capita respectively 23.4 %.
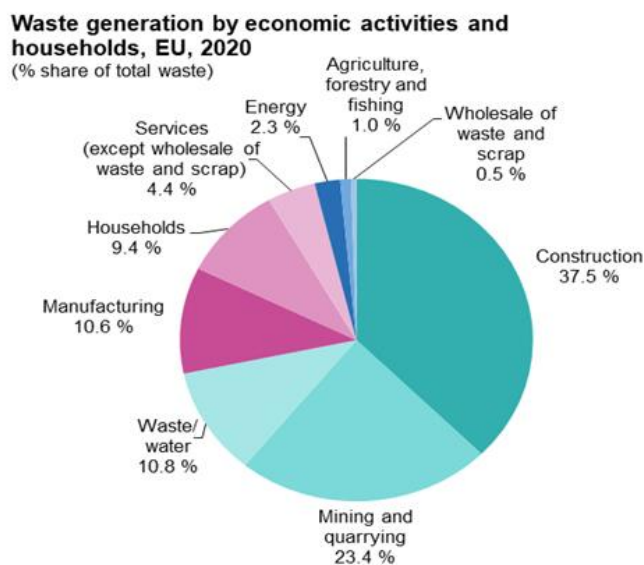
Figure 1: Waste generation (percent) in the European Union 2020 [1]

The quantities of construction and demolition waste without stones, soil and dredged spoil generated in the different EU member states range between 0.02 and 2 t/capita*year (Figure 2). This wide range is caused, on the one hand, by the different quality of the data collection and by differences in the data assessment methods. On the other hand, technical aspects such as the regionally preferred types of materials and constructions or the age and the condition of the existing building stock play a role.
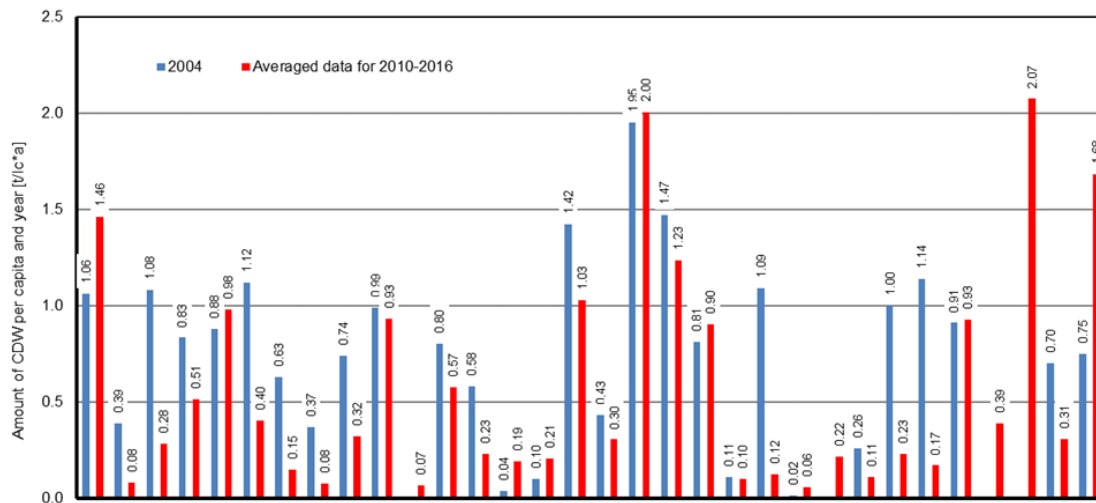
Figure 2: Per capita amount of construction waste excluding excavated soil in European countries for 2004 resp. as average for 2010 to 2016 [2]

In addition, there are influences from the respective economic situation in the construction industry. The realization of large-scale projects in the period under consideration, which required the demolition of residential, commercial and industrial buildings, can also have an influence. The temporal fluctuations may be due to all of these factors.

2 State of the art of processing

A simplified scheme of the processing of demolished concrete and masonry is shown in Figure 3. The process steps crushing - classification - sorting are passed through (Table 1).
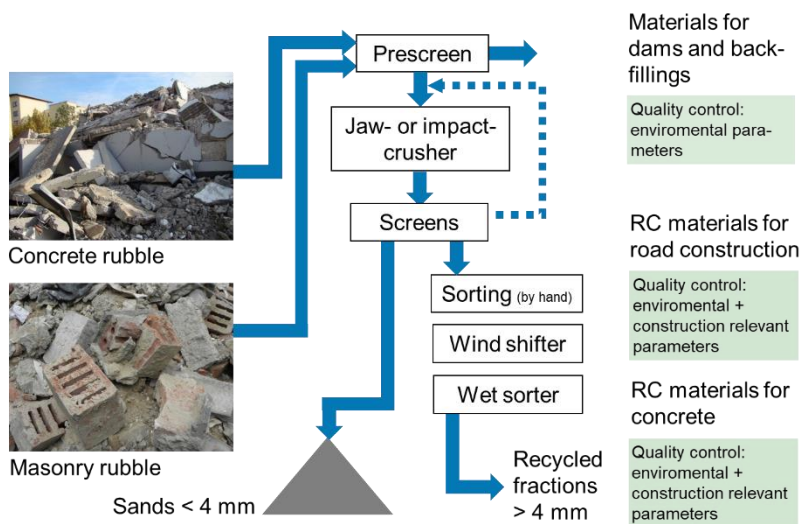
Figure 3: Processing scheme for concrete and masonry rubble

Table 1: Basic operations of CDW processing

Basic operation	Objectives
Pre-screening	— Separation of soil and/or oversized boulders
Crushing: Using mechanical forces to split up a solid body	— Reduction of the largest particle size — Production of polydisperse particle mixtures — Disintegration of "adhesions", i.e. exposure of the individual components of composites
Classification by screening: Separation of processed polydisperse mixtures according to geometrical dimensions into different particle size fractions	— Limitation of the upper particle size — Generation of certain particle size distributions for subsequent recycling — Separation of coarse materials to protect downstream crusher from damages and overloading — Separation of fine particles to relieve the load on crushing equipment, to secure against wear and to prevent blockages — Preparation for sorting if this is only possible for a narrow range of particle size Sorting the material if specific substances are enriched in certain particle size fractions
Sorting: Separating a mixture of materials according to substance types using physical characteristics	— Removal of pollutants and impurities — Separating mixed construction waste into its mineral components

The most important step to produce recyclates with a defined composition is sorting. "State of the arte" feature for the sorting of non-metallic components of CDW is the particle density. It ranges from 30 kg/m³ for insulating materials up to 3,000 kg/m³ for certain natural rocks. With dry sorting methods, lightweight materials such as paper, plastic foils and insulation fragments can be separated. Wood is also usually discharged, if it is not present as a very compact fragment. With wet sorting methods, low-density contaminants can be removed. It is not possible to separate mineral building material by their type with exception of aerated concrete and other low-density building materials. The sorting of mixtures of brick, sand-lime brick, concrete or natural stone is usually done by hand. As an advanced technology, sensor-based sorting machines began to be used in waste management about 30 years ago and have since become established in the sorting of end-of-life plastics, waste paper or waste glass. In the sorting of construction waste they have been used only very sporadically up to now (Figure 4, left).

The newest development is sorting by "heavy pickers" (Figure 4, right). The entire sorting device consists of a conveyor belt, one or more sensors, the process computer, the actual pickers, to each of which 4 drop boxes are assigned. The components of the building rubble, as delivered, are transported on the flat conveyor belt and pass the sensors individually. Impurities or recyclables and their position on the belt are detected. This information is transmitted to the sorting gripper, which picks up the materials and drops them into the box provided for the

respective type of material. This sorting method offers advantages because only a few "hand movements" are required to separate the coarse fragments. However, the basic principle of processing technology is not taken into account, namely that a breakdown/separation of the composites must take place before sorting in order to keep "valuable material losses" low. However, this aspect is less important when sorting CDW.
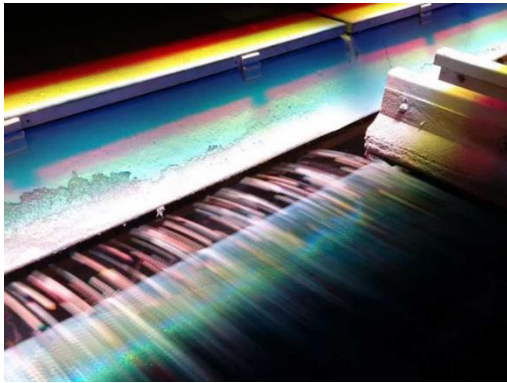
Figure 4: Sensor-based sorting device for the separation of brick and concrete in action in a recycling plant left [3] and heavy picker for sorting construction and demolition waste right [4]

3   State of the art of reuse of processed CDW

3.1   Reuse for earthwork and road construction

Industrially produced recycled building materials from demolished concrete or masonry consist mainly of concrete, natural aggregates, bricks and mortar. The sum of these components ranges between 90 and 100 mass-%. They have a comparatively wide range of applications between "Using (only) the volume" of the recycled materials for filling cavities etc. and "Using their mechanical properties" for layers in road construction or as aggregates in concrete.

In earthworks and road construction (Figure 5, left), the possible fields of application depend on the components of the recycled aggregates. If the recycled building material consists of the material groups concrete, natural stone, sand and gravel, there are no restrictions on use in geotechnical applications, provided that the environmental parameters fulfil the requirements. In road construction (Figure 5, right), requirements on particle size distribution, material composition, particle strength and frost resistance exist, which can be met in most cases.
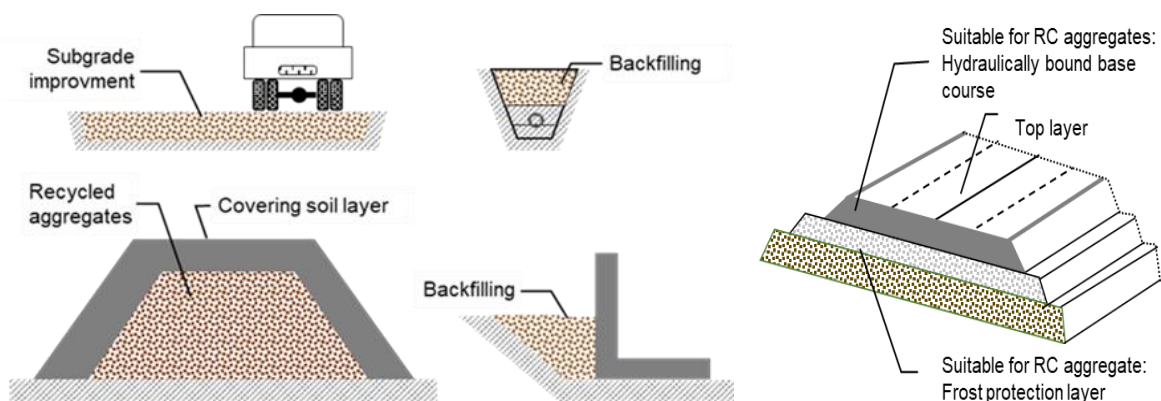
Figure 5: Examples for the use of recycled aggregates in geotechnical applications (left) and in in road construction (right) [2]

The content of gypsum is strictly limited to < 0.5 mass-% in the fraction > 4 mm resp. < 300 SO_4^{2-} mg/l in the fraction < 4 mm, because gypsum can cause liftings etc. Roads with frost protection layers made of recycled materials, which were built in the 1980s, are still functional today without any complaints.

3.2 Reuse for the production of concrete

Decades of basic and applied research have been carried out on the properties of concrete recyclates and the effects of their use for the renewed production of concrete. The crucial fact that concrete is a composite of coarse aggregates and mortar was already pointed out by Hansen in his 1985 report [5]. The more accurate definition that concrete is a composite of fine and coarse aggregates on the one hand and cement paste on the other has still not been fully accepted. Consequences of the composite character are, among others:

- The composition of the aggregates can vary from grain to grain.
- Additional (old) cement paste is introduced into the second-generation concrete by the recycled aggregates.

Due to the additional entry of hardened cement paste, the effects on the strength and the modulus of elasticity are unavoidable. The simplified model consideration of "multiple recycling" and the investigations carried out on this topic illustrate the increase in the cement paste content (Figure 6).
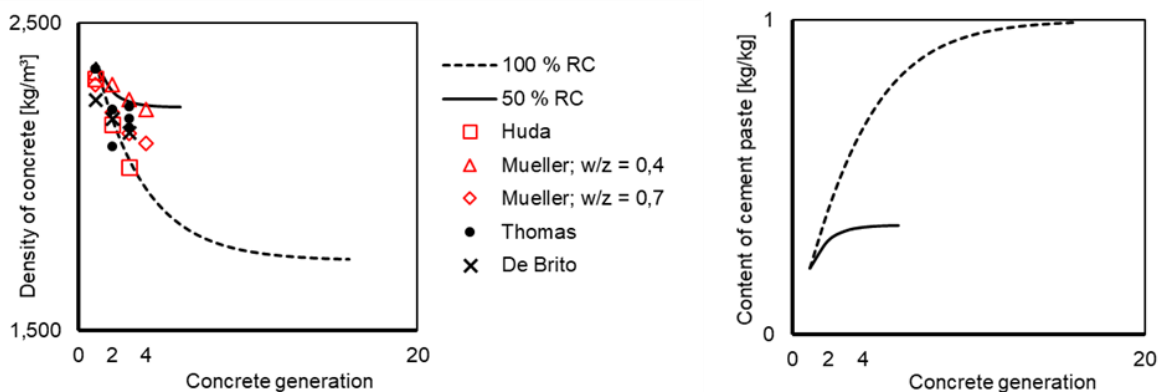
Figure 6: Systematic changes of density and cement paste content as result of "multiple recycling" of concrete [2]

The lengthy process of knowledge generation is also reflected in the timing of the standardization process. In Germany, the first specification for the use of recycled aggregates in the renewed production of concrete was available as early as 1998 [6]. The largest addition of 35 vol.-% concrete chippings > 2 mm plus 7 vol.-% crushed concrete sand ≤ 2 mm was possible for interior walls up to strength class B 25. In concretes that shall be used outdoors and therefore exposed to higher stresses were allowed to contain a maximum of 20 vol.-% of recycled aggregates > 2 mm. Based on this the apartment house "Waldspirale" designed by Friedensreich Hundertwasser was built. The (for the time being) final standard was published in 2023 [7]. According to this, a maximum of 45 vol.-% of the coarse aggregates may be replaced by concrete recyclates > 2 mm. Concrete sands from the same production as the coarse aggregates

may be used in a quantity of < 20 vol.-%. In the meantime, a number of less spectacular buildings have been constructed using R-concrete. First visible advantages in the properties of concretes with recycled aggregates are emerging. The absorption behaviour of the recycled material noticeably reduces the number of blowholes and water runs on the surface of concrete components. This makes R-concrete suitable for use as exposed concrete. Another possibility is to make the aggregates contained in the R-concrete visible by sandblasting the surface. Especially when using aggregates containing bricks, this results in an attractive appearance.

4 Progress in recycling technologies for certain components of CDW

4.1 Gypsum cardboard

Gypsum is a building material increasingly used because of its favourable properties. If this building material is not demounted during deconstruction or separated during processing, the recycled building materials produced cannot be used because they do not meet the environmental and construction requirements. At the same time, there are signs of an increasing shortage of raw materials for the production of gypsum, because flue gas desulfurization gypsum (FGD) will no longer be available in the future as a result of changes in energy production. Therefore, the development, construction and commissioning of gypsum processing plants started about 10 years ago in Germany.

The first step of processing is a visual inspection of the incoming waste after the unloading of the transport truck. A second batch-wise quality control follows before the material is fed in the recycling device. The processing starts with the coarse crushing. Subsequently, the metallic components and other impurities are sorted out. This is followed by a multiple secondary crushing that allows selective comminution of the components gypsum and cardboard, based on the fact that the comminution behaviour of these two materials is different. Gypsum can be crushed by pressure or impact loads. Shear stresses are suitable for disintegration, i.e. the physical separation of the cardboard from the plaster body. The cardboard itself can be comminuted by cutting stress. Crushing is followed by screening. The cardboard, which is present in coarse flakes, is separated. The screen passing consists of gypsum particles up to a size of about 10 mm (Figure 7). The secondary gypsum has to fulfil certain quality parameters. Among others, the gypsum content must be above 85 mass-% [8]. These and the other requirements can be met. So the recycled gypsum can be used for the renewed production of plasterboard, for example.

Figure 7: Products of the processing of gypsum plasterboard: Gypsum grains left, cardboard flakes right

4.2 Tar containing asphalt

Increasing efforts are made to eliminate asphalts containing tar pitch from the material cycle completely. Therefore, since 2018, tar contaminated road construction material may no longer be reused in road construction in Germany. One option of waste management of this material is to deposit it in a landfill. Apart from the fact that this approach runs counter to the idea of recycling, the high-quality aggregates contained in the asphalt granulate are lost too. Thermal recycling, in which the tar pitch is burned and the aggregates are recovered, is a suitable alternative [9]. This is done, first time, in two plants in the port of Rotterdam. The feed material is heated up to temperatures of 850 to 950 °C in a gas-fired rotary kiln. The tar pitch is combusted. The hot aggregates leaving the rotary kiln serve to preheat the combustion air. The dusts are separated in a multi-stage flue gas cleaning and desulfurization system. The products are coarse and fine aggregates, filler and flue gas desulphurization gypsum (FDG). In addition, the energy of flue gas is used for the production of electricity. Following the first plant, which was started up in 2006, a second plant with higher throughput and significantly improved energy efficiency was commissioned in 2020 (Figure 8).

Figure 8: Thermal plants for the treatment of asphalt containing tar [9]

4.3 Masonry rubble

The permissible proportion of clay bricks in recycled aggregates for concrete production is limited according to the above-mentioned regulation. Contrary to this, the production of prefabricated elements is technically possible even with higher proportions of clay bricks, but requires approval by the building authorities. This approval was granted for the first time in Germany for the so-called "Büscher wall", which is used in modular housing construction. The concrete for this wall consists of 100 mass-% recycled aggregates, which can contain up to 50 mass-% brick [10]. The contents of asphalt, glass, non-floating components and floating components are limited, as is the sulfate content. The strength class C20/25 must be achieved as a minimum. Since the approval was granted, a large number of precast elements have been produced (Figure 9) and installed in residential buildings.

Figure 9: Prefabricated concrete elements "Büscher wall" from masonry rubble [11]

4.4 Non-recyclable masonry rubble

In the acceptance and price lists of recycling and disposal companies, construction waste mixtures of lightweight concrete, pumice, aerated autoclaved concrete, bricks and gypsum are often described as "non-recyclable". However, they represent not only a useful but even a favourable starting material for the production of lightweight aggregates. These new lightweight aggregates are on a par with commercial aggregates made from clay or fly ash, such as Leca, Fibo-Exclay, Liapor, Argex.

The production of the lightweight aggregates from mixed rubble begins with the treatment of input materials, similar to the process used in the recycling industry. The resulting material with a maximum particle size < 45 mm is the input material for the production of the lightweight aggregates [12]. The production process of the aggregates themselves starts with grinding under addition of an expanding agent. Then the powdered masonry rubble is pelletized. Thermal stabilization and expanding in a rotary kiln follow. The main characteristic of the lightweight aggregates produced in an pilot plant is their density of 600 g/cm³ on average. They were already used to produce light concrete blocks on a technical scale.
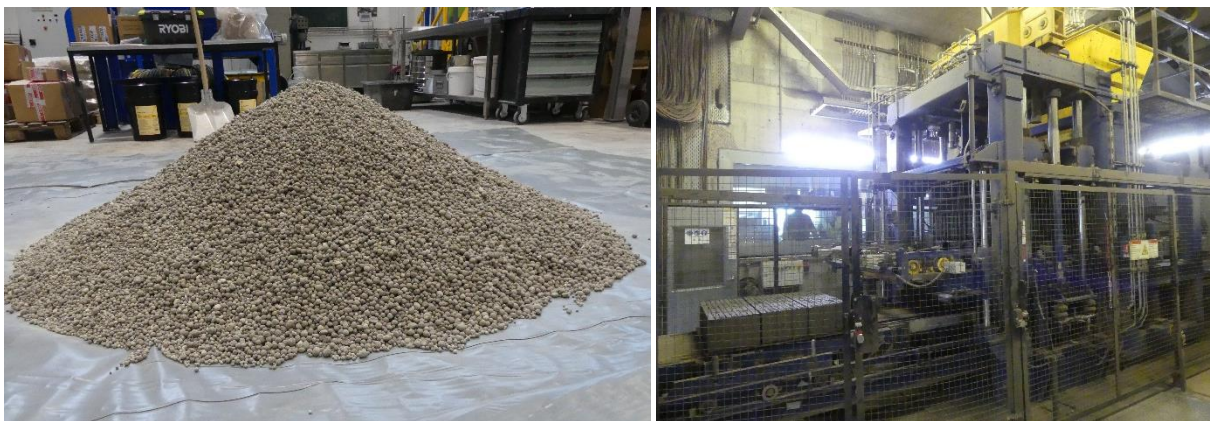
Figure 10: Lightweight aggregates from mixed rubble and the production of lightweight concrete blocks in a production facility

In terms of consumption of resources, the in this way manufactured lightweight aggregates from masonry rubble represent a nearly ''primary raw material free'' product. Only the expanding

agent SiC, which undergoes oxidation at temperatures of around 1100 °C, releasing the necessary bloating gas and a considerable amount of heat, needs to be added. A second decisive advantage of the developed process is that gypsum-containing material can be processed. The gypsum decomposes at the necessary burning temperature and can be recovered from the flue gas as FGD gypsum.

5   Summary

After a long period of stagnation in the recycling of construction and demolition waste, various developments have recently begun to emerge. In processing, the focus is on sorting methods based on sensor technology and machine learning. In recycling, concrete production from recycled aggregates is increasingly finding its way into construction practice. Special processes have been developed for types of construction waste that previously could not be recycled or could only be recycled at the lowest level. A promising process that has been successfully tested at a pilot plant is the production of lightweight aggregates using non-recyclable CDW including gypsum as raw material. The products generated are lightweight aggregates and FGD gypsum.

6   Literature

[1] Data from https://ec.europa.eu/eurostat/statistics-explained/index.php?title=Waste_statistics

[2] Müller, A.; Martins, I.: Recycling of Building Materials. SpringerVieweg 2022.

[3] https://beton-rc.ch/

[4] Heavy picker https://www.terex.com/zenrobotics/robots/heavy-picker

[5] Hansen, T., C.: Recycled aggregates and recycled aggregate concrete second state-of-the-art report. Rilem Technical Committee-37-DRC DEMOLITION AND RECYCLING OF CONCRETE 1985.

[6] Zuschläge Deutscher Ausschuss für Stahlbeton: DAfStb-Richtlinie Beton mit rezykliertem Zuschlag. Deutscher Ausschuss für Stahlbeton im DIN Deutsches Institut für Normung. Beuth-Verlag. Berlin 1998.

[7] E DIN 1045-2:2022-07 Tragwerke aus Beton, Stahlbeton und Spannbeton - Teil 2: Beton

[8] Bundesverband der Gipsindustrie e.V.: Recyclinggips (RC-Gips) Erstprüfung für Recyclinganlagen, Qualitätsmanagement, Qualitätsempfehlungen und Analyseverfahren. 2020.

[9] https://www.recovery-worldwide.com/en/artikel/thermal-cleaning-plants-by-reko-b-v-3566145.html

[10] Deutsches Institut für Bautechnik: Allgemeine bauaufsichtliche Zulassung Z-3.51-2184 „R-Beton der Borex GmbH & co. KG für die Büscher-Wand.

[11] Betonwerk Büscher Verwaltungs-GmbH

[12] Müller, A.; Liebezeit, S.; Palzer, U.: Aufbaukörnungen aus gipshaltigem Mauerwerkbruch – Teil 2: Untersuchungen im Pilotmaßstab. Chem. Ing. Tech. 2022, pp. 1642-1653.

ADVANCED DATASET ACQUISITION FOR IMPROVED CONSTRUCTION AND DEMOLITION WASTE CLASSIFICATION USING MACHINE LEARNING

Tomáš Zbíral (1), Matěj Hužvár (1), Stanislav Vítek (1), and Václav Nežerka (1)

(1) Czech Technical University in Prague, Jugoslávských partyzánů 1580/3, Praha 6, 160 00, Czech Republic

Abstract

Efficient sorting and recycling of construction and demolition waste (CDW) are vital to sustainable development and a circular economy in the construction industry. Building on our previous study that achieved up to 92.3% accuracy using RGB camera data, we propose an improved data set acquisition and feature extraction approach to improving classification performance. We introduce a customized measurement line with industrial RGB cameras, force transducers for volume and mass estimation, and acoustic transducers for ultrasound frequencies. By integrating these additional data sources and exploring various feature extraction techniques, such as shape indices, texture entropy, and mean intensity gradients, our approach aims to enrich the set of features for machine learning algorithms and increase classification accuracy. This research addresses the challenge of improper sorting in CDW recycling, which limits the value of recycled aggregates in high-quality applications.

1.   Introduction

Construction and demolition waste (CDW, Figure 1) constitutes a significant proportion of the total waste generated worldwide. CDW is a complex mixture of different materials, some of which can be recycled, and it is important to improve the efficiency and effectiveness of CDW sorting and recycling [1]. Traditional methods of sorting CDW are time-consuming, labor-intensive, and can be potentially hazardous for workers, particularly when dealing with contaminated materials. Automating the sorting process using machine learning techniques provides a promising avenue for improving both safety and efficiency.

In recent years, machine-learning algorithms have been successfully employed for object recognition tasks, demonstrating high accuracy and reliability. With the rise of deep learning, especially convolutional neural networks, applications for image classification and object detection have expanded rapidly. There are several studies employing these techniques in the context of CDW classification, yielding promising results [2, 3].

Figure 1: Mixed CDW being landfilled.

However, one of the limitations of these approaches is that they primarily rely on visual data captured by RGB cameras. Despite their capability of recognizing and classifying different waste materials, these models face challenges when dealing with materials that are visually similar or when fragments are covered with dust or other residues. This issue highlights the need for more comprehensive data acquisition techniques to enhance the performance of machine-learning models in CDW classification.

To overcome these limitations, we put forward a specialized measurement line that synergizes multiple sensors, namely, an RGB camera, an acoustic sensor, and a weight-measuring device, integrated with a conveyor belt system for efficient CDW transportation. This setup aspires to generate a more comprehensive dataset for machine-learning models, encompassing visual, acoustic, and weight attributes of CDW fragments. The overarching goal is to devise a robust, high-accuracy classification system capable of differentiating between various CDW types, thereby streamlining the recycling and reusing processes of CDW.

This paper presents the development of this comprehensive measurement line, demonstrating its potential for improving CDW sorting and recycling.

2.   Development of the Multimodal Data Acquisition System

The central component of our system is a conveyor belt mechanism, selected for its efficiency in transporting a steady stream of CDW fragments (Figure 2). The conveyor belt ensures a consistent presentation of the material to the sensors, maintaining a regular distance and orientation, which is crucial for obtaining reliable and reproducible data. Furthermore, the speed of the conveyor can be adjusted to match the requirements of the data acquisition process.

Above the conveyor belt, an RGB camera is placed to capture high-resolution images of the CDW fragments. The frame is equipped with an adjustable light source to control illumination conditions, ensuring consistent lighting across different imaging sessions.

Beyond visual data (Figure 3), our system integrates an acoustic sensor and a weight-measuring device to expand the spectrum of collected data. The weight-measuring device operates based on the force exerted onto the rollers that guide the conveyor belt, providing insightful data about the weight characteristics of different CDW fragments.
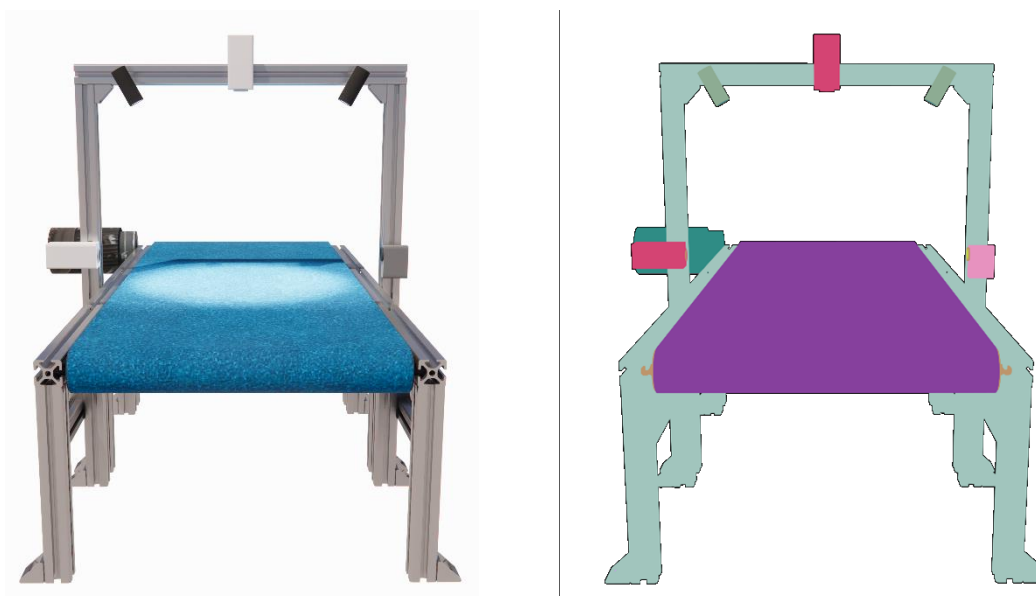
Figure 2: Prototype of the developed multimodal acquisition system; the colored components (right) represent: (i) a frame (light turquoise), (ii) a motor (teal), (iii) a conveyor belt (purple), (iv) cameras (red), (v) acoustic unit (pink), and (vi) lights (green); the computational unit and weight measuring transducers are not visible in these images.

The classification is based on the detection of ultrasonic waves reflected by the surface of the material under the test (Figure 4). HC-SR04 ultrasonic sensors were employed for the measurements, with the transducers positioned to maximize the radiation characteristics towards the target sample. These sensors are operated using an Arduino UNO microcontroller connected to a PC. Additionally, a 1/8" Brüel & Kjær measurement microphone is affixed to the mount to capture the signal reflected from the sample's surface. The obtained signal is further processed using a Brüel & Kjær Nexus measurement amplifier, with a conversion setting of 100 mV/Pa. Subsequently, the amplified signal is displayed on a Rigol MSO5074 digital oscilloscope.

The measured signals exhibit a short, narrowband signal at approximately 40 kHz. The dataset comprises 8 sets of 20 measurement instances. Initially, the signals were normalized by subtracting their mean value. Although this normalization procedure eliminates potential information regarding the acoustic absorption of the material, it is deemed acceptable given the intended robustness of the classification method under uncalibrated field conditions. Notably, all signals demonstrate a prominent amplitude peak followed by a smaller peak, often preceded by minor activity. To facilitate a more comprehensive analysis, two-time windows were selected.

Figure 5 illustrates the first (green) window, which encompasses the period preceding the large peak to ensure the inclusion of the smaller peak whenever present. The second (red) window is a narrowed-down interval surrounding the two larger peaks. Examining the peak ratio within the second window proved instrumental in segregating the data into three clusters, with one cluster exclusively containing one specific material. Furthermore, the variance observed in the first window facilitated the division of one of the remaining clusters into two

distinct materials, while the other cluster was split into two as well. The outcome of this analysis is presented in Figure 6.
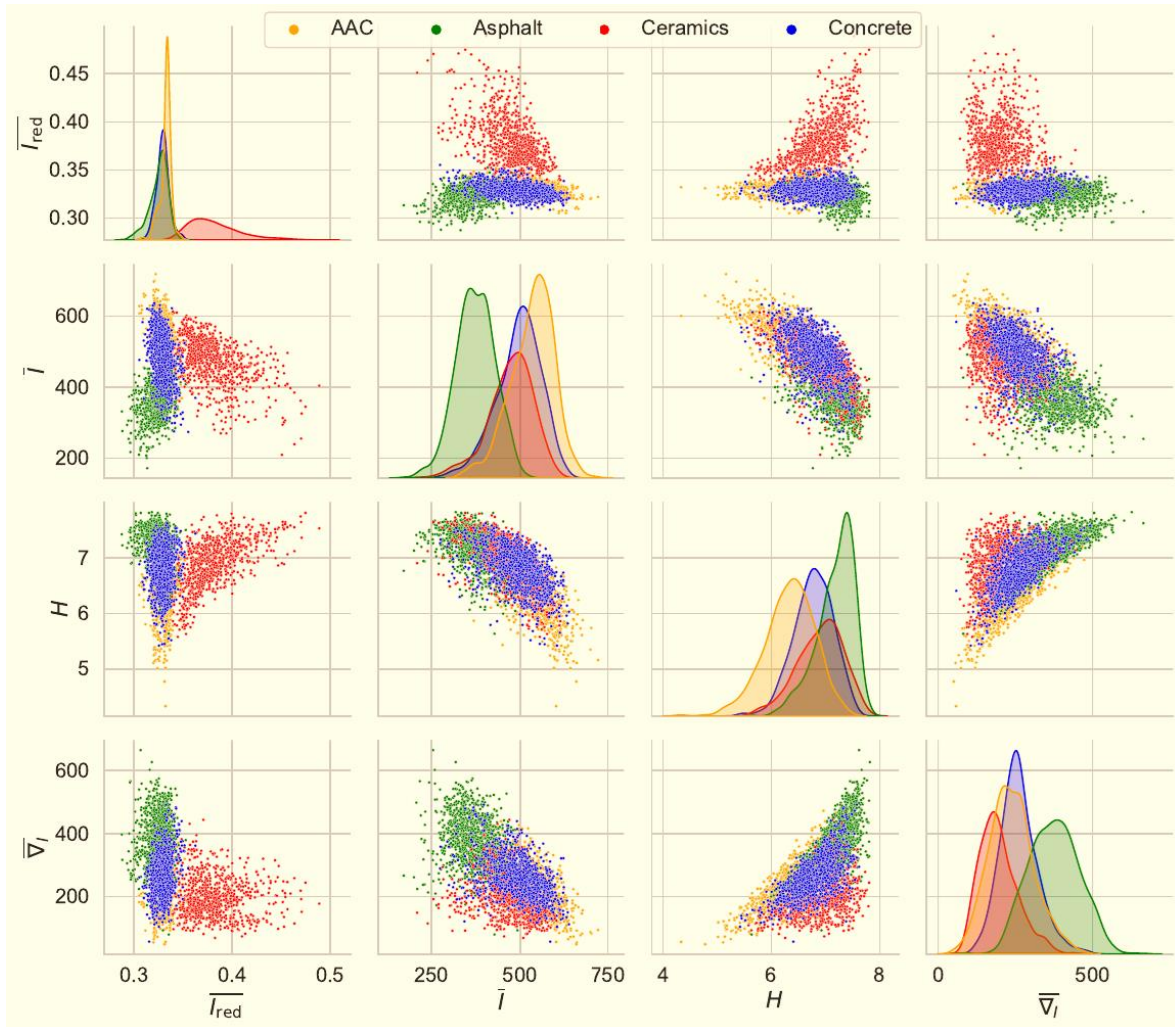
Figure 3: Correlation of features extracted from RGB images [4].
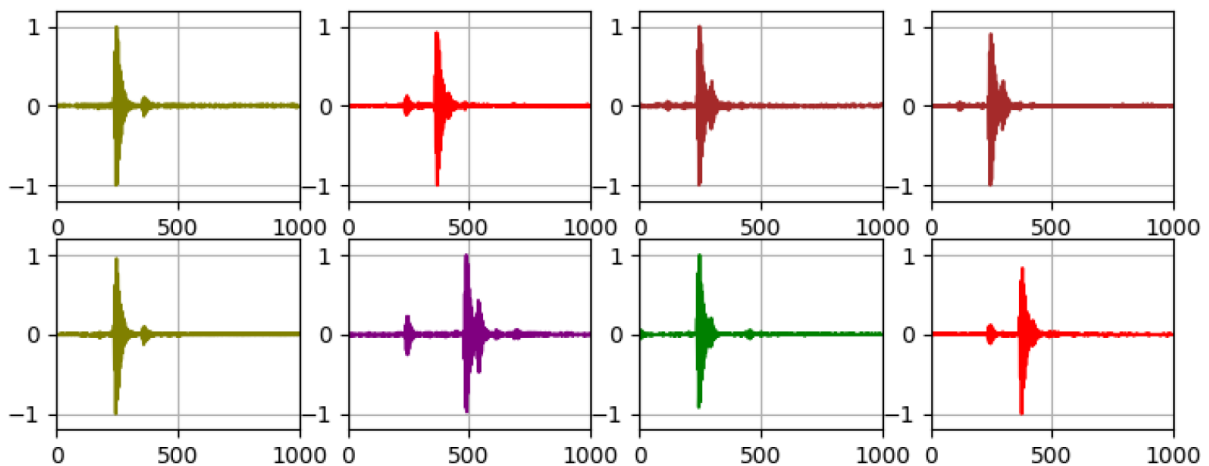
Figure 4: Variability of reflected signals measured for different materials.
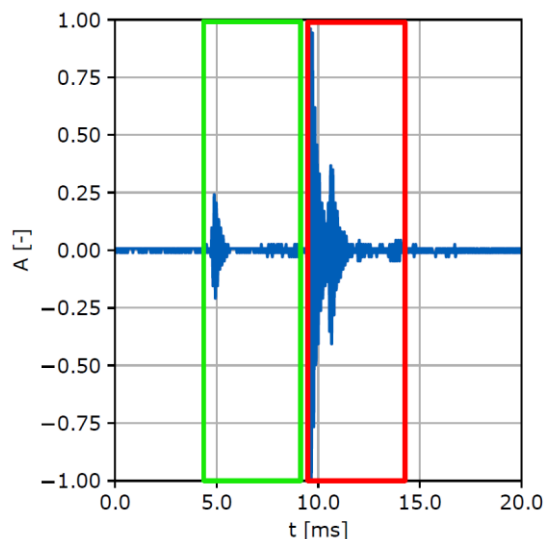
Figure 5: Windows to extract features from the retrieved ultrasound signal.
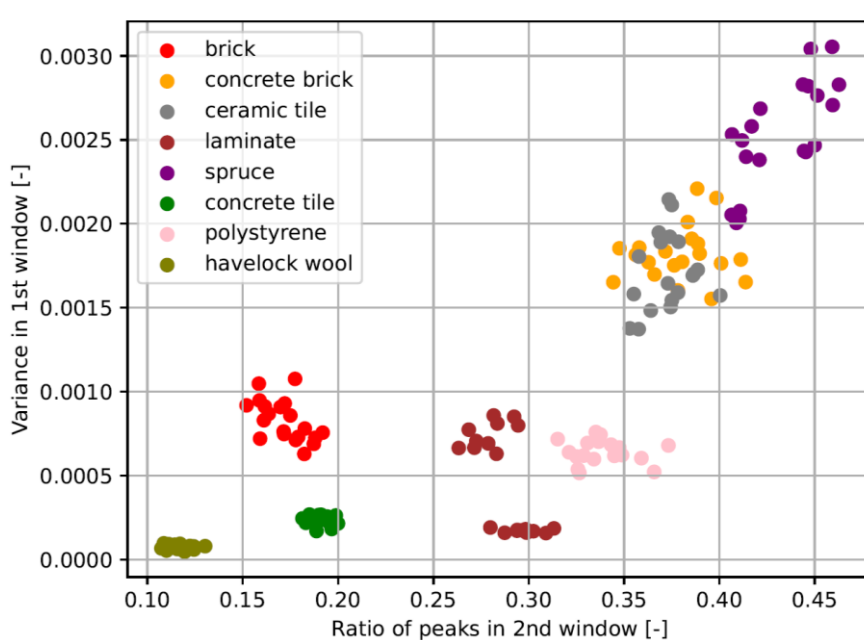
Figure 6: Clustering of materials in the space of extracted features from the measurements of reflected ultrasound signal.

3.   Fusion of Data from Different Sensors

Effective use of multimodal data in a classification task requires not just the collection of data from different sensors, but also the strategic fusion of these data. The process of data fusion combines the information from each sensor, exploiting the unique strengths of each data type to improve the overall classification performance. In the context of CDW classification, this

means integrating the information derived from RGB images and acoustic sensor measurements to better differentiate between different types of CDW fragments.

The first step in this process is the independent feature extraction from each sensor's data. For the visual data, we continue to use the methodology described in our previous work [4], which includes the extraction of various textural features from high-resolution images. Meanwhile, for the acoustic data, we apply standard signal processing techniques to extract spectral and temporal features, such as presented in Section 2.

Once the feature sets from all sensors have been extracted, the next step is their fusion. There exist several strategies for data fusion, commonly categorized into three levels: early (or data level) fusion, intermediate (or feature level) fusion, and late (or decision level) fusion.

In early fusion, the raw data from each sensor is combined before any processing or feature extraction takes place. However, due to the disparate nature of visual and acoustic data, early fusion is not feasible in our case.

In intermediate fusion, the feature sets from each sensor are combined into a single, high-dimensional feature vector, which is then fed into the classification model. This approach allows the classifier to make decisions based on all available information, but it also increases the dimensionality of the input data, which may lead to challenges associated with the so-called "curse of dimensionality."

Lastly, in late fusion, each sensor's feature set is independently fed into separate classifiers, and the final decision is made based on the combination of these separate decisions. This approach exploits the strength of each sensor in recognizing certain types of CDW fragments but relies heavily on a robust strategy for decision-making.

In this study, we opt for the intermediate fusion approach, mainly due to its capability to leverage the complementary nature of visual and acoustic features. The fused high-dimensional feature vector will then be fed to machine learning classifiers, including gradient-boosting decision trees (GB) and multi-layer perceptron (MLP), which have demonstrated promising results in our previous work.

4. Training Machine Learning Models for CDW Classification

The first step in the training process is to split the entire dataset into two subsets: a training set and a validation set. The training set is used for teaching the model, while the validation set is utilized for testing the model's accuracy on unseen data and tuning the hyperparameters. The standard practice is to use around 70-80% of the dataset for training, and the remaining 20-30% for validation.

The training process involves adjusting the model's parameters so that the model's predictions on the training data are as accurate as possible. This is done by defining a loss function that quantifies the discrepancy between the model's predictions and the actual labels. The model's parameters are then iteratively updated using optimization algorithms, such as gradient descent, in a way that minimizes this loss.

For both GB and MLP models, the training process involves several rounds of iterative learning. In the case of GB, a series of weak learners (decision trees) are trained, where each successive learner tries to correct the mistakes of the previous one. For MLP, a different approach is used, where the model learns to map the input (features) to the output (labels) using

several layers of artificial neurons (or perceptrons), and the weights of these neurons are adjusted during the training process.

Once the training is complete, the model's performance is evaluated on the validation set. This step is crucial to ensure the model's ability to generalize well to unseen data and avoid overfitting, a scenario where the model performs well on the training data but poorly on new, unseen data.

Finally, once the models are well-trained and have demonstrated satisfactory performance on the validation set, they can be deployed for the real-time classification of CDW fragments in the sorting and recycling plants.

5. Transition to Industrial-Scale CDW Sorting

An industrial-scale sorting line would first and foremost require the development of a robust conveyor system able to accommodate high volumes of CDW. The system described in our study, while effective for research-scale analysis, would need to be significantly upscaled in terms of both size and speed. Notably, this would involve careful design considerations to maintain the precision of data capture while increasing the throughput of the system.

The sensor network we have developed, comprised of acoustic, weight, and RGB camera sensors, could also be effectively scaled to meet the demands of an industrial environment. Large-scale applications would require a comprehensive setup of sensors at multiple points along the conveyor line to ensure comprehensive data capture for each CDW fragment. This would involve additional hardware and installation requirements but could potentially be offset by significant increases in sorting efficiency and recycling rates.

Training machine learning models for industrial-scale applications would entail processing and analyzing substantially larger volumes of data. This might require more powerful computational resources and potentially the application of distributed computing or cloud-based machine learning services. However, the benefits of this approach are significant, with the potential for the models to continuously improve over time as they process more data, increasing the efficiency and accuracy of CDW sorting.

The models would also need to be made robust against variances in CDW types, lighting conditions, sensor calibration, and other factors that might be more variable in an industrial setting compared to a controlled research environment. This could be achieved by continuously updating the training datasets with new data from the industrial sorting line, effectively enabling the models to learn and adapt to changing conditions.

Importantly, while our research provides a proof-of-concept for a sensor-fused, machine-learning-based approach to CDW sorting, the transition to the industrial-scale application would require significant collaboration with industry partners, government agencies, and other stakeholders. The practicalities of implementing such a system, such as financial costs, regulatory requirements, and operational logistics, would all need to be carefully considered.

8. Conclusion

In this study, we have showcased a pioneering approach to construction and demolition waste (CDW) sorting and recognition using a fusion of multiple sensor data and machine-learning models. Our work underscores the significant potential of integrating acoustic, weight,

and RGB imaging data to enhance the classification accuracy of CDW fragments, overcoming the limitations inherent in relying on visual data alone.

The prospect of applying these methodologies on an industrial scale presents exciting possibilities for the field of waste management and recycling. While there are practical considerations for transitioning our research-scale system to an industrial context, our study offers a roadmap for implementing a sophisticated, sensor-fused, machine-learning-based CDW sorting line. This could revolutionize the CDW recycling industry, enhancing efficiency, and increasing recycling rates, thereby contributing to a more sustainable construction industry.

However, it is crucial to note that transitioning to such a system will require significant collaboration among industry partners, government agencies, and other stakeholders. Further research and development will also be needed to fine-tune the models and adapt them to the variable conditions of an industrial setting.

Acknowledgments

References

[1] Hoong, J.D.L.H., Lux, J., Mahieux, P.Y., Turcry, P., & Aït-Mokhtar, A. 2020. "Determination of the Composition of Recycled Aggregates Using a Deep Learning-Based Image Analysis." *Automation in Construction* 116: 103204. https://doi.org/10.1016/j.autcon.2020.103204.

[2] Ku, Y., Yang, J., Fang, H., Xiao, W., & Zhuang, J. 2020. "Deep Learning of Grasping Detection for a Robot Used in Sorting Construction and Demolition Waste." *Journal of Material Cycles and Waste Management* 23: 84–95. https://doi.org/10.1007/s10163-020-01098-z.

[3] Lin, K., Zhou, T., Gao, X., Li, Z., Duan, H., Wu, H., Lu, G., & Zhao, Y. 2022. "Deep Convolutional Neural Networks for Construction and Demolition Waste Classification: VGGNet Structures, Cyclical Learning Rate, and Knowledge Transfer." *Journal of Environmental Management* 318: 115501. https://doi.org/10.1016/j.jenvman.2022.115501.

[4] Nežerka, V., Zbíral, T., & Trejbal, J. 2023. "Machine-Learning-Assisted Classification of Construction and Demolition Waste Fragments Using Computer Vision: Convolution versus Extraction of Selected Features." Submitted to *Automation in Construction*.

STEEL RECOVERY FROM REINFORCED CONCRETE ELEMENTS

Leonardo C. Machado[1,*], Gabriel V. Z. Silva[1], Guilherme S. Moreira[1], Renata C. Pétta[1], Sergio C. Angulo[1]

(1) University of São Paulo, Escola Politécnica - Brazil

* email of the corresponding author(s): *leonardo.machado@lme.pcc.usp.br*

Abstract

Strategies to increase the lifecycle of products are needed to reduce environmental impacts and provide new business opportunities. In old cities, demolitions are increasing, and some companies are interested in reusing steel rebars from the demolition of reinforced concrete elements. However, there is lack of studies once reuse of steel can pose structural risks. Twenty-four rebars were collected from the demolitions of three buildings near the city of São Paulo, Brazil. Those were characterized based on the building age, demolition equipment used, the type of element (slab, pillar, etc.), and the physical condition of the steel rebar in terms of alignment and corrosion aspect. After, the samples were cleaned mechanically and manually realigned using levers, and some of them were subjected to tensile testing. All rebars met the yield strength criteria; however, the ductility criteria did not. The rebars behavior may be influenced by the structural element, the demolition technique used, the building's prior use, and the realignment process. Although more studies are needed, the steel can be used for construction purpose only, without significant structural risk in reinforced concrete elements. This strategy could add value to the material and potentially reduce environmental impacts.

Keywords: STEEL REBARS RECOVERY ; DEMOLITION ; CIRCULAR ECONOMY

## 1.	Introduction

Urbanization leads to stock buildings to accommodate the growing population, and the old growing building stocks will result in an increase of demolition operations over time [1]–[4]. In the mechanical process of demolitions, excavators and hydraulic breakers were used and the steel rebars of the reinforced concrete structures become separated. A remaining steel fraction is separated after the crushing of the concrete fragments in the construction and demolition waste (CDW) recycling plants. Both extractions of steel are done without care for reuse. A significant portion of this resulting scrap can be recovered and recycled in steel producers. The steel scrap presents the highest secondary material price in the CDW types [5]. In Brazil, the total steel production reached in 2020 31.4 million tons [6]. 30% of it is obtained from steel scrap [7]; therefore, 9 million tons of steel scrap was recycled in Brazil in 2020.

"Selective Demolition" (SDM) [8] is a process that can preserve the functional components, and it can increase the selling price of the reuse steel rebar, 3 times more than that of scrap recycling [9]. Steel rebar is usually recovered more carefully from the structural reinforced concrete elements and reuse can be explored without passing it in a recycling process.

In Brazil, it is common to encounter an average ratio of 23kg of steel rebars/m² (0,023ton/m²) in typical residential building construction with reinforced concrete structure [10]. Steel scrap is usually sold for US$201/ton, while the recovered steel rebars could be sold for US$604/ton in Brazilian market. As a result, during a demolition of a 10,000m² residential building, the recovering of all rebars could potentially boost the financial gains derived. This could elevate the earnings from US$ 46,000 to US$139,000 (Eq 1).

$$10,000 m^2 \times \frac{0,023 ton}{m^2} \times (US\$604) = US\$138,920.00 \qquad \text{(Eq. 1)}$$

Other research indicate that the metals content (although it is not specified) during the demolition of a non-residential building (constructed using a reinforced concrete structure) could reach up to 53kg/m² [11], potentially enhancing those financial benefits. The production of 1 ton of steel usually generates 1.6 tons of CO_2 [6].Although further studies are needed, this analysis show that we could not only improve the added value of the steel in a circular economy scenario, but also minimize energy consumption and significantly the CO_2 emissions [12], [13].

The Fig. 1a shows the typical steel scrap after a mechanical demolition process. It is hard to think the reuse of rebars. However, certain companies in the Brazilian market introduced an equipment designed to "realign" these steel rebars. The Fig. 1b shows a commercially available equipment called "Rebar recycler". According to the producer, this equipment has a productivity of 8 tons/day. Some recycling plants and demolition companies are already implementing a similar process, not necessarily using this specific equipment (Fig. 1c).
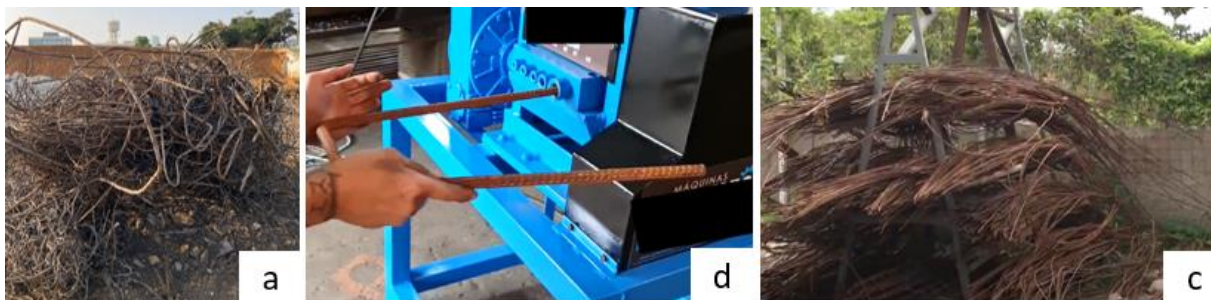
Fig. 1 – (a) Steel scrap; (b) Entrance of twisted rebar in the Machine for "realignment"; (c) Rebar after passing through "realignment" [16].

In literature, only two studies have been identified about reused steel rebars; one from Poland and other from Jordan [14], [15].These studies primarily focused on assessing the rebar's mechanical properties, including tensile and bonding strength, as well as bending capability. In both studies, the rebars were only manually realigned, similar of that was observed in Brazil.

The utilization of realigned rebars can be promising in non-structural applications, where the main parameter is not the steel's strength. In some contexts, steel is used to help the construction process, or to mitigate shrinkage, such as urban seats, sidewalks, with neglectable structural risks. However, in Brazil, reused rebars has been employed to construct informal buildings, posing structural risks. Therefore, and the properties of the reuse steel needs to be assessed.

Steel reuse presents certain risks, particularly, regarding the consumption of plastic deformation, or local damages by impact which can lead to fatigue and brittle rupture. Various inquiries, not yet addressed in existing literature, must be resolved before this practice can be

considered valid. For instance, does the mechanical behavior of these rebars present acceptable properties after years of use, or when submitted to realignment? Does the demolition technique affect the steel bar mechanical property? Is the ductility enough to lay rebars again ?

1.1 Objective

This work aimed to evaluate the physical condition, the tensile strength and ductility of steel rebars recovered from demolition of reinforced concrete elements.

2. Methodology

Three demolition sites were visited near the city of São Paulo, Brazil in 2022: The first one in São Bernardo do Campo (ID 1-SBC), a commercial building over 40-years-old and 2,970m²; the second in Santo André (ID 2 – SA), a 14-years-old factory over 7,800m²; the third in São Paulo, a 60-years-old factory covering 45,000m² (ID 3 – SP).

Eight rebars (1.5~2m) were collected from each demolition site, totaling 24 steel rebars. The rebars were characterized *in situ* in four items: 1) Type of element (beams, columns, slabs, foundation); 2) Position in the building (Outside, inside); 3) Twisting degree (low, regular, intense) – Visually defined by the angle of deformation (α) as follows: Low ($\alpha < 10^{\circ}$), Regular ($10^{\circ} < \alpha < 45^{\circ}$), Intense ($\alpha > 45^{\circ}$); 4) Conservation against corrosion (Deteriorated, Not deteriorated) - visually defined by the significant presence or not of corrosion residue adhered to steel rebars. It was also identified which type of machinery were used in the demolition process to obtain each rebar (Hydraulic breaker, Hydraulic shear). The Table 1 shows the summary of the characteristics of the collected rebars.

Table 1 - Summary of collected rebars.

Category	Item	Demolition Site			Total	Total %
		1 – SBC	2 – SA	3 - SP		
Type of element	Slabs	4	7	8	19	79%
	Columns	4	0	0	4	17%
	Foundation	0	1	0	1	4%
Position in the Building	Outside	2	1	0	3	13%
	Inside	6	7	8	21	88%
Machinery	Hydraulic breaker	0	8	8	16	67%
	Hydraulic Shear	8	0	0	8	33%

These rebars underwent a laboratory-based manual realignment process using levers (the mechanical realignment was not possible at this moment of the research). After this, the rebars were mechanically cleaned using a bench grinder. Twelve rebars were sectioned into 65cm lengths and submitted to a tensile test in accordance with the Brazilian standard code ABNT NBR 7480:2022 [19]. The Brazilian standard code presents four main requirements for the steel rebars CA-50 (focus of this work):I. Yield Strength (f_y) (500MPa); II. Maximum strength ($1,08*f_y$); III. Elongation at maximum force (5%); IV. Elongation at fracture (8%).

3. Results and discussions

3.1 Rebars physical characteristics

The elements collected were visually evaluated for the twisting degree and their conservation against corrosion. The Table 2 shows a summary of this evaluation for each building.

Table 2 – Visual evaluation about physical state of the steel rebars

Category	Item	Demolition Site			Total	Total %
		1 – SBC	2 – SA	3 - SP		
Twisting Degree	Low ($\alpha < 10°$)	6	5	4	15	63%
	Regular ($10° < \alpha < 45°$)	2	2	3	7	29%
	Intense ($\alpha > 45°$)	0	1	1	2	8%
Conservation	Deteriorated	0	3	2	5	21%
	Not Deteriorated	8	5	6	19	79%

The elements were collected from within concrete elements inside of the building, and although the buildings have been standing for 14-70 years since the construction, no correlation between the building age and the conservation against corrosion was identified. On the other hand, the Table 3 shows the relationship between the twisting degree and conservation against corrosion for different elements. The rebars collected from slabs exhibit higher twisting degrees and poorer conservation than other elements.

Table 3 – Twisting degree and conservation against corrosion by elements.

Element	Twisting degree						Conservation against corrosion			
	Low		Regular		Intense		Not deteriorated		Deteriorated	
Slabs	10	53%	7	37%	2	10%	14	74%	5	26%
Columns	4	100%					4	100%		
Foundation	1	100%					1	100%		

The worsened condition state of slab's rebars can be attributed to the quality of execution and concrete cover. This often results from the absence of plastic spacers during the concreting, which is a common construction error in Brazil. Furthermore, the authors identified two possible factors that could explain the higher twisting degrees of slab's rebars: Firstly, the reduced diameter (typically smaller than those in columns and beams) - Fig. 2a, which may contribute to greater deformability. Secondly, the type of machinery employed during slabs demolitions (Hydraulic breakers) - (Fig. 2b) - , could have a greater impact on the pieces, whereas the columns (which exhibit better twisting degrees) were demolished using hydraulic shears (this machinery could result in less impact on the pieces). To gain a statistically significant understanding of these circumstances, further investigations involving a larger sample size, varying diameters and machinery are needed.

| | (a) | (b) |
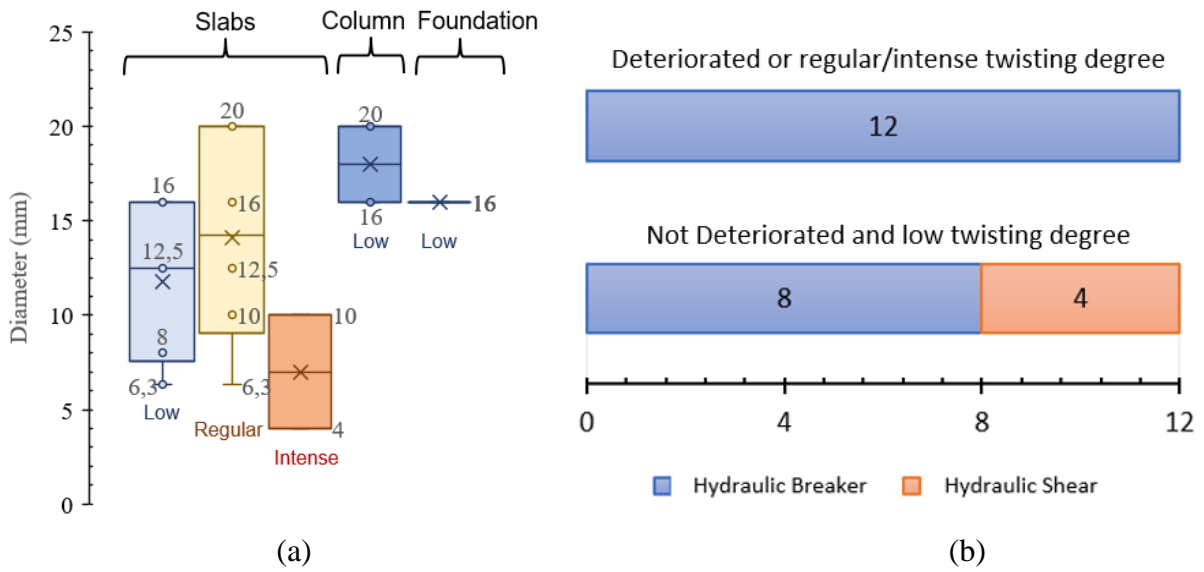
Fig. 2 – (a) Diameter of rebars vs type of element vs Twisting degree (b) Machinery vs twisting degree and conservation degree.

3.2   Mechanical properties

During the evaluation of the rebar's mechanical properties, two aspects were considered: their stress-strain behavior, and the standard requirements. Upon conducting the tensile strength test, the rebars exhibited a nonlinear behavior in the beginning of the strength application. This behavior could be attributed to a residual deformation that was not eliminated in the manual realignment process (Fig. 3a). Once the linear behavior was established, the strength was released and the test restarted, returning the diagram to the expected linear behavior. However, only two rebars demonstrated a clear yielding point, highlighting the need for careful consideration in the reuse of rebars (Fig. 3b)

| | (a) | (b) |
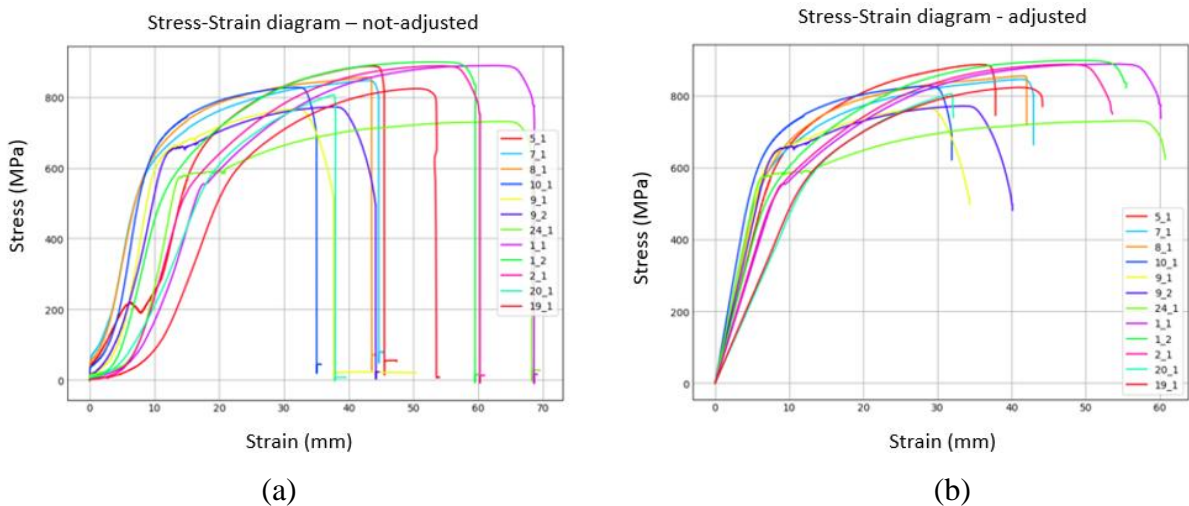
Fig. 3 – Stress-Strain steel diagram

Upon evaluating the requirements in the ABNT NBR 7480:2022 all rebars meet the strength criteria. However, the ductility requirements were not always met. Only 42% of rebars meet both strength and ductility requirements simultaneously, while the others did not attain either the Elongation in the Maximum force (83% attained) or the Elongation after breakage in 10 diameters (just 58% attained).

Some rebars presented brittle failure. The authors suspect that these rebars have undergone a fatigue process during their life cycle, which may have reduced their ductility. This needs further investigation in future research.

(a)   (b)

Fig. 4 – Brittle failure of steel rebars (a) rebar collected at the factory building at São Paulo ID3-SP, from an industrial floor, showing signs of fatigue (b) rebar collected from the commercial building at São Bernardo do Campo ID 1 - SBC

The Table 4 presents a summary of the ductility evaluation and the influence of the type of element, the twisting degree, and the machinery (HB means Hydraulic Breaker, HS means Hydraulic Shear).

Table 4 – Summary of ductility evaluation

Evaluation	By type of element		By Twisting degree		By machinery			
	Slab	Column	Low	Regular	ID 2 - SA HB	ID 1 - SBC HB	ID 3 - SP HB	ID 1 - SBC HS
Approved	23%	100%	50%	25%	33%	0%	33%	100%
Disapproved	77%	-	50%	75%	67%	100%	67%	0%

A significant majority of slab rebars did not meet the approval criteria. This could be attributed to two potential factors: the higher twisting degree, resulting from smaller diameters; or due to the building's usage (factory floors, subjected to cyclic loads). The twisting degree may affect the ductility. The results show that the higher the twisting degree, the lower the ductility approval. Furthermore, hydraulic shears demonstrated a 100% approval rate, outperforming the Hydraulic breaker. However, it should be noted that all the rebars collected from the hydraulic shear were sourced from columns, with larger diameters, which presented lower twisting degrees compared to slab rebars. No correlation was found between the tensile test and the conservation against corrosion. These parameters may be interconnected and challenging to isolate. Nevertheless, this research serves as an initial step for future investigations, where more variables and statistical analysis should be done.

4.   Conclusions

As the demolitions are expanding worldwide, this paper presents an investigation about the physical state and mechanical properties of steel rebar recovered for reuse from demolition. The results are promising, potentially adding more value to the material in the future. All the evaluated rebars met the yield strength criterion; however, only 42% of the rebars met the ductility criterion. It was not found any correlation between the building age and the corrosion condition of the rebars. However, the rebars herein were collected mainly inside the building. The type of element, the use of the building and the demolition techniques may affect the characteristics of the recovered steel rebars. Rebars from Columns, demolished with hydraulic shears, present significantly better results than slab rebars demolished with impact breakers. Also, some rebars collected in industries involving intense machine movement on floors presented brittle failure due to fatigue. The findings highlight that the primary challenge lies not in the tensile strength of rebars, but rather in their ductility. However, more research should be done to understand the effects of all the variables. Use of steel for constructive need in non-structural elements seems to be promising. Although it requires further investigation, the reuse of steel rebars could potentially reduce environmental impacts by decreasing energy consumption and CO_2 emissions in the manufacturing process.

5.   Research needs

To continue the study, samples should be evaluated outside of buildings and in different environmental exposure classes. The realignment method requires further investigation to ensure that initial residual deformation is eliminated and based on industrial-scale implementation. A statistical assessment about mechanical properties should be performed. An economic and environmental comparison between recycled rebars and reused steel rebars should also be conducted.

6.   Acknowledgements

7.   References

[1]   IBGE, "IBGE | Projeção da população". Acesso em: 8 de novembro de 2022. [Online]. Disponível em: https://www.ibge.gov.br/apps/populacao/projecao/index.html

[2]   Folha de São Paulo, "SP precisa construir 698 mil casas até 2030, aponta estudo", Folha de São Paulo. Acesso em: 8 de novembro de 2022. [Online]. Disponível em: https://www1.folha.uol.com.br/cotidiano/2022/06/sp-tera-de-construir-698-mil-moradias-para-suprir-a-demanda-ate-2030-aponta-estudo.shtml

[3]   E. Martínez, Y. Nuñez, e E. Sobaberas, "End of life of buildings: three alternatives, two scenarios. A case study", *Int J Life Cycle Assess*, vol. 18, nº 5, p. 1082–1088, jun. 2013, doi: 10.1007/s11367-013-0566-4.

[4]   R. Moura, "Exploração imobiliária aumenta em São Paulo - Estadão Imóveis", Imóveis - Estadão. Acesso em: 8 de novembro de 2022. [Online]. Disponível em:

https://imoveis.estadao.com.br/noticias/aumenta-exploracao-imobiliaria-em-sao-paulo-estadao-imoveis/

[5]   F. Pacheco-Torgal, V. W. Y. Tam, J. A. Labrincha, Y. Ding, e J. de Brito, Orgs., "Woodhead Publishing Series in Civil and Structural Engineering", em *Handbook of Recycled Concrete and Demolition Waste*, em Woodhead Publishing Series in Civil and Structural Engineering. , Woodhead Publishing, 2013, p. xxi–xxiii. doi: 10.1016/B978-0-85709-682-1.50028-2.

[6]   Instituto Aço Brasil, "Relatório de Sustantabilidade 2020", Instituto Aço Brasil, RIO DE JANEIRO, 2020.

[7]   Benite, Anderson e Taniguti, Eliana;, *Manual da sustentabilidade da construção em aço*, 1º ed. em Série Manual de Construção em Aço). RIO DE JANEIRO, 2019.

[8]   E. M. Lund, N. R. Center, e P. Yost (Building-wright), *Deconstruction, Building Disassembly and Material Salvage: The Riverdale Case Study*. NAHB Research Center, 1997.

[9]   European Comission, "Guidelines for the waste audits before demolition and renovation works of buildings". 2018. [Online]. Disponível em: https://ec.europa.eu/docsroom/documents/31521

[10]   M. H. C. Botelho e O. Marchetti, *Concreto Armado - Eu te Amo - Vol. 2*. Blucher. Acesso em: 16 de outubro de 2022. [Online]. Disponível em: https://www.blucher.com.br

[11]   M. Mália, J. de Brito, M. D. Pinheiro, e M. Bravo, "Construction and demolition waste indicators", *Waste Manag Res*, vol. 31, nº 3, p. 241–255, mar. 2013, doi: 10.1177/0734242X12471707.

[12]   P. Morseletto, "Targets for a circular economy", *Resources, Conservation and Recycling*, vol. 153, p. 104553, fev. 2020, doi: 10.1016/j.resconrec.2019.104553.

[13]   M. Arora, F. Raspall, L. Cheah, e A. Silva, "Buildings and the circular economy: Estimating urban mining, recovery and reuse potential of building components", *Resources, Conservation and Recycling*, vol. 154, p. 104581, mar. 2020, doi: 10.1016/j.resconrec.2019.104581.

[14]   J. Domski, J. Katzer, e M. Zakrzewski, *Mechanical characteristics of used bent rebars as a factor limiting their reuse*. 2016.

[15]   K. Bsisu e Z. Abusalem, "Recycling of Steel Bars from Demolished Structures", *International Journal of Engineering Research and Technology*, vol. 13, p. 94, jan. 2020, doi: 10.37624/IJERT/13.1.2020.94-99.

[16]   *Reciclagem de VIGAS E COLUNAS - Fortaleza - CE*, (28 de janeiro de 2022). Acesso em: 8 de novembro de 2022. [Online Vídeo]. Disponível em: https://www.youtube.com/watch?v=e8J-pQ7CHGM

[17]   "JP BOTELHO MAQUINAS – JP BOTELHO MAQUINAS". Acesso em: 8 de novembro de 2022. [Online]. Disponível em: https://jpbotelho.com.br/

[18]   *RECICLADORA DE VERGALHÃO MDV 16 Máquina para desentortar e alinhar vergalhão.*, (14 de setembro de 2021). Acesso em: 8 de novembro de 2022. [Online Vídeo]. Disponível em: https://www.youtube.com/watch?v=hOfNUwdXRAA

[19]   Associação Brasileira de Normas Técnicas, "NBR 7480 - Aço destinado às armaduras para estruturas de concreto armado — Requisitos", ABNT, RIO DE JANEIRO, 2022.

CHARACTERISATION OF POZZOLANIC ACTIVITY OF MASONRY RUBBLE BY SPECTROPHOTOMETRY

Alexander Winkel (1), Katrin Severins (2)

(1) Institut für Ziegelforschung Essen e.V., Germany

(2) VDZ Technology gGmbh, Germany

Abstract

Masonry rubble is a mixture of concrete, brick, lime sand brick, mortar and plaster. Due to their pozzolanic activity and the future shortage of fly ash, bricks are of special interest for the cement industry as a potential substitute. There have been numerous research projects dealing with optical sorting of masonry rubble to produce brick rich granulate or the use of waste brick powder as pozzolan. Yet there has been no research trying to directly determine the pozzolanic activity of brick rich masonry rubble with optical methods. In this work masonry rubble from a recycling facility and backing bricks from a brick manufacturer were investigated. Sample colour was measured by spectrophotometry and pozzolanic activity by hydration heat. Also Fe_2O_3 and Al_2O_3 were measured with X-ray fluorescence, since Fe_2O_3 is responsible for the reddish colour of bricks and Al_2O_3 content is an indicator for the clay type the bricks are made of. The results show good positive correlation between Fe_2O_3 and Al_2O_3 content and the hydration heat. Colour measurement enables to determine the brick content of masonry rubble and thus the results indicate the pozzolanic activity. Future determination of pozzolanic activity of masonry rubble already in the recycling facility is likely to be possible.

1.   Introduction

The production of cement clinker requires a lot of energy and resources and is responsible for around 8 % of the global CO_2 emissions. Many measures have to be taken to reduce this environmental impact. One of them is the replacement of cement clinker by pozzolanic by-products from other industries like fly ash from coal-fired power plants or slag sand from steel production. But the ongoing process of decarbonisation of energy production leads to a shortage of fly ash in the near future. Also the amount and quality of slag sand is expected to decline. Thus, new resources for the replacement of cement clinker with broad availability and low environmental impact have to be found.

The biggest potential is currently seen in calcined clays. Since highly reactive metakaolin is too expensive, latest research is dealing with the use of "common" clays containing other clay minerals like illite or smectite. Numerous research projects showed their potential as substitute for cement clinker depending on mineralogy and firing temperature [1–4]. The disadvantage of

calcined clays is that, though to a lower extent than for cement clinker, there is still required energy for the calcination process. Therefore, already existing calcined clay products could be used as pozzolans, namely fired clay bricks. The knowledge of pozzolanic activity of crushed brick exists since the Roman empire and in the last years the subject gained new attention [5, 6]. The firing temperature of backing bricks reaching from 900 to 950 °C lies in a range where clay minerals show pozzolanic activity. Since in Germany around 30 % of residential buildings are made of brick masonry, there is a big potential for pozzolanic material. Furthermore, backing bricks are produced of calcareous clays and the calcite might have a positive effect on pozzolanic activity due to formation of an amorphous phase [7].

But when a building made of bricks is demolished, there is usually a mix of different mineral constituents and in the recycling plant the material might also be mixed with other construction waste from the surrounding area so the brick content in the masonry rubble and its pozzolanic activity is unknown. But for the use as cement substitute the determination of pozzolanic activity of masonry rubble already in the recycling plant would be helpful. There are several methods to measure the reactivity, e.g. measuring the fixed quantity of calcium hydroxide (Chapelle test), measuring the amount of soluble Al- and Si-ions (Surana test) or measuring the hydration heat (ASTM C1897-20). Each of them is non-automatic and too time consuming to be applied in a recycling plant.

Colour measurement might be a promising way to estimate the pozzolanic activity. Unlike other building materials bricks have a reddish colour which distinguishes from colourless cement based materials. And since brick is the only pozzolanic material in masonry rubble, there should be a link between the reddish colour of masonry rubble and its pozzolanic activity. This paper shows a way to indirectly estimate the hydration heat by measuring the brick content in masonry rubble via spectrophotometry, supplemented with X-ray flurescence.

2.   Experimental procedure

In this project 8 samples from a recycling plant and 13 samples from a backing brick manufacturer were investigated. In the recycling plant an optical sorting of arriving masonry rubble by human eye was conducted to increase the brick content. There was no further machine sorting. Sample 4 and sample 8 are special. The first one is an ordinary sample from daily recycling process and the second one is rich in roof tiles that were collected by hand. The brick manufacturer has three different plants and its own recycling facility where he crushes damaged bricks and bricks that return from construction sites. The first samples were referred to as brick plant 1 to 3 and the latter as brick recycling. Besides these backing bricks, also old roof tiles that were produced many years ago in one of the brick plants were investigated.

For the measurement of hydration heat at 7d the samples were ground to 90 µm and then tested with an isothermal calorimeter (TAM Air, TA Instruments) according to ASTM C1897-20. For the colour measurement the samples were ground to 0.5 mm to obtain a homogeneous colour, then compacted to a flat surface and measured with a spectrophotometer (CM-600d, Konica Minolta). The measurement area was about 8 mm in diameter, a D65 illuminant and a 10° vision angle were selected to measure lightness (L*) and chromatic coordinates (a* and b*). The L*a*b* colour space as shown in Figure 1 was used for evaluation. It describes all perceptible colors, where each colour in the colour space is defined by a position with the Cartesian coordinates L*, a* and b*. On the a* axis green (negative values) and red (positive values) are opposite each other and the b* axis runs between blue (negative values) and yellow (positive values). The L* axis describes the brightness of the color with values from 0 to 100 and can

also be called neutral gray axis, because between the end points black ($L^* = 0$) and white ($L^* = 100$) all achromatic colors (gray) are contained.
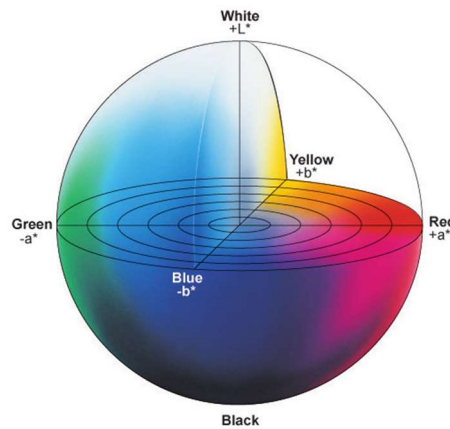
Figure 1: The spectrophotometer describes the samples using colour measurements adopted by the Commission Internationale d'Eclairage (CIE) in 1976 (image source: Konica Minolta Sensing)

Also the content of Fe_2O_3 and Al_2O_3 was measured as Fe_2O_3 in the form of hematite is responsible for the reddish colour of bricks and Al_2O_3 is an indicator for the amount and type of clay minerals in the brick clay. The chemical composition of the samples is determined by quantitative X-ray fluorescence analysis according to DIN EN ISO 12677. For the analyses, one melt tablet is prepared from each sample material, which has been previously dried at 105 ºC, then representatively divided and ground to an analytical fineness (< 63 μm). The analysis is performed on a Malvern PANalytical AXIOS advanced X-ray fluorescence spectrometer.

Since there should be a linear relation between brick content in masonry rubble, its reddish colour and in consequence its pozzolanic activity a simple linear regression analysis was performed with the software Design Expert. The dependent variable was the hydration heat and the independent variables were a^* and b^* value and Fe_2O_3 and Al_2O_3 content. The p-value and the adjusted coefficient of determination (R^2_{adj}) were evaluated to determine if the variables have a significant influence and how well they predict the hydration heat.

3. Results and discussion

Figure 2 shows the measured $L^*a^*b^*$ values of masonry rubble and brick samples. The chromatic values of the masonry rubble samples are, except for sample 8, lower than for brick samples. There is a tendency in the L^* value for masonry rubble to decline with increasing chromatic value which might be due to increasing brick content. Yet there is also a strong variance in L^* value for the brick samples. The roof tile samples are the darkest samples so the L^* value is probably a result of brick content and brick firing temperature. Since only sample 8 is in the colour space of the brick samples, the other masonry rubble samples must be contaminated to different degrees by other constituents like mortar and plaster. The values for the different brick plants are close together as the colour depends on mineralogy of the clay, firing temperature and kiln atmosphere and these factors do not change much in a backing brick
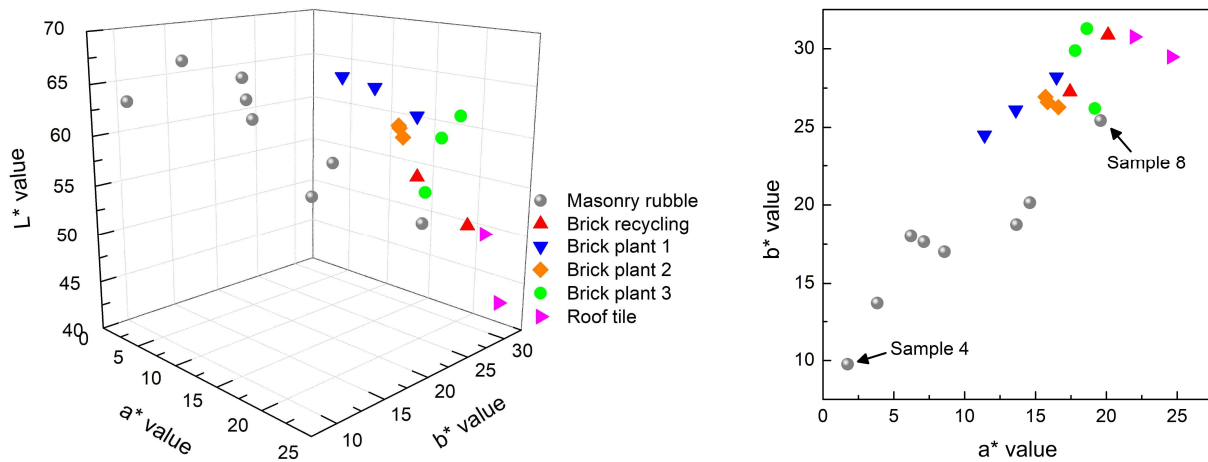
Figure 2: L*a*b* values of masonry rubble and brick samples

Table 1: Hydration heat and Fe_2O_3/Al_2O_3 content for samples of masonry rubble and brick

Sample	Hydr. heat [J/g]	Fe₂O₃ [wt.%]	Al₂O₃ [wt.%]	Sample	Hydr. heat [J/g]	Fe₂O₃ [wt.%]	Al₂O₃ [wt.%]
Masonry rubble				*Brick*			
Sample 1	79,9	2,41	6,99	Brick recycling	115,7	4,77	12,99
Sample 2	58,0	1,95	6,27	Brick recycling	123,8	4,77	12,73
Sample 3	80,2	3,26	9,02	Brick plant 1	142,8	5,24	14,69
Sample 4	32,6	1,89	4,36	Brick plant 1	117,2	4,85	12,70
Sample 5	80,2	2,69	7,90	Brick plant 1	106,0	4,99	12,77
Sample 6	66,8	2,11	6,94	Brick plant 2	250,3	5,07	16,67
Sample 7	67,6	2,69	8,30	Brick plant 2	191,0	4,64	15,56
Sample 8	125,7	3,69	10,53	Brick plant 2	220,0	4,13	14,40
				Brick plant 3	168,8	5,85	15,39
				Brick plant 3	178,0	6,36	16,35
				Brick plant 3	118,0	5,63	14,82
				Roof tile	126,0	6,29	16,22
				Roof tile	140,0	6,68	17,28

plant, especially in the short time period where the samples were collected. The variance in the a* value is much higher than in the b* value which is probably caused by different iron oxide contents, since the samples of brick plant 3 and the roof tiles have the highest Fe_2O_3 content and exhibit the highest a* values. It seems sufficient to measure just the a* and b* value as the L* value does not contain colour information.

Table 1 contains the data for hydration heat at 7d, Fe_2O_3 and Al_2O_3 content. In Figure 3 the hydration heat of the samples is correlated with a* and b* value. For the masonry rubble sample 4 shows the lowest hydration heat and sample 8 the highest. The hydration heat slightly increases with increasing a* and b* values which shows there is a link between the colour of masonry rubble and its pozzolanic activity. Since sample 8 is the masonry rubble with the highest brick content, its hydration heat is similar to that of the brick samples. The values measured for the different brick types are higher than for the masonry rubble as they are not contaminated. Moreover, samples from the same brick plant are close to each other, indicating a correlation between heat of hydration and clay mineralogy. All brick samples show a similar hydration heat except for the samples from brick plant 2 that show significantly higher values.
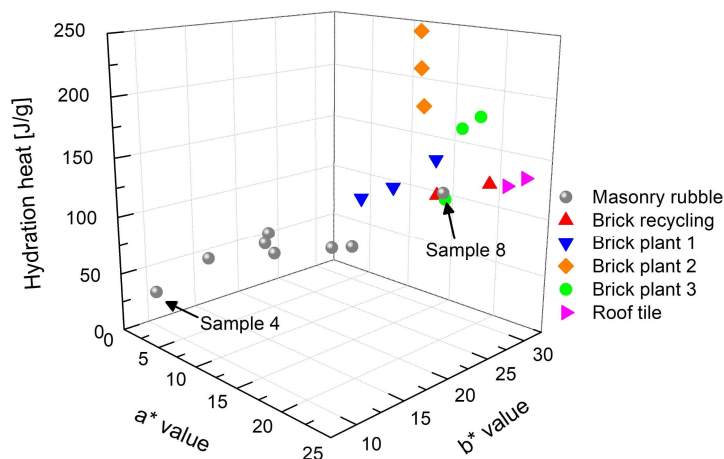
Figure 3: Hydration heat in dependence of a*b* values for all samples

Table 2 shows the results of the linear regression analysis which was performed with the data of Table 1 and the a*b* values. All p-values are lower than 0.05 which indicates that the relationship between hydration heat and the four independent variables is statistically significant and that these variables can be used to describe the hydration heat. The coefficient of determination is highest for Al_2O_3 content and b* value and lowest for Fe_2O_3 and a* value. The value for Al_2O_3 means that 67.6 % of the variance can be explained by this variable which shows the major influence of the clay mineral content on hydration heat.

Table 2: P-value and adjusted coefficient of determination

	a*	b*	Fe_2O_3	Al_2O_3
p-value	0.0015	< 0.0001	0.0013	< 0.0001
R^2_{adj}	0.387	0.591	0.397	0.676

Figure 4 shows the linear regression plots. For each variable the predicted hydration heat is compared to the measured hydration heat. A high coefficient of determination means that the values are close to the dotted line. All variables show a positive linear correlation with hydration heat. The b* value (yellow) correlates better with the hydration heat than the a* value (red) despite its lower variance (see Figure 4 a and b). The red colour of bricks is caused by hematite which is the most important colouring pigment in iron containing ceramics fired under oxidizing conditions. Its origin are iron containing minerals or the clay minerals [8]. Bricks made of calcareous clays are rather orange than red. The yellow part of the colour is caused by partly incorporation of iron in new crystal phases like melilite or pyroxene [9, 10]. The correlation of Fe_2O_3 with hydration heat is worse than for Al_2O_3 but the position and the relative arrangement of the brick samples to each other is nearly the same, since iron and aluminium highly correlate with the clay mineral content in brick clays and consequently with the brick content in masonry rubble.
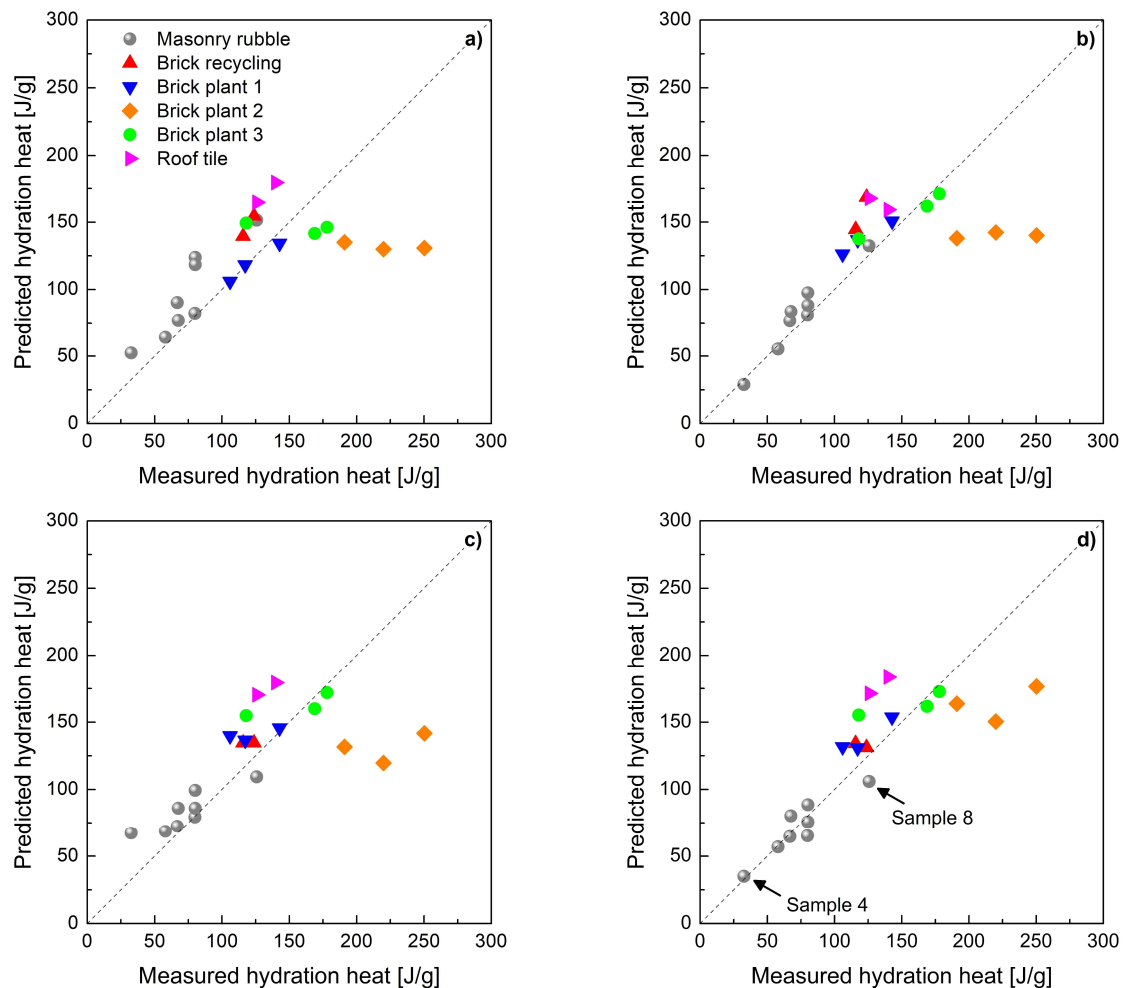
Figure 4: Linear regression analysis of hydration heat in dependence of a* and b* value (a, b) and Fe_2O_3 and Al_2O_3 content (c, d)

In all four diagrams it can be seen that the samples from brick plant 2 are special because the measured values are much higher than the predicted ones. Since the samples of brick plant 2 have the same colour as the others, the clay mineralogy, especially the Al_2O_3 content, must be responsible for the difference in hydration heat. This assumption is supported by the fact that

R^2_{adj} is highest for Al_2O_3 and that the samples of brick plant 2 in Figure 4 d are closer to the dotted line compared to the other diagrams. The main source of Aluminium in clay are the clay minerals in which it is part of the crystal lattice. Iron can always be found in ordinary brick clay and it can be part of the crystal lattice, absorbed on the surface or exist as a mineral. In brick plant 2 a so called opalinus clay with a kaolinite content of 18 wt.% is processed. The clays from brick plants 1 and 3 each contain only 4 wt.%. Since kaolinite is a 1:1 clay mineral, it contains more Al_2O_3 than 2:1 clay minerals like illite or smectite. Furthermore, aluminium in the kaolinite lattice is not replaced by iron which is the case for other clay minerals like chlorite and illite [11]. Consequently the ratio of Al_2O_3 to Fe_2O_3 is higher for bricks made out of this clay type (see Figure 5 a). Kaolinite is the clay mineral with the highest pozzolanic activity and studies showed that the kaolinite content also determines the compressive strength of calcined clay limestone cements [12]. So there are two factors influencing the hydration heat of brick waste and therefore of masonry rubble. One is the Al_2O_3 content which correlates with the amount of clay minerals and the other is the Al_2O_3/Fe_2O_3 ratio which is an indicator for the kaolinite content. The influence of these factors on the hydration heat can be seen in Figure 5 b where the x-axis is the product of these two parameters. There is a good positive correlation between the measured hydration heat and $(Al_2O_3)^2/Fe_2O_3$ indicating that by knowing the chemical composition of masonry rubble or brick waste the pozzolanic activity can be estimated.
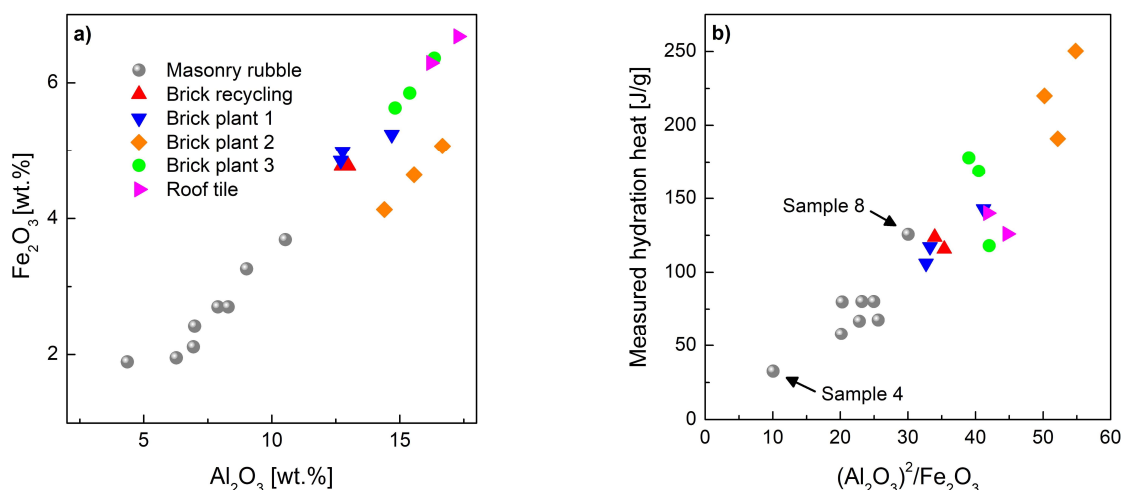
Figure 5: Ratio of Fe_2O_3 to Al_2O_3 for all samples (a) and dependence of measured hydration heat on $(Al_2O_3)^2/Fe_2O_3$ ratio (b)

4.   Conclusion

Estimating the pozzolanic activity of masonry rubble by means of colour measurement is possible. However, the chemical composition, especially the Fe_2O_3 and Al_2O_3 content, is needed as additional information as spectrophotometry can only measure the brick content in the rubble. But the pozzolanic activity of the brick also strongly depends on the mineralogical composition of the original clay, which is reflected in its chemical composition. Bricks made of kaolinitic clay contain more Al_2O_3 and are more reactive than bricks made of illitic clay. The combination of spectrophotometry with an automated and fast measurement method for determining the chemical composition such as LIBS, supported by machine learning and AI, could enable an even better prediction [13]. Furthermore, for the industrial application of this method, the sorting of masonry rubble with the aim of high brick content is of great importance.

Acknowledgements

References

[1] He, C., Makovicky, E. and Osbæck, B., 'Thermal stability and pozzolanic activity of calcined kaolin', *Applied Clay Science* **9** (3) (1994) 165–187

[2] Fernandez, R., Martirena, F. and Scrivener, K., 'The origin of the pozzolanic activity of calcined clay minerals: A comparison between kaolinite, illite and montmorillonite', *Cement and Concrete Research* **41** (1) (2011) 113–122

[3] Truemer, A., Ludwig, H.-M and Rohioff, K., 'Investigations into the application of calcined clays as composite material in cement', *ZKG International* **67** (9) (2014) 52–57

[4] Beuntner, N., 'Zur Eignung und Wirkungsweise calcinierter Tone als reaktive Bindemittelkomponente im Zement', Dissertation, Universität der Bundeswehr München (2017)

[5] Lum Wong, C., Hung Mo, K., Poh Yap, S., Alengaram, U. J. and Ling, T. C., 'Potential use of brick waste as alternate concrete-making materials: A review', *Journal of Cleaner Production* **195** (2018) 226–239

[6] Msinjili, N.S., Gluth, G.J.G., Sturm, P., Vogler, N. and Kühne, H. C., 'Comparison of calcined illitic clays (brick clays) and low-grade kaolinitic clays as supplementary cementitious materials', *Materials and Structures* **52** (5) (2019) 94

[7] Danner, T., Norden, G. and Justnes, H., 'The Effect of Calcite in the Raw Clay on the Pozzolanic Activity of Calcined Illite and Smectite', in *Calcined Clays for Sustainable Concrete* 131–138

[8] Valanciene, V., Siauciunas, R. and Baltusnikaite, J., 'The influence of mineralogical composition on the colour of clay body', *Journal of the European Ceramic Society* **30** (7) (2010) 1609–1617

[9] Pérez-Monserrat, E.M., Maritan, L., Garbin, E. and Cultrone, G., 'Production Technologies of Ancient Bricks from Padua, Italy: Changing Colors and Resistance over Time', *Minerals* **11** (7) (2021) 744

[10] Pérez-Monserrat, E.M., Maritan, L. and Cultrone, G., 'Firing and post-firing dynamics of Mg- and Ca-rich bricks used in the built heritage of the city of Padua (northeastern Italy)', *European Journal of Mineralogy* **34** (3) (2022) 301–319

[11] Finck, N., 'Iron speciation in Opalinus clay minerals', *Applied Clay Science* **193** (2020)

[12] Scrivener, K., Martirena, F., Bishnoi, B., Maity, S., 'Calcined clay limestone cements (LC3)', *Cement and Concrete Research* **114** (2018) 49–56

[13] Klewe, T., Völker, T., Götz, J., Landmann, M., Wilsch, G. and Kruschwitz, S., 'Sorting of construction and demolition waste by combining LIBS with NIR spectroscopy', *NDT-CE 2022 - The International Symposium* (2022)

DETERMINATION OF MATERIAL PARAMETERS USING MULTISPECTRAL SENSING

Ina Reichert (1), Jurij Walz (1), Patrick Hunhold (1) and Elske Linß (1)

(1) MFPA - Materials Research and Testing Institute, Weimar, Germany

Abstract

This paper studies the potential of determining material parameters of recycled aggregates of construction and demolition waste (CDW) by means of multispectral sensing.

Multispectral data in the range from visible light over near-infrared to short-wavelength infrared of different kinds of CDW are taken, covering wavelengths from 300 nm to 2500 nm in total.

One key aspect is the classification of the assorted CDW. In order to resolve this task features of the spectral information are extracted and multivariate statistics techniques, such as principal component analysis (PCA) and linear discriminant analysis (LDA), are used to distinguish between the groups of CDW. Once the detection rate is sufficiently large, further investigations within the classes can be performed.

For the estimation of the water content three different characteristic parameters utilizing spectral information are introduced: mean absorption, water index and absorption difference. Their calculation is based on the absorption spectrum of the covered water band at approximately 1950 nm. All three approaches are applied to several kinds of CDW and compared according to their quality and applicability.

In conclusion, the LDA emerges as a promising tool for the classification of CDW. The estimation of the water content utilizing the absorption difference looks most auspicious considering quality and efficacy.

Keywords: recycling, CDW, recycled aggregates, material composition, multispectral sensing, classification, multivariate statistics

1.   Introduction

In the last twenty years about 50 million tons of mineral CDW were produced annually in Germany [1]. For high-quality reuse instead of disposal, it is necessary to monitor the structural properties of the recycled material according to [2-4]. Within the scope of this research work, an automated analysis for the classification of recycled aggregates and the corresponding water content will be developed (Figure 1). For this purpose, spectral information from the visual to the near-infrared (NIR) wavelength range (300 nm to 2500 nm) will be used in combination

with different dimensionality reduction methods like principal component analysis (PCA) [5] and linear discriminant analysis (LDA) [6].
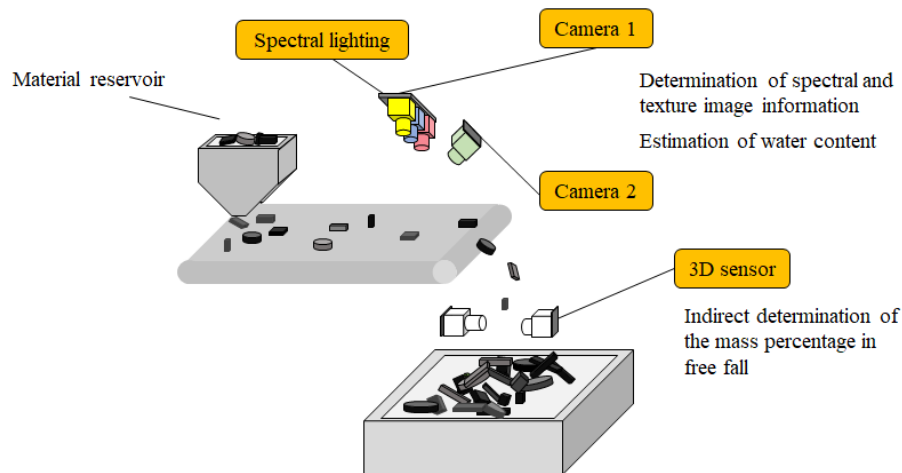
Figure 1: Device for material composition analysis and water content estimation

For the determination of the water content, there exist many well-known methodologies, which can be found in [7] [8]. Nevertheless, the aim is to rapidly gain information about the water content non-destructively and contact-free. The estimation of the water content by using spectral information was already described by [9] [10] for vegetation and by [11]-[12][14] for the curing of concrete and mortar, respectively. This paper deals with investigations on the application of water content estimation methods for spectral data in the range from 1000 nm to 2300 nm.

2. Investigations on the determination of the material composition

2.1 Material and Methods

The investigations were realised on selected building material samples (concrete, calcium silicate brick, roof tiles, masonry bricks, lightweight concrete, autoclaved aerated concrete). The material parameters (pure and bulk density, water absorption, mineralogy) of the partly recycled and partly new building materials were analysed.

After an unsupervised dimension reduction method, PCA was used, where the class membership does not have to be known. LDA was applied as a supervised dimension reduction method in a complementary way. The goal of using LDA is to increase the interclass variance of samples while decreasing the intraclass variance between samples in one class, such that a much clearer separation of classes can be achieved. Information in greater depth can be gained in [5] and [6].

2.2 Application

The spectrometer measurements were done by the Agilent Cary 5000 UV-VIS-NIR spectrometer. The recordings are taken within the range of 300 nm to 2500 nm with a spectral resolution of 1 nm. To gain information of commonalities and differences within the recorded point spectra without knowledge of class membership, the data set was examined using PCA and LDA.

2.3 Results

The investigations carried out with PCA and LDA show cluster formations, i.e. that a separation of the considered building material categories is possible based on spectral information. LDA proves to be most suitable for a separation of the considered building material classes. The following Figure 2 shows the PCA and LDA analysis results in the wavelength range from 401 to 2500 nm.

- ● Concrete
- ● Calcium silicate brick
- ● Roof tile
- ● Brick
- ● Lightweight concrete
- ● Autoclaved aerated concrete
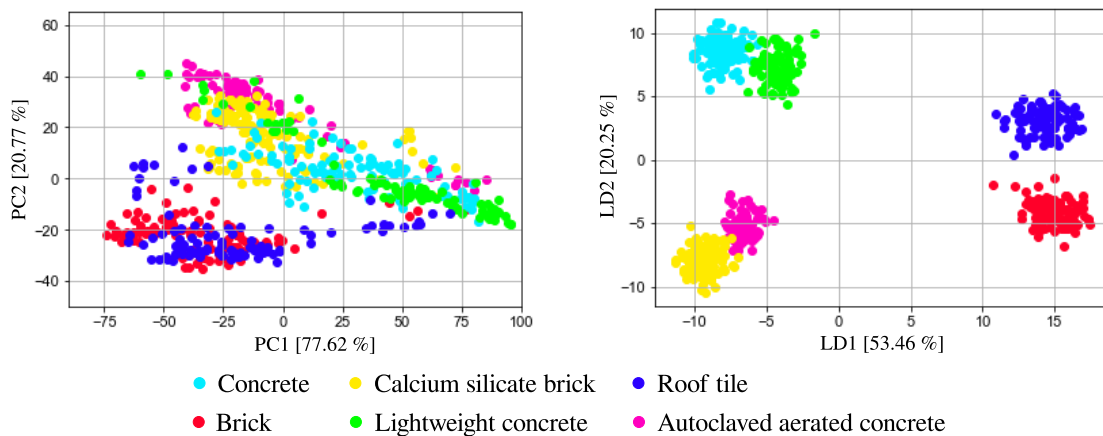
Figure 2: PCA (left) and LDA (right) analyses in the range from 401 nm to 2500 nm

3. Investigations to estimate the water content

3.1 Material and Methods

Figure 3 is exemplarily showing several reflection measurements of recycled brick with different water contents and the corresponding absorption. The water bands around 1950 nm and 1450 nm are best recognized when the water content is relatively high. It has to be noted that the total water including free and bonded water on the surface is measured. With decreasing water content, the amplitude of the extreme values is dropping.
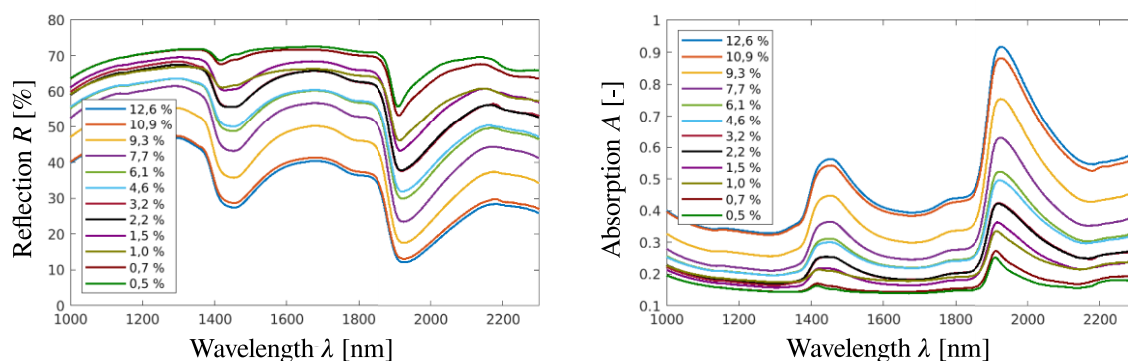
Figure 3: Reflection (left) and absorption curves (right) of selected measurements of one aggregate of recycled brick material with indicated the water content in the legend

The absorption spectrum allows formulating several estimates for the water content. Three of them are presented and used on recycled aggregates in the following.

3.1.1 Mean absorption

The mean absorption is depicted in Figure 4. Here, the mean value of the absorption is calculated between the points of inflection of the absorption curve for the 1950 nm water band.
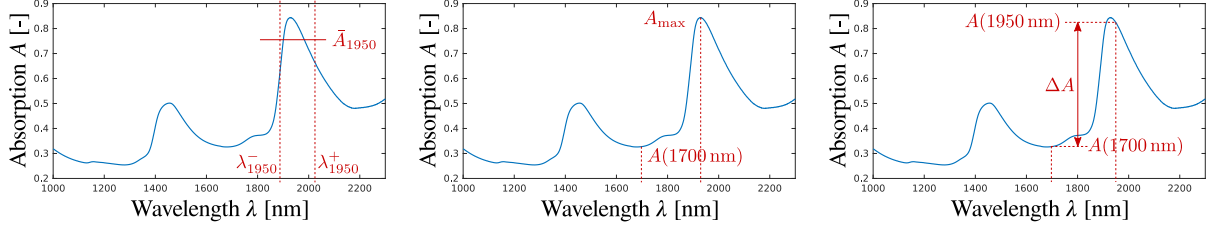
Figure 4: Water content estimation approaches: mean absorption, water index and absorption difference (from left to right)

Additionally, a baseline correction is performed to achieve a sorting of the measurements according to the value of water content. In this case, the absorption value at 1700 nm, which is a nearly constant band, is subtracted. Hence, the mean absorption is calculated by

$$\overline{A_{1950}}(w) = \frac{1}{N}\sum_{j=1}^{N}\big(A(\lambda_j; w) - A(1700\text{nm}; w)\big),$$

(2)

where A is the absorption, λ is the wavelength, w is the water content and N is the number of measurements between the inflection points.

3.1.2 Water index

The water index, as depicted in Figure 4, is calculated as the quotient

$$\text{I}(w) = \frac{1}{A(1700\text{nm}; w)} \max_{\lambda \in \Lambda} A(\lambda; w) \text{ with } \Lambda = \left[\lambda_{1950}^{-}, \lambda_{1950}^{+}\right]$$

(4)

between the maximal absorption value of the water band around 1950 nm and the value of absorption at 1700 nm (see [9]-[11]).

3.1.3 Absorption difference

For the absorption difference

$$\Delta A(w) = A(1950\text{nm}; w) - A(1700\text{nm}; w)$$

(5)

the difference between the absorption values of 1950 nm and 1700 nm as shown in Figure 4 is used.

3.1.4 Material

The samples consist of three aggregates of each of the following materials: concrete, autoclaved aerated concrete, lightweight concrete, brick, roof tile, and calcium silicate brick. Before starting the measurements to estimate the water content, each of the samples lay in water for a minimum of 12 hours. In Table 1 the water content at saturation w_0 as well as the particle sizes are given.

Table 1: Overview of investigated samples with water content at saturation

material	Concrete	Autoclaved aerated concrete	Light-weight concrete	Brick	Roof tile	Calcium silicate brick
Image of sample						
Water content at saturation w_0 [%]	6.6 ± 0.4	24.4 ± 0.6	63.8 ± 3.1	14.3 ± 0.5	9.5 ± 1.3	6.8 ± 0.5
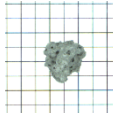
3.2 Application

The experiment was performed in a predefined sequence for all material samples. The near-infrared spectra were gained by the workflow shown in Figure 5.
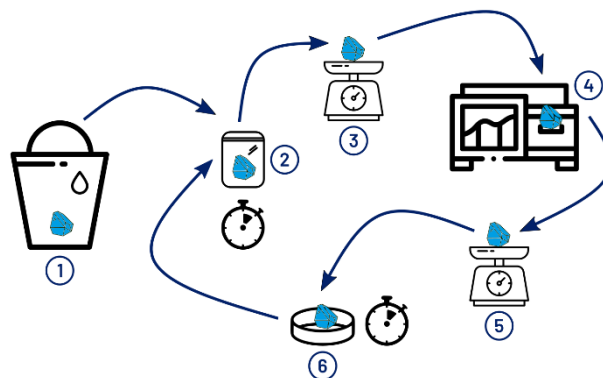
Figure 5: Workflow of the experiment execution

First, the samples was kept under water for at least 12 hours (1). Hereafter, the specimen was put in an airtight plastic bag for a minimum of five minutes (2) to balance the water distribution between the surface and the inside. Before (3) and after (5) the spectrometer measurement (4), the specimen was being weighed. The average between the two weight measurements m_i forms the basis to calculate the water content w_i belonging to each spectrum that was taken. After the second weighing, a drying under ambient conditions for another five minutes (6) was performed. As long as there is a reduction in mass between successive loops, steps (2) to (6) are repeated.

According to this workflow, it is possible to measure NIR spectra at different levels of water content. Finally, the specimen were oven-dried to gain the dry mass m_{dry}, which is needed for the calculation of the water content

$$w_i = \left(\frac{m_i}{m_{dry}} - 1 \right) \cdot 100\% \qquad (6)$$

belonging to each of the spectral data taken.

3.3 Results

The methods, suggested in section 3.1, were used on the spectral data of the samples. Figure 6 is showing the linear regressions for each of the water content estimation methods over the water content that was calculated by the weighing method.

a) Mean absorption

b) Water index

c) Absorption difference
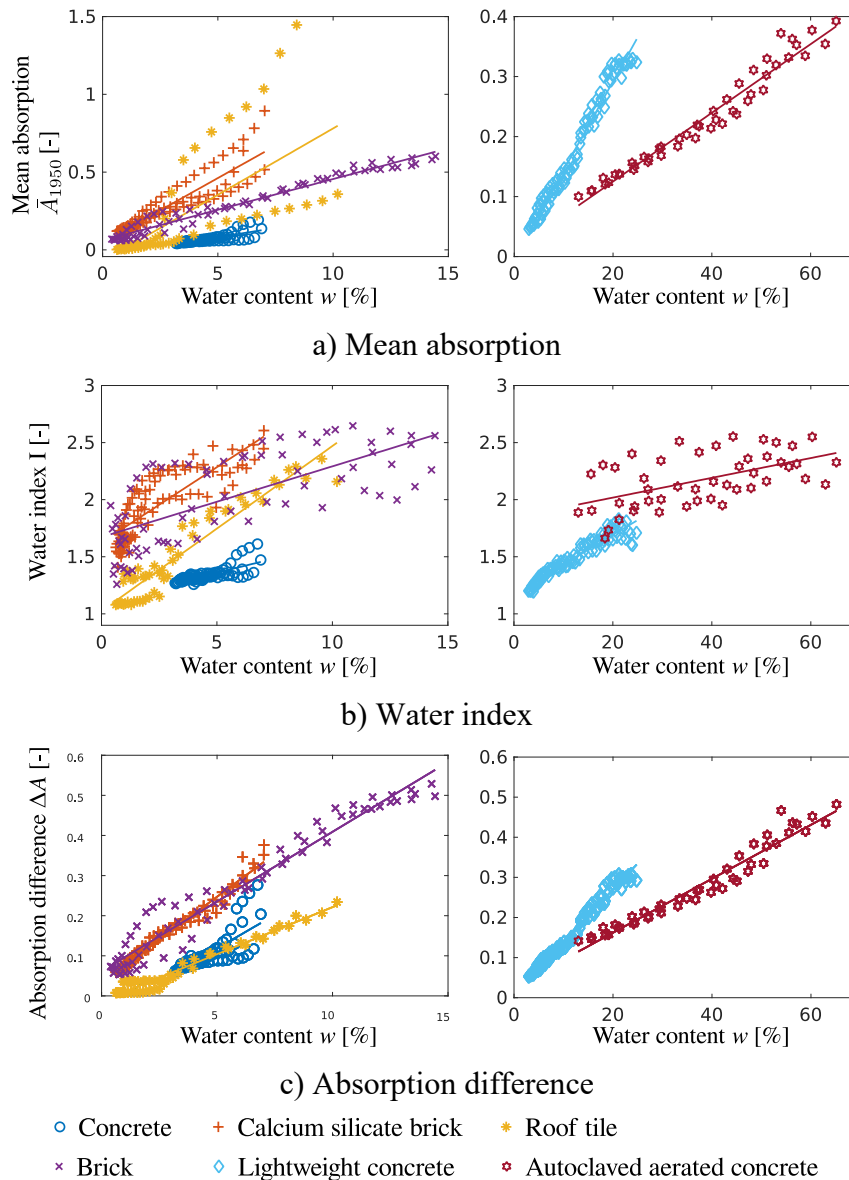
Figure 6: Linear regression of the water content estimates for investigated samples

The quality of the key parameters of each water content estimation varies for different materials. To measure this, the coefficient of determination R^2 was calculated for each water content estimation approach depending on the material and is summarized in Table 2. Apparent from Table 2 a value of the coefficient of determination $R^2 > 0.9$ can be achieved for several materials.

Table 2: Coefficient of determination R^2 for each water content estimation method depending on the material (values greater than 0.9 are marked in italic and bold)

material	Concrete	Autoclaved aerated concrete	Light-weight concrete	Brick	Roof tile	Calcium silicate brick
Mean absorption	0.585	***0.960***	***0.976***	***0.967***	0.444	0.835
Water Index	0.537	0.301	***0.909***	0.500	***0.905***	0.683
Absorption difference	0.585	***0.949***	***0.975***	***0.954***	***0.957***	***0.975***

The only exception is concrete, where none of the water estimation methods achieves a high coefficient of determination. The absorption difference is suitable for most of the materials to estimate the amount of water. It is followed by the mean absorption and the water index is most applicable for lightweight concrete and roof tile.

4.   Discussion and conclusion

A separation of the CDW materials by spectral information in the wavelength range between 401 nm to 2500 nm is best accomplished by the LDA method.

The estimation of the water content using spectral data in the NIR range is possible. For all three investigated approaches, a dependency on the material is observed. Nevertheless, further measurements need to be done to put the investigations on a solid database. Especially, the behavior of the concrete material emphasizes this, because the differences may be caused by its heterogeneous structure.

The results also show that the absorption difference and the mean absorption are best suited, but for the water index variations appear. Additionally, the absorption difference needs only two measuring points for the water content estimation, which makes it very effective.

Acknowledgements

References

[1] BAU, Kreislaufwirtschaft (2020) *Mineralische Bauabfälle – Monitoring 2020* [online]. https://kreislaufwirtschaft-bau.de/Download/Bericht-13.pdf [last downloaded 30.03.2023]

[2] DIN 4226-101: 2017-08 (2017) *Rezyklierte Gesteinskörnungen für Beton nach DIN EN 12620 – Teil 101: Typen und geregelte gefährliche Substanzen*. Beuth, Berlin. August 2017.

[3] DIN EN 933-11:2009 (2011) *Prüfverfahren für geometrische Eigenschaften von Gesteinskörnungen – Teil 11: Einteilung der Bestandteile in grober recyclierter Gesteinskörnung*. Beuth, Berlin. Mai 2011.

[4] DIN EN ISO 12570:2018-07 (2018) *Wärme- und feuchtetechnisches Verhalten von Baustoffen und Bauprodukten – Bestimmung des Feuchtegehaltes durch Trocknen bei erhöhter Temperatur*. Beuth,

Berlin. Juli 2018.

[5] Sidharth, M. et al., (2017) *Multivariate Statistical Data Analysis- Principal Component Analysis (PCA)*, International Journal of Livestock Research, Vol 7 (5), S. 60-78. doi: 10.5455/ijlr.20170415115235

[6] Tharwat, A.; Gaber, T.; Ibrahim, A.; Hassanien, A. E. (2017) *Linear discriminant analysis: A detailed tutorial. AI Communications*, Vol. 30, No. 2, S. 169–190. doi:10.3233/AIC-170729

[7] Kropp, J. (2005). *Bestimmung der Kernfeuchte wassergesättigter: Bauschuttrezyklate anhand des Trocknungsverhaltens*. Amtliche Materialprüfungsanstalt Bremen.

[8] Kupfer, K. (1997). *Materialfeuchtemessung. Grundlagen – Meßverfahren – Applikationen - Normen*. expert verlag. Renningen-Malmsheim. Kontakt und Studium. Band 513.

[9] Mauch, U. (2019) *Untersuchung der land-und forstwirtschaftlichen Trockenheit von 2018 in der Schweiz anhand Sentinel-2-Satellitenbildern* [Bachelorarbeit]. ZHAW Zürcher Hochschule für Angewandte Wissenschaften. 2019.

[10] Thiel, M. (2018) *Bildgebende NIR-Hyperspektral-Technologie zur in-situ Erfassung des Blattwassergehalts* [Dissertation]. Leibniz Universität Hannover. 2018.

[11] Brook, A.; Ben-Dor, E. (2011) *Reflectance spectroscopy as a tool to assess the quality of concrete in situ*. Journal of Civil Engineering and Construction Tehnology, August 2011, Vol. 2(8), S. 169-188.

[12] Fan, L., et al. (2019) *Assessing moisture content on the surface of mortar samples from hyperspectral imaging*. Proceedings of 9th International Conference on Structural Health Monitoring of Intelligent Infrastructure, St. Louis, Missouri USA, August 2019, S. 1150-1155.

[13] Gastaldi, D.; Canonico, F.; Boccaleri, E. (2009) *Ettringite and calcium sulfoaluminate cement: investigation of water content by near-infrared spectroscopy*. Journal of materials science, 2009, 44. Jg., S. 5788-5794.

[14] Gastaldi, D., et al. (2010) *Near-infrared spectroscopy investigation on the hydration degree of a cement paste*. Journal of materials science, 2010, 45. Jg., S. 3169-3174.

RECYCLEBIM: A FRAMEWORK FOR THE CIRCULARITY OF CONSTRUCTION MATERIALS THROUGH DIGITAL MODELLING

Manuel Parente[1],*, José Granja[1], Vasco Vieira[1], Artur Kuzminykh[1], Veracruz González[2], Antonio Fernández[2], Lucia Díaz-Vilariño[2], Donglin Cao[3], Neven Ukrainczyk[3], Luciano Sambataro[3], Eduardus Koenders[3], John Babafemi[4], Wibke de Villiers[4], Gideon van Zijl[4], Leslie Petrik[5], Erik Sandonis[6] and Miguel Azenha[1]

(1) University of Minho, ISISE, ARISE, Department of Civil Engineering, Portugal

(2) University of Vigo, Spain

(3) Technical University of Darmstadt, Germany

(4) Stellenbosch University, South Africa

(5) University of the Western Cape, South Africa

(6) Lezama Demoliciones, Spain

* map@civil.uminho.pt

Abstract

Despite the extensive research conducted in BIM applications in construction and the built environment, fields such as demolition and circularity of construction and demolition waste (CDW) materials can still be subject to significant breakthroughs stemming from BIM-inspired frameworks. The circular economy concept in the context of CDW aims to minimize waste, reuse materials, and reduce pollution and emissions. However, the increasing amount of CDW reflects that circularity has not been well implemented in the construction field so far.

The RecycleBIM project aims to propose an integrated framework for the circularity of raw materials in construction leveraging on the wealth of information provided by BIM, while enabling key technologies such as scan-to-BIM, open data formats (e.g., IFC), distributed marketplaces, and 3D printing. This framework not only supports scan-to-BIM of to-be-demolished buildings and subsequent quantitative prediction of CDW reuse/recycling potential from a circularity viewpoint, but it also explores the potential of integrating the latter both within a global circularity marketplace and in CDW-incorporating 3D printing. Thus, this paper highlights the global perspective of RecycleBIM as well as the most recent developments in its course, particularly in the definition of data templates and inspection methods to set the stage for further progress within the project.

1.   Introduction

The Construction Industry is enduring important digital evolutions, particularly through the introduction of BIM [1]. At the same time, new normalization is pushing structural engineers towards a culture of proper information/data management in view of the recently issued

ISO19650 series [2,3], which keeps expanding, as well as the definitions of interoperability based on the IFC format and open BIM principles, promoted by buildingSMART [4]. All the above are promoting increased BIM adoption worldwide [5], with increased awareness of the need to adequately set the information to be exchanged according to protocols that set 'Exchange Information Requirements' (EIR) [3], the definition of 'Model View Definitions' for better IFC exchange, and even the progress towards digital permits is on the horizon, with initiatives such as eubim.eu and the European Network for Digital Building Permits [Noa20]. Whereas there have been some interesting BIM tools already oriented to demolition, they tend to fall short in regards to the more holistic approaches such as circularity or life cycle assessment (LCA) and life cycle costing (LCC) [6,7]. Concurrently, issues such as the cost of creating BIM models for to-be-demolished structures, as well as opportunities brought about by integration of CDW with novel trends such as additive manufacturing and distributed global markets have yet to be fully explored [8, 9].

The RecycleBIM project aims to propose an integrated framework for the circularity of raw materials in construction leveraging on the wealth of information provided by BIM, while enabling key technologies such as scan-to-BIM, open data formats (e.g., IFC), distributed marketplaces, and 3D printing. In fact, this framework not only supports scan-to-BIM of to-be-demolished buildings and subsequent quantitative prediction of CDW reuse/recycling potential from a circularity viewpoint, but it also explores the potential of integrating the latter both within a global circularity marketplace and in CDW-incorporating 3D printing. Thus, this paper highlights the global perspective of RecycleBIM as well as the most recent developments in its course, particularly in the definition of data templates and inspection methods to set the stage for further progress within the project.

While the project contemplates both new constructions from a design to demolition viewpoint and to-be-demolished buildings at their end-of-life, this paper focused on the to-be-demolished track, as it has been the subject of greater progress at this stage in the project. In this context, one could argue that, in the project, the combination of aforementioned technologies come together into an information flow structure consistent with the depiction of Figure 1. Indeed, it is easy to infer that BIM data comprises the central source of information for most of the project applications, including an LCA/LCC IFC-based tool, the exploration of the viability of incorporating CDW into 3D printing constructions, and the creation of distributed marketplaces aimed at making CDW materials locally available. In turn, the data included into the BIM models originates from surveying to-be-demolished structures by resorting to technologies such as handheld LiDAR, as well as simple and cost-effective surveying techniques.
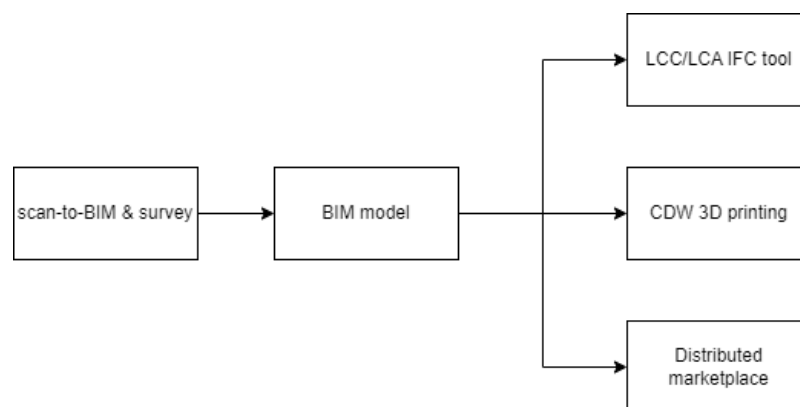

Figure 1: Flow of information in RecycleBIM (to-be-demolished track)

Hence, the structure of this paper resembles the information flow illustrated in Figure 1, beginning by a description of the scan-to-BIM process in Section 2, followed by the resulting specifications and requirements for the resulting BIM data in Section 3. Sections 4 and 5 respectively describe the progress of the development of the IFC-based optimization and LCA/LCC analysis tool, and the exploration of the viability of incorporating CDW into 3D printing. Finally, since the creation of distributed marketplaces is planned to be a future development in the project, its connection to the previous technologies is discussed together with the expected impact of the project in the Conclusions Section.

2.　　To-be-demolished scan-to-BIM

As depicted in Figure 1, the framework features a to-be-demolished BIM model as one of the central elements in which data is compiled and made readily available to support not only the demolition process, but also some of the downstream developments of the project, such as the LCA/LCC tool or the circularity material marketplace. Yet, a BIM model capable of encompassing all the necessary information for those purposes may not always be available beforehand. Hence, the focus of this Section pertains to the development of a methodology to assist the semi-automated creation of BIM models based on already available and affordable technology such as LiDAR-based handheld systems. Considering that building a BIM model can be an expensive enterprise, two fundamental self-imposed goals for this methodology are related with implementation expediency and effortlessness, and cost-effectiveness, aiming to mitigate the BIM model creation burden.

In this context, the full scope of the development of this methodology encompasses the implementation of strategies not only for the efficient planning of scanning activities using hand-held LiDAR systems, with the aim of minimizing the time needed for scanning while maximizing data completeness, but also for cost-effective surveys, which may include mild-destructive techniques to gather clear information on thicknesses and composition of building elements. These survey strategies and activities will provide the basis for the development of methods for the semantic segmentation and inventory of building elements (i.e. external walls, ceilings, slabs, interior walls and doors, etc.), through knowledge-based and machine learning approaches which are capable of singling out, identifying, and carrying out the parametrization of building elements and materials from point LiDAR-originated cloud models. Ultimately, the resulting data will directly support and facilitate the creation of IFC-based to-be-demolished BIM models.

At the current stage of the project, scan-to-BIM development efforts are twofold. On one hand, geospatial data preprocessing tools are being developed to improve data quality for further processing. In this context, a set of computation methods for *subsampling*, *denoising* and *removing outdoor points* are being implemented. On the other hand, automated methods are being designed to hierarchically segment the point cloud at three levels: *floorplan segmentation*, *room/space segmentation* and *building element segmentation*. This strategy is useful from different perspectives. The hierarchical segmentation of building point clouds into floorplans and rooms makes the building element segmentation simpler. In addition, the procedure inherently establishes topological relationships which are essential for BIM reconstruction and useful for material and element location. Figure 2 shows a workflow of a room/space segmentation procedure. The method starts by implementing a preprocessing tool consisting on removing outdoor points. Next, mathematical morphology is directly implemented to segment

the floorplan into rooms and the trajectory followed by the system during the acquisition is used to detect doors. As a result, the point cloud corresponding to a building floorplan is segmented in a set of rooms connected by doors.
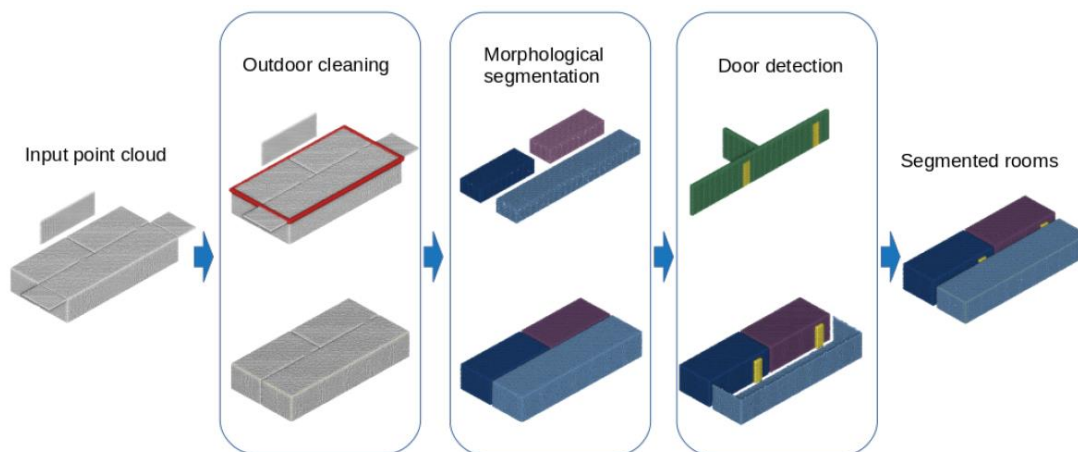
Figure 2. Workflow of a method for segmenting rooms within floorplans.

3.   BIM data specifications

Beyond supporting any demolition efforts themselves, the produced to-be-demolished BIM models need to compile enough information to support all the analyses and integration efforts carried out by the downstream applications that depend on the data provided by the models. This includes the LCA/LCC analyses and the distributed construction and demolition waste (CDW) marketplace, as well as any potential CDW-incorporating additive manufacturing applications to some extent. Besides these requirements, the BIM data must also align with the requirements of the most recent standards pertinent to the subject at hand, namely ISO-19650:2018 and EN 17412-1:2020. This effort not only sets up a normalized, machine-readable structure to the data, but it also facilitates to owners the opportunity to set their own requirements for information (i.e., exchange information requirements, EIR). Bearing once again in mind that the need for creation of a BIM model for a 'to-be-demolished' construction might be perceived as an expensive activity, special attention is given towards the minimization of the effort required to produce these models.

The definition of data specifications ranges from the creation of a specific set of information management rules according to the most recent standards of ISO and CEN and following a "lean information" approach (i.e., enough information, but no more than enough), to translating those rules into ISO19650-compliant EIR and BIM execution plan (BEP) templates for owners and appointed parties, respectively. Concurrently, to ensure interoperability between the information in these BIM models and the other developed tools and applications in the project, all information management rules should foresee the adoption of openIFC formats.

To achieve these goals, the first steps have encompassed the development of a database of Product Data Templates (PDT, as put forward by regulations such as EN23386 and EN23387) in the context of circularity of construction materials. In these PDT, two approaches have been considered for the recycling of an object from a circular economy in buildings perspective: either each object is recycled as a complete system (e.g., a whole window), or it is broken down into the materials that comprise (e.g., the window would be broken down into glass and

wood/aluminium, depending on the material that comprises the frame). Naturally, the former approach has clear advantageous in comparison with the latter, as the system can be reused as is in, as opposed to having to go through the disassembly process. In both cases, however, the definition of each object's parameters is paramount, so as to allow for this type of analysis to be carried out and subsequently translated into a machine-interpretable way. As such, the proposed structure for a circularity PDT embraces the parameters described in Table 1 and exemplified in Figure 3.

Table 1: Circularity PDT parameters

On the product level	On the material level
• The quantification of construction and demolition waste (CDW) materials as calculated from the BIM model (further described in Section 4); • The statement of whether the product can be reused as-is, i.e., without the need to decompose it into its material components; • The analysis of deconstruction possibilities of the product (e.g., fully dismountable mechanical joints, or element is attached/welded/walled up, requiring machinery or extra human effort to achieve disassembly) • A representative image of the product; and • An array of quantity of materials present in the product that can be sorted for recycling.	• The European waste code of the material(s) comprising the product; • The analysis of whether these materials can be collected and sorted for recycling or reuse; • The analysis of deconstruction possibilities; and • Material characteristics (e.g., density).
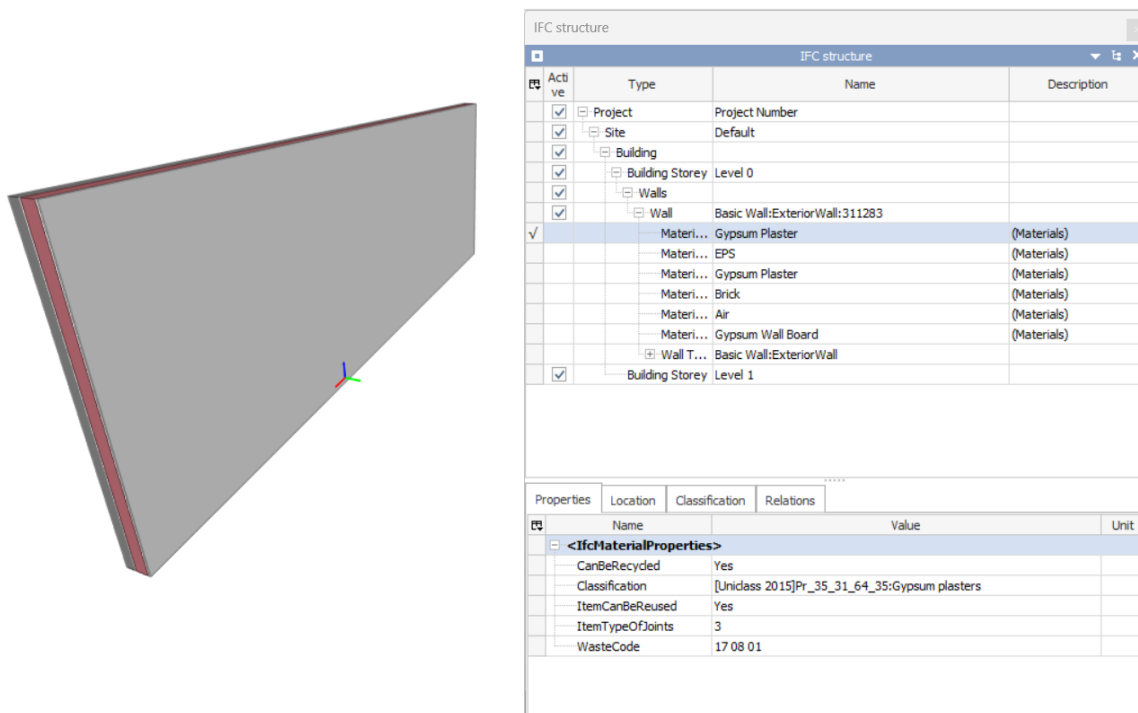
Figure 3: Example wall product model in IFC file format with the corresponding PDT parameter structure

4. IFC based LCA/LCC

The tool for optimisation and scenario studying leverages on an IFC BIM model file as input to deploy multicriteria analyses (e.g., optimisation algorithms and artificial intelligence), enabling decision support regarding design choices of materials and solutions considering LCA/LCC, and with specific focus on circularity impacts. In such a context, the tool is aimed at allowing informed decisions to be carried out, supported by the quantification of subsequent impacts. Specifically, in the to-be-demolished context, the IFC-based tool provides insight on the quantities of materials that feature the potential for circularity and provide advice to the stakeholders responsible for demolition regarding the best choices of techniques and sequences of demolition, so as to maximise re-use and recycling.

The development of the tool follows the establishment of an access strategy between itself and the various free and commercially available environmental databases, so as to gather the necessary data for LCA/LCC and circularity analyses. In its core, it comprises a CDW prediction model based on de-construction and demolition techniques, together with an advanced LCA/LCC objective function-based optimization tool for real-time feedback visualisation of the environmental impact. In the latter, the optimization process encompasses geometries, materials properties, heating systems and de-construction techniques in terms of performance versus environmental impact.

Currently, a web-based platform has been developed to predict CDW (Figure 4). While it is naturally expected that most of the CDW will be comprised of demolition debris, the platform takes into account that reusing or recycling entire construction elements may be advantageous in terms of circularity and LCA/LCC. Thus, the aim of this predictive model is to make precise predictions based on deconstruction and demolition methods. The building demolition waste predictor consists of two modules:

- Python-based IFC file analyzer: Classifies the reuse/recycling potential of building components and materials based on their properties, and storage of the data in MySQL.

- Web-based prediction model: Takes into account the waste production associated with demolition techniques. It allows for users to make informed decisions on the disposal procedure per material or component, based on the potential outcomes of each option. The forecasted waste flows include reuse as components, reuse as materials, pre-sorting and recycling as clean waste, pre-sorting of hazardous substances, and mixed waste after demolition.

Figure 4: The user interface for defining the disassembly

V International Conference Progress of Recycling in the Built Environment

10-12 October 2023 – Weimar, Germany

5. 3D printing and new opportunities for circularity

With regard to 3D printing for optimized use of recycled demolition waste, the focus is on bringing clarity and mainstream application of materials collected from demolition. This includes the partial replacement of aggregates in 3D printing for concrete/mortar, as well as the use of low-carbon cement as binder (e.g., limestone calcined clay cement (LC^3) and waste ashes), while preserving required pumpability, extrudability and buildability. The use of waste construction material indeed aligns with the concepts of urban mining of metals, though adapted to a different reality and waste materials.

In the long term, the achievement of the set goals features the inventory and characterization of CDW for use as aggregate and binder in high technology 3D construction printing. This task precedes the actual development of CDW-incorporated 3D printed concrete technology, mix design guidelines and quality assurance tests, including the mechanical and durability characterization of resulting 3D printed elements for demonstration and validation.

Throughout the duration of the project so far, CDW has been sourced from several localities in South Africa and characterised in terms of elemental composition and mineralogy (Figure 5). The results in Figure 5 illustrate that CDW is not a homogeneous material, being comprised of a variety of mineral phases depending on the source, although quartz is the predominant mineral phase and SiO2 and CaO the predominant elemental components. The presence of these elements indicate that the CDW may act as a supplementary binder.
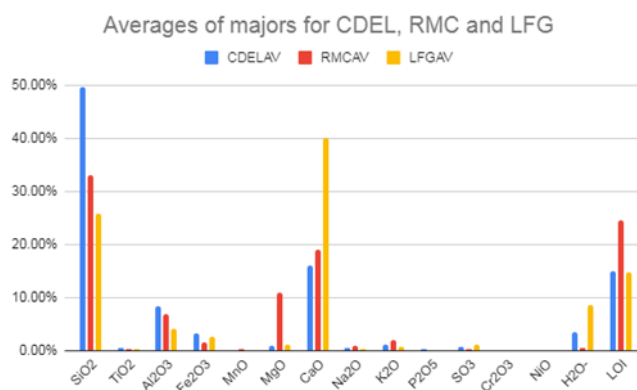
(a)
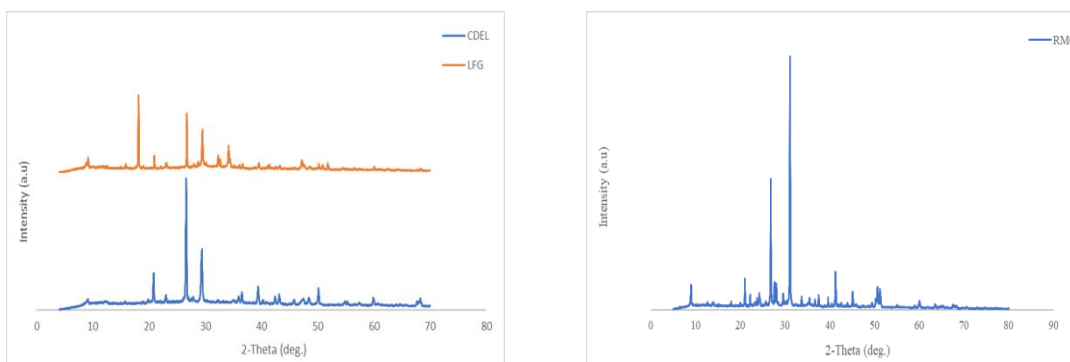
(b)

Figure 5: (a) Elemental composition of CDW from three sources (b) Mineralogy of CDW

The total non-clinker binder content, including fly ash, slag, metakaolin and LC^3, and the aggregate volume fractions were increased in 3D printed concrete categories (i) containing supplementary cement materials (3DPSCM), (ii) limestone calcined clay (3DPLC^3) and (iii) geopolymer concrete (3DPGPC). In conventional concrete (CC), up to 80% of the volume comprises aggregate. Self-compacting concrete (SCC) requires more paste for smearing, hence contains lower aggregate volume of up to about 70%. Printed concrete originally contained a low aggregate volume, recently increased up to 50%, and in exceptional cases approach 60%. Larger aggregate content increases dimensional stability, and the potential use of CDW to replace natural aggregate. Figure 6 shows a printed wall part containing CDW replacing 64% of the natural sand by mass.
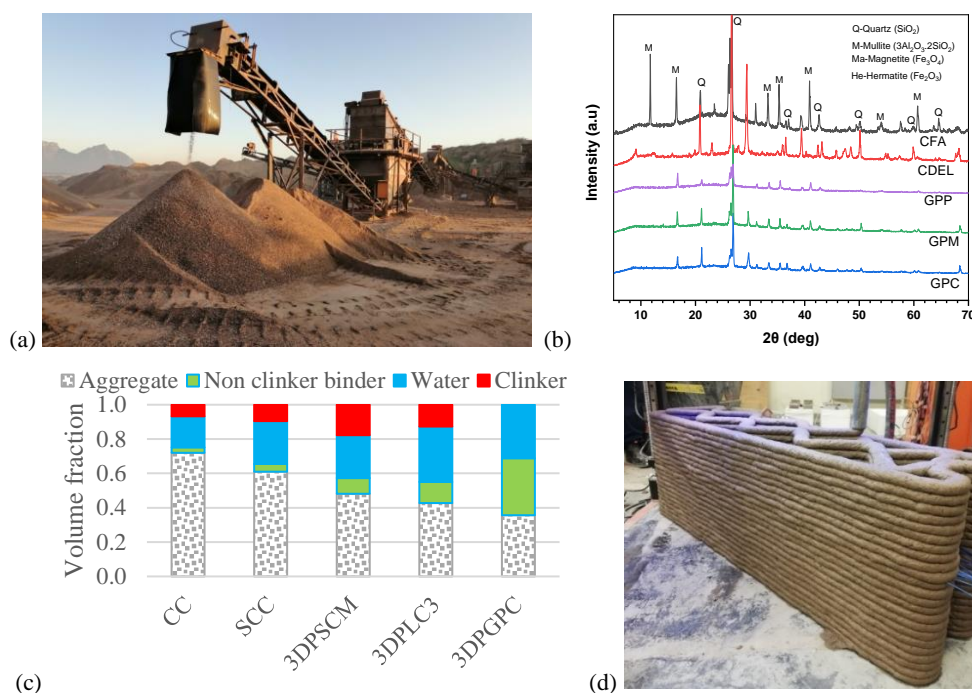
Figure 6: (a) Local CDW works and (b) XRD results of CDW from local supplier CDEL, and those of geopolymer paste (GPC), mortar (GPM) and concrete (GPC). (c) Volume fractions in conventional (CC), self-compacting (SCC) and 3 categories of 3D printed concrete. (d) 3DCP load-bearing wall element with CDW replacing 64% of natural aggregate [10].

Establishing realistic CDW data is an essential step in ensuring the technical, economic and logistical viability of using CDW in 3DPC. A dualism exists in the South African waste sector, where a local recovery, reuse and recycling sector thrives, owing to extensive and active informal waste management practices. However, this creates an environment rife for systemic underreporting of CDW generation rates, necessitating the estimation of CDW amounts through alternative methods. Of the methods considered, the lifetime material analysis and per capita multiplier methods are the most appropriate for the context and available seed data and result in a concrete and masonry CDW estimate of 24.3Mt and 12.2 Mt per annum in South Africa, respectively. Projections of material usage in 3DPC are difficult to quantify. However, in order to contextualise the estimated availability of CDW material for use in concrete in general, the demand for coarse and fine aggregate and supplementary cementitious material in South Africa is quantified as 77.9Mt. However, this overall annual demand for coarse and fine aggregates and SCM in South Africa far exceeds the estimated CDW material (12.2 – 24.3Mt) available as alternative material source for concrete.

6.   Conclusions

This paper showcases the global perspective of the RecycleBIM project focused on its to-be-demolished track and specifics, as well as the most recent developments in its course. The project combines different fields of application into a framework tailored for material circularity especially in relation to construction and demolition waste materials. So far, the project team has explored fields such as LiDAR-based scan-to-BIM, the structuring and management of to-be-demolished BIM data and its requirements, optimization and LCA/LCC analyses, and 3D printing.

One of the major future aspects of the project in which several of the aforementioned developments will culminate (and from which a significant societal impact can be achieved) is related with the creation of a distributed CDW marketplace. Indeed, even though the use of demolition residues is not necessarily highly competitive at the current stage, it is anticipated that the rules for incorporation of demolition waste in EU/worldwide will bring a significant value to this marketplace, as soon as significant minimum rates of incorporation of residues in new constructions become mandatory. As conditions are created to pursue this goal throughout the development of the project, the initial steps concern the important matter of definition of the relevant information and parameters to include in a freely accessible web-based database of materials. The ensuing marketplace itself is aimed at local commercialisation of materials recycled from CDW, including their requirements, environmental and economic data. Aspects such as the possibility to store samples stemming from the surveying processes of to-be-demolished buildings (see Section 2), upon which further mechanical and physical characterization tests can be carried out by the seller (i.e., demolition company) if prompted by a potential buyer, are also envisioned to be enabled by the marketplace web-based application.

Besides the obvious impacts on owners and designers, who will attain the capacity to prescribe and respond to sustainability and circularity requirements (via EIR) clearly and in detail through OpenBIM, the project's outputs will also positively impact contractors, demolition companies, municipalities and 3D printing construction companies. Indeed, as present-day constructions approach their end-of-life, their characteristics as banks of CDW materials becomes emphasized, impacting the activities of actors such as municipalities and contractors who have a better knowledge of and access to locally available recycled raw materials, brokered in a distributed marketplace. Conversely, demolition and waste sorting companies garner direct advantages not only from better prescribed demolitions (both in terms of methods and materials to harvest), but also from a better placement as sellers in the marketplace of recycled products, increasing their productivity and profitability. Lastly, by exploring and demonstrating the feasibility of incorporating CDW into 3D printed constructions, the project acts as an enabler of 3D printing construction companies, further facilitating their establishment as thriving businesses worldwide and contributing for a better optimization of material usage in general for the future.

Acknowledgements

References

[1] Sacks, R., Eastman, C., Lee, G., Teicholz, P. (2018) BIM handbook: A guide to building information modeling for owners, managers, designers, engineers, and contractors. Hoboken, N.J: Wiley. 3rd Edition. ISBN: 978-1-119-28753-7

[2] ISO 19650-1:2018 Organization and digitization of information about buildings and civil engineering works, including building information modelling (BIM) — Information management using building information modelling. Part 1: Concepts and principles

[3] ISO 19650-1:2018 Organization and digitization of information about buildings and civil engineering works, including building information modelling (BIM) — Information management using building information modelling. Part 2: Delivery phase of the assets

[4] ISO 16739-1:2018 Industry Foundation Classes (IFC) for data sharing in the construction and facility management industries — Part 1: Data schema

[5] Faisal Shehzad, H. M., Binti Ibrahim, R., Yusof, A. F., Mohamed khaidzir, K. A., Shawkat, S., & Ahmad, S. (2020). Recent developments of BIM adoption based on categorization, identification and factors: A systematic literature review. International Journal of Construction Management, doi:10.1080/15623599.2020.1837719

[6] Obrecht, T.; Röck, M.; Hoxha, E.; Passer, A. BIM and LCA Integration: A Systematic Literature Review. Sustainability 2020, 12, 5534. https://doi.org/10.3390/su12145534

[7] Xue, K.; Hossain, M..U.; Liu, M.; Ma, M.; Zhang, Y.; Hu, M.; Chen, X.; Cao, G. BIM Integrated LCA for Promoting Circular Economy towards Sustainable Construction: An Analytical Review. Sustainability 2021, 13, 1310. https://doi.org/10.3390/su13031310

[8] Paul SC, Van Zijl GPAG, Tan MJ, Gibson I 2018. A review of 3D concrete printing systems printing concrete – Current status and future research prospects. Rapid Prototyping Journal DOI: 10.1108/RPJ-09-2016-0154, 24/4 (2018) 784-798

[9] Caldera S, Ryley T, Zatyko N. Enablers and Barriers for Creating a Marketplace for Construction and Demolition Waste: A Systematic Literature Review. Sustainability. 2020; 12(23):9931. https://doi.org/10.3390/su12239931

[10] Christen HE, van Zijl GPAG, de Villiers WI, 2022. The incorporation of recycled brick aggregate in 3D printed concrete. Journal of Cleaner Materials 4 (June 2022) 100090 https://doi.org/10.1016/j.clema.2022.100090

PURE BRICK SAND FROM CONSTRUCTION AND DEMOLITION WASTE (CDW) THROUGH MAGNETIC SORTING

Annett Lipowsky, Jenny Goetz, Anette Müller

IAB – Weimar Institute of Applied Construction Research

Abstract

In the processing of CDW, the sorting of the delivered mixtures is one of the decisive process steps in order to produce pure recyclates, which can be used, for example, as a cement substitute or as a raw material component for the brick production. A previously unused method for the separation of fine particles as sand utilises rare-earth magnets. This method is based on differences in magnetic susceptibility, which have been confirmed by measurements on bricks and concretes. Sorting tests carried out using a roll magnetic separator with a field strength of 1.4 Tesla at a belt thickness of 0,7 mm confirmed the separability of brick-concrete-mixtures and provided insights into the most important influencing variables. In addition to manual sorting the quantification of the contents of concrete or brick in the magnetic and non-magnetic fractions was determined by calculation using the loss on ignition, laser-induced breakdown spectroscopy (LIBS) and artificial intelligence-based optical quality assurance. Thus, in addition to the proof of separability, a first step to faster ways for quality control has been accomplished.

Introduction

In the processing of construction waste, the sorting of the delivered mixtures is one of the decisive process steps in the production of new construction materials. On the one hand, well-known methods such as air classification or wet sorting processes are used. These processes are essentially based on density differences. On the other hand, manual sorting is still used, which in some cases has already been replaced by sensor-based processes.

With the techniques mentioned above, mineral particles with sizes in the centimetre range can be sorted. There are far fewer methods available for sorting sands. Jigs, aquamators and spiral separators are possible wet processes that are suitable for grain sizes in the sand range. They are rarely used in the processing of fine-grained recyclates.

A possibility not yet used in the processing of construction waste is magnetic sorting at high field strengths on the basis of paramagnetic properties. First indications from the literature on the distinguishability of brick and concrete sands to due of magnetic properties were already available in 2004 [1], [2]. Using a Frantz Isodynamic Separator, brick particles were separated from cement mortar particles due to of their Fe_2O_3 content, which was < 1.25 wt.% in the mortar

and 3 to 4 wt.% in the bricks used. After that, this possibility was not or only very scarcely [3], [4] revisited.

In contrast to fine, unsorted masonry rubble, for which there are hardly any recycling possibilities so far, there are additional areas of use for the brick sands besides vegetation applications. For example, they can be used as a proportionate raw material substitute for the renewed production of bricks [5]. They can also be used as "additional cementitious material" and thus contribute to reducing the use of clinker in cement [6], [7], [8]. Additionally the concrete sand can be upgraded by separation of unwanted foreign particles and used as fine aggregate for mortar and concrete.

Material

Different brick and concrete samples were collected from diverse locations in Germany. The aim was to test a wide range of brick samples produced from different feedstock sources and at different firing temperatures. As concrete samples such with different concrete aggregates such as limestone were used.

In order to characterize their chemical and mineralogical composition samples of the feed materials were subjected to a number of analyses, (Table 1 and 2). There are differences typical for these building materials. For example, the SiO_2, Al_2O_3 and Fe_2O_3 contents of the bricks are significantly higher than those of the concretes, while the concretes have more CaO. These differences are also reflected in the mineralogical composition.

Table 1:   Loss on ignition and chemical composition of concrete and brick samples

Material	LOI 950°C	SiO_2	Al_2O_3	Fe_2O_3	CaO	MgO	MnO	TiO_2	K_2O	Na_2O	SO_3
	Mass-%										
Concrete 1	29.0	27.3	1.90	0.49	39.5	0.50	0.02	0.06	0.42	0.14	0.55
Concrete 2	6.56	64.2	5.92	3.74	13.7	1.50	0.07	0.62	1.75	0.94	0.67
Concrete 3	9.27	62.9	5.44	1.42	16.6	0.47	0.05	0.16	1.55	0.92	1.00
Clinker. red (RC)	0.33	70.7	18.15	4.20	0.57	1.05	0.04	1.00	2.61	0.69	0.04
Clinker. black (BC)	0.12	71.2	15.18	7.73	0.36	0.76	1.00	1.19	1.83	0.16	0.02
Clinker. yellow (YC)	0.09	69.7	22.12	3.15	0.38	0.37	0.02	2.06	1.76	0.22	0.00
Insulating brick (IB)	1.4	52.5	17.8	5.93	13.5	3.85	0.11	0.91	2.88	0.47	0.17
Brick. old (OB)	0.31	73.4	13.6	6.11	0.87	0.84	0.07	1.04	2.87	0.69	0.02
Brick from demolation (WB)	1.64	70.4	13.56	4.15	4.63	1.07	0.06	0.82	2.55	0.46	0.41

Table 2: Mineralogical composition of concrete and brick samples

Material (%)	Quartz	Plagioclase	Orthoclase	Diopside	Hypersthene	Hematite	Calcite
				Mass-%			
Concrete 1	17.67	7.47	2.47	0.00	1.26	0.00	0.00
Concrete 2	52.88	0.00	9.90	0.00	3.58	3.58	22.89
Concrete 3	48.48	10.86	9.15	2.53	0.00	1.43	21.10
Clinker. red (RC)	57.19	4.26	15.17	0.00	2.56	4.10	0.77
Clinker. black (BC)	62.15	1.95	10.86	0.00	1.89	7.76	0.27
Clinker. yellow (YC)	61.64	0.98	10.39	0.00	0.93	3.14	0.46
Insulating brick (IB)	13.20	41.52	17.02	12.28	3.91	5.94	3.20
Brick. old (OB)	57.43	5.24	16.94	0.00	2.07	6.09	1.35
Brick from demolation (WB)	53.10	13.23	15.10	0.00	2.68	4.16	3.74

The measurements of the magnetic susceptibility of the samples showed values below $1500*10^{-9} \text{m}^3\text{kg}^{-1}$ for the concrete samples. Exceptions are to be found in the range of coloured concretes or concretes with soiled surfaces. The susceptibilities of the bricks range from 1500 to $11000*10^{-9} \text{m}^3\text{kg}^{-1}$.

Magnetic separation tests

Magnetic separation tests were conducted using a laboratory scale dry rare-earth separator (Figure 1). Main parts of the separator are the rare-earth head roll and the Kevlar belt with 0.15 mm thickness. The field intensity of the head roll was approximately 2.1 T. The intensity is reduced to 1.4 T due to the influence of the belt. The experiments were carried out at narrow size fractions of 0.063/0.5 mm, 0.5/1.0 mm as well as 1.0/2.8 mm. The separator includes an adjustable splitter that separates the non-magnetic from the magnetic material (Figure 2). Other parameters that may have an influence on the sorting result are the speed of rotation of the head roll, the number of passes and the humidity of the materials.

Figure 1: Dry rare-earth separator used in the tests
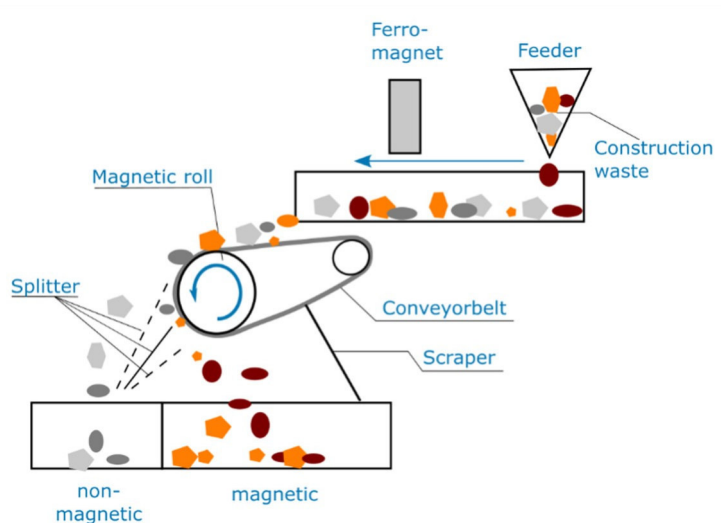
Figure 2: Schematic diagram of dry rare-earth separator

In the experiments, mixtures of 50 wt.% brick and 50 wt.% concrete were used. The particle sizes (Figure 3) and the material combinations were tested as parameters. The products resulting from magnetic separation were immediately weighed after each experiment. The separation success was assessed visually at first (Figure 4). Visual assessment of the rejected non-magnetic material and the material adhering to the magnet showed obvious differences. The magnetic fraction is predominantly red, while grey particles dominate in the fraction not adhering to the magnet.

A quantitative analysis based on counting red brick and gray concrete particles on the microscope proved to be extremely time-consuming and was carried out only for the fraction of 1.0-2.8 mm. Therefore, an initial quantitative evaluation was made by comparing the loss on ignition. Low losses on ignition are typical for bricks. Concrete has significantly higher ignition losses, which originate from the chemically bound water but also from the CO_2 absorbed as a result of carbonation.

The proportion of bricks in the magnetic output was calculated from mass of this product and the losses on ignition of the input materials and the products by a simple mixture calculation.

Figure 3: Different fraction of concrete-/brick-mixture before sorting
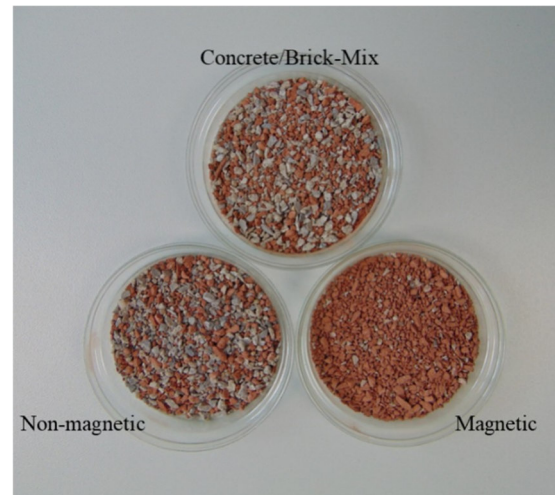
Figure 4: Concrete-brick-mixture before sorting (above) and the magnetic and non-magnetic product after separation (below)

Results

To make sure that there are no differences in the composition of single fractions of the individual materials, they were examined chemically again. Table 3 shows the differences in the iron oxide content of the respective fractions. The measured differences could be explained by differences in the sorting properties. The fractions are composed differently, fraction 0.063 – 0.5 mm contains more cement paste, the fraction 0.5 – 1.0 mm contains quartz sand and the coarsest fraction (1.0 – 2.8 mm) contains more aggregate.

Table 3: Total iron oxide content of the single fractions of tested bricks and concrete

Brick	RC	BC	YC	IB	OB	WB
			Fe_2O_3 [wt. %]			
0.063/0.5 mm	3.98	6.41	2.04	5.97	5.30	3.78
0.5/1.0 mm	4.36	7.33	2.40	6.12	5.22	4.04
1.0/2.8 mm	4.26	7.48	2.37	6.10	5.12	4.16

Concrete	C1	C2	C3			
		Fe_2O_3				
0.063/0.5 mm	0.91	2.54	1.37			
0.5/1.0 mm	0.64	1.89	1.16			
1.0/2.8 mm	0.65	2.50	1.53			

The proportion of brick in the magnetic yield varied significantly with the type of concrete as well as the size fraction, exemplary shown in Figure 5 for mixtures of an insulating and an old masonry brick combined with three different concretes.

The best sorting result is achieved for the concrete 1 in all tested three fractions and for both brick combinations. This is due to its relatively low Fe_2O_3 content in all three size fractions (Table 3). Then the results of the concrete 3 with a mean Fe_2O_3 content of 1.42 wt.% follows. Here the influence of the particle size is diffuse (Table 1). Concrete 2 shows the worst results because this concrete shows the highest Fe_2O_3 content of all tested concretes in all size fractions.
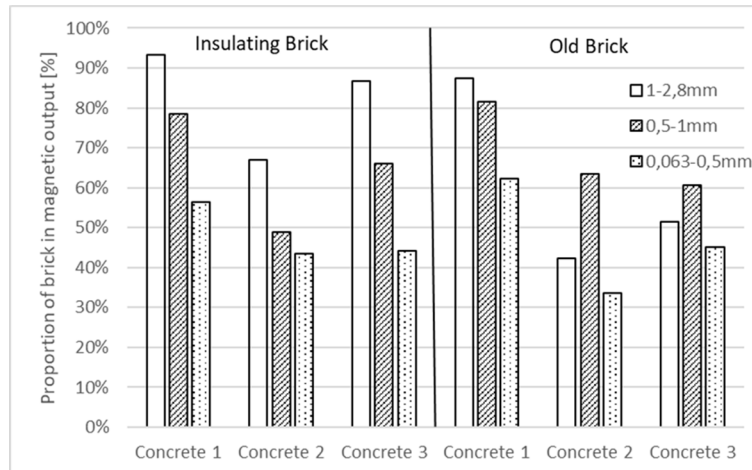
Figure 5: Proportion of brick in the magnetic fraction of two brick samples mixed with three different concretes of the size fractions 0.063-0.5 mm, 0.5-1 mm, 1-2.8 mm

A summary of all data from the magnetic separation tests is presented in Figure 6. Two parameters that influence the sorting results are taken into consideration:

- the particle size
- the ratio of the Fe_2O_3-contents of the combined bricks and concretes.

The particle size is an important parameter. In the fraction 0.063/0.5 mm a decrease of the brick content in the magnetic fraction compared with the input material occurs until a Fe_2O_3-ratio of about 4. One of the reasons of this effect may be the method of determination of the brick content on base of the loss of ignition.

In the fractions 0.5/1.0 mm and 1.0/2.8 mm there is no enrichment for a Fe_2O_3-ratio of 1, i.e. for the same Fe_2O_3 content in the brick and in the concrete. With increasing Fe_2O_3-ratio the enrichment of the brick particles in the magnetic fraction increases. I.e. larger ratios result in a higher brick content in the magnetic material. The results show a considerable scattering. One reason could be that the quality determination by means of the loss on ignition method is slightly prone to errors.
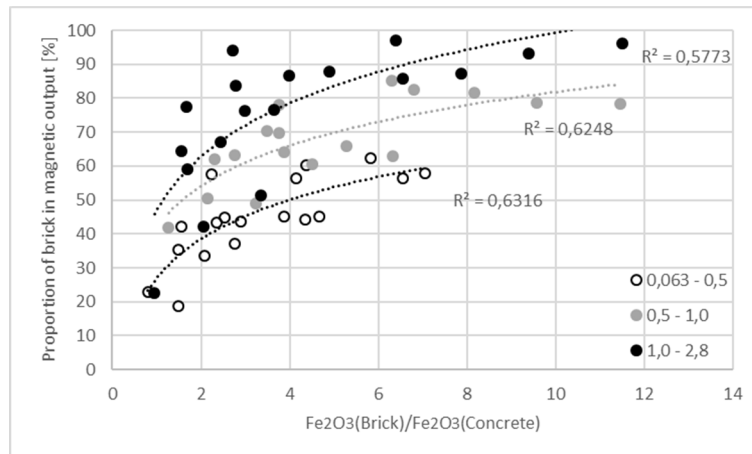
Figure 6: Brick material in the magnetic yield versus Fe_2O_3
content of brick and concrete in the starting mixture

In future investigations, the magnetic iron oxide should also be determined in addition to the total iron oxide content. Because the total iron oxide content in the respective material does not completely explain its magnetic properties or the presence of other magnetic minerals.

The machine parameters tested have a rather low influence on the sorting results. A higher portion of the magnetic product is always connected with a lower enrichment of the brick in this product. There has been found no evident differences in the yield and the quality of this yield whether the material was sorted at initial moisture (up to 6 wt.%) or oven-dried at 105°C.

Conclusions

In the paper results on the sorting of fine particles as sand using a rare-earth magnet separator are described. Mixtures of 50 wt.% concrete and 50 wt.% brick have been tested. The achieved magnetic enrichment of bricks is based on their significantly higher magnetic susceptibility compared to concrete, which in turn depends, among other influences, significantly on the Fe_2O_3 content. Enrichments of brick particles in the magnetic output up to 95 wt.% are possible. However, improvements in the evaluation methods are necessary in order to be able to deduce more precise statements on the influencing variables of the separability.

Acknowledgements

References

[1]   Weihong, X. 'Quality Improvement of Granular Secondary Raw Building Materials by Separation and Cleansing Techniques' in *Proefschrift. Technische Universiteit Delft* 2004.

[2]   Weihong, X., Hendriks, C.F., Fraaij, A. and Rem, P. 'Quality Improvement of Granular Wastes - The Effective Way to Recycle Secondary Raw Building Materials', *Journal of Wuhan University of Technology - Mater. Sci. Ed.* **19** (4) (2004) 87-90.

[3]   André, F.P., Miceli H., Moura, L.C., Neumann, R. and Tavares, L.M. 'Upgrading a manufactured fine aggregate for use in concrete using dry rare-earth magnetic separation', *Miner.Eng.* **143** (2019)

[4]   Carriço, A. Bogas, J.A., Hu, S., Real, S. and Costa Pereira, M.F. 'Novel separation process for obtaining recycled cement and high-quality recycled sand from waste hardened concrete', *J. Clean. Prod.*, **309** (2021) Article 127375.

[5]   Müller, A., Döring, I., Knorr, M., Lipowsky, A., Palzer, U., Leydolph, B., 'Developments in the recycling of clay bricks and brick masonry ', *Zi – Brick and Tile Industry International* **3** (Part 2) (2020) 20-26

[6]   Müller, A., Lipowsky, A. and Palzer, U. 'Brick powders as pozzolanic additives in cement production', *Zement Kalk Gips* **7-8** (2020) 38-45.

[7]   Müller, A.; Lipowsky, A. and Palzer, U. 'Mehle aus Ziegelbruch als Flugascheersatz bei der Betonherstellung', *BWI – BetonWerk International* **3** (2020) 44-50.

[8]   IZF VDZ Abschlussbericht: 'Verbesserung der Energieeffizienz und Reaktivität durch separate Mahlung von Ziegelbrechsand für den Einsatz in Portlandpuzzolanzementen' *Bericht zum IGF-Forschungsvorhaben Nr. 20920 N*, 23.12.2022.

NEW SOURCES FOR SECONDARY GYPSUM

K. Weimann (1), P. Farago (2) and F. Mayer (3)

(1) BAM Bundesanstalt für Materialforschung und -prüfung, Berlin, Germany

(2) MUEG Mitteldeutsche Umwelt- und Entsorgung GmbH, Braunsbedra, Germany

(3) Öko-Institut e.V., Darmstadt, Germany

Abstract

In order to protect natural gypsum deposits and to compensate for the decreasing amount of Flue Gas Desulfurization (FGD) gypsum it is necessary to develop and explore new sources of gypsum. For this purpose, the potentials of different gypsum wastes are investigated in the study "GipsRec 2.0", funded by the Federal Ministry of Education and Research (Germany).

On the one hand, the project worked on a new processing technology for gypsum fibreboards (GFB). While the recycling of gypsum plasterboards (GPB) has already been carried out on an industrial scale for several years, the recycling of gypsum fibreboards has proven to be challenging. Gypsum fibreboards from demolition sites and offcuts from GFB production were used for these investigations. The tests were conducted on a technical scale. Furthermore, various synthetic gypsums are being investigated with regard to their suitability for gypsum production. The analyses are carried out on production residues.

In this project, a promising process for gypsum fibreboard recycling could be developed, as well as other waste gypsums are investigated and evaluated in relation to their potential as secondary raw material. In addition, selected process routes are assessed for their environmental impact using a life cycle assessment (LCA) approach.

1. Introduction

Due to its excellent building material properties gypsum has been widely used in constructions during the last decades in many countries. In the European Union, there is a demand for around 57 million tons of gypsum per year. Approximately 17 million tons of gypsum are generated in incineration plants, primarily coal-fired plants through the process of flue gas desulfurization (FGD) [1]. Due to efforts in reducing CO_2-emissions in Europe, the operation of coal-fired power plants will be severely restricted in the coming years. Additionally, mining of natural gypsum affects the environment, which further worsens the situation. Therefore, it is crucial to close the emerging gap in gypsum production.

Until recent years, Germany, the largest producer and consumer of gypsum in the EU, covered more than 60% of its demand with FGD gypsum. In 2019, the share of FGD gypsum had already declined to 44% [2], a trend that is deemed to continue due to Germany's coal exit law and the related decommissioning of coal-fired power plants. Consequently, the pursuit for alternative sources of secondary gypsum is becoming increasingly important.
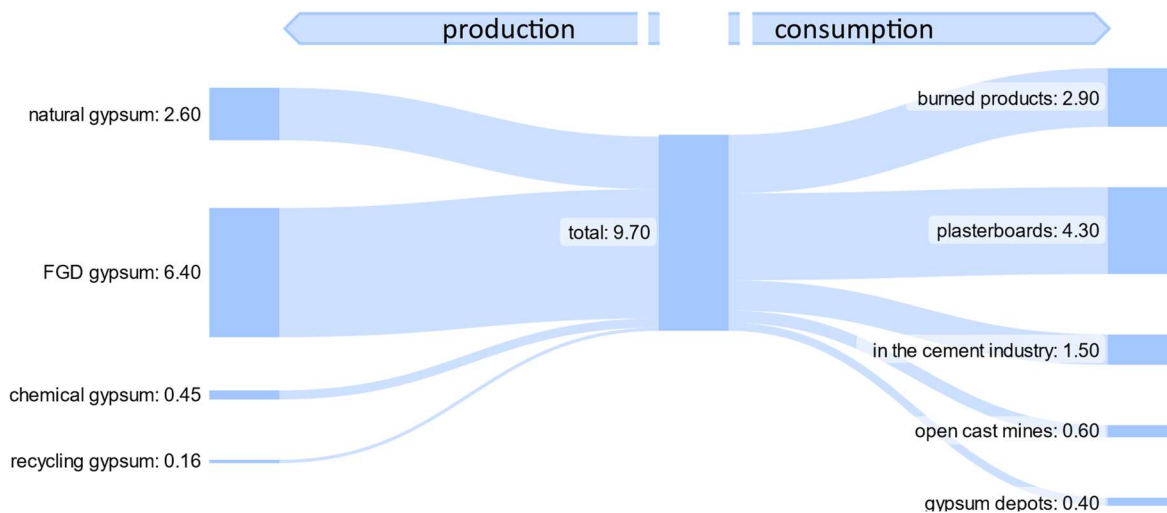
Figure 1:   Gypsum production and consumption in reference year 2018, in million tons per year [3]

Due to an extensive use of gypsum boards in construction activities over the past decades, it is expected that gypsum waste in construction and demolition waste (CDW) increases in the upcoming years. If the high-quality requirements for recycled gypsum – especially regarding the sorting accuracy – are met, waste gypsum from CDW can be fed into the gypsum production. Gypsum plasterboards (GPB) have been successfully recycled on an industrial scale for several years now [4]. However, in view of the quantities of gypsum that need to be substituted, it is essential to explore additional sources of secondary gypsum. On the one hand synthetic gypsum are particularly suitable for this purpose. On the other hand, waste gypsum boards apart from GPB may also contribute to substitution efforts.

2.   Recycling of gypsum fibre boards

2.1   Market Research

Regarding the production of gypsum boards in Germany, around 250 million tons of GPB and gypsum fibreboards are produced annually (Figure 2). In comparison to GPB, there has been a significantly lower production and installation of GFB. The share of GFB produced in square metres is on average only 13% of the gypsum board production. However, due to the boards' higher weight this translates to about 19% of the total tonnage produced. Both types of gypsum board are comparatively easy to deconstruct and recycle separately from other CDW.

Gypsum board production in Germany
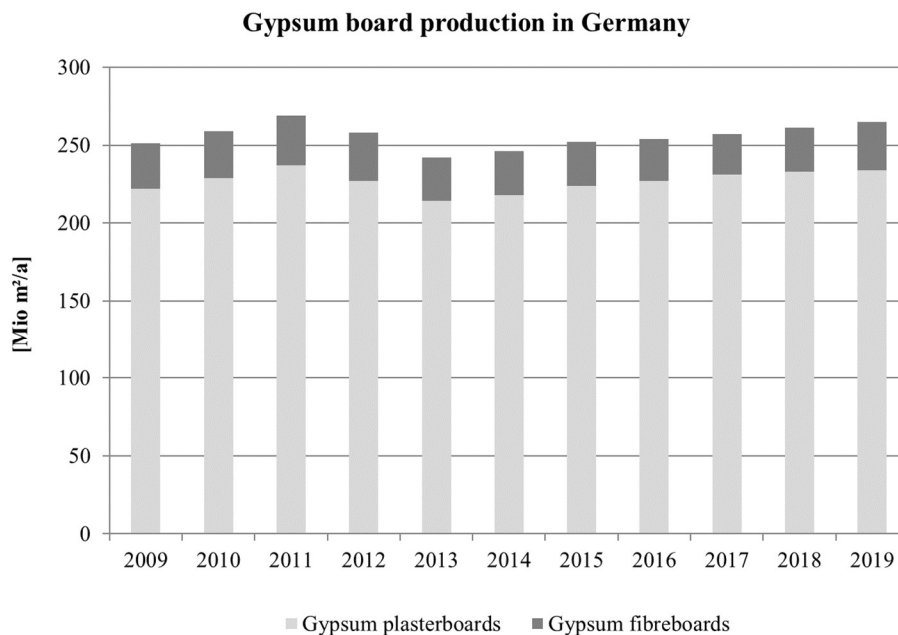
Figure 2:   Gypsum board production in Germany 2009-2019 in million m² per year [5]

As part of the project, a survey was conducted together with the German Demolition Association on the handling of gypsum boards during demolition in Germany. It was found that more than 90% of the companies surveyed engage in selective deconstruction of gypsum boards. However, only few companies transport the gypsum boards to a gypsum recycling plant. This is primarily due to long transport distances to recycling plants and comparatively inexpensive landfill costs. Another reason hindering the recycling, is the concern of potential contamination with asbestos fibres. Finally, there is still a need for clarification with regard to the distinction between GPB and GFB on the construction sites. A distinction is necessary so that the gypsum boards can be recycled in an optimized manner. In the case of GPB, the separation of gypsum and cardboard is comparatively easy to carry out due to the coarse cardboard fragments. For GFB however, the separation of paper from gypsum is challenging because of the fine paper fibres.

2.2   Processing of used gypsum fibre boards

Another goal of the project is to develop a processing route for the recycling of GFB. To evaluate the efficiency of processing routes for GFB recycling, it is essential to determine the composition of GFB. Therefore, two different grades of GFB from the demolition site were examinated. The analysis focused on the amount of gypsum in the gypsum-, fibre and additives-fraction and their chemical composition. The results indicated that the mixture of GFB is ~80% gypsum and ~20% fibre and additives.

The processing route contains two elementary steps, shredding and screening. Shredding was achieved by a hammer mill with different screen baskets of 4 mm and 8 mm each inserted. The aim of using the hammer mill was to achieve an optimum disintegration of the paper-gypsum compound of the manufacturer-specific GFB-mixture. This was done in preparation for the subsequent screening step, which aimed at separating the GFBs main components. Screening was achieved by a screening machine. Due to the material grades and sieve baskets, a total of 12 sieve test with mesh sizes of 125 µm and 400 µm were performed.

The separated fibre and gypsum fractions were analysed in the laboratory (Figure 3). Target parameters were moisture content and calcium sulfate to determine the amount of gypsum in the gypsum fraction. Secondly, the amounts of fibre and additives were determined. In addition, the gypsum samples were analysed for crystal water and TOC.
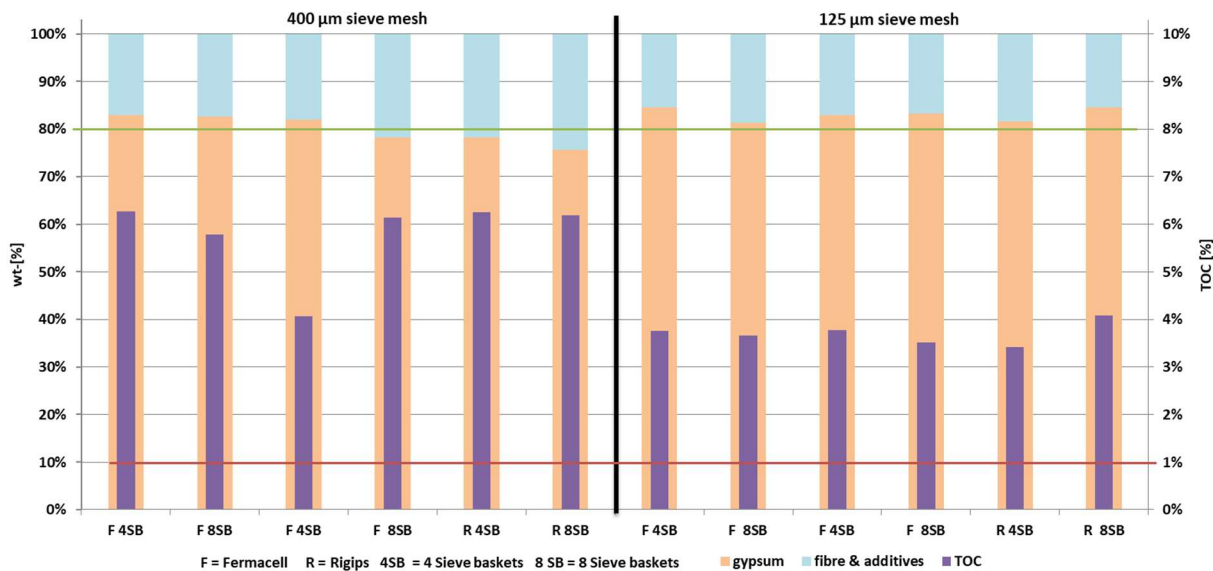
Figure 3: The results of the processing route with GFB of two brands, each processing step of two settings yielded the amount of gypsum (salmon bar) in the gypsum and fibre & additive fraction. The green bar at 80 wt-% showing a suspected component mixture and the red bar at 1 wt-% TOC represents the maximum content of TOC recommended by the gypsum association

The results show fibre contents between 10.1 wt-% and 23.4 wt-% and gypsum contents of 62.9 wt-% and 83.4 wt-% with additive matters of 6.5 wt-% and 13.7 wt-%. Samples screened by the 400 µm sieve mesh show a humidity content of 0.56 wt-%-0.72 wt-% for the gypsum fraction. In the paper fraction the humidity content is between 0.13 wt-%-0.54 wt-%. The samples screened by the 125 µm sieve mesh show a humidity content of 0.32 wt-%-0.45 wt-%. The humidity content in the fibre and additives range from 0.23%-0,86%.

When compared to the 400 µm sieve mesh the TOC content exhibits a decrease. For the 400 µm sieve mesh the TOC and ranges between 3.41 wt-%-6.27 wt-% and is ≤ 4,08% when screened with the 125 µm sieve mesh. The decrease in the TOC indicates a higher purity. Still the specification of the gypsum association, which allows for a maximum TOC content of 1.0 wt-% [6], is not met. To achieve a TOC content <1 wt-% further treatment needs to be integrated into the process chain.

3. Preliminary investigations on synthetic gypsums

Synthetic gypsum is usually produced as a residual material or by-product in various industrial processes. The best-known example is the FGD gypsum already mentioned, which is produced during flue gas cleaning in coal-fired power plants. In addition, there are various methods and processes that can produce gypsum of varying quality. Table 1 provides an overview.

Table 1   Overview of various synthetic gypsums

Source of synthetic gypsum	Description
Fertilizer production	By product from the production of phosphoric acid. The treatment of phosphate ore with sulfuric acid results in phosphogypsum
Municipal waste incineration	FGD-gypsum from the desulphurization of flue gas analogous to FGD-gypsum from coal power plants
Lead-acid batteries	Sulfuric acid within lead acid batteries is neutralized with milk of lime (or similar)
Phosphorus-extraction from sewage sludge ash	During the extraction of phosphorus from sewage sludge ash by means of leaching, gypsum may be obtained as by-product.
Fruit acid production	Gypsum is obtained as by-product from the production of organic fruit acid, such as tartaric acid, citric acid or oxalic acid.
Titanium dioxide production	If titanium dioxide is produced via the sulfide process, gypsum is obtained as by-product.
Hydrofluoric acid production	In the course of the reaction between fluorite and sulphuric acid, gypsum and hydrofluoric acid are formed as products.
Lithium production	In the course of lithium extraction, gypsum may be obtained as by-product.

Data available show that mostly comparatively small quantities of synthetic gypsums are generated. Relevant criteria for synthetic gypsum are high grade purity, compliance with quality criteria for e.g. heavy metals or salts, and the quantity of waste. Furthermore, grain size, grain shape and water content are important for usability of gypsum as a secondary raw material. Some of these gypsums, e.g. fluorogypsum, are already recycled in their entirety. Gypsum from citric acid production can also be utilized to a large extent, while tartaric acid gypsum is of no further significance due to the very small quantity produced.

The largest quantities of gypsum residues are to be found in phosphogypsum from fertilizer production: several million tons are produced worldwide each year. However, due to their different origins, phosphogypsums are not homogeneous in composition and usually contain different impurities such as heavy metals, phosphates or even radioactive contamination. Accordingly, there are large stockpiles of phosphogypsum in the world, the total magnitude of which is several hundred million tons. In addition, further synthetic gypsum potentials may arise from comparatively new technologies, such as lithium production for electric car batteries or sewage sludge treatment.

In this project, various types of gypsum from different sources are being investigated for their suitability as secondary raw materials for the gypsum industry. All materials are tested for their heavy metal content and gypsum content. Additionally, investigations using a scanning electron microscope (SEM) are conducted to draw conclusions about the grain size and grain shape and

thus about the reactive surface of the samples. Figure 4 shows exemplary gypsum crystals from an Italian titanium dioxide production and from phoshogypsum, which originates from Croatia.
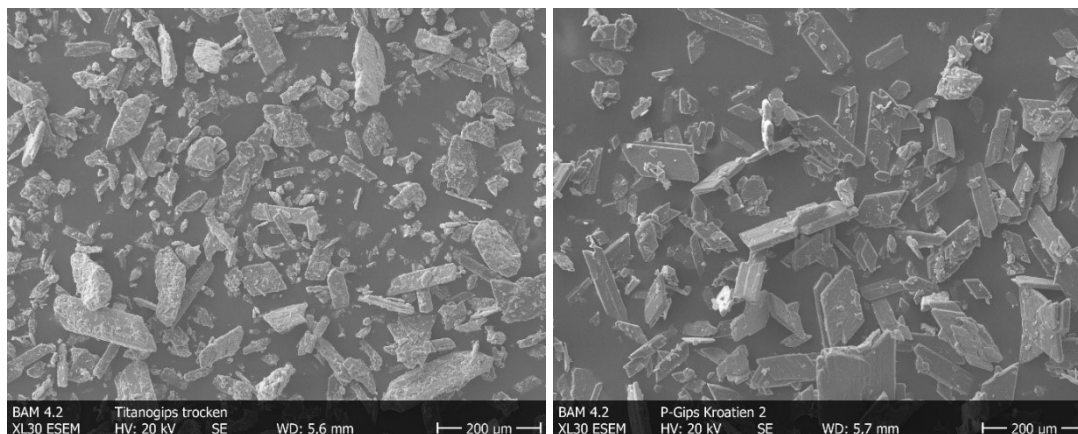
Figure 4:   Gypsum crystals from Titanogypsum and Phosphogypsum (right), SEM

In contrast to used gypsum boards from demolition, synthetic gypsums have a comparatively high water content depending on the preceding processes. Before further processing in the gypsum industry, synthetic gypsum must therefore usually be dried. In view of the required energy consumption, it is particularly important to evaluate these recycling processes in terms of life cycle assessment.

4.   Life cycle assessment of secondary gypsum

To determine whether alternative gypsum resources should be tapped into, their viability needs to be evaluated against an assessment scale. Next to the economic efficiency and social aspects, resource criticality and environmental aspects may be used as benchmark. Within the scope of this project the latter two are addressed by means of environmental life cycle assessment (LCA). One source for secondary gypsum investigated is recycled gypsum from waste GFB. Furthermore, an assessment of synthetic gypsum from the recycling of end-of-life (EoL) lead acid batteries is in preparation. Further secondary gypsum sources may be considered later in the project.

LCA has established as best possible method to assess a variety of environmental impact categories and the depletion potential of natural resources. Thereby the entire life cycle of a product or serviced is considered. Both, the ISO 14040 and 14044 provide fundamental guidelines to conduct a standardized LCA. Alongside four iterative steps – (1) the definition of the goal and scope, (2) the life cycle inventory, (3) the life cycle impact assessment and (4) interpretation – environmental impacts are quantified. Despite the formalized procedure, practitioners of LCA are confronted with many degrees of freedom while modelling and evaluating the life cycle of products and/or services. Thereof, modelling choices have to be concretised during the definition of the goal and scope.

4.1   Definition of goal and scope

The modelling choices made for the LCA of secondary gypsum are summarized in Table 2. The scope for the assessment is Germany and the reference year 2020. In the case of GFB, the modelling starts at the point, where GFB become waste and are collected (demolition site). For

gypsum from EoL lead acid batteries the modelling starts at the recycling plant (the transportation of lead acid batteries to the recycling facility and the separation of diluted sulfuric acid is entirely allocated to the recovery of lead, as it represents the primary product sought in lead acid battery recycling). The modelling ends with the production of a marketable gypsum product (CaSO$_4$-Dihydrate). This represents a gate-to-gate approach.

Within this LCA secondary gypsum is offset against gypsum obtained from flue gas desulfurization systems in coal power plants (FGD-gypsum) and natural gypsum. This is accomplished by a method referred to as the substitution method. Here, burdens associated with the production of gypsum from FGD- and natural gypsum are subtracted from the burdens of producing secondary gypsum. For the LCA an attributional approach is chosen, which – in comparison to a consequential approach - provides a description of the status of a product system with regard to its environmental impacts. The product systems are modelled within openLCA (v. 2.0). Background processes are mainly taken from the ecoinvent database (v. 3.9.1).

Table 2   Modelling choices in the conducted LCA

Parameter	Modelling choice
Geographical scope	Germany
Temporal scope	Reference year 2020
Considered life cycle	Gate-to-gate
LCA method	Attributional LCA
Allocation method	Substitution method
Software and database	openLCA 2.0 in connection with the ecoinvent 3.9.1, APOS database

4.2   Life cycle inventory

Prior to compiling the life cycle inventory, a process chain is developed for the considered product systems. An overview is given in Figure . For the recycling of GFB, the separately collected GFB are transported to the recycling plant at which gypsum is separated from impurities (i.e. plastics, metals, paper-rich fraction and other mineral waste) in several process steps: First, manual sorting takes place, then GFB are freed from Fe-metals via magnetic separators and form non-ferrous metals via a eddy flow separator. Paper fibres are extracted by means of milling and sieving. Impurities are treated in energy (plastics, paper) or material recovery plants (metals) or are landfilled (other mineral waste). Raw gypsum is transported to the gypsum plant and replaces gypsum from primary sources. To maintain comparability between the different moisture contents in gypsum from secondary sources and FGD and natural gypsum, a drying step is included in the process chain. Hereby the burdens for drying gypsum to 0% water content are balanced.

For the production of synthetic gypsum from EoL lead acid batteries, the diluted sulfuric acid within the batteries enters the product system "burden-free" (see 4.1). With the aid of a reactant such as lime milk or calcium carbonate, gypsum is synthesized. The mother liquor remains as

by-product and undergoes further treatment. Similar to gypsum from GFB, the obtained synthetic gypsum is transported to the gypsum plant and for reasons of comparability a drying step is balanced.
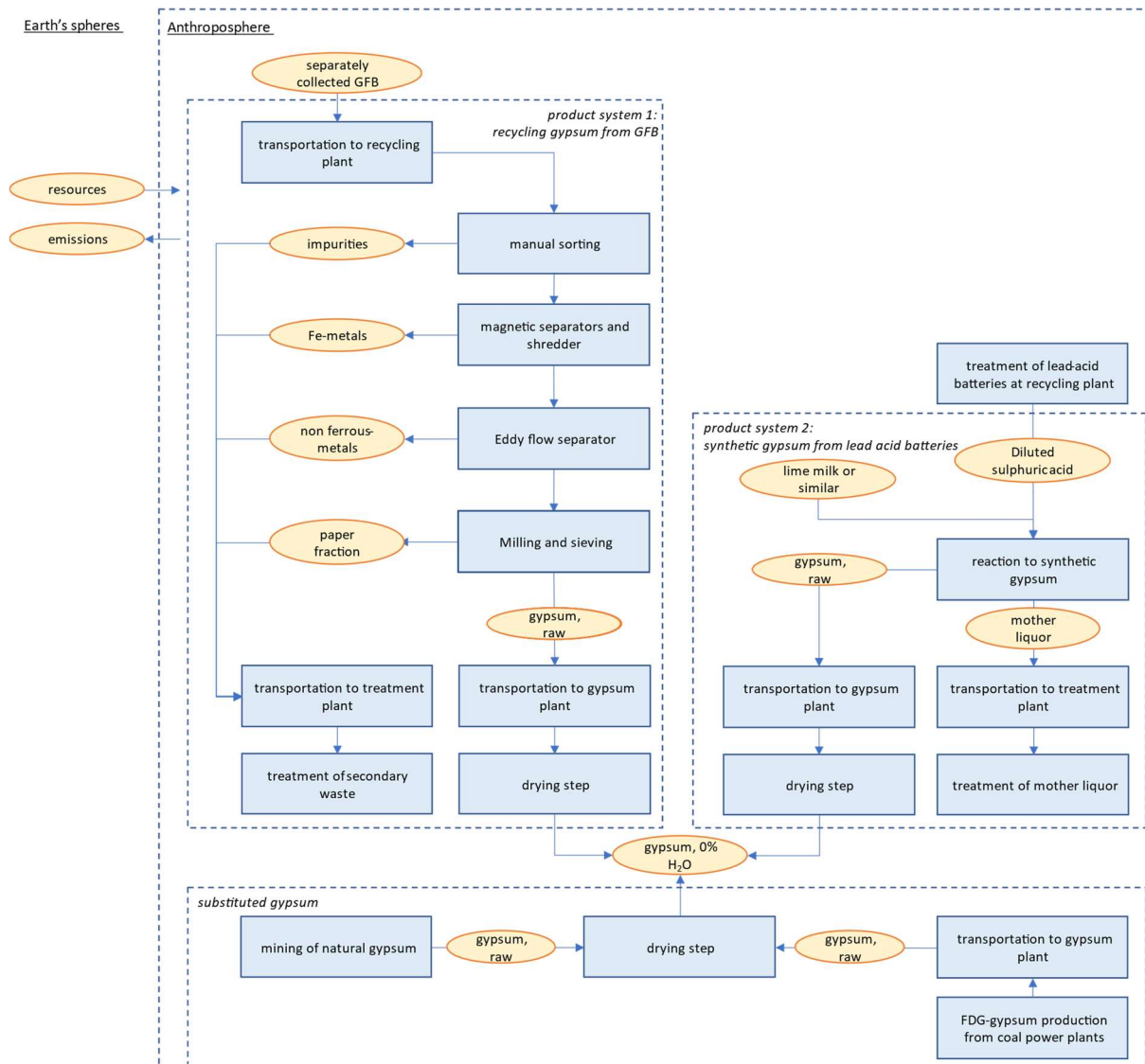
Figure 5: Simplified flow chart of two considered product systems and the primary production of gypsum

4.3 Life cycle impact assessment and interpretation

In this project the development of a LCA on secondary gypsum sources is currently still at an early stage and the results are still pending. Based on the evaluation of the results, relevant impact categories will be chosen and both environmental hot spots and a comparative analysis of different secondary gypsum sources shall be provided. It should be noted that the goal and scope definition as well as the life cycle inventory and process chains are still subject to adjustments, given the iterative nature of LCA. Based on previous studies, it can be assumed that the impact categories global warming potential and land use will be of importance [7, 8].

## 5.	Conclusions

In summary the emerging gap in FGD will increase while mining of natural gypsum shall remain steady. Therefore, to cover the demand of gypsum alternative sources of secondary gypsum become more and more important. As for GPB the recycling process and efficiency is established, but not yet for GFB and synthetic gypsum. From the separation of GFB followed that the amount of gypsum meets the expectations of an 80/20 ratio gypsum to fibre. The separation rate of GPB can only be approached, so the recommendation of TOC by the gypsum association. The process route will and has to implement a further treatment stage to address this.

In addition, certain synthetic gypsums are particularly suitable as secondary gypsum. Their viability needs to be evaluated against an assessment scale. To do so their potential and ecological impact have to be investigated by mentioned system with given parameters and modelling choices within LCA, to determine whether alternative gypsum resources should be tapped into. Furthermore, transport distances and thus the points of origin probably also have a particular influence on the results of the environmental evaluations.

Complementary to the life cycle assessment of the two investigated routes for the extraction of gypsum from secondary sources, an economic analysis is also indispensable. Particularly in the case of materials that - like gypsum - are not cost-intensive, substitution of the primary product must not lead to higher costs. Influencing parameters such as transport distances or energy consumption during processing are also essential here. Last, but not least: the resulting saving of disposal expenses may have a decisive influence on the economic efficiency.

Acknowledgements

References

[1]	European Commission, Directorate-General for Internal Market, Industry, Entrepreneurship and SMEs, Blengini, G., El Latunussa, C., Eynard, U., et al., Study on the EU's list of critical raw materials: final report, Publications Office, https://data.europa.eu/doi/10.2873/904613 (2020).

[2]	Demmich, J., 'Impact of the coal phase-out on Germany's gypsum supply' (in German), REWIMET Symposium August 2021 Ressourcenmanagement, Clausthal-Zellerfeld, (2021).

[3]	Alwast, H. 'Nachhaltige Ausstiegsszenarien für Naturgips und REA-Gips für die nächsten 25 Jahre' (in German), available online: https://www.rewimet.de/images/downloads/symposium2021_alwast.pdf (2021) (accessed 24.05.2023).

[4]	Bunzel, J., Wilczek, M. ,Industrielles Recycling von gipshaltigen Abfällen' in: Mineralische Nebenprodukte und Abfälle, 3. Auflage, TK Verlag Karl Thomé-Kozmiensky, Neuruppin, ISBN: 978-3-944310-282 (2016) 487-497.

[5]	Statista: Produktion von Gipsplatten in Deutschland in den Jahren 2010 bis 2021. Available online: https://de.statista.com/statistik/daten/studie/589581/umfrage/produktion-von-gipsplatten-in-deutschland/ (accessed 26.05.2023).

[6]	Bundesverband der Gipsindustrie e. V.: Recyclinggips (RC-Gips) Erstprüfung für Recyclinganlagen, Qualitätsmanagement, Qualitätsempfehlungen und Analyseverfahren. Available online:

https://www.gips.de/fileadmin/user_upload/aktuelles/Qualitaetsempfehlungen_Gipsrecycling_Analyseverfahren_Stand_Juni_2020.pdf (2020) (accessed: 25.05.2023).

[7] Weimann, K.; Matyschik, J.; Adam, C.; Schulz, T.; Linß, E.; Mueller, A. Optimization of demolition/dismantling of buildings for the recovery and treatment of building materials considering the reduction of harmful substances (in particular sulphates) in the recycled building material and aspects of life-cycle analyses (in German). In *Umweltforschungsplan*; FKZ 3709 33 317, Report; German Environment Agency: Dessau, Germany (2012).

[8] Buchert, M.; Sutter, J.; Alwast, H.; Schuetz, N.; Weimann, K. Life cycle assessment of gypsum plasterboard recycling (in German). In *Umweltforschungsplan*; FKZ 3715 34 320, Report; German Environment Agency: Dessau, Germany (2017).

HYDRATION KINETICS OF CEMENT-LIME BINDERS WITH CONSTRUCTION AND DEMOLITION WASTE FINES FOR MASONRY APPLICATIONS

V. Grigorjev (1), J.M. Etcheverry (1), M. Azenha (2), N. De Belie (1)

(1) Magnel-Vandepitte Laboratory, Ghent University, Belgium

(2) ISISE, University of Minho, Portugal

Abstract

Effective reuse of construction and demolition waste requires solutions for the use of all recycled material fractions. Recycled fines (<63 µm) still pose major challenges in the processing and application of recycled aggregates in new construction. However, masonry structures may present opportunities for the utilization of recycled waste fines. In masonry mortars, which are normally subjected to lower mechanical loads and milder environmental conditions than concrete, recycled fines could potentially be used as a partial binder replacement. This study showcases a certain level of reactivity of recycled concrete fines and mixed fines through R^3 reactivity testing (ASTM C1897). Furthermore, the effect on hydration kinetics of cement is showcased in isothermal calorimetry testing by gradually increasing the content of recycled fines in cement and cement-lime binders. For comparison, quartz powder is used at identical replacement levels to distinguish between a known filler effect and the changes in cement hydration induced by recycled concrete fines and mixed fines. The obtained results indicate that the addition of lime increases the rate of cement hydration, while recycled concrete fines and mixed fines are comparable to quartz filler at low binder replacement levels, whereas at higher replacement levels they demonstrate different, possibly chemically-induced effects**.**

1.   Introduction

The premise of circular economy relies on full recyclability of materials which allows to keep materials in use rather than using them up [1, 2]. Construction and demolition waste (CDW) is one area in which there is a significant potential for innovation, since the amounts of such waste generated account for around a third of all waste in EU [3], whereas the use is still challenged by many of the inherent problems and limited by current legislative systems in place. Even though the primary pathway for recycled CDW is destined for the generation of coarse recycled aggregates for use in new concrete and road building, there are substantial amounts of fine recycled aggregates produced at the same time [4, 5]. Whilst there have been many attempts to explore the use of fine recycled aggregates for various new applications [6], the performance of such materials is usually infringed by the lower quality of recycled materials compared to raw ones. Even so, the lower quality is largely the result of a large proportion of recycled fines (<63 μm) present in these aggregates, which bear many of the negative aspects, including high water absorption capacity, high porosity, low density and strength.

However, recycled fines, originating either from select sources such as concrete and ceramics, or from mixed sources, can potentially exhibit some reactivity. Many studies have relied on this assumption in order to justify the use of recycled fines as partial binder replacement, yet the results have often demonstrated that the reactivity is not on par with cement or other types of waste, used as supplementary cementitious materials [7, 8, 9, 10].

Whilst concrete applications have been primary area of study for recycled fines' potential use, there are some less-explored destinations for this type of waste materials. One possibility is masonry-related applications, particularly the binder systems in mortars for masonry. Some research has revealed interesting results of recycled fine waste incorporation in masonry mortar binders [11, 12], but the effects have been studied from a mortar performance viewpoint.

To develop a better understanding of the possible implications of using recycled fines in masonry mortars, this study has been designed to indirectly assess the hydration behaviour of cement and cement-lime binders with partial replacement of the binding raw material by recycled powders. First, the reactivity of fines was assessed against that of a quartz filler using isothermal calorimetry by the ASTM C1897 R^3 method [13] and then the hydration kinetics of cement were evaluated by adding lime to formulate masonry mortar-analogous binder mixtures and gradually replace part of these binders by recycled concrete fines and recycled mixed fines.

2.   Materials and methods

Main binding materials explored in this study were Portland-limestone cement CEM II/A-L 32.5 R [14] and hydrated lime CL90 S [15]. Bulk density of cement and lime was 1045 kg/m^3 and 420 kg/m^3, respectively. Two types of recycled materials were sourced – fine recycled concrete aggregates (FRCA) and fine recycled mixed aggregates, both originating from unknown demolished structures. Recycled concrete fines (RCF) and recycled mixed fines (RMF) were manually separated from dried recycled aggregates using a 63 μm sieve and were otherwise untreated. Quartz filler was also used for comparison.

Particle size distributions of all studied materials were evaluated using laser diffractometry and are summarized in Table 1.

Table 1: Particle size distribution of studied materials

Laser diffraction results (μm)	D_{10}	D_{50}	D_{90}
Cement	2.7	10.9	28.6
Lime	1.4	6.8	15.4
Quartz filler	4.1	25.4	60.9
Recycled concrete fines	5.0	31.1	77.6
Recycled mixed fines	5.2	34.1	74.0

The assessment of combined hydraulic and pozzolanic reactivity of recycled fines was performed in accordance with the R^3 method [13], where fines were used in specified proportions for supplementary cementitious materials, tested at 40 ºC. The same procedure was applied for inert quartz filler.

Hydration kinetics of cement and cement-lime binders were evaluated using isothermal calorimetry [16] at 20 ºC. Masonry-specific binders were formulated in volumetric proportions of cement/lime of 1:0 (pure cement), 2:1 and 1:1. The water to binder (w/b) ratio was set to 1.0 in order to reflect the w/b ratios in mortars for masonry. Recycled fines and quartz filler were used at 5, 10, 20 and 30% replacement levels of the total binder mass.

The paste samples were mixed outside the calorimeter using an overhead mixer at 600 rpm and were inserted into the testing channels as fast as possible, at approximately 3-4 minute intervals.

3. Results and discussion

Reactivity of both types of recycled fines and quartz filler, as tested using the R^3 method, is showcased in Table 2. As specified in the standard, the cumulative heat release from 75 minutes after sample insertion was recorded until 7 days, whilst values were shown for 3 and 7-day cumulative heat.

Quartz filler was tested to set the baseline for comparison of fines with a known inert filler. Recycled concrete fines have shown a heat release of ~25 J/g_{fines}, which mostly occurred during the first 3 days, with very limited development during later age of hydration. This indicates potential hydraulic reactivity remaining in the fines, most likely attributed to the unhydrated cement phases. Recycled mixed fines were evidently more reactive during the first 3 days of measurement, compared to concrete fines, but there was also a considerable heat development from 3 to 7 days. Overall, both recycled materials exhibited a degree of reactivity well above inert material, but RCF reactivity is far from any conventional supplementary cementitious materials, whilst that of RMF is barely approaching the range for pozzolanic materials (50-300 J/g_{SCM}) [17].

Table 2: R^3 reactivity test results for quartz filler and recycled fines

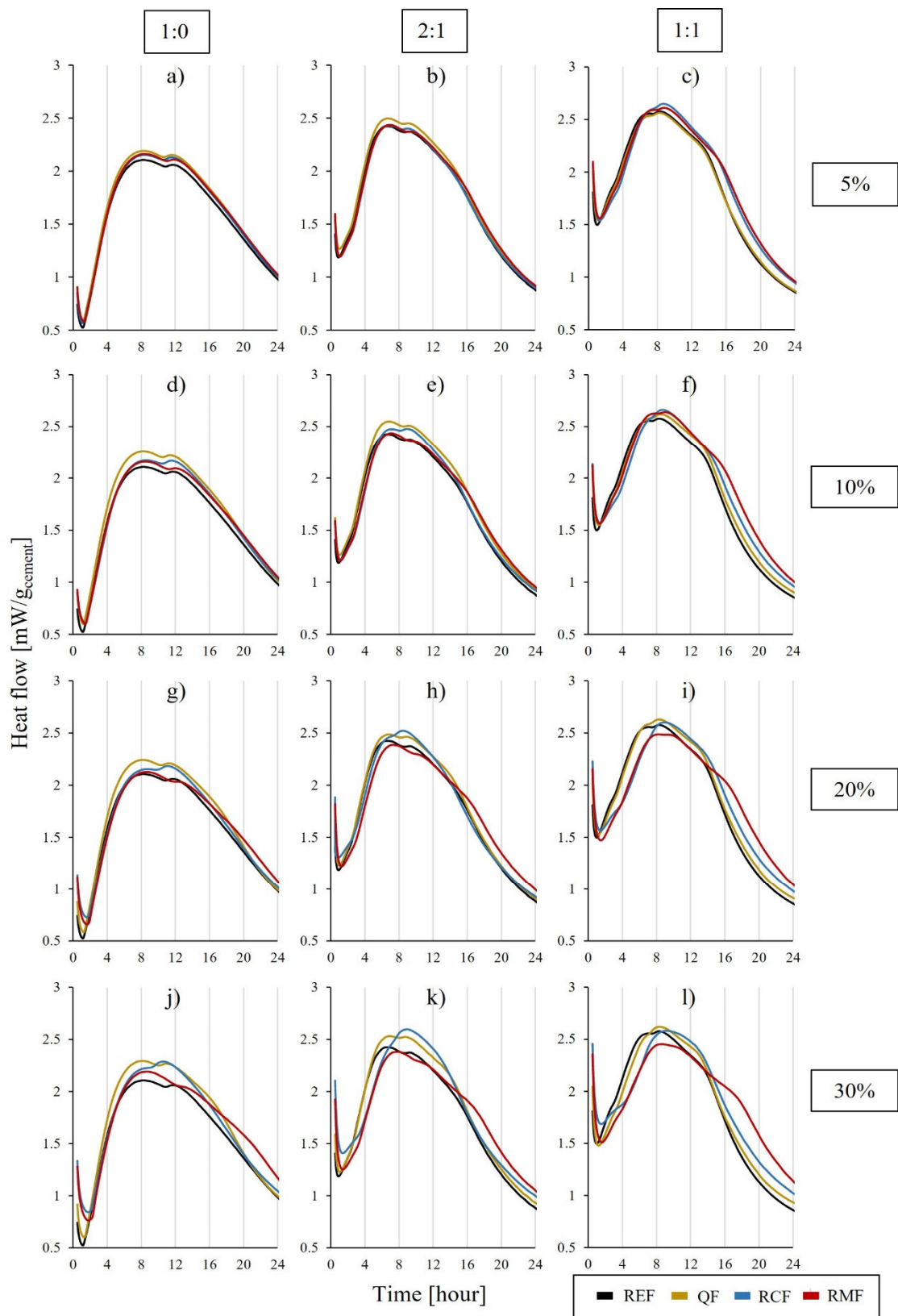| Cumulative heat release [J/g_{fines}]	75 min to 3 days	75 min to 7 days
Quartz filler (QF)	4.3	4.6
Recycled concrete fines (RCF)	24.8	24.9
Recycled mixed fines (RMF)	37.9	44.7

Figure 1: Isothermal calorimetry results of three different binder systems (denoted REF) with partial replacement of cement and lime by quartz filler (QF), recycled concrete fines (RCF) and recycled mixed fines (RMF)

Hydration kinetics of cement and cement-lime pastes with partial replacement of raw binders are showcased in Figure 1, which presents the main hydration peaks developed during the first 24 hours in the isothermal calorimeter. All of the results are normalized with respect to the mass of cement in all the studied mixes to aid the comparison between cement and cement-lime binders, as well as between different recycled materials and an inert filler at different replacement levels.

Based on Figure 1 (a to c), the addition of lime appears to facilitate cement hydration by increasing the heat released during the dormant period and accelerating the main peak formation during the 24 hour period. As a consequence, the height of the two peaks during the induction period is increased as well. These peaks are mostly associated with Portland-limestone cement hydration followed by a shoulder-like formation at ~8-14 hours of hydration where the variable replacement of raw binders by recycled fines seems to have an apparent effect.

At 5% and 10% replacement of cement (Figure 1 a and d), both recycled concrete fines and mixed fines resemble the filler effect of quartz powder, albeit less pronounced. Similar behaviour is observed with a 2:1 cement:lime binder (Figure 1 b and e), whereas at a 1:1 volumetric cement and lime proportion, both recycled fines present a greater filler effect, possibly due to higher replacement of the non-hydraulic lime – Figure 1 c and f.

At 20% replacement of raw binders, further distinction between recycled materials and quartz filler are noticeable. In pure cement paste (Figure 1 g) quartz powder presents the highest filler effect, but with increasing lime content – Figure 1 h – a higher peak from RCF is noted, and the addition of 20% RMF lowers the peak, but broadens the shoulder formation. This effect is even more pronounced in a 1:1 binder, with the evident addition of delayed peak formation from both recycled materials – Figure 1 i.

The differences between QF, RCF and RMF are clearly visible at a 30% binder replacement. Based on Figure 1 j, quartz powder still shows the highest peak, whereas recycled concrete fines manifest in an increased second peak formation and recycled mixed fines – a broadening of the double peak shape and a more prominent shoulder. In 2:1 and 1:1 cement and lime pastes, the effects of both recycled materials are similar to the 20% replacement case, only more distinguishable – Figure 1 k and l.

Overall the influence of recycled materials on cement hydration kinetics appears to be different from that of an inert quartz powder, and even though their influence has been directly compared to a physical filler effect, the changes in cement hydration might be chemical too. A certain degree of reactivity was found in these recycled fines, but isothermal calorimetry tests on binder paste samples did not present an opportunity to evaluate any potential chemical effects due to limited heat release, especially past the initial 24 hour hydration period.

4.   Conclusions

This study has provided new insights into the reactivity of recycled fine powders originating from different construction and demolition waste. Furthermore, their effect on the hydration kinetics of cementitious masonry binder systems has been evaluated as well. Based on the results presented here, a few important points can be presented.

- Recycled concrete fines and recycled mixed fines exhibit a certain degree of reactivity above the inert quartz filler, based on the R^3 method.

- Recycled mixed fines are almost 2 times more reactive than recycled concrete fines and there is an indication of later-age reactivity.

- Hydrated lime has accelerated and increased cement hydration.

- When used in a cementitious masonry mortar binder, both recycled fines manifest a slightly increased cement hydration effect at 5 and 10% replacement levels. This effect is comparable to quartz filler in intensity, but the nature may be both physical and chemical. It is also more pronounced when binder system contains a higher proportion of hydrated lime.

- In lime containing binders at higher replacement levels of 20-30%, recycled concrete fines present a visibly reduced filler effect compared to quartz powder and there is a slight delay in cement hydration. However, hydration peak is broadened. Recycled mixed fines display even a further decrease in the main peak, but broadening is even more pronounced with a noticeable shoulder formation, especially at higher lime content in the binder.

Acknowledgements

References

[1] European Commission, A new Circular Economy Action Plan For a cleaner and more competitive Europe. (2020). Available from: https://eur-lex.europa.eu/legal-content/EN/TXT/?qid=1583933814386&uri=COM:2020:98:FIN

[2] Ellen MacArthur Foundation, Universal Circular Economy Policy Goals (2021). Available from: https://ellenmacarthurfoundation.org/universal-policy-goals/overview#upg-paper

[3] European Commission, Construction and demolition waste (no date). Available from: https://environment.ec.europa.eu/topics/waste-and-recycling/construction-and-demolition-waste_en

[4] Pacheco, J.; de Brito, J. Recycled Aggregates Produced from Construction and Demolition Waste for Structural Concrete: Constituents, Properties and Production. *Materials* **2021**, *14*, 5748. https://doi.org/10.3390/ma14195748

[5] Schoon, J., de Buysser, K., van Driessche, I., & de Belie, N. (2015). Fines extracted from recycled concrete as alternative raw material for Portland cement clinker production. *Cement and Concrete Composites*, *58*, 70–80. https://doi.org/10.1016/J.CEMCONCOMP.2015.01.003

[6] Villagrán-Zaccardi, Y. A., Marsh, A. T. M., Sosa, M. E., Zega, C. J., de Belie, N., & Bernal, S. A. (2022). Complete re-utilization of waste concretes–Valorisation pathways and research needs. *Resources, Conservation and Recycling*, *177*, 105955. https://doi.org/10.1016/J.RESCONREC.2021.105955

[7] Nedeljković, M., Visser, J., Nijland, T. G., Valcke, S., & Schlangen, E. (2021). Physical, chemical and mineralogical characterization of Dutch fine recycled concrete aggregates: A comparative

study. *Construction and Building Materials*, *270*, 121475. https://doi.org/10.1016/J.CONBUILDMAT.2020.121475

[8] Letelier, V., Tarela, E., & Moriconi, G. (2017). Mechanical Properties of Concretes with Recycled Aggregates and Waste Brick Powder as Cement Replacement. *Procedia Engineering*, *171*, 627–632. https://doi.org/10.1016/J.PROENG.2017.01.396

[9] Kim, J., & Jang, H. (2022). Closed-loop recycling of C&D waste: Mechanical properties of concrete with the repeatedly recycled C&D powder as partial cement replacement. *Journal of Cleaner Production*, *343*, 130977. https://doi.org/10.1016/J.JCLEPRO.2022.130977

[10] Li, Z., Bian, Y., Zhao, J., Wang, Y., & Yuan, Z. (2022). Recycled concrete fine powder (RFP) as cement partial replacement: Influences on the physical properties, hydration characteristics, and microstructure of blended cement. *Journal of Building Engineering*, *62*, 105326. https://doi.org/10.1016/J.JOBE.2022.105326

[11] Corinaldesi, V., Giuggiolini, M., & Moriconi, G. (2002). Use of rubble from building demolition in mortars. *Waste Management*, *22*(8), 893–899. https://doi.org/10.1016/S0956-053X(02)00087-9

[12] Hu, Z., Kong, Z., Cai, G., Li, Q., Guo, Y., Su, D., Liu, J., & Zheng, S. (2021). Study of the properties of full component recycled dry-mixed masonry mortar and concrete prepared from construction solid waste. *Sustainability (Switzerland)*, *13*(15). https://doi.org/10.3390/su13158385

[13] ASTM C1897, Standard Test Methods for Measuring the Reactivity of Supplementary Cementitious Materials by Isothermal Calorimetry and Bound Water Measurements, ASTM International, West Conshohocken, PA, 2020. https://doi.org/10.1520/C1897-20.2.

[14] EN 197-1:2011 - Cement - Part 1: Composition, specifications and conformity criteria for common cements.

[15] EN 459-1:2015 - Building lime - Part 1: Definitions, specifications and conformity criteria.

[16] ASTM C1679-17. Standard Practice for Measuring Hydration Kinetics of Hydraulic Cementitious Mixtures Using Isothermal Calorimetry, ASTM International, West Conshohocken, PA, 2017 https://doi.org/10.1520/C1679-17

[17] Londono-Zuluaga, D., Gholizadeh-Vayghan, A., Winnefeld, F. *et al.* Report of RILEM TC 267-TRM phase 3: validation of the R^3 reactivity test across a wide range of materials. *Mater Struct* **55**, 142 (2022). https://doi.org/10.1617/s11527-022-01947-3

USE OF LIMESTONE FILLER TO PROMOTE SEPARABILITY BETWEEN CEMENT PASTE AND NATURAL AGGREGATE: A CIRCULAR ECONOMY STRATEGY FOR CONCRETE

Tatiane I. Hentges[1,*], Luis M. M. Tavares[2], Vanderley M. John[1], and Sérgio C. Angulo[1,*]

(1) Civil and Urban Construction Engineering Department, Polytechnic School of University of São Paulo

(2) Metallurgical & Materials Engineering Department, Federal University of Rio de Janeiro, Rio de Janeiro, Brazil

* tatiane.hentges@lme.pcc.usp.br

*sergio.angulo@lme.pcc.usp.br

Abstract

The phases of concrete (cement, fine aggregate, coarse aggregate) are not fully separated by comminution. The circularity of concrete would be improved if clean natural aggregates and cement were obtained. Using of limestone filler (LF) in concrete may help detach the aggregate once it can modify the fracture energy of the concrete and the separation mechanism by comminution. The aim of this research was to evaluate the effect of LF on the fracture energy (Gf) of pastes and concretes and in the detaching or fracturing coarse aggregates. In the mixtures the cement was replaced by filler and the water content adjusted. The Gf was measured by wedge splitting test (WST) and the percent of detached and fractured aggregates was determined by image analysis. For pastes, the Gf with LF was slightly higher than that of the reference due to the toughening effect. The Gf of concrete was much higher than pastes due to the longer crack path to bypass the aggregate. In concretes, the presence of filler reduced the Gf due to the increase of porosity, and the fracture process was more prone to detach the aggregates.

Keywords: concrete, fracture energy, coarse aggregate, limestone filler, recycling

1.   Introduction

A concrete structure recycling process comprises comminution and size reduction. The comminution is made by crusher, mill, or combining both strategies [1,2]. The recycled concrete aggregate (RCA) produced contains adhered cement paste, elevating its porosity and reducing the aggregate strength. These characteristics are the reason to limit the replacement of natural aggregates by the recycled ones in standards for the application in structural and non-structural concretes [3,4].

Increasing the RCA quality and remove cement paste as fines would promote the circular economy of concrete. Strategies for strengthening or removing the adhered cement paste have been proposed. The strengthening was made, in general, by carbonation or coating (immersing) the RCAs in pozzolan slurries previously of its insertion on concrete mixtures [5–9]. However, the amount of work seems not worth due to the slight RCA improvement.

On the other hand, removing the adhered paste results in an RCA equivalent to the natural aggregate. Among the studies process are: immersion of ARCs in acidic solutions, thermo-mechanical method, electrical discharge crushing method, freeze-thaw method and microwave method [10–16]. These procedures, however, are not viable nowadays due to their high cost or significant environmental impacts.

In this paper, we proposed using limestone filler (LF) in the concrete formulation as a strategy to change the fracture process of the cement paste and the interfacial transition zone during comminution, resulting in an RCA without adhered paste. This proposal is based on the fact that LF does not react chemically with the cement during hydration, reducing the water demand and keeping the mechanical and durability properties [17]. In the hardened state of concrete, the presence of LF contributes to the toughening post-cracking mechanism, resulting in a higher uniformity of the load distribution in all the materials, as Das et al. [18] demonstrated. This toughening effect may promote more damage during the comminution of the cement matrix composite waste and will help detach of the cement paste from the natural aggregates.

Therefore, this works aims to analyze the effect of limestone filler on the fracture energy bond strength of cement paste and concretes.

2. Experimental program

Cement pastes and concrete mixtures composed with and without limestone filler were produced in this work. The fracture energy of those mixtures was determined once this property indicates the amount of work necessary to create a unit of crack area and, thus, can be related to the energy required for concrete comminution. Furthermore, when determined by the Wedge Splitting Test (WST), the fracture energy curve shows more details as the toughening effect. After the WST, the fractured surfaces of the samples were analysed, relating the energy to the fracture or detachment of aggregates.

2.1 Materials

The characteristics of the materials used in this work are presented in Table 1. Also, their discrete (a) and cumulative (b) particle size distribution are in Figure 1. **Ordinary Portland cement** (OPC) was used in this work (classified as CPV in Brazil). This cement type was chosen because it has the lowest per cent of addition available in the Brazilian market. A thermogravimetric analysis showed that it is composed of 10% of limestone. Two types of **limestone filler** (LF) were used in this work, called PF1 and PC5, both composed of 100% of $CaCO_3$. They were chosen due to their size difference, aiming to replace the cement and fill the smaller pores of the cement paste. The **fine aggregate** was a river sand whose dimensions are between 0.184 and 1.03 mm. Lastly, the **coarse aggregate** used was river gravel with particle size between 4.75 and 16.5 mm.

Table 1: Materials characteristic

Material	Density (g/cm³)	D50 (μm)	VSA (m²/m³)
Cement	3.08	17.41	0.836
Limestone Filler PF1	2.76	2.49	3.1784
Limestone Filler PC5	2.74	8.83	10.287
River sand	2.65	398	0.031
River gravel	2.64	11,526	0.0008

The insertion of filler in cement paste was made by 40% of mass replacement and the water to binder ratio was reduced with the aim to obtain similar strength. Consequently, the total paste content in the mixture was slightly reduced, and the coarse aggregate content increased, as shown in Table 2. All the LF used in this work comprised 50% of PF1 and 50% of PC5.
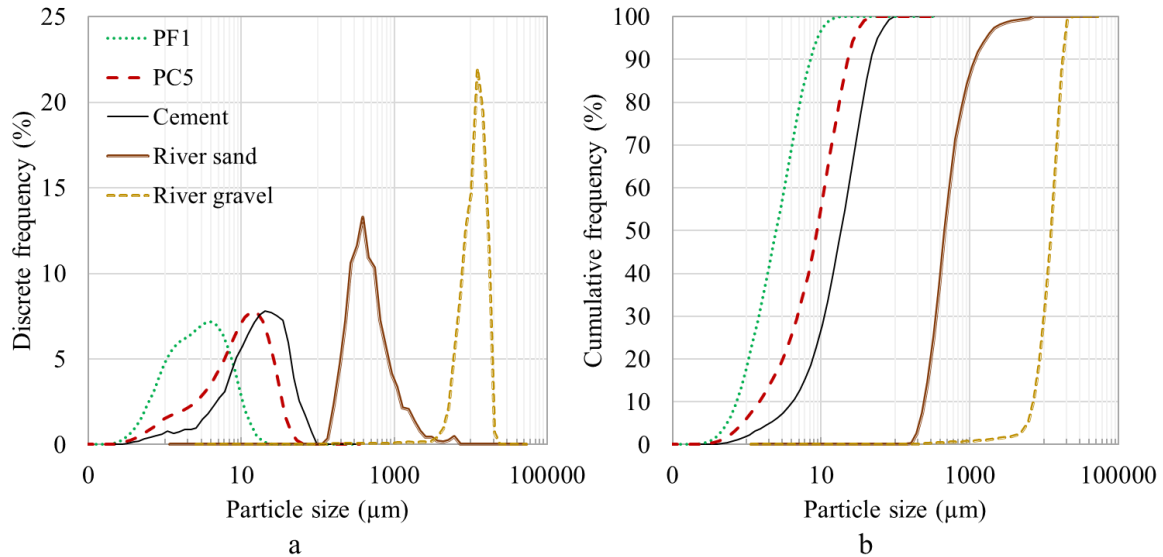
Figure 1: Discrete (a) and cumulative (b) particle size distribution of the materials used in this work.

Table 2: Mix proportion in kg/m³ and properties of produced mixtures

Mixture	Name	C	LF	FA	CA	W	Fc (MPa)	E (GPa)
Paste	P	1240.3	-	-	-	596.8	48.3	18.7
Paste with LF	PF	778.7	519.1	-	-	558.1	26.0	10.6
Reference concrete	C	375.0	-	796.9	1148.8	180.8	62.2	34.3
Concrete with LF	CF	235.4	157.0	796.8	1119.9	168.7	40.6	30.5

C = cement; LF = limestone filler; FA = fine aggregate; CA = coarse aggregate; Fc = compressive strength; E = Elastic Modulus

2.2 Methods

The mixing was performed in a rheometer until the total homogeneity of the mixture. After that, the samples were casted in a vibrating table and kept at environmental conditions. After 24 hours they were cured immersed in lime water for 28 days.

Fracture energy

The Wedge Splitting Test (WST) was performed to determine the fracture energy, in which the samples had dimensions presented in Figure 2 (a).   mixture using an electromechanical dual-column testing machine with a 50 kN load cell. A vertical load was applied at 3 µm/min by the machine in the wedge and distributed horizontally in the sample by the rollers and plates accommodated in the groove. A clip gauge measured the crack opening from a metallic support fixed on the sample (Figure 2 (b)).

Thickness = 75 mm

(a)   (b)
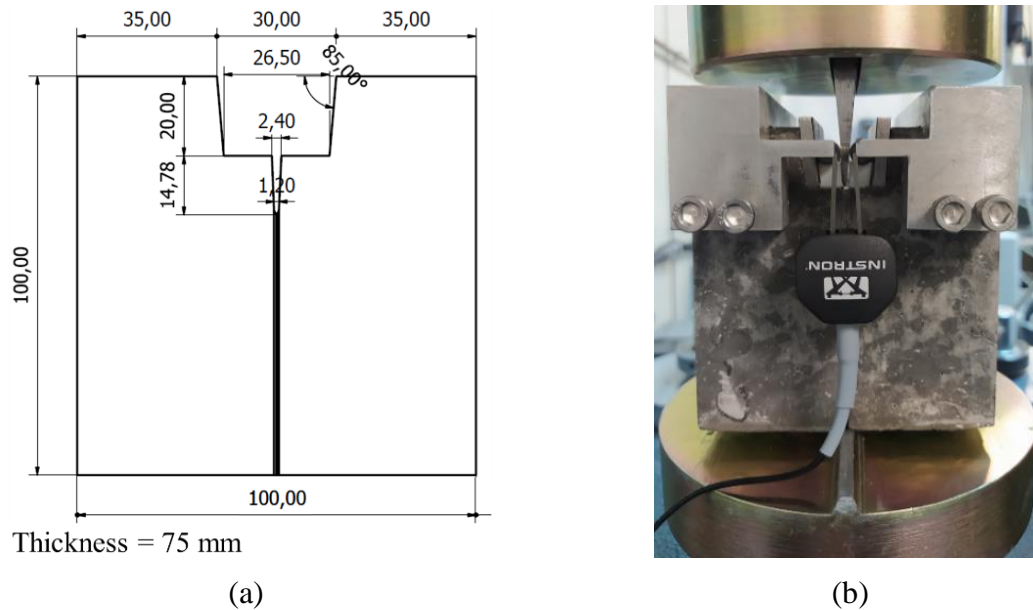
Figure 2: WST sample dimensions (a) and apparatus for carrying out the test, including the frontal clip gage (b)

Load-displacement curves were plotted, and from them, the fracture energy could be calculated using Equation (1), where GF is the fracture energy in (N/m); P is the horizontal load applied in N; δ is the displacement in m measured by the clip gauge (and divided by two sample halves); A is the sample fracture area in m².

$$G_F = \frac{\int_0^\delta P d\delta}{A} \tag{1}$$

Fractured and detached aggregates

After the WST, all the broken samples were identified, and pictures were taken from the fracture surface of the pairs. From this, the number of aggregates on the surface was counted and organised into fractured and detached. The fractured aggregates were considered the ones whose parts are visible in both sample halves. The detached were the ones in that one fracture surface presented only the hole, and the other presented the entire aggregate. Also, up to 10% of broken aggregate was considered detached.

3. Results

3.1 Fracture energy

The average fracture energy (Gf) of mixtures is presented in Figure 3. The Gf of concretes was more than 12 times higher than pastes. Also, the presence of LF in pastes resulted in Gf 48% higher than the reference. In concretes, however, the Gf of C was 18% superior to CF. This ambiguous result occurs due to the different crack courses in the presence of particles. In pastes, when the crack meets a filler particle during crack propagation, it tends to surround the particle and, sometimes, divides itself into two or more microcracks. This effect caused larger deformation for the same load [18]. In concrete, however, in addition to micrometric filler particles, the crack must deflect larger aggregate particles, requiring more energy.

The load-displacement curves of pastes and concretes explain the values of Gf (Figure 4). The pastes reached lower values of load and displacement when compared to concretes. Also, in pastes, the end of the tests was due to the collapse of the samples, which did not happen for the concretes. These results demonstrate that the aggregates are the main ones responsible for the resistance to the formation and propagation of cracks, thus, for the fracture energy.

The presence of LF in pastes reduced the maximum load but also demonstrated a curve tail, reaching larger deformations before collapsing. The maximum load supported is related mainly to the higher porosity of the system, once even though the water-to-solids ratio was lower for LF mixtures, the water-to-cement ratio was higher. Instead of it, the toughening effect of LF suggests that more microcracks appeared during the crack propagation, demanding more energy for the fracture process. The same LF effect was seen for concretes, where the reference (C) reached a higher maximum load, but the CF curve tail demonstrated higher strength for crack propagation.
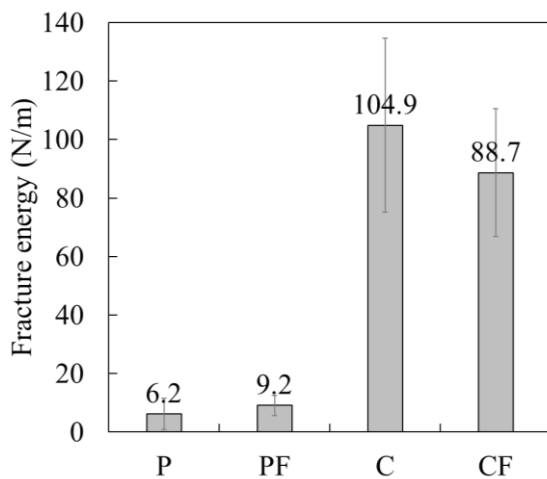
Figure 3: Total fracture energy of mixtures studied in this work
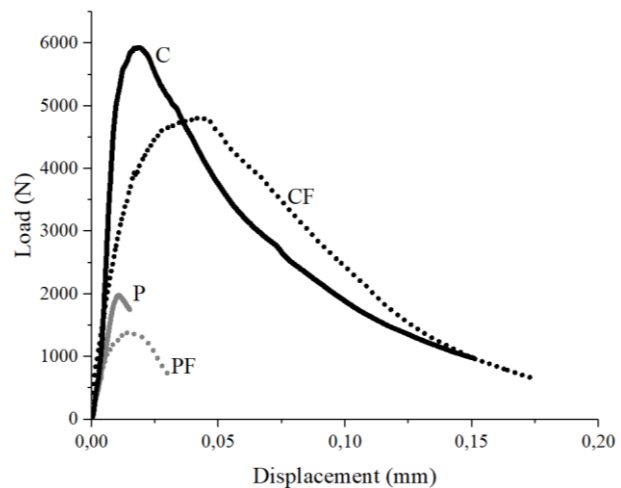
Figure 4: Load-displacement curves from WST

3.2   Fractured and detached aggregates

The average detached coarse aggregates of the concretes were reduced by 15% with cement replacement by filler, as seen in Figure 5. This indicates that the higher energy necessary to break the samples is also related to break a river gravel. It still means that the crack path was easier through the aggregate than bypassing it. On CF, however, the main crack was more prone to bypass the coarse aggregate. This effect is possible due to the microcracks generated by the LF presence on the crack path. Then, with the existence of a microcrack, it was easier for the main crack to surround the aggregate than to pass through it.
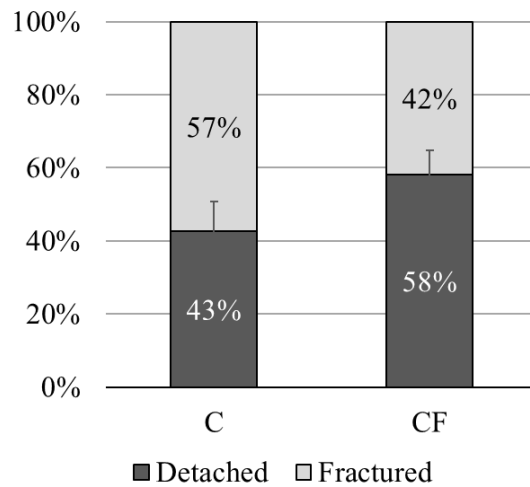
Figure 5: Amount of detached and fractured aggregates in the fracture surface of WST samples

The graph results are illustrated in Figure 6, where one fractured area of each concrete is depicted. Some fractured and whole river gravel can be seen in the pictures, and some grooves are left in the mortar due to detachment. Comparing the concrete without and with LF, more fractured aggregates are identified in the surface in the first, while more detached aggregates are seen in the last. Finally, the aggregates from both concretes have no adhered pastes on their surfaces.
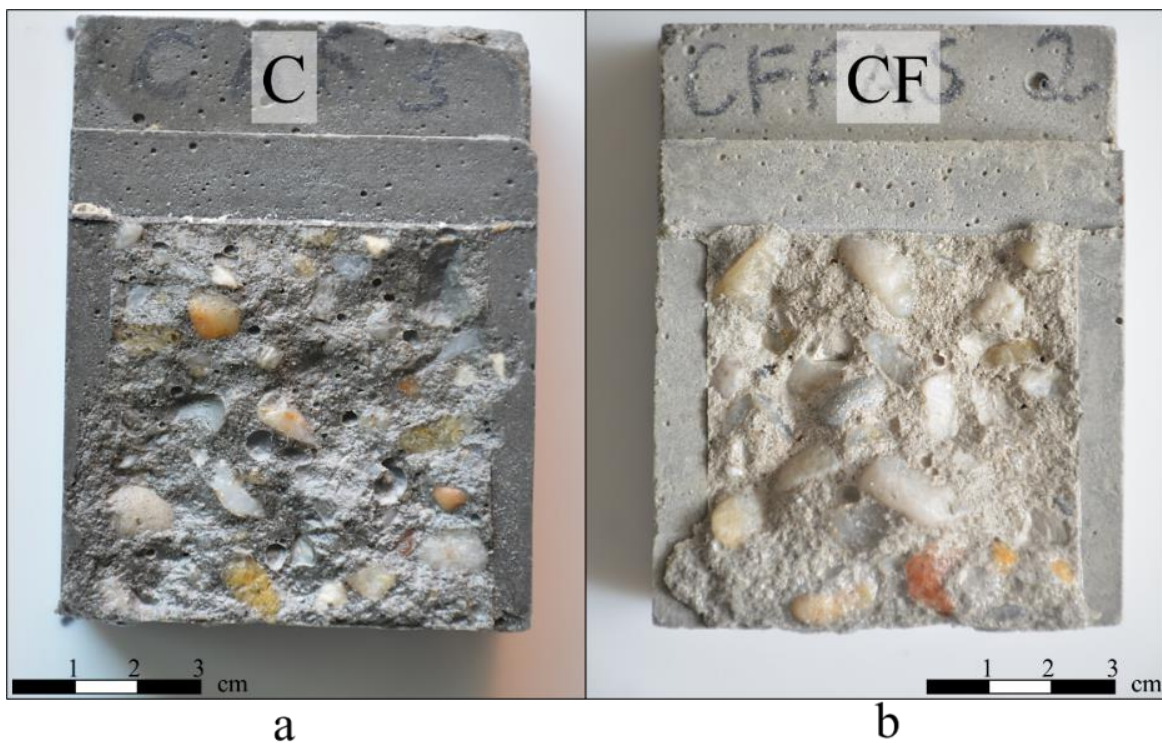
Figure 6: Fracture surface of WST used for counting detached and fractured aggregates. a: reference concrete; b: concrete with filler

4. Conclusions

Limestone filler was used by cement replacement in this work as strategy to improve the recyclability of concretes. Fracture energy and counting of fractured and detached aggregates were carried out. It can be concluded that:

- Pastes containing LF presented higher fracture energy than reference pastes and this is explained by the load-displacement curves. Due to the higher water-to-cement ratio, the LF pastes reached lower maximum load, but the filler toughening effect led to larger deformations;
- Concretes had fracture energy 12 times higher than pastes. The crack path is more tortuous in the presence of aggregates, increasing the need of energy to break the sample;
- Concrete with LF had Gf lower than reference one. Lower maximum load was supported by filler concrete due to its higher porosity and the effect of toughening was smaller than the effect of aggregates in the crack path. Also, the fracture process was more prone to bypasses the aggregates in filler concrete and more prone to break the aggregates in reference concrete.

Different results could be obtained for higher contents of filler (50%) and high water-to-solid ratios that may influence on the quantity of detached aggregates. Further investigations on those directions are necessary.

Acknowledgements

References

[1] C. Ulsen, H. Kahn, G. Hawlitschek, E.A. Masini, S.C. Angulo, Separability studies of construction and demolition waste recycled sand, Waste Manag. 33 (2013) 656–662. doi:10.1016/j.wasman.2012.06.018.

[2] P.C.C. Gomes, C. Ulsen, F.A. Pereira, M. Quattrone, S.C. Angulo, Comminution and sizing processes of concrete block waste as recycled aggregates, Waste Manag. 45 (2015) 171–179. doi:10.1016/j.wasman.2015.07.008.

[3] A. Kiouranis, L.F.R. Miranda, A.A. de Melo Neto, Agregados reciclados em concretos : uma análise crítica das propriedades e classificações, in: XVI Encontro Nac. Tecnol. Do Ambient. Construído, ENTAC, São Paulo, 2016: pp. 4209–4220.

[4] E. Güneyisi, M. Gesoglu, Z. Algin, H. Yazici, Rheological and fresh properties of self-compacting concretes containing coarse and fine recycled concrete aggregates, Constr. Build. Mater. 113 (2016) 622–630. doi:10.1016/j.conbuildmat.2016.03.073.

[5] C. Shi, Y. Li, J. Zhang, W. Li, L. Chong, Z. Xie, Performance enhancement of recycled concrete aggregate - A review, J. Clean. Prod. 112 (2016) 466–472. doi:10.1016/j.jclepro.2015.08.057.

[6] Q. Zhu, Y. xin Yuan, J. hao Chen, L. Fan, H. Yang, Research on the high-temperature resistance of recycled aggregate concrete with iron tailing sand, Constr. Build. Mater. 327 (2022) 126889. doi:10.1016/j.conbuildmat.2022.126889.

[7] J. Wu, Y. Zhang, P. Zhu, J. Feng, K. Hu, Mechanical Properties and ITZ Microstructure of Recycled Aggregate Concrete Using Carbonated Recycled Coarse Aggregate, J. Wuhan Univ. Technol. Mater. Sci. Ed. 33 (2018) 648–653. doi:10.1007/s11595-018-1873-1.

[8] B. Lu, C. Shi, Z. Cao, M. Guo, J. Zheng, Effect of carbonated coarse recycled concrete aggregate on the properties and microstructure of recycled concrete, J. Clean. Prod. 233 (2019) 421–428. doi:10.1016/j.jclepro.2019.05.350.

[9] S.M.S. Kazmi, M.J. Munir, Y.F. Wu, I. Patnaikuni, Y. Zhou, F. Xing, Effect of recycled aggregate treatment techniques on the durability of concrete: A comparative evaluation, Constr. Build. Mater. 264 (2020). doi:10.1016/j.conbuildmat.2020.120284.

[10] V.W.Y. Tam, C.M. Tam, K.N. Le, Removal of cement mortar remains from recycled aggregate using pre-soaking approaches, Resour. Conserv. Recycl. 50 (2007) 82–101. doi:10.1016/j.resconrec.2006.05.012.

[11] M.S. Juan, P.A. Gutiérrez, Study on the influence of attached mortar content on the properties of recycled concrete aggregate, Constr. Build. Mater. 23 (2009) 872–877. doi:10.1016/j.conbuildmat.2008.04.012.

[12] A. Akbarnezhad, K.C.G. Ong, M.H. Zhang, C.T. Tam, T.W.J. Foo, Microwave-assisted beneficiation of recycled concrete aggregates, Constr. Build. Mater. 25 (2011) 3469–3479. doi:10.1016/j.conbuildmat.2011.03.038.

[13] R. Movassaghi, Durability of Reinforced Concrete Incorporating Recycled Concrete as Aggregate (RCA), University of Waterloo, 2006.

[14] A. Abbas, G. Fathifazl, O. Burkan Isgor, A.G. Razaqpur, B. Fournier, S. Foo, Proposed method for determining the residual mortar content of recycled concrete aggregates, J. ASTM Int. 5 (2008) 1–12. doi:10.1520/JAI101087.

[15] K. Kalinowska-Wichrowska, E. Pawluczuk, M. Bołtryk, Waste-free technology for recycling concrete rubble, Constr. Build. Mater. 234 (2020) 117407. doi:10.1016/j.conbuildmat.2019.117407.

[16] S. Touzé, K. Bru, Y. Ménard, A. Weh, F. Von der Weid, Electrical fragmentation applied to the recycling of concrete waste – Effect on aggregate liberation, Int. J. Miner. Process. 158 (2017) 68–75. doi:10.1016/j.minpro.2016.11.009.

[17] H. Moosberg-Bustnes, B. Lagerblad, E. Forssberg, The function of fillers in concrete, Mater. Struct. 37 (2004) 74–81. doi:10.1007/bf02486602.

[18] S. Das, M. Aguayo, G. Sant, B. Mobasher, N. Neithalath, Fracture process zone and tensile behavior of blended binders containing limestone powder, Cem. Concr. Res. 73 (2015) 51–62. doi:10.1016/j.cemconres.2015.03.002.

LIGHTWEIGHT AGGREGATES MADE FROM CONSTRUCTION AND DEMOLITION WASTE – APPLICATION IN LIGHTWEIGHT CONCRETE AND MORTARS

Julia Seher[1],*, Katrin Rübner[1],*, Constanze Müller[1], Falk Martin[2], Nicole Pniok[3] and Bianca Dreisow[3]

(1) Bundanstalt für Materialforschung und -prüfung (BAM), Berlin, Germany

(2) Beton- und Naturstein Babelsberg GmbH, Potsdam, Germany

(3) Opus Denkmalpflege GmbH, Berlin, Germany

* *julia.seher@bam.de*, *katrin.ruebner@bam.de*

Abstract

Heterogeneous construction and demolition waste can be used as raw material to produce lightweight aggregates (LWA) similar to expanded clays. In the joint research project "REALight", LWA were produced from masonry rubble in a thermal expanding process using a pilot production plant with a rotary kiln. Our research focuses on the characterisation of the novel LWA and their use in different hydraulically bound applications.

Infra-lightweight concrete (ILC) was produced with the novel LWA, which accounts for two thirds of total aggregate volume, and Celitement, which is a hydraulic binder with a low carbon footprint. Its dry bulk density is ≤ 800 kg/m³. Strength and durability properties are comparable to ILC data from the literature.

Lime-based repair mortars (LRM) containing LWA are beneficial for sandstone conservation due to their similar properties regarding porosity, water absorption and strength. A two-layer repair mortar system, which consists of a filling mortar to fill large voids and a covering mortar to modulate the surface texture to the historic sandstone, was developed.

In our contribution, we present results of the LWA characterisation according to the European standard EN 13055:2016. Requirements and challenges of the use of the novel LWA in ILC and LRM are discussed.

1. Introduction

The utilization of mixed masonry rubble is limited due to its very heterogenous composition of various building materials e. g. concrete, bricks, aerated concrete, calcium silicate blocks, natural stones, plaster and mortar. Each material has different physical, mechanical and chemical properties and can contain different amounts of contaminates like sulphate. Therefore, mixed masonry rubble fines are mainly used for applications with low quality requirements, such as backfilling or profiling on landfills. Furthermore, if the masonry rubble has a high

sulphate content, the use will be forbidden due to groundwater protection or the risk of sulphate attack on concrete [1].

The idea of producing LWA from masonry rubble dates back to the early 2000s [2]. Initial studies were carried out at the Bauhaus-Universität Weimar [3-5]. Based on these results, the production process of LWA from mixed masonry rubble fines was developed from laboratory to pilot scale by the Weimar Institute of Applied Construction Research (IAB) [6-7]. The first step of this process is the production of green granules. They are produced in a multi-stage mechanical process, which consists of the following steps: crushing, screening, grinding, addition of an expanding agent (often SiC powder), homogenisation and wet granulation. Finally, the green granules are thermally treated in a rotary kiln, which causes expanding of the granules due to the thermal decomposition of the expanding agent. This process is very similar to the production of expanded clays. Today, a pilot plant with a 6-metre-long rotary kiln is operated by IAB. Over 2.4 tons of LWA were successfully produced for different application studies within the joint research project "REALight" [8-9].

In our contribution, we present the characteristics of the novel LWA, which were tested according to the European standard EN 13055:2016. Furthermore, we present results on application studies on infra-lightweight concrete (ILC) and lime-based repair mortars (LRM) containing the novel LWA.

2. Lightweight aggregates

2.1 Experimental

LWA were produced by IAB. Expanded granules were obtained from masonry rubble fines containing at least 60 % brick with an addition of 2 % SiC powder. LWA used for ILC were screened to the desired granule fractions of 2-4 mm and 4-8 mm. For the use in LRM, LWA 4-16 mm were crushed in a jaw crusher and screened into the granule fractions of 0-0.5 mm, 0.5-1 mm, 1-2 mm, 2-4 mm and 4-8 mm afterwards.

The characterisation of LWA was carried out according to EN 13055:2016. The particle size distributions were obtained by dry sieving according to EN 993-1:2012 and the particle shapes were studied with dynamic image analysis (CAMSIZER®, Retsch). The water absorption and the particle bulk density of granule fractions with sizes ≤ 2 mm were tested according to EN 13055:2016, Annex D and the BVK method [10]. The water suction time was extended to 10 min. Granule fractions with particle sizes ≥ 2 mm were tested according to EN 1097-6:2013, Annex C. The particle skeletal density was tested with helium pycnometry according to DIN 66137-2:2019. For this purpose, LWA were dried and ground to powder. The total porosity was calculated from particle bulk density and particle skeletal density according to DIN 66137-1:2019. The loose bulk density was tested according to EN 1097-3:1998.

To evaluate the environmental compatibility, eluates of each granule fraction (water/solid = 10 L/kg) were produced according to EN 12457-4:2002. The eluate composition was analysed with ion chromatography (IC) and inductively coupled plasma optical emission spectroscopy (ICP-OES).

2.2 Characterisation

All expanded granules, round and crushed, can be classified as lightweight aggregates according to EN 13055:2016. All granule fractions consist of 20-30 % undersized and no oversized particles (grading curves not shown). The loose bulk density of each granule fraction

is ≤ 1000 kg/m^3 and the particle bulk density is ≤ 2000 kg/m^3, which meet the requirements of the standard (Table 1). The total porosity of the round LWA is slightly higher than that of the crushed LWA. When the LWA, which are mostly macroporous [11], are crushed in the jaw crusher, the total porosity decreases with decreasing particle size. Cracks occur mainly along the pore walls. Therefore, the smaller the fragments, the more pores are broken down, which led to the loss of total porosity and rise in particle bulk density.

The appearance of round and crushed LWA is very different. Round LWA have an almost spherical shape whereas the crushed LWA are irregular formed. The difference in shape is expressed in the sphericity values and the aspect ratios of the LWA. For round LWA, these parameters are close to 1, which is typical for perfect spheres, whereas the values for crushed LWA decrease with decreasing particle size (Table 1).

The results of the environmental analysis of the different LWA fractions show that all values are below the limits according to German regulations [1]. No environmental risk for soil and water is to be expected from the novel LWA.

Table 1: Properties of round and crushed LWA [12-13].

Fraction [mm]	Loose bulk density [kg/m^3]	Particle bulk density [kg/m^3]	Particle skeletal density [kg/m^3]	Total porosity [%]	Water absorption [%]	Sphericity	Aspect ratio
				round			
2-4	518	1020	2680	61.9	19.9	0.922	0.828
4-8	467	890	2660	66.4	16.0	0.930	0.848
				crushed			
0-0.5	997	1980	2690	26.5	13.6	-	-
0.5-1	662	1760	2680	34.5	18.9	0.693	0.673
1-2	527	1490	2660	44.0	23.1	0.765	0.699
2-4	465	1230	2660	53.7	20.5	0.777	0.699
4-8	495	1130	2660	57.5	19.0	0.816	0.734

3. Infra-lightweight concrete

3.1 Background

Lightweight concrete has a very low dry bulk density (800-2000 kg/m³) compared to normal concrete. The reduction of the dry bulk density is primarily induced by using lightweight aggregates (e. g. pumice, expanded clay, expanded glass). In addition, infra-lightweight concrete (ILC) has a dry bulk density of less than 800 kg/m³. The development of ILC started more than a decade ago. The great thermal insulation properties of ILC make it interesting for building houses because no further thermal insulation is needed. Architects and civil engineers have more freedom for the design and construction of future buildings. Furthermore, the

absence of additional insulation material has a positive impact on the environment and the recycling of the building components is simplified. Until today, several houses have been built with ILC for demonstration purpose [14].

3.2 Experimental

Beton und Naturstein Babelsberg GmbH developed formulations for ILC using the expanded glass Liaver [15] and the low-CO_2 binder Celitement [16]. This concrete mixture was adapted for the use of the novel LWA. 65 Vol.-% of the aggregates were substituted by the round LWA fractions 2-4 mm and 4-8 mm. LWA were pre-wetted before use. The composition of the fresh ILC is given in Table 2. The w/b value was 0.46. Mixing was carried out in a Teka THZ 250 concrete mixer. The fresh concrete was transferred to specific moulds and stored according to the requirements of each test.

Table 2: Composition of infra-lightweight concrete with round LWA.

Material	Binder	Water	Silica	PCE SP	SRA	Liaver 0.5-1 mm	Liaver 1-2 mm	LWA 2-4 mm	LWA 4-8 mm
Amount [kg]	52.2	23.9	10.2	1.5	0.2	9.0	7.0	24.8	30.1

PCE SP = polycarboxylate ether superplasticizer, SRA = shrinkage reducing admixture

The compressive strength was tested on cubes (150 mm) and cylinders (d: 100 mm, h: 300 mm) according to EN 12390-3:2019. The flexural strength was determined on prisms (150 mm x 150 mm x 300 mm) according to EN 12390-5:2019. The dry bulk density was tested according to EN 12390-7:2019. The skeletal density was tested with helium pycnometry according to DIN 66137-2:2019. For this purpose, ILC cubes were dried and ground to powder. Afterwards, the total porosity was calculated from the dry bulk density and the skeletal density according to DIN 66137-1:2019. The static modulus of elasticity was determined according to EN 12390-13:2021 and the change in elongation (swelling and shrinkage) according to EN 12617-4:2002.

3.3 Results

The properties of hardened ILC at the age of 28 days are summarized in Table 3. The concrete can be just classified as infra-lightweight concrete due to its dry bulk density of 800 kg/m³. It could be assigned to compressive strength class L8/9. The concrete properties are similar to those reported in literature on other ILC, which contain expanded clay as LWA and ordinary cement [14, 17-18].

Table 3: Properties of infra-lightweight concrete with round LWA at the age of 28 days [13].

Compressive strength (cube) [MPa]	Compressive strength (cylinder) [MPa]	Flexural strength [MPa]	Dry bulk density [kg/m³]	Skeletal density [kg/m³]	Total porosity [%]	Static E-modulus [MPa]	Shrinkage [mm/m]
10.8	8.7	1.4	800	2200	63.5	4200	-0.43

Some exemplary photographs of ILC specimens are shown in Figure 1. Because of its low dry bulk density, ILC floats on water, making under water curing challenging. The low weight of

ILC is caused by the high total porosity due to the macroporous LWA [11] and many air voids, respectively.

Figure 1: Infra-lightweight concrete floating on water (left), close-up of cut surface area of an infra-lightweight concrete cylinder (right).

4. Lime-based repair mortars

4.1 Background

Lightweight mortars are preferred for sandstone conservation due to their lower weight compared to conventional repair mortars. Especially for the conservation of overhanging parts, the total weight of the mortar is crucial for a successful repair. The chemical, physical and mechanical properties as well as the appearance of the repair mortar must adapted to the specific conservation object. A long-lasting bond must be formed between the repair mortar and the damaged stone to avoid new damages during and after the restoration. Physical and mechanical mortar parameters to be considered include compressive strength, shrinkage, dynamic modulus of elasticity, moisture expansion, thermal expansion, water absorption coefficient, water vapour permeability and adhesive strength [19].

Opus Denkmalpflege GmbH and BAM are developing lightweight, lime-based repair mortars (LRM) using fine crushed LWA for the conservation of objects made from Cotta sandstone. This natural stone is often used for decorative building elements in Germany. A two-layer mortar system consisting of a filling and a covering mortar is suitable to repair large areas. The filling mortar is used to fill large voids, while the covering mortar is used to modulate the surface texture to the damaged stone. LRM are preferred in conservation. The repair mortar must be the weakest part of the system. If the repair mortar is lost or damaged, the system should fail either in the mortar itself or at the interface to the stone but never in the restored object. Therefore, the compressive strength of the mortar should be less than 60 % of the compressive strength of the damaged stone [19].

4.2 Experimental

Crushed LWA 0-0.5 mm were used for the covering LRM and crushed LWA 0-0.5 mm, 0.5-1 mm and 1-2 mm for the filling LRM. Different combinations of binders were used. As lime-based binders CL 90 and NHL 3.5 were selected. Tuff powder and Portland cement CEM I 42.5 were used as pozzolanic and hydraulic binder, respectively. The composition of each mortar mixture is given in Table 4.

Table 4: Composition of lime-based repair mortars with fine crushed LWA [12].

Material	C1	C2	C3	C4	F1	F2	F3	F4
	% by volume of dry mortar mixture							
CL 90	22.5	12.4	-	-	25.9	14.1	-	-
NHL 3.5	-	-	22.5	12.4	-	-	25.9	14.1
CEM I 42.5	-	12.4		12.4	-	14.1		14.1
Tuff powder	9.0	-	9.0		10.4	-	10.4	-
Tylose	0.7	0.7	0.7	0.7	0.7	0.6	0.7	0.6
Quartz 0.04-0.25 mm	45.1	49.5	45.1	49.5	-	-	-	-
LWA 0-0.5 mm	22.7	25.0	22.7	25.0	23.6	28.4	23.6	28.4
LWA 0.5-1 mm	-	-	-	-	22.1	28.7	22.1	28.7
LWA 1-2 mm	-	-	-	-	17.4	14.1	17.4	14.1
w/b	0.97	1.23	0.97	1.23	0.94	1.20	0.94	1.20

C = covering mortar, F = filling mortar

The mortars were prepared manually. Water was placed in a bowl, the previously prepared dry mortar mixture was added and everything was mixed for 1-2 minutes. The fresh mortar was left to stand for approx. 2 minutes and then filled into moulds. Cubes (20 mm) were produced for all tests. The moulds were stored at 23 °C and 65 % relative humidity.

The approach of EN 1097-6:2013 was adapted for the determination of the dry bulk density of the hardened mortar at the age of approx. 40 days. The compressive strength test was carried out on at least 3 cubes per mortar mixture at the age of 28 days with a ToniPRAX testing device (240 N/s, F_{max} 10 kN). The cubes were demoulded directly before the test.

4.3 Results

The determined physical and mechanical properties of LRM are summarized in Table 5. All filling LRM can be classified as lightweight mortar according to EN 998-2:2017 due to their low dry bulk density ($\leq$ 1250 kg/m^3). The covering mortars have a slightly higher dry bulk density ($\leq$ 1430 kg/m^3) because of the use of LWA fractions with higher particle bulk density (Table 1) and smaller amounts of LWA in the mortar mixtures (Table 5). For the restoration of Cotta sandstone, mortars assigned to mortar class M 2.5 or M 5 are desirable. Almost, all covering and filling mortars develop adequate compressive strength at the age of 28 days. Depending on the binder composition, the LRM achieve a compressive strength of 1.2-5.2 MPa.

Table 5: Properties of lime-based repair mortars with fine crushed LWA [12].

	C1	C2	C3	C4	F1	F2	F3	F4
Dry bulk density [kg/m^3]	1360	1430	1380	1430	1250	1190	1250	1230
Compressive strength [MPa]	2.0	3.3	3.0	5.2	1.2	2.7	2.1	4.1

Two exemplary micrographs of LRM are shown in Figure 2. These LRM were made with CL 90 and tuff powder. The difference in microstructure can be clearly seen from the micrographs: The covering mortar C1 consists of smaller particles with a denser packing, while the filling mortar F1 has a looser packing and some air voids.
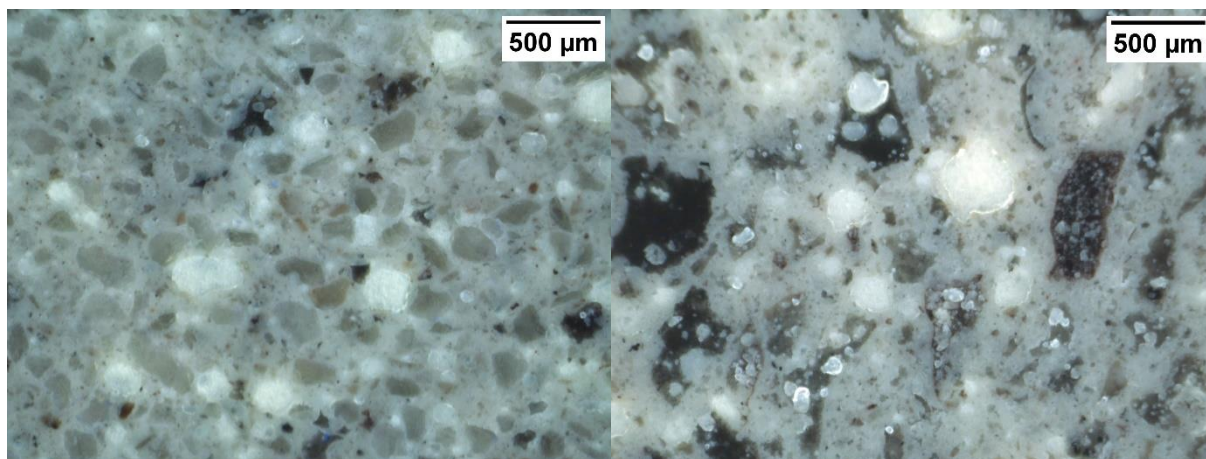
Figure 2: Micrographs of covering (left) and filling lime-based repair mortars (right). Crushed LWA appear as black asymmetric spots, air voids as white areas.

5. Conclusions

In the joint research project "REALight", LWA were produced from mixed masonry rubble fines in a thermal expanding process. These novel LWA, round and crushed, were tested as aggregates in lightweight concrete and mortars. The following results are achieved:
- successful production of an infra-lightweight concrete
- development of lightweight lime-based repair mortars for sandstone restoration

The development and comprehensive characterisation of lightweight concrete and mortars will be continued. The production of an infra-lightweight concrete made with expanded clay for comparison as well as the production of concrete elements for a pavilion will be performed. Moreover, optimised lime-based repair mortars will be applied on Cotta sandstone objects.

6. Acknowledgements

7. References

[1] Deutsches Institut für Bautechnik (Ed.) 'Muster-Verwaltungsvorschrift Technische Baubestimmungen (MVV TB), Ausgabe 2023/1, Anhang 10, Anforderungen an bauliche Anlagen bezüglich der Auswirkungen auf Boden und Gewässer (ABuG), Tabelle A-2' (DIfB, Berlin, 2023).

[2] Reinhold, M. and Müller, A. 'Lightweight aggregate produced from fine fractions of construction and demolition waste' Proceedings of the CIB Task Group 39 – Deconstruction Meeting, Karlsruhe, April, 2002, CIB Publication 272, Paper 3.

[3]   Schnell, A., Müller, A. and Rübner, K., 'Entwicklung von Leichtgranulaten aus Mauerwerkbruch für die Betonherstellung', in 'Innovative Technologien für Ressourceneffizienz in rohstoffintensiven Produktionsprozessen' (Fraunhofer Verlag, Stuttgart, 2013) 300-316.

[4]   Müller, A., Schnell, A. and Rübner, K., 'The Manufacture of Lightweight Aggregates from Recycled Masonry Rubble', *Construction and Building Materials* **98** (2015) 376-387.

[5]   Rübner, K., Schnell, A., Ihlenfeldt, T. and Vöge, M., 'Lightweight concrete with recycling aggregates made from masonry rubble and rubble-clay mixtures', Proceedings of IV International Conference Progress of Recycling in the Built Environment, Lisbon, October, 2018, (RILEM Publications SARL, Paris, 2018) 323-331.

[6]   Müller, A., Liebezeit, S. and Palzer, U. 'Building Aggregates from Gypsum-Containing Masonry Rubble – Part 1: Laboratory-Scale Tests' *Chemie Ingenieur Technik* (2022).

[7]   Müller, A., Liebezeit, S. and Palzer, U. 'Building 'Building Aggregates from Gypsum-Containing Masonry Rubble – Part 2: Investigations in Pilot Scale' *Chemie Ingenieur Technik* (2022).

[8]   Schnell, A., Rübner K., Seher, J., Liebezeit, S., Müller, A., Fenner, J., Martin, F. and Pniok, N. 'REALight – Leichtgranulate und REA-Gips aus feinkörnigen sulfatbelasteten Bau- und Abbruchabfällen und industriellen Nebenprodukten', Proceedings of 21st International Conference on Building Materials (ibausil 2023), Weimar, September, 2023 (ce/papers, Ernst & Sohn, Berlin, 2023) (in press).

[9]   Liebezeit, S., Müller, A. and Palzer, U. (2023) 'Leichte Gesteinskörnungen aus Mauerwerkbruch', Proceedings of 21st International Conference on Building Materials (ibausil 2023), Weimar, September, 2023 (ce/papers, Ernst & Sohn, Berlin, 2023) (in press).

[10] Wirtschaftsverband Mineralische Nebenprodukte e. V., 'Merkblatt BVK-Prüfverfahren für Leichtzuschläge' (WIN, Düsseldorf, 2016).

[11] Rübner, K., Prinz, C., Adolphs, J., Hempel, S. and Schnell, A. 'Microstructural Characterisation of Lightweight Granules Made from Masonry Rubble' *Microporous and Mesoporous Materials* **209** (2015) 113-121.

[12] Seher, J., Rübner, K., Müller, C., Pniok, N. and Dreisow B. 'Leichte Gesteinskörnungen hergestellt aus Bau- und Abbruchabfällen – Applikation in der Denkmalpflege', Proceedings of 21st International Conference on Building Materials (ibausil 2023), Weimar, September, 2023 (ce/papers, Ernst & Sohn, Berlin, 2023) (in press).

[13] Rübner, K., Seher, J., Müller, A., Schnell, A., Müller, C., Liebezeit, S. and Martin, F. 'REALight – Leichtgranulate und REA-Gips aus feinkörnigen sulfatbelasteten Bau- und Abbruchabfällen und industriellen Nebenprodukten' in 'Mauerwerk-Kalender 2024' (Ernst & Sohn, Berlin, 2024) (accepted).

[14] Elshahawi, M., Hückler, A. and Schlaich, M. 'Infra Lightweight Concrete: A Decade of Investigation (A Review) ' *Structural Concrete* **22** (S1) (2020) E152-E168.

[15] Liaver – Expanded Glass technologies, www.liaver.com, accessed: 14.03.2023.

[16] Celitement – advanced processing, www.celitement.de, accessed: 14.03.2023.

[17] Schlaich, M. and Hückler, A. 'Infraleichtbeton: Reif für die Praxis' *Beton- und Stahlbetonbau* **112** (2017) 772-783.

[18] Lösch, C., Hückler, A. and Schlaich, M. 'Infraleichtbeton' *Bauphysik* **41** (2019) 1-6.

[19] Snethlage, R. and Pfanner, M. 'Leitfaden Steinkonservierung, Planung von Untersuchungen und Maßnahmen zur Erhaltung von Denkmälern aus Naturstein', 5th Edn (Fraunhofer IRB Verlag, Stuttgart, 2020).

COMPARATIVE STUDY OF LIGHTWEIGHT EXPANDED AGGREGATES MADE FROM MASONRY RUBBLE OR CLAY

K. Rübner (1), A. Schnell (2), A. Müller (3)

(1) Bundesanstalt für Materialforschung und -prüfung (BAM), Germany

(2) Bauhaus-Universität Weimar, Germany

(3) Weimar Institute of Applied Construction Research, Germany

Abstract

Lightweight aggregates can be manufactured from masonry rubble by a thermal expanding process pursuing the idea of feedstock recycling. Throughout a series of research projects, the manufacturing process has been developed, optimized and scaled up. Various test results prove that the engineering properties of the new expanded masonry rubble aggregates are similar to those of traditional expanded clays. The aggregates show a heterogeneous and macroporous pore structure. The grains consist of cracks, cavities, large bulky pores and a solid skeleton containing small capillary pores as well as partly melted areas. But which differences and similarities exist to expanded clay aggregates, which are made from a relatively homogeneous clayey raw material? To answer this question, comparative studies on the chemical, physical, mineralogical and microstructural characteristics of expanded masonry rubble aggregates and commercial expanded clay aggregates have been conducted. In our contribution, results of particle shape and porosity measurements, mercury intrusion porosimetry and electron microscopy are presented. The microstructural characteristics are correlated with engineering properties, such as water absorption and particle strength.

1.   Introduction

The reuse of heterogeneous and fine-grained mineral construction and demolition waste (CDW) as building material is limited because of its unfavourable intrinsic properties. However, masonry rubble can be used as raw material for the manufacture of lightweight aggregates by a thermo-chemical material conversion process. The manufacturing technology has been developed from lab scale to pilot scale in a series of research projects [1-4]. The lightweight expanded masonry rubble aggregates are produced in a multistage process. The finely ground rubble, which is blended with 1-3 % silicon carbide powder (SiC) as expanding agent, is granulated. The green granules are burnt at about 1180 °C in a rotary kiln [1-6]. Similar to the manufacturing process of expanded clay, expansion occurs due to gas release (here from the SiC powder) at the same temperature where the material reaches a visco-plastic and partly melted or vitreous state [2, 5, 6]. The thermo-chemical material conversion leads to a successful

feedstock recycling of CDW. Today the Weimar Institute of Applied Construction Research is able to produce tonnes of lightweight expanded aggregates from masonry rubble in campaigns.

Lightweight aggregates are porous and almost spherical mineral grains. They are characterized by a particle bulk density smaller than 2000 kg/m³ or a loose particle bulk density smaller than 1200 kg/m³ according to EN 13055:2016. Commercially available aggregates are mechanical processed from natural stones, like pumice, tuff and other volcanic rocks, or produced by thermal treatment of natural raw materials, like clay, shale and perlite. To produce structural lightweight concretes the lightweight aggregates should possess sufficient particle strength beside the appropriate low intrinsic weight. Furthermore, a relatively high total porosity but moderate water absorption arising from well-proportioned fractions of open and closed pores is required. These properties are best met using lightweight expanded aggregates made from clay, which are usually used to produce lightweight concretes [7-9].

According to first applications in structural lightweight concretes, the expanded masonry rubble aggregates are said to be similar to expanded clay [3, 9-11]. To prove this statement, it is necessary to provide information on the basic characteristics of the aggregates. This paper gives a brief overview about the results of an experimental study on the textural and microstructural characteristics of lightweight expanded aggregates from masonry rubble (referred to as EMR) compared to expanded clay (referred to as EC).

2.   Experimental

2.1   Lightweight expanded aggregates

To produce the expanded masonry rubble aggregates, different masonry rubbles containing about 25 % or 50 % brick material served as raw material. The produced aggregates were divided by screening into the grain fractions 2-4 mm and 4-8 mm, which are typically used to produce lightweight concrete. Depending on the burning conditions and each detailed raw material preparation, aggregates with different particle bulk densities varying from 580 kg/m³ to 1800 kg/m³ were produced. For comparison, commercially available round or crushed expanded clays with particle bulk densities between 750 kg/m³ and 1400 kg/m³ were used.

All results are presented depending on the particle bulk density of the aggregates. Therefor the different EMR and EC samples are labelled with each density in kg/m³.

For the pore structure analyses, the following characteristic samples were selected: EMR 640, EMR 720, EMR 1160, EMR 1390, EMR 1410, EC 1040 and EC 1240. Before the analyses, the aggregates were washed and then dried at 105 °C.

2.2   Measuring methods

The particle shape of the aggregates was determined by means of the photo-optical particle analysis system CAMSIZER (Retsch). According to the principle of digital image processing, the particles pass in free fall through an extended LED strobe light source and two CCD cameras. The projected particle shadows are recorded at a rate of more than 60 images per second.

The micrographs of individual aggregates were taken using a camera NIKON with 105 mm focal length and an environmental scanning electron microscope XL 30 ESEM (Philips). The ESEM technique enables the investigation of the sample in a low vacuum atmosphere without applying a conductive layer on its surface.

For pore structure analyses, mercury intrusion porosimetry (MIP) is used. This method is based on the principle that mercury as a non-wetting liquid only intrudes into a porous system under pressure [12]. The volume of mercury that is injected into the sample was measured in dependence of the pressure applied. The MIP analyses were carried out by an Auto Pore III 9400 porosimeter system (Micromeritics) applying a maximum pressure of 405 MPa according to ISO 15901-1:2016. A collective of 10 to 20 grains was analysed during each run. Assuming a contact angle of 140° and a mercury surface tension of 0.48 N/m, a range of pores and pore entrances, respectively, from 4 nm to 320 µm pore diameter were assessable by mercury.

The total porosity of the lightweight aggregates was calculated from the ratio of particle bulk density and skeletal density according to DIN 66137-1:2003. The particle bulk density is understood as the ratio between mass of dry sample and the sample volume including the volume of closed and open pores but excluding the void spaces between particles. It was determined during the water absorption measurements according to EN 1097-6:2008. The skeletal density is understood as the ratio between mass of dry sample and the sample volume including the volume of closed (if present) but excluding open pores in the particles and void spaces between particles. It was measured with a gas pycnometer Accupyc 1330 (Micromeritics) using helium according to DIN 66137-2:2004. For the pycnometer analyses, the granules from water absorption experiments were dried and ground to powdered samples.

The water absorption after 24 hours was determined according to EN 1097-6:2008 by means of the pycnometer method. This method measures the mass increase of the oven dry aggregates due to water sucked by open pores and cavities under atmospheric pressure. The sample masses of water saturated aggregates and oven dry aggregates were determined.

The particle strength of the lightweight aggregates was measured on a particle collective using a test cylinder of 200 cm³ volume according to EN 13055-1:2002.

3.   Results and discussion

For expanded aggregates from masonry rubble as well as from clay, the thermal treatment in the rotary kiln leads to a structural hardening simultaneously with expansion of the grain volume and formation of the porous skeletal system. Depending on the nature and the quantity of expanding components as well as the burning conditions, lightweight aggregates with different particle bulk densities are produced.

3.1   Particle shape, surface texture and macroscopic structure

Visual observation alone shows that EMR aggregates consist of almost spherical grains just as the EC aggregates. The aggregates have a sphericity greater than 0.9 and an aspect ratio (ratio of particle length to particle width) between 1.1 and 1.2. The parameters in Figure 1 show that the particle shape of EMR is between round and crushed EC grains. The photographic micrographs of cut surfaces of EMR and EC embedded in cementitious paste are compared in Figure 2. ESEM micrographs of the aggregate's outer surface and inner core are shown in Figure 3. Both, EMR and EC aggregates, have macroscopically a relatively smooth outer surface (Fig. 2, right). But microscopically the surface texture is rather rough and porous due

to differently shaped crystals covering the surface (Fig. 3, left). Additionally, cavities and rough pores are visible.

Inside the grains, the micrographs of EMR and EC (Fig. 2, right and Fig. 3, right) show cracks, cavities and rough pores of millimetre size beside bulky macropores of micrometre size. The outer grain layer of varying thickness shows another porosity than the inner core. Considering a mixed bunch of EMR aggregates (not shown in the figures), differently porous grains are found. Beside fully expanded particles, least expanded or unexpanded grains with a small porous layer around an unexpanded core exist. Probably, the proportion of differently expanded grains determine the particle bulk density of EMR. In contrast, all EC grains show a macroscopically denser structure with an uniform expanding degree. This means that the varying particle bulk densities are reached by different expansion of all grains in a bunch.
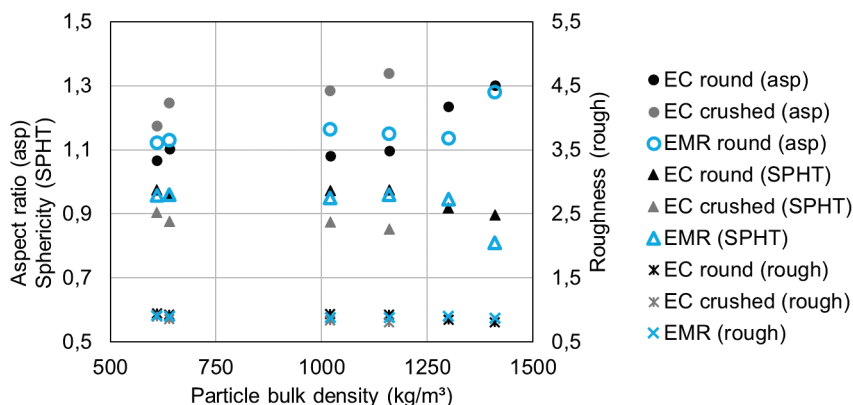
Figure 1: Particle shape parameters of expanded aggregates from masonry rubble (EMR) and clay (EC, round and crushed particles) depending on particle bulk density
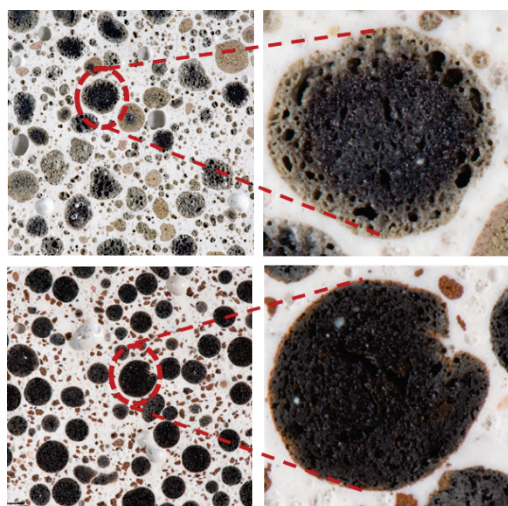
Figure 2: Photographic micrographs of cut grains of expanded aggregates 4-8 mm from masonry rubble (above) and clay (below) embedded in cementitious paste
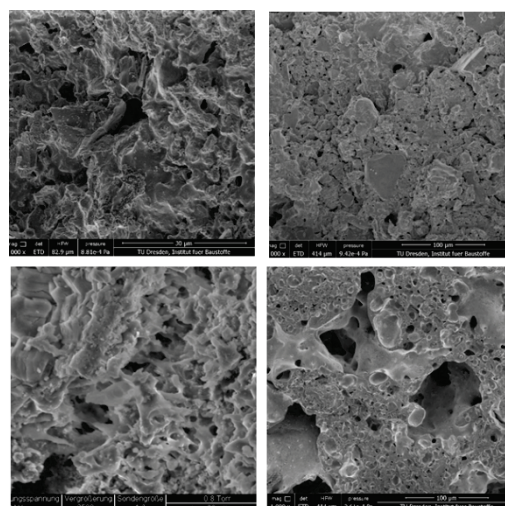
Figure 3: ESEM micrographs of the outer surface (left) and the fresh fractured inner core (right) of expanded aggregates from masonry rubble (above) and clay (below)

3.2 Microstructure

Looking deeper into the aggregate microstructure and considering smaller pores in micrometre and nanometre range, the ESEM micrographs in Fig. 3 on the right side show a heterogeneous pore structure of EMR and EC. Beside the macropores, smaller pores in the skeletal solid walls and partly melted vitreous areas exist. The finding of vitreous amorphous phases is proved by the results of XRD analysis [6].

A quantitative insight into the pore structure is provided by the results of MIP analysis. Typical cumulative and differential pore size distributions of EMR and EC aggregates are shown in Figure 4. Both, aggregates made from masonry rubble or clay, show a large intrusion/extrusion hysteresis. Almost all mercury remains entrapped into the pore system during extrusion. This phenomenon characterizes a completely non-uniform pore system with large macropores with sizes much greater than that of the pores leading into them. Such behaviour is known from bricks and high-burnt clay minerals [8, 12-14]. It proves that the EMR achieve the desired material characteristics similar to expanded clay. The qualitatively finding from ESEM that the two aggregates contain an irregular pore network consisting of non-uniform shaped pores is confirmed. Probably, large pores are randomly connected to each other or smaller pores via narrow throats (ink-bottle pores e.g.). These large pores remain filled with mercury during extrusion when the continuous mercury flow towards the sample surface is interrupted by the narrow pore throats.

The parameters total pore volume, apparent bulk density and most frequent pore diameter, which are derived from MIP analyses, are visualized in the bar charts in Figure 5. The total pore volumes of both types of aggregates, EMR and EC, are relatively high and vary between 250 kg/m³ und 1100 kg/m³ depending on the particle bulk density. The total pore volumes as well as the apparent porosities decrease with growing bulk densities. The two studied aggregate types have mainly macropores with pore sizes above 0.1 µm diameter (pore classification according to IUPAC and Setzer summarized in [15]). But the maxima of the pore volume distributions are different. The EMR aggregates contain mainly capillary pores with diameters greater than 5 µm. For expanded clays, the distribution maximum is shifted to smaller capillary and microcapillary pores of 0.1 to 5 µm diameter. Thus, the most frequent pore diameter is between 10 µm and 30 µm for EMR and at about 2 µm for EC, respectively.
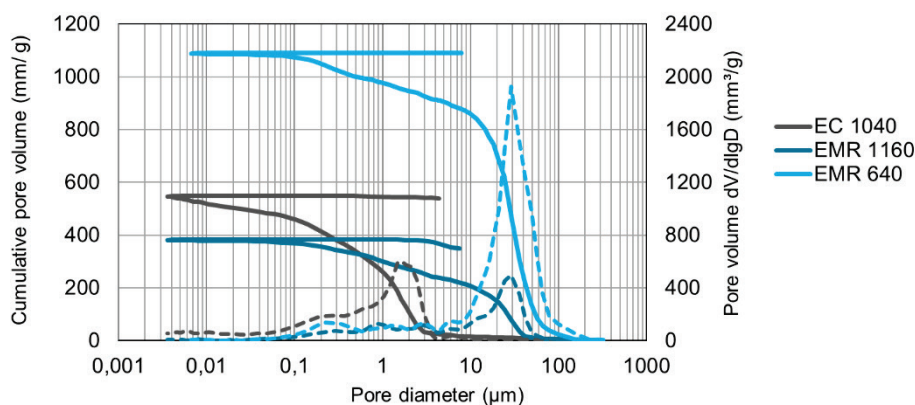
Figure 4: Typical pore size distributions of expanded masonry rubble aggregates (EMR) compared to expanded clay aggregates (EC) measured by mercury intrusion porosimetry
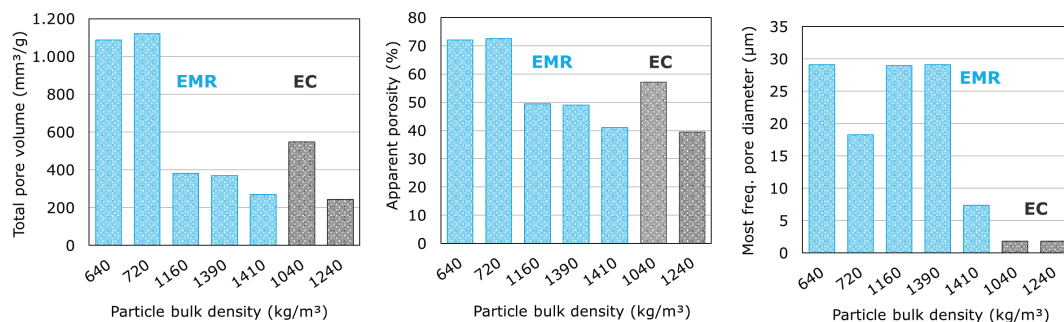
Figure 5: Results from MIP analyses of expanded masonry rubble aggregates (EMR) compared to expanded clay aggregates (EC) (from left to right: total pore volume, apparent porosity, most frequent pore diameter depending on particle bulk density)

3.3   Total porosity, water absorption and particle strength

The total porosity of EMR and EC, which has been calculated from particle bulk density and skeletal density, is shown depending on the particle bulk density in Figure 6. The porosity, which is important for the low intrinsic weight of the aggregates, is between 30 % and 80 %. Due to the almost similar solid density of all aggregates of about 2700 kg/m³, the total porosity decreases linearly with growing bulk densities regardless of the raw material and manufacturing conditions. The values are in accordance with the course of the apparent porosities determined by MIP but they are in general 1 % to 10 % higher. The difference can be related to the presence of closed pores as well as pores greater than 320 μm, which are outside the MIP measuring range.
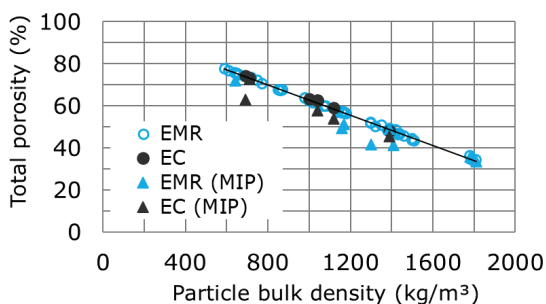
Figure 6: Total porosity of masonry rubble aggregates (EMR) compared to expanded clay aggregates (EC) depending on particle bulk density, values of apparent porosity from MIP are added
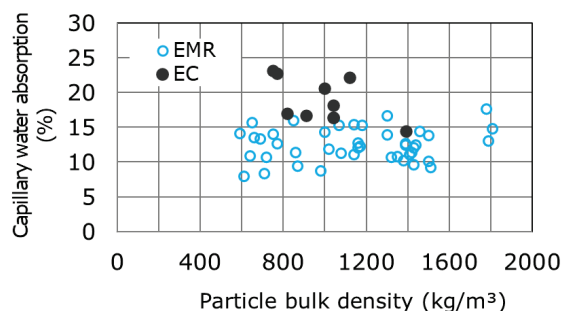
Figure 7: Water absorption of masonry rubble aggregates (EMR) compared to expanded clay aggregates (EC) depending on particle bulk density

The water absorption of all measured lightweight aggregates is shown depending on the particle bulk density in Figure 7. Due to the heterogeneous micro- and macrostructure and the partially vitreous surface areas, the two aggregate types show typically a moderate capillary water absorption with 8-16 % for EMR and 15-25 % for EC, respectively. The water absorption does

not show a systematic dependence on the particle bulk density for both, EMR and EC samples. The randomly interconnected pores of different sizes and shapes including ink-bottle and dead-end pores apparently cause the capillary suction of the aggregates to be sporadically slowed down or interrupted, for example when a narrow pore opens into a large-volume cavity. The microstructure of the EMR aggregates seems to have a more favourable effect on a low water absorption than the expanded clay.

Beside the low intrinsic weight that is provided by the porosity, the particle strength of the aggregates is important. The particle strength of EMR and EC samples increases with growing particle bulk density. The particle strength varies between 1.5 MPa and 8 MPa for the EMR as well the EC aggregates, which all reach a sufficient particle strength to be used in lightweight concretes [7, 8].

5.   Conclusions

The macro- and microstructural characteristics, the porosity, the water absorption and the particle strength of lightweight expanded aggregates from masonry rubble (EMR) and clay (EC), respectively, were compared.

Both lightweight aggregates, EMR and EC, consist of almost spherical particles.

Macroscopically, EC grains are evenly porous whereas EMR contain fully-, half- and non-expanded grains but both have same total porosities depending on the particle bulk density.

EMR and EC show a heterogeneous microstructure with partly melted vitreous surface areas, rough pores and bulky macropores as well as capillary pores in the skeletal walls. EC contains additionally a proportion of smaller sized microcapillaries < 2 μm diameter.

Despite the different starting materials, EMR and EC have in general similar macro- and microstructural characteristics so that they show the same engineering properties in dependence on the particle bulk density. Differences in pore structure are found, but they do not substantially influence the macroscopic properties.

The engineering properties of EMR and EC aggregates are well explained by the findings of porosity and microstructure measurements.

Acknowledgements

References

[1] Schnell, A., Müller, A. and Rübner, K., 'Entwicklung von Leichtgranulaten aus Mauerwerkbruch für die Betonherstellung', in 'Innovative Technologien für Ressourceneffizienz in rohstoffintensiven Produktionsprozessen' (Fraunhofer Verlag, Stuttgart, 2013) 300-316.

[2] Müller, A., Schnell, A. and Rübner, K., 'The Manufacture of Lightweight Aggregates from Recycled Masonry Rubble', *Constr. and Build. Mat.* **98** (2015) 376-387.

[3] Rübner, K., Schnell, A., Ihlenfeldt, T. and Vöge, M., ,Lightweight concrete with recycling aggregates made from masonry rubble and rubble-clay mixtures', 'Progress of Recycling in the Built Environment', RILEM Proc. PRO 124 (RILEM Publications S.A.R.L., Paris, 2018) 323-331.

[4] Schnell, A., Rübner, K., Seher, J.; Müller, C., Liebezeit, S., Müller, A., Fenner, J., Martin and F. Pniok, N., 'REALight - Leichtgranulate und REA-Gips aus feinkörnigen sulfatbelasteten Bau- und Abbruchabfällen und industriellen Nebenprodukten', '21. Internationale Baustofftagung ibausil' (F.A. Finger-Institut für Baustoffkunde, Bauhaus-Universität Weimar, Weimar, 2023).

[5] Schnell, A., Müller, A., Rübner, K. and Ludwig, H.-M., 'Mineralische Bauabfälle als Rohstoff für die Herstellung leichter Gesteinskörnungen', 'Recycling und Rohstoffe', Band 5 (TK Verlag, Neuruppin, 2012) 469-494.

[6] Rübner, K., Peplinski, B., Hempel, S., Schnell, A. and Müller, A., 'Novel lightweight aggregates from masonry rubble', '1st Int. Conference on the Chemistry of Construction Materials', GDCh monograph Vol. 46 (Gesellschaft Deutscher Chemiker, Frankfurt am Main, 2013) 27-30.

[7] Zhang, M.-H., Gjorv, O.E., 'Characteristics of lightweight aggregates for high-strength concrete', *ACI Material Journal* (1991) 150-158.

[8] Faust, T., 'Leichtbeton im Konstruktiven Ingenieurbau' (Ernst & Sohn, Berlin, 2003).

[9] Rübner K, Schnell A, Haamkens F, Jakubcová P. and Müller A., 'Leichtbeton aus Aufbaukörnungen', *Chem. Ing. Tech.* **84** (10) (2012)1792-1797.

[10] Rübner, K., Prinz, C., Adolphs, J., Hempel, S. and Schnell, A., 'Microstructural characterisation of lightweight granules made from masonry rubble', *Micropor. Mesopor. Mater.* **209** (2015) 113-121.

[11] Rübner, K., Schnell, A., Peplinski, B., Zimathies, A. and Hempel, S., 'Mikrostrukturelle und mineralogische Eigenschaften leichter Gesteinskörnungen aus Mauerwerkbruch', '19. Internationale Baustofftagung ibausil', Band 2 (F.A. Finger-Institut für Baustoffkunde, Bauhaus-Universität Weimar, Weimar, 2015) 1329-1336.

[12] Rübner K. and Hoffmann D., 'Characterization of mineral Building materials by mercury-intrusion porosimetry', *Part. Part. Syst. Charact.* **23** (2006) 20-28.

[13] Garderen, N., Clemens, F.J., Kaufmann, J., Urbanek, M., Binkowski, M., Graule, T. and Aneziris, C.G., 'Pore analysis of highly porous diatomite and clay based materials for fluidized bed reactors', *Micropor. Mesopor. Mater.* **151** (2012) 255–263.

[14] Hill, R.D., 'A study of pore-size distribution of fired clay bodies', *Trans. Br. Ceram. Soc.* **59** (1960) 189–212.

[15] Meyer, K., Lorenz, P., Röhl-Kuhn, B. and Klobes, P., 'Porous solids and their characterization', *Cryst. Res. Technol.* **29** (7) (1994) 903-930.

OPTIMIZATION OF MIXTURE DESIGN OF 3D PRINTABLE CONCRETE PRODUCED WITH RECYCLED AGGREGATES FROM 3D PRINTED CONCRETE WASTE

Pawel Sikora[1],*, Szymon Skibicki[1], Karol Federowicz[1], Marcin Hoffmann[2], Daniel Sibera[1], Krzysztof Cendrowski[1], Mateusz Techman[1] and João Nuno Pacheco[3],*

(1) Faculty of Civil and Environmental Engineering, West Pomeranian University of Technology in Szczecin, Poland

(2) Faculty of Mechanical Engineering and Mechatronics, West Pomeranian University of Technology in Szczecin, Poland

(3) CERIS / c5Lab – Sustainable Construction Materials Association, Portugal

* pawel.sikora@zut.edu.pl; jpacheco@c5lab.pt

Abstract

Additive manufacturing is an emerging technology that optimizes construction process, leading to environmental benefits. However, a large content of cement is required (at high environmental cost by volume of material) and end-of-life solutions for 3D printed concrete (3DPC) have not been investigated so far. This paper studies a circular model that uses 3DPC waste to replace cement for 3DPC production. This study optimizes 3DPC mixes by incorporation of fine recycled aggregates (fRA), obtained from recycling 3DPC waste, as partial cement replacement. Cement was replaced by 30 vol.% and 50 vol.% with this fRA. Rheological and early-age mechanical properties were evaluated. Study showed that it is possible to produce mixes with the addition of fRA instead of cement, and thus increasing the sand contribution in the mix substantially (aggregate-to-binder ratio from a/b=1.58 to a/b=2.86). However, rheological measurements confirmed substantial loss in static yield stress and recovery rate of the newly developed mixes, resulting in lower buildability and quality of material during printing. Loss in mechanical performance was also reported, however all mixes meet the mechanical criteria for structural applications. As an outcome an introduction of chemical admixtures is advised to produce mixes containing fRA with satisfactory fresh-state performance.

1.   Introduction

Construction and demolition waste (CDW) constitutes one of the largest materials flows globally, accounting for over 36% of all waste generated in the EU [1]. In this context, the EU sets an ambition goal towards reuse and recycling of CDW. The recovery of CDW as a secondary raw material has a twofold environmental advantage: the decrease of the consumption of mineral natural resources and the reduction of landfill disposals. Fine recycled aggregate (fRA) is commonly used for backfilling (which leads to low added value), landfilled (without any added value) or stockpiled at CDW plants indefinitely (in practical

terms, landfilling). Therefore, finding end-goals for fRA is particularly relevant in the current context of the EU's Circular Economy Action Plan [2]. In this context, the market uptake of fRA can be driven by developing its use in higher-grade applications through innovation such as additive manufacturing of concrete.

The mixture design of 3D printed concrete (3DPC) substantially differs from that of conventional concrete. The design of 3DPC requires substantial mixture modifications in order to meet special requirements on extrudability, buildability and setting time. The material requires high-static yield stress and low-dynamic yield stress of concrete, therefore highly thixotropic behaviour is intended. This implies use of binder (mostly composed of cement) with amounts exceeding 700 kg/m^3 (roughly two times higher than in conventional concrete). According to a literature survey performed by Pacheco et al. [3], the binder content of 96% of all 3DPC mixes found (total of 165) is higher than 500 kg/m^3 (Figure 1a). In addition, due to rheological and technical limitations of pumps, as well as the requirement that the individual layers of 3DPC have small cross-section (both height and width are typically smaller than 25 mm), coarse aggregates (>4 mm) are typically absent in 3DPC mix design. Figure 1 presents the size of aggregates used for 3DPC confirming that, in most of the mixes (total of: 218), the aggregate size does not exceed 2 mm (Figure 1b). Similarly, 3D printed concrete has a high content of fine aggregates, a major threat to natural resources.
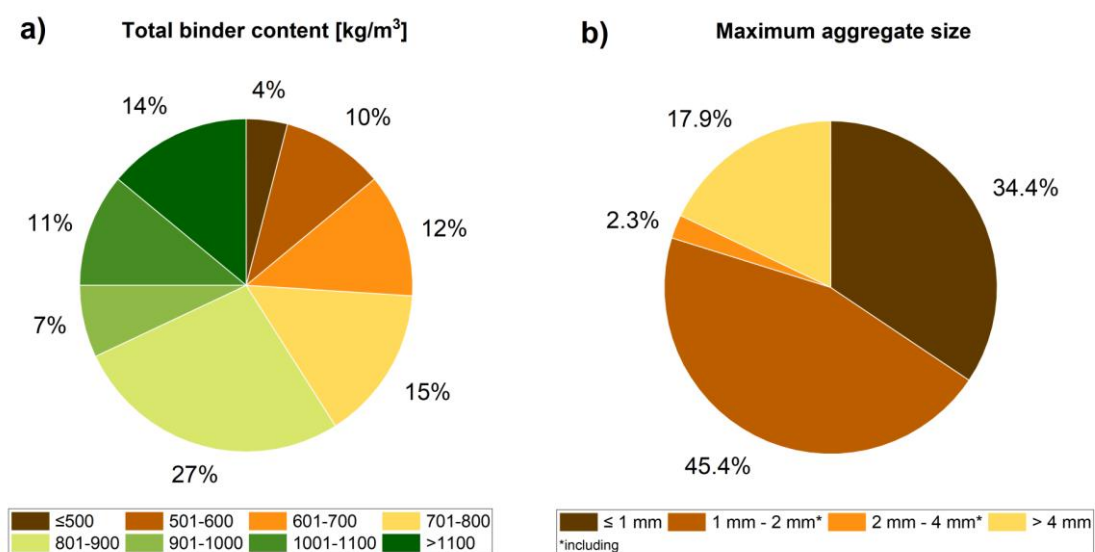
Figure 1: Percentage distribution of the typical binder content (a) and maximum aggregate size used in 3D printed mixtures (b). Reprinted from Pacheco et al. [3] (Creative Commons Attribution 4.0 International)

Although, some of the characteristics of fRA such as high water absorption and irregularity in shape could be considered as undesired in conventional concretes, they could be taken in account while designing 3D printed concrete mixes towards tailoring the rheological properties of 3D printed mix. To date limited knowledge on application of fRA for 3D printing applications, however some research groups confirmed its satisfactory performance in 3D printed concrete [4-6].

Based on the abovementioned literature and scarce information on the design of 3DPC with fRA, a preliminary study was held towards optimizing the mix design by inclusion of fRA produced from recycling of 3DPC. The following assumptions have been made:

- It is possible to produce a mixture design with lower cement content by introducing fRA in the mix.

- Due to high water absorption of the fRA, cement could be potentially replaced with fRA without significant effects on rheological performance.

- To better understand the influence of the fRA in the properties of 3DPC, the superplasticizer dosage remained fixed for all mixes.

- 3D printing process of testing columns was performed in the same printing conditions (fixed printing parameters, including speed and methodology).

As a first approximation, it was assumed that no changes to the water content of the mix were needed. This is based on the fact that the replacement of cement (lower particle size and higher surface area) is replaced by fRA, which are rough and have high water absorption. This hypothesis was confirmed. Otherwise, the water content of the mix would have been adjusted.

The assumptions and experimental design are part of a comprehensive research programme that aims at finding alternatives for the use of fRA in 3DPC. The present study aims at a simplified mix design procedure that maximizes the environmental benefits of this replacement (since cement is replaced with fRA without additional changes to the mix design), at technical cost (presumed loss of open time, workability and extrudability). Other experiments are ongoing and aim at maximizing fresh and hardened-state technical performance.

2.   Materials and Methods

CEM I 42.5 R, fly ash and silica fume were used as a binder component. Natural river sand (NA) in size of <2 mm obtained from Bielinek, Poland was used. The fRA were produced from waste 3D printed concrete produced at the West Pomeranian University of Technology in Szczecin and using the same raw materials used in the present research. In all cases, the compressive strength material exceeded 50 MPa and examples of the compositions if these 3DPC are shown in e.g. [7-8]. The material was crushed using a jaw crusher (LAB-08-240, EKO-LAB, Poland) and sieved below 2 mm. The morphological features of NA and fRA is presented in Figure 2.

A reference mix (R0) and two mixes containing 30 vol% (R30) and 50 vol% (R50) replacement of cement with fRA were produced. The mixture design is presented in Table 1. The proposed optimization strategy allowed to reduce the cement content in the mixture from 560 kg/m^3 to 280 kg/m^3 along with increasing the a/b ratio by 81%.
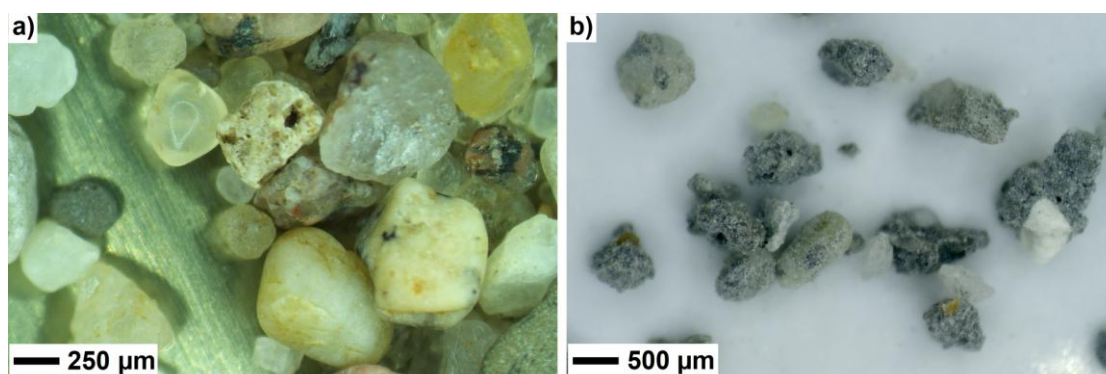
Figure 2: Optical microscope image of NA (a) and fRA produced from waste 3DPC (b).

Table 1: Mixture design of 3DPC (kg/m^3) and aggregate-to-binder ratio

Mix	Cement	Fly ash	Silica fume	NA	fRA	Water	SP	a/b ratio
R0	560	160	80	1266	0	225	2.20	1.58
R30	392	160	80	1266	132	225	2.20	2.21
R50	280	160	80	1266	220	225	2.20	2.86

Rheological properties were determined using a modular compact rheometer MCR 72 (Anton Paar). A vane geometry was used along with a customized ribbed cup (v=120 cm^3) to exclude potential wall-slip effect. The static yield stress was determined at shear rate of 0.1 s^{-1} in function of time (up to 45 min) following the methodology presented by Chen et al. [9]. Similarly, three interval thixotropy test (3iTT) was performed to observe the apparent viscosity recovery after the 3DPC structure has been broken down (recovery rate). The consistency of developed material was measured through the flow table test conforming EN 1015-3. Green strength of 3DPC was assessed by uniaxial unconfined compressive test. The tests were performed by special precision press device with precise LVDT and force sensor (up to 500 N). The device and testing methodology was described comprehensively in [10]. Flexural and compressive strength was determined on cast prismatic specimens in size of 40×40×160 mm^3 after 2 and 28 d of curing. The tests were performed according to EN 1015-11. The printing process was performed by a 3-degree-of-freedom Cartesian robot attached to a pump. The printing test consisted of printing a column with a diameter of 150 mm and a height of 420 mm with speed of 100 mm/s.

If the buildability of the mix was not sufficient to achieve the mentioned height, the test was ended due to structure collapse. In this case, the maximum height of the specimen was measured as the height limit. Additionally, visual inspection of element quality was performed.

3.   Results and Discussion

3.1.   Fresh properties

Figure 3 presents the static yield stress of mixes as function of time. Clearly a loss in static yield stress of mixes is visible in specimens containing higher fRA content. After 45 min, the static yield stress values of R30 and R50 were comparable to the value obtained for mix R0 after 10 min. Recovery rate determined by 3iTT is summarized in Table 2. Clearly a decrement of thixotropic behaviour of mixture can be observed with higher aggregate content reaching up to 20% loss in recovery rate when 50 vol.% of fRA is present. The green properties, including green strength and green Young's modulus significantly decrease with the addition of fRA. It should be noted that the green strength for mixes R30 and R50 is reduced by 52.1% and 71.9%, respectively. The decrement in green Young's modulus is 48% and 69% for R30 and R50, respectively. The green strength for all mixes ranged between 6.3 kPa and 22.3 kPa. These values agree with other studies [11-12] and are sufficient for printing the structure. The relation between spread flow obtained by flow table method is opposite to the green strength properties. With the addition with fRA, the spread flow decreases by 11.70% and 20.9% for R30 and R50, respectively. This phenomenon shows that for the examined mixes, there is no relationship between spread flow (as a simple rheology test) and green strength. The similar observation was described by [13-14]. In this paper, this observation is due to the incorporation of fRA being associated with a reduction of the content of cement.
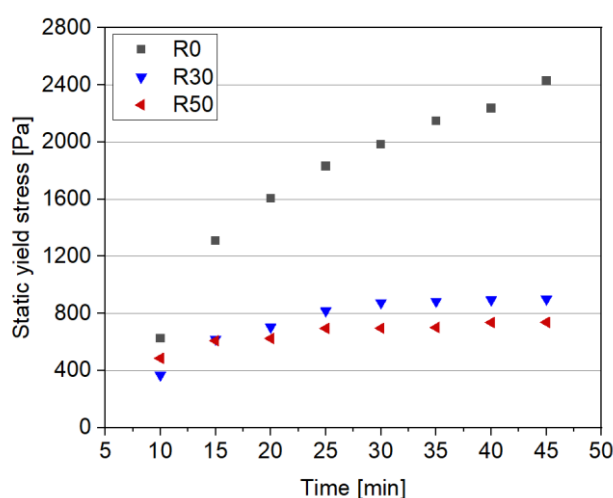
Figure 3: Static yield stress development of 3DPC as function of time

Table 2: Results of flow table, green strength and recovery rate (3IT)

Mix	Spread flow [mm]	σ_{max} [kPa]	Green Young's modulus [kPa]	Recovery rate [%]
R0	163	22.29	352.4	100
R30	144	10.68	184.9	88
R50	129	6.26	109.5	80

3.2. Hardened mechanical properties

The mechanical properties results are present in Table 3. The presented data contain mean values for compressive (f_c) and flexural (f_f) strength and standard deviation (StD) for each result. The addition of fRA influences the mechanical properties negatively due to the reduction in the amount of cement in the mix. The results show that the reduction in compressive strength is up to 67.6% for the R50 mix. In the case of flexural strength, the reduction is up to 46.7%. The differences between specimens with fRA and without fRA are higher in the first days of curing (i.e., for compressive strength, the reduction is up to 45.0% and 67.6% for 2 days and 28 days of curing, respectively). However, it is worth noting that, even with the highest fRA incorporation rate, the 28 days mechanical properties are sufficient to considered material for structural applications.

Table 3: Results of compressive and flexural strength

Mix	Compressive strength				Flexural strength			
	2 days		28 days		2 days		28 days	
	f_c [MPa]	StD [MPa]	f_c [MPa]	StD [MPa]	f_f [MPa]	StD [MPa]	f_f [MPa]	StD [MPa]
R0	33.7	2.81	82.1	14.29	5.4	0.18	8.7	0.94
R30	18.6	1.61	61.3	2.19	3.8	0.09	6.8	0.53
R50	10.9	1.32	41.6	5.53	2.9	0.38	5.1	0.34

3.3. Extrusion and print quality testing

The printing process was carried out according to the procedure described in Section 2. Figure 4 presents an example of the printing process. The printing test shows that the reference mix, R0 (without fRA), exhibits the highest buildability values. This mix was able to successfully print a column with a height of 420 mm (29 layers) without collapse. The printing process of the mentioned column is presented in Figure 4a. However, for specimens with 30% and 50% of fRA, the printing process ended in collapse. For R30, it was possible to print 14 layers (21 cm height), and for R50, only 10 layers (15 cm height) could be printed. The collapse of the column was classified as a plastic collapse (Figure 4b). Due to the overload on the bottom layers, the maximum stress was exceeded, resulting in a plastic collapse. This is a consequence of the low green strength observed in the fresh properties tests. Additionally, it should be noted that, as the amount of fRA increases, the number of surface defects also increases, leading to a deterioration in surface quality (Figure 4). For the reference mix (R0), the surface has only minor defects, which is in contrast to the specimens containing fRA.

Figure 4: Printing process results: a) specimen R0 during printing; b) specimen R30 after collapse; c) specimen R50 during printing process

4. Conclusions

The following conclusions can be drawn from this work:

- It is possible to print mixes with the replacement of cement by fRA, and thus increasing the sand contribution in the mix substantially (aggregate-to-binder ratio from a/b=1.58 to a/b=2.86) without any additional mix modification. However, rheological measurements confirmed substantial loss in static yield stress and recovery rate of the newly developed mixes. These mixes should be directed to non-demanding applications such as small scale non-bearing elements etc.

- The tests show that the addition of fRA deteriorates the green strength by up to 71.9%. Nevertheless, the results obtained are still suitable for printing small structures at a speed of 100 mm/s. This was confirmed by the buildability test, which allowed the printing of structures with heights of 21 cm and 15 cm for R30 and R50 mixes, respectively.

- The hardened mechanical properties were reduced in mixes with the addition of fRA and this phenomenon is significantly noticeable in the early stages of curing. However, the reduction in compressive and flexural strength at 28 days is up to 49.3% and 41%, respectively (for the R50 mix).

This preliminary research shows that the idea of replacing cement with fRA is suitable for 3D printing. Despite the fact that the addition of fRA deteriorates the green properties of the 3DPC, this approach aligns with sustainable development goals, such as reducing CO_2 emissions and preserving natural aggregates. Further works on optimization/introduction of chemical additives are required towards achieving better buildability, green strength, and hardened properties. Moreover, further studies related to conventional replacement of natural sand with fRA as well as research on the possible advantages that arise from the water absorption of the RA (increase of buildability and internal curing to mitigate shrinkage) should be performed.

5. Acknowledgements

6.   References

[1]   EUROSTAT (2022). ENV_WAS: European statistics on waste, EUROSTAT

[2]   European Commission (2020). COM/2020/98 final - Communication from the Commission to the European Parliament, the Council, the European Economic and Social Committee and the Committee of Regions: A new circular economy Action Plan for a cleaner and more competitive Europe.

[3]   Pacheco, J., Santos, K., Sikora, P., Skibicki, S., Techman, M., Federowicz, K., Reales, O., Vieira, M., Leporace-Guimil, B., Tošić, N., Pepe, M., 'Recycled Aggregates and 3D printing technology: production requirements, printability and way forward (Recycl3D project report D.1.1.)', *Zenodo* (2023) https://doi.org/10.5281/zenodo.7866197.

[4]   Ding, T., Xiao, J., Zou, S., Wang, Y., 'Hardened properties of layered 3D printed concrete with recycled sand', *Cem Concr Compos.* **113** (2020) 103724.

[5]   Duan, Z., H, S., Xiao, J., Singh, A., 'Rheological properties of mortar containing recycled powders from construction and demolition wastes', *Constr Build Mater.* **237** (2020) 117622.

[6]   Xiao, J., Zou, S., Yu, Y., Wang., Y., Ding, T., Zhu, Y., Yu, J., Li, S., Duan, Z., Wu., Y., Li, L., '3D recycled mortar printing: System development, process design, material properties and on-site printing', *J. Build. Eng*. **32** (2020) 101779.

[7]   Sikora, P., Techman, M., Federowicz, K., El-Khayatt, A. M., Saudi, H.A., Elrahman, M.A., Hoffmann, M., Stephan, D., Chung, S-Y., 'Insight into the microstructural and durability characteristics of 3D printed concrete: Cast versus printed specimens', *Case Stud. Constr. Mater.* **17** (2022) e01320.

[8]   Skibicki, S., Techman, M., Federowicz, K., Olczyk, N., Hoffmann, M., 'Experimental Study of Hardened Young's Modulus for 3D Printed Mortar', *Materials* **14**(24) (2021) 7643.

[9]   Chen, M., Yang, L., Zheng, Y., Huang, Y., Li, L., Zhao, P., Wang, S., Lu, L., Cheng, X., 'Yield stress and thixotropy control of 3D-printed calcium sulfoaluminate cement composites with metakaolin related to structural build-up', *Constr Build Mater.* **252** (2020) 119090.

[10] Skibicki, S., Jakubowska, P., Kaszyńska, M., Sibera, D., Cendrowski, K., Hoffmann, M., 'Early-Age Mechanical Properties of 3D-Printed Mortar with Spent Garnet', *Materials* **15**(1) (2021).

[11] Wolfs, R., Bos, F.P., Salet, T., 'Early age mechanical behaviour of 3D printed concrete: Numerical modelling and experimental testing', *Cem Concr Res.* **106** (2018) 103–16.

[12] Casagrande, L., Esposito, L., Menna, C., Asprone, D., Auricchio, F., 'Effect of testing procedures on buildability properties of 3D-printable concrete', *Constr Build Mater.* **245** (2020) 118286.

[13] Jones, S.Z., Bentz, D.P., Martys, N.S., George, W.L., Thomas, A., 'Rheological Control of 3D Printable Cement Paste and Mortars', in: 'First RILEM International Conference on Concrete and Digital Fabrication - Digital Concrete 2018'. Cham, Switzerland: Springer; 2019.

[14] Kawashima, S., Chaouche, M., Corr, D.J., Shah, S.P., 'Rate of thixotropic rebuilding of cement pastes modified with highly purified attapulgite clays', *Cem Concr Res.* **53** (2013) 112–8.

ECO-MORTARS FOR SHOTCRETING IN CIRCULAR CONSTRUCTION

Valoni, N.A.[1],*, Barroso, M.[1], Sáez del Bosque, I.F. [1], Medina, G.[2], Corroto, M.[3], Sánchez de Rojas, M.I.[4] and Medina, C.[1],**

(1) Cáceres Polytechnic School, University of Extremadura, Cáceres, Spain.

(2) School of Industrial and Computer Engineering, University of Leon, Leon, Spain

(3) MC OTIFA, Alcorcón, Madrid, Spain

(4) Eduardo Torroja Institute of Construction Sciences, Higher Council for Scientific Research, Madrid, Spain.

* nvaloni@unex.es/ ** cmedinam@unex.es

Abstract

The construction industry as a whole and construction material manufacturers in particular are making an effort to use raw materials and energy more efficiently and shrink the carbon footprint of their end products in response to the need to transition to a circular economy, a model geared to minimal resource and energy consumption.

This research work evaluates the feasibility of incorporating recycled fines from mixed construction and demolition waste in the formulation of eco-mortars for shotcreting, which will contribute to reducing the carbon footprint of construction projects. To achieve this objective, the physical properties (density and consistence) in the fresh state and the mechanical performance (compressive and tensile strength) in the hardened state of the formulated mortars were evaluated. The results show the technical feasibility of using these new secondary raw materials in formulating this type of eco-mortar.

1. Introduction

The building sector is a key target in this policy for circular economy, a regenerative economic system in which material and energy consumption must be minimized. The construction sector requires vast amounts of resources and accounts for about 50% of all extracted material [1], of 40% of global energy consumption and consumes 16% of the water in the world [2]. Additionally, a recent report [3] revealed that the EU-27 generates around 374 Mt of Construction and Demolition Waste (CDW), which represents 35% of the solid waste generated each year. Despite the great efforts and the potential for recovering these waste streams, the level of recycling and material recovery of construction and demolition waste differ significantly across the EU, ranging from less than 24% to over 90% in 2018, (88% in UE-28 and 75% in Spain). Within the recycled aggregates from CDW, mixed recycled aggregates (CDWm) stand out for their importance with 67% of the total volume of CDW [4]. The range of particle size distribution in this aggregate (fine particles 0 - 4 mm) may be an obstacle to specifying it in new product design. These fractions are not currently included in the different international regulations, so their recovery as granular skeleton represents an advance in their knowledge and application.

Mortars are frequently used as bedding mortars, to layer masonry units, to re-point masonry joints, to coat outdoor and indoor walls and ceilings (renders and plasters, respectively) or as screeds in floor [5] and to repair other infrastructures (i.e., tunnels, bridges…). The selection of appropriate components (i.e., reduce to natural resources by recycled materials), and of their proportion, to achieve adequate workability, strength and durability requirements, are key challenges for mortars production more sustainable.

In this context, in the last decade, the scientific community has increased the amount of research into investigating the potential use of CDW fine aggregates (<4.75 mm) in the manufacture of rendering mortars, observing that for percentages lower than 30%, its performance was equal to or higher than reference mortars [6, 7]. Along this same line, Jesus et al. [8] established that the optimal recycled sand percentage in concrete and mixed with a particle size of 0-0.149 mm is 20% and 15% substitution, respectively.

The objective of this research work is the optimal formulation of an eco-mortar for shotcreting that has 100% mixed fine aggregate as a substitute for natural aggregate through an initial classification of them. This classification entailed determining the physical properties (density and consistency) and mechanical properties (compressive and flexural strength) in the fresh and hardened state, respectively.

2. Materials and methods

2.1 Materials and formulated mortars

The materials used are classified into three large groups: i) binder (cement); ii) minerals that make up the granular skeleton (calcium hydroxide, metakaolin, natural sand, mixed recycled sand and light aggregates); and iii) other components (fibres and additives).

Table 1: Mix A and Mix B composition.

Materials (% en peso)	Mix A	Mix B
Cement	24.0	24.0
Calcium hydroxide	6.0	6.0
Metakaolin	6.0	6.0
Mixed recycled sand	-	40.2
Natural sand	40.2	-
Light aggregates	21.0	21.0
Others*	2.8	2.8
Water/solid ratio	0.84	0.84

*Note. - *Fibres and additives (fluidiser, water-retentive and air entraining).*

As for the aggregates, a natural crushed greywacke sand (0/6 mm) and a recycled sand (0/6 mm) from mixed CDW from the ARAPLASA waste management plant in the north of Cáceres, Spain were used. The recycled sand consists mainly of concrete components (~44% by weight), unbound aggregate (~43% by weight) and ceramic material (~11% by weight) and has an apparent density of 2.70 kg/dm^3, a lower value to that of natural sand (2.99 kg/dm^3). Both

aggregates were screened, selecting the fraction less than 2 mm. Regarding the lightweight aggregates, perlite and vermiculite with a maximum size of 2 mm were used.

The cement used was an ordinary Portland cement CEM I 42.5R that meets the requirements of the European EN 197-1 standard [9].

Finally, Table 1 shows the composition of the mix as a percentage by weight of each of the components that make up the new eco-mortars.

2.2 Methods

The mixing process of the constituent components of eco-mortars (Mix A and Mix B), together with the subsequent mixing process, plays a fundamental role in their final performance. A specific methodology for the mixing order has therefore been developed, establishing the mixing of the heaviest components, with the highest density, to the lightest ones, as a criterion. The mixing process consisted of the following phases: i) 45 seconds at slow speed (150±5 rpm); ii) 60 seconds at fast speed (285±10 rpm). The mixer used was a Matest model E093 series E093/AI/0017.

The physical classification of the powder mixes shown in table 1 consisted of determining the granulometric curve according to the EN 1015-1 standard [10] and the apparent powder density according to the calibrated funnel method [11], mixing only those granular components (binder and mineral charges) that constitute the working formula.

Subsequently, Mixes A and B were mixed according to the previously described protocol, evaluating the physical run-off and apparent density properties on these eco-mortars in the fresh state according to the methodology included in the EN 1015-3 [12] and EN 1015-6 [13] standards, respectively. Next, the 4x4x16 cm prismatic moulds were filled (three test tubes/blend and breaking age). These moulds were de-moulded 48 hours after their manufacture and maintained at a temperature of 20ºC±3ºC and relative humidity 65±5% for 7 and 28 days. Finally, these specimens were subjected to the flexural and compression strength test according to the EN 1015-11 standard [14], in an Eptisa model S-120 and series 10 4230 multi-test press.

3. Results

3.1 Physical properties of powder mixes

Figure 1 shows the granulometric curve of the mix of granular components (binders and mineral) that make up Mix A and Mix B, noting that both are continuous and have a maximum size of 2 mm. It can also be seen that the percentage of particles less than 0.080 mm is ~27% and ~30% by weight for Mix A and B. These values are within the theoretical optimal range of fines (24-35%) for the granular skeleton of this type of protection and coating mortars.
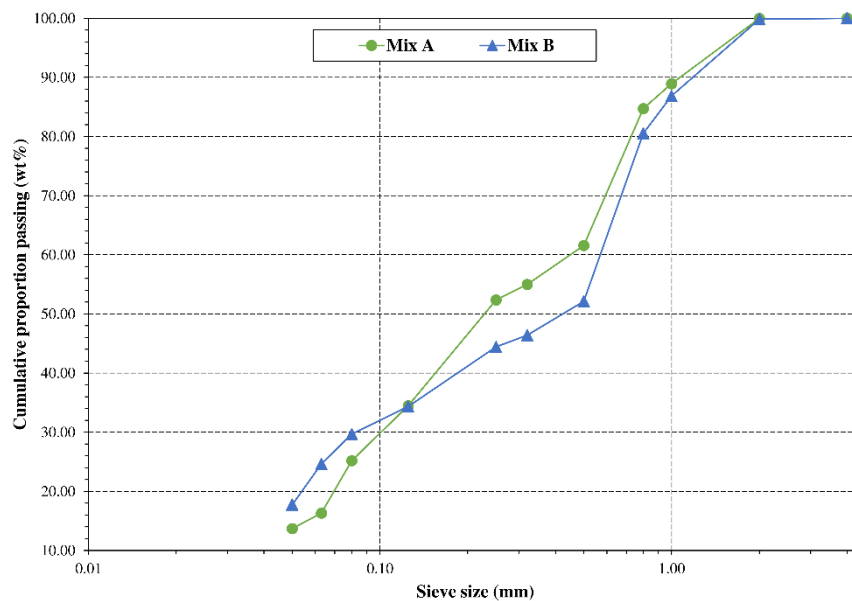
Figure 1: Mix A and B granulometric curve

Finally, the apparent powder density of Mixes A and B is 529.88 kg/L and 504.74 kg/L, respectively. These values are important for the subsequent industrialisation process, as they are industrial products that are marketed in bags of 8-15 kg/bag.

3.2 Physical properties of eco-mortars in the fresh state

Table 2 shows the apparent density and consistency values of the formulated eco-mortars. It shows that the apparent density of the eco-mortar made with Mix B is lower ($\Delta\rho_{mix\ B}$ B~1.3% compared to Mix A) than that formulated with Mix A, due to the lower density of the recycled aggregate compared to Mix A to the natural aggregate associated with its more porous micro-structure. This trend has previously been recorded by Silva et al. [15] who observed that for percentages of 100% CDW recycled aggregate in coating and masonry mortars, values of 1.08 – 0.72 times lower than the reference mortars were recorded.

Table 2: Physical properties in fresh state of formulated eco-mortars.

Property	Eco - mortar	
	Mix A	Mix B
Bulk density (kg/m^3)	643.42	635.06
Consistence (mm)	166.77	161.64

Regarding the consistency values, both eco-mortars have a plastic consistency (140-200 mm) according to EN 1015-6 [13], revealing that the addition of mixed recycled aggregate has no significant effect on the rheological property. Once again, it is evident that the addition of mixed recycled aggregate translates into a small decrease of ~3% compared to the eco-mortar made with Mix A. This trend was previously observed by Miranda et al. [16] who recorded a linear decrease in density with the addition of recycled aggregate, which is due to water absorption and the shape of the aggregates used.

3.3 Mechanical properties

Figure 2a) and 2b) present the results of flexural and compressive strength of the eco-mortars made with Mix A and B at 7 and 28 days of curing. Regarding the values obtained for compressive strength at 28 days, note that the mortars made with Mix A and Mix B can be classified as CS I (0.4 MPa – 2.5 MPa), according to the classification proposed by the EN 998-1 standard [17] for rendering and plastering mortars.
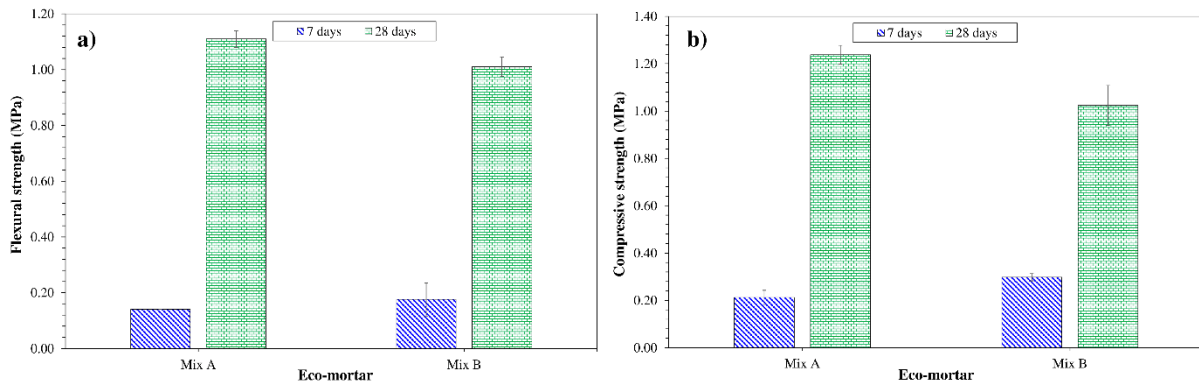
Figure 2: Mechanical strength of Mix A and Mix B.

Figure 2 also shows that the addition of mixed recycled aggregate in Mix B implies performance loss, with this decrease in flexural and compressive strength at 28 days at ~9% and ~17% compared to the reference mortar manufactured with Mix A. This decrease is much lower than the addition percentage, as identified by Silva et al. [15] in their research. These authors observed that for percentages of 100% recycled aggregate in masonry mortars, the compressive strength decrease between 23% - 64% respect to reference mortar. This smaller, negative effect in flexural than in compressive strength is associated with the fact that the mechanical behaviour of the aggregates has a greater influence on compressive strength, which is higher in natural aggregates than in recycled aggregates that have adhered mortar and a more porous micro-structure than the properties of the interfacial transition zone (ITZ) aggregate/paste (figure 3). However, the ITZ properties have a greater effect on flexural strength, in this case showing better insertion of the recycled aggregates as they have a rougher texture than the natural fine aggregate, as well as the possible pozzolanic reaction of the fine fraction (<0.063 mm) of this mixed recycled aggregate. This aspect was previously observed by Sáez del Bosque et al. [18] and Velardo et al. [19] for mixed recycled aggregates as aggregate or supplementary cementitious materials in concrete or cement, respectively.
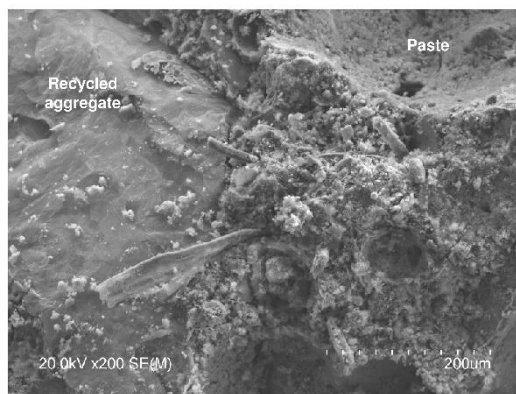
Figure 3. Micrographs of the recycled aggregate/ paste ITZ

4. Conclusions

The conclusions obtained from this research work were:

- Mixes A and B have a continuous granulometric curve and a maximum size of 2 mm.

- The addition of mixed recycled aggregate decreases the apparent density in powder and in the fresh state of the eco-mortars.

- The mortars made with Mix A and B have a plastic consistency.

- The addition of the mixed recycled granular skeleton of CDW decreases the tested mechanical performance, which was much lower than the addition percentage.

Finally, the formulated eco-mortars could logically be used as protection and coating mortars, which would require evaluation of the elastic, acoustic, water absorption and thermal conductivity properties in a second research phase.

Acknowledgements

5. References

[1] European Commission. Building and construction. 2023. https://single-market-economy.ec.europa.eu/industry/sustainability/buildings-and-construction_en

[2] Heravi, G. and Abdolvand, M.M. "Assessment of water consumption during production of material and construction phases of residential building projects". *Sust. Cities Soc.* **51** (2019)

[3] Concrete Centre "UK Concrete and Cement Industry Roadmap to Beyond Net Zero". *Sustainable Concrete, part of The Concrete Centre*, 2021.

[4] Díaz, M., Plaza, P., Blanco, D., Jordán, M.M., Sáez del Bosque, I.F. and Medina, C. "The design and development of recycled concretes in a circular economy using mixed construction and demolition waste". *Materials* **14** (2021), 4762.

[5] Santos, T., Almeida, J., Silvestre, J.D. and Faria, P. "Life cycle assessment of mortars: a review on technical potential and drawbacks". *Constr. Build. Mater.* **288** (2021), 123069.

[6] Ruviaro, A.S., Silvestro, L., Pelisser, F., Garcez, A.R., de Mateos, P.R. and Guerra, A. "Long-term effect of recycled aggregate on microstructure, mechanical properties, and CO_2 sequestration of rendering mortars". *Constr. Build. Mater.* **321** (2022), 126357.

[7] Jesus, S., Pedermeiras, C.M., Farinha, C., de Brito, J. and Veiga, R. "Reduction of the cement content by incorporation of fine recycled aggregate from construction and demolition waste in rendering mortars". *Infrastructures* **6** (2021).

[8] Jesus, S., Cinthia, M., Brazao, C., de Brito, J. and Veiga, R. "Rendering mortars with incorporation of very fine aggregates from construction and demolition waste". *Constr. Build. Mater.* **229** (2019), 116844.

[9] European Committee for Standardization, "EN 197-1. Cement - Part 1: Composition, specifications and conformity criteria for common cements", 2011.

[10] European Committee for Standardization, "EN 1015-1. Methods of test for mortar for masonry - Part 1: Determination of particle size distribution (by sieve analysis)", 1999.

[11] Centre Scientifique Et Technique Du Batiment, "Mortiers et produits connexes. Document technique 11-04. Mortiers de montage á joint mince pour petits éléments de maçonnerie", 2022.

[12] European Committee for Standardization, "EN 1015-3. Methods of test for mortar for masonry - Part 3: Determination of consistence of fresh mortar (by flow table)", 2000.

[13] European Committee for Standardization, "EN 1015-6-1999. methods of test for mortar for masonry - Part 6: Determination of bulk density of fresh mortar", 1999.

[14] European Committee for Standardization, "EN 1015-11. Methods of test for mortar for masonry - Part 11: Determination of flexural and compressive strength of hardened mortar", 2020

[15] Silva, R.V., de Brito, J. and Dhir, R.K. "Performance of cementitious renderings and masonry mortars containing recycled aggregates from construction and demolition wastes". *Constr. Build. Mater.* **105** (2019), 400-415.

[16] Miranda, I.F.R. and Selmo, S.M.S. "A case study on the variation in the quality mortars using CDW recycled sands". International RILEM conference on the use of recycled materials in building and structures. RILEM Publications SARL., Barcelona, Spain (2004), 483-492

[17] European Committee for Standardization, "EN 998-1. Specification for mortar for masonry. Part 1: Rendering and plastering mortar", 2018.

[18] Sáez del Bosque, I.F., Zhu, W., Howind, T., Matías, A., Sánchez de Rojas, M.I. and Medina, C. "Properties of interfacial transition zones (ITZs) in concrete containing recycled mixed aggregate". *Cem. Concr. Comp.* **81** (2017), 25-34

[19] Velardo, P., Sáez del Bosque, I.F., Sánchez de Rojas, M.I.; De Belie, N., Medina, C. "Design and evaluation of physical, mechanical and microstructural properties of eco-friendly binary-blended mortars using biomass bottom ash or construction and demolition waste powder". *Cem. Concr. Comp.* 143 (2023), 105252.

THE COMBINED ROLES OF CEMENT TYPE AND RECYCLED CONCRETE AGGREGATE ON THE FORMATION OF THE INTERFACIAL TRANSITION ZONE

Bruno Fernandes (1), Sreejith Krishnan (1), Alice Macente (1), Yury Villagrán-Zaccardi (2,3), Leon Black (1) and Susan A. Bernal (1)

(1) School of Civil Engineering, University of Leeds, Leeds, UK

(2) VITO, Mol, Belgium

(3) CONICET, La Plata, Argentina

Abstract

This study evaluates the microstructural features of the interfacial transition zone (ITZ) between different aggregates (natural and recycled) and cement systems - Portland cement (PC) and slag-limestone ternary composite cement. Scanning electron microscopy (SEM) using backscattered electron imaging and greyscale analysis was used to analyse the porosity and reaction products in the zone surrounding the aggregates. Line scans obtained by energy dispersive X-ray spectroscopy (EDX) revealed the chemical changes in the vicinity of aggregates. Results indicate a higher porosity in the ITZ when RCA was used, compared to NA for both cements. Slag-limestone cement systems developed a thinner but more porous ITZ, especially when compared to NA-PC. The EDX line scans indicated a narrower ITZ than the width suggested by BSE imaging. Lastly, X-ray Computed Tomography (XCT) revealed a higher overall porosity in slag-limestone composite cements compared with PC systems, independent of the aggregate type. This study elucidates that the cementitious binder significantly impacts the chemical and physical features of the ITZ.

1.   Introduction

The interfacial transition zone (ITZ) plays a crucial role in mortars and concrete, as it has a significant influence on the mechanical and transport properties of the material. This region, typically measuring around 15 to 50 μm in width, is characterised by higher porosity, a concentration of portlandite, and smaller cement grains [1,2]. The properties of this interface depend on several factors, such as the water/binder ratio the and size and type of aggregate [3].

In the case of recycled concrete aggregate (RCA), the ITZ is even more complex. The RCA includes the original natural aggregate to which original mortar is attached (old matrix). This leads to RCA having a higher porosity and increased absorption. This can affect concrete behaviour. Furthermore, concrete made with RCA presents more than one ITZ: (i) between the old aggregate and the attached mortar, (ii) between the old aggregate and the new matrix and

(ii) between the new and the old matrix [4]. These features can also affect performance.

The ITZ and its properties can be investigated using different imaging techniques, such as scanning electron microscopy (SEM) coupled with energy dispersive X-Ray spectroscopy (EDX). This technique can give valuable information related to the elemental composition, phase assemblage, and porosity. Some previous studies have evaluated the particular properties of the ITZ of RCA concrete [4,5], with the key findings that the ITZ of these systems show greater porosity when compared to NA [4], they may present similar thickness [5], and that the ITZ is sensitive to the initial moisture content and to the RCA strength [5].

Although previous studies have characterised the ITZ formation and properties, the influence of the cement type on ITZ properties is largely unknown, particularly for cements with low clinker contents. This study focuses on the combined influence of the cement type and the recycled concrete aggregate on shaping the interfacial transition zone. In addition, X-ray Computed Tomography (XCT) was employed to explore the three-dimensional microstructure and evaluate the influence of different aggregates and binders on the overall pore structure.

2.   Experimental Program

2.1   Materials and mixes

Two different cements were investigated: a commercial Portland cement (PC) CEM I 52.5 R and a ternary slag-limestone cement (SL). The latter was blended in the laboratory, by mixing CEM I 52.5 R (54%), blast furnace slag (30%), limestone (15%) and gypsum (1%). Table 1 shows the chemical composition (determined by XRF) and the densities (determined by Helium Pycnometer) of the studied binders.

Two different types of aggregate were used: a commercial siliceous natural aggregate (NA) and recycled concrete aggregate (RCA) obtained from a CEM I 52.5N concrete with a water/binder ratio of 0.42 and original f_{c28} of 40 MPa. Table 2 presents some of the aggregate properties. For NA, the specific gravity and absorption were determined based on BS EN 1097-6 [6]. Since the cone method is less suitable for RCA [7], the centrifuge method, based on the work of Li et al [8], was used to determine the water absorption of the recycled material. Specific gravity of the RCA was measured using the helium pycnometer. It is noteworthy that the specific gravity is high, but still in the range of previous works [9]. The attached paste content was estimated on the basis of the solubility of RCA in (hydrochloric) acid [10].

The NA and RCA fraction were chosen to pass a 5 mm sieve and be retained on a 2.36 mm sieve. This was to achieve two requirements: (i) a fraction that allows the production of small specimens (especially for XCT) and (ii) a fraction with a sufficiently large quantity of attached mortar. Notably, the selected fraction of NA was mainly siliceous, and most of their particles were spherical.

Specimens were produced with a cement paste matrix and a constant volume proportion of aggregates (V_{agg}/V_{paste}=0.25) to facilitate quantitative and comparative testing. The cement pastes were produced with a water/binder (w/b) ratio of 0.35 and a polycarboxylate superplasticizer (SIKA ViscoCrete 650MK) dosed 0.15% for the CEM I mix and 0.075% for limestone slag cement mix (dosage by weight of binder). Two sizes of samples were produced: a Ø35 mm cylinder for SEM-EDX and Ø13 mm cylinder for XCT.

Table 1: Binder properties

	CaO (%)	Al$_2$O$_3$ (%)	SiO$_2$ (%)	MgO (%)	SO$_3$ (%)	Traces (%)	LOI * (%)	Density (g/cm^3)
PC	65.01	3.65	22.5	0.83	3.36	2.62	1.82	3.11
Limestone	52.7	0.98	3.51	0.53	0.11	0.71	41.5	2.63
Slag	40.25	11.52	35.6	7.98	2.41	2.29	-	2.92

*LOI stands for loss on ignition at 900°C determined using a muffle furnace

Table 2: Aggregate properties

Physical Properties	NA	RCA
Size (mm)	5 - 2.36	5 - 2.36
Specific gravity (g/cm^3)	2.61	2.48
Water absorption (%)	2.59	10.12
Attached paste content (%)	-	36.98

One of the critical points when using recycled aggregates is the water compensation to correct their higher water absorption. Different approaches can be followed, ranging from using saturated aggregates to using dried aggregates followed by a correction of the mixing water [11]. In this study, aggregates were initially dried before use. Before mixing, they were pre-saturated with 80% of the total water absorption for 10 minutes. This strategy was adopted considering that recycled aggregates do not absorb 100% of their water absorption capacity and most of the absorption happens in the initial minutes (after 10 minutes) [7,12]. Similar approaches were reported in previous work [12,13]. The impact of the uncertainty in the effective water-to-binder ratio was minimized with the low value adopted for V_{agg}/V_{paste}.

For the mixing process, the pre-soaked aggregates and cement were hand mixed for 1 minute. Then, water and superplasticizer were added and mixed for 3 minutes at a low speed using a high-shear mixer. After mixing, the mixes were cast into the plastic vials. Samples were cured in water at 20°C until the test age (28d).

2.2 Experimental methods

At 28 days, the Ø35 mm cylinders were cut into 3 mm thick disks. These slices were cut into smaller parts and immersed in isopropanol for 7 days to stop hydration. After this, samples were kept in a vacuum desiccator for 2 days and subsequently impregnated under vacuum using an epoxy resin. After resin curing for 1 day at 40 °C, samples were coarse polished with SiC papers (600, 1200 and 2500 grit) for about 3 min each, followed by polishing with 6, 3, 1 and 0.25 µm diamond pastes. Finally, samples were cleaned in an isopropanol ultrasonic bath for 5 min and stored in vacuum desiccator. After 1 day of vacuum, samples were carbon coated.

Scanning electron microscopy (SEM) in backscattered electron mode (BSE) coupled with the energy-dispersive x-ray spectroscopy (EDX) was used to understand the microstructural and chemical variations in the specimens. A Zeiss Evo 15 scanning electron microscope, operating at a voltage of 20kV was used for image analysis. Images were obtained at different ITZ regions with magnifications from 500x to 1500x. Line scans were collected using the EDX module (Oxford Instrument XMAX150) and the Aztec software.

For porosity segmentation and quantification, images were taken at 750x magnification at different spots in the ITZ between aggregate and paste. Then, these images were split into successive strips from the aggregate boundaries. For each image, 15 successive 10 µm strips were obtained. The image segmentation is strongly dependent on the value of the grey level chosen from the image histogram (threshold, T) and different approaches can be used for this selection [14]. Since the main interest of this study was to evaluate the porosity, it was chosen to use the overflow criterion method described in Wong et al. [14].

Complementary analysis was made using XCT. For this analysis, the Ø13mm samples were used without any further preparation. XCT data acquisition was performed using a ZEISS Versa 410. The objective of the XCT scan was to identify the air void volume and their 3D spatial distribution in relation to the aggregates. Data were collected using a 0.4X objective, a beam energy of 120kV/12W, with a 4s exposure time, and 2401 projections acquired over 360° rotation. The final reconstructed pixel size was 13.7 µm. It is worth noting that, at this spatial resolution, the XCT is not able to identify the same porosity as the SEM analysis.

3.   Results and Discussion

Typical backscattered images (BSE) of the four systems are shown in Figure 1. For NA systems (Figure 1a and Figure 1c), both aggregate and paste are easily identified, as well as the interface. The interface between old and new paste was less pronounced for RCA systems (Figure 1b and Figure 1d), given the similarities between the pastes. In the RCA, it was possible to locate the old natural aggregate, the old cement paste, and the old interface between them. Other relevant features in the pastes are anhydrous cement grains (U) observed as bright areas in the Portland cement systems, and slag particles (SL) and limestone (L) in slag-limestone cement.

(a) NA-PC

(b) RCA-PC

(c) NA-SL

(d) RCA-SL
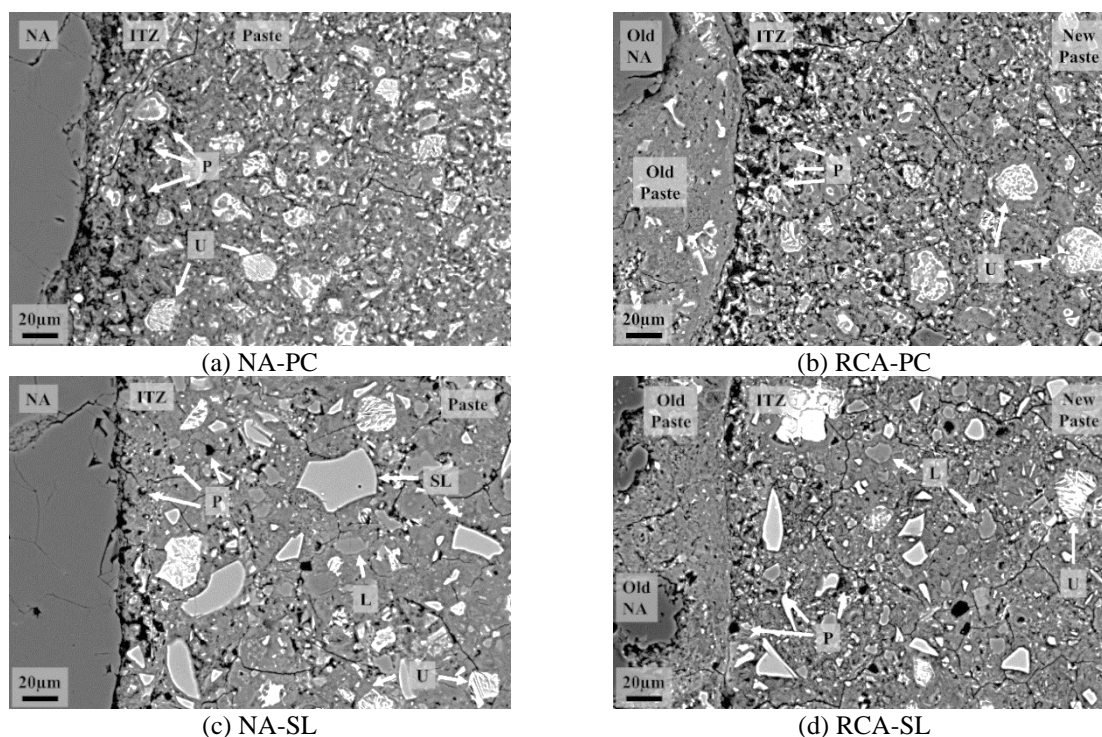
Figure 1: BSE images (1000x magnification) of the studied mixes (NA=natural aggregates; RCA=recycled concrete aggregates; ITZ=interfacial transition zone; P=pores; U=unhydrated cement particles; L=limestone; SL=slag)

The images also revealed the ITZ features. Usually, this region presented higher porosity, denoted by darker zones (pores) closer to the vicinity of the aggregate. This was observed in both systems using Portland cement, but the one with RCA (Figure 1b) appeared more porous than the NA sample (Figure 1a). Possible explanations for this behaviour may be associated with the RCA's higher porosity. Even though the water absorption was corrected with a reduced (80%) content, the RCA may have released water into the paste, increasing the effective w/b and the porosity. This increase in porosity was also reported in previous studies that have used aggregates in the SSD condition [4,5]. Notably, the uncertainty in RCA's water uptake is normally reported in the literature [15]. These differences were also observed in the slag limestone cement systems but less pronounced (Figure 1c and Figure 1d). However, the paste appeared denser when compared to PC systems.

To highlight some of these differences, the initial quantification of the porosity is presented in Figure 2. In these graphs, the detectable porosity (by % of the strip area) is plotted against the distance from the aggregate. The end of the ITZ and the beginning of the bulk paste are identified when the porosity line starts to flatten. Comparing NA and RCA made with Portland cement (Figure 2a and Figure 2b), the ITZ thickness was similar in both cases, at around 70 µm. However, the porosity was higher for RCA, even in the bulk paste, confirming the visual observations. For example, in the bulk paste, RCA showed around 20% porosity (Figure 2b), while NA showed around 10% (Figure 2a). Similar differences in profiles were observed in the work of Djerbi [4].

(a) NA-PC	(b) RCA-PC
(c) NA-SL	(d) RCA-SL
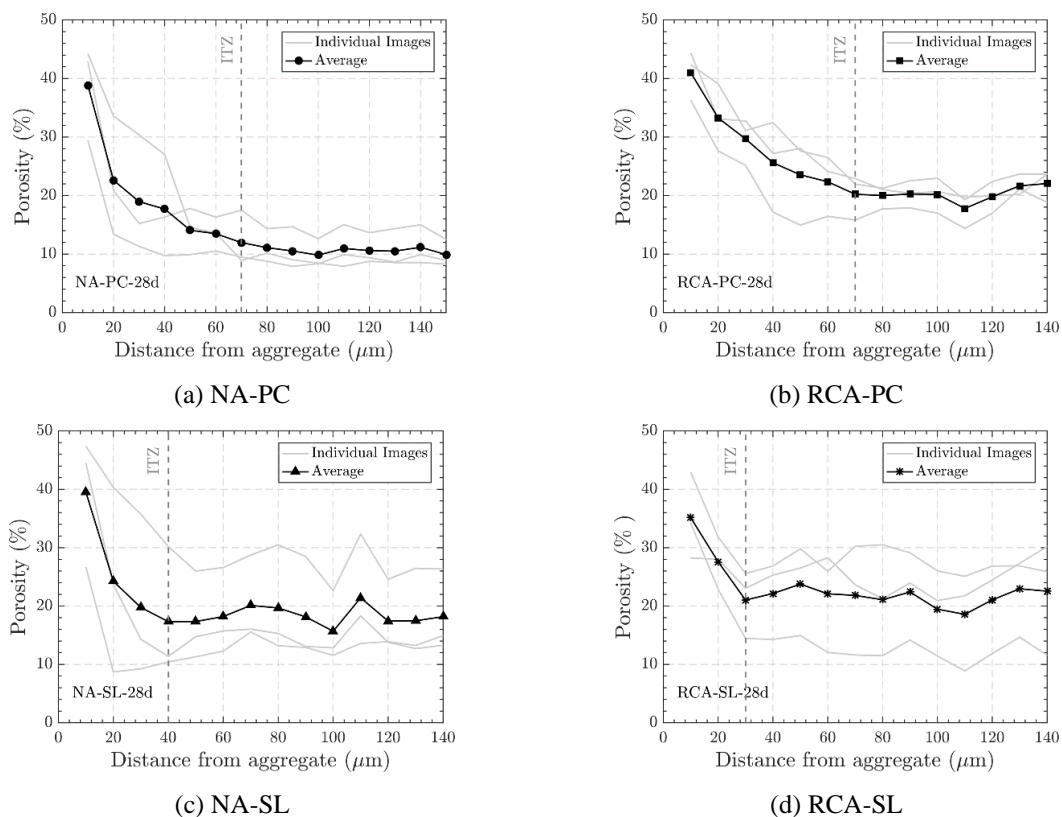
Figure 2: Detectable porosity as a function of the distance from the aggregate

A reduced ITZ thickness (around 30-40 µm) was observed in slag-limestone ternary cement when compared to the PC system. The porosity was similar for both types of aggregate, with a bulk paste porosity around 20% (Figure 2c and Figure 2d). This value is closer to the RCA-PC

(Figure 2b) and higher than the NA-PC (Figure 2a), despite the visual refinement of the microstructure. However, the lower total porosity of PC when compared to ternary cements is consistent with previous work [16]. The potential causes for the higher porosity include the dilution effect of the limestone and the partial reaction degree of the slag [17]. This is evident from the presence of large unreacted particles in the SEM images (Figure 1c and Figure 1d). Notably, the slag-system showed higher variability in the porosity, and further quantification is necessary.

Figure 3 presents results from EDX line scans made on selected images (3-line scans per image). In these images, specific elements are plotted against the distance from the aggregate. The counts for each element were normalised by the combined number of counts (y-axis). As shown in Figure 3, there were variations in composition, especially in the first 10 to 20 µm. In NA-based systems (Figure 3a and Figure 3c), the ITZ is identified by the inversion between Si and Ca (around 10-15µm). In RCA-based systems (Figure 3b and Figure 3d), the ITZ may be identified by the Si content, which shows a consistent trend in the vicinity of aggregate (up to 20 µm). In general, the width observed in the EDX line scan is narrower than the ITZ observed in the SEM-BSE imaging.

(a) NA-PC

(b) RCA-PC

(c) NA-SL

(d) RCA-SL
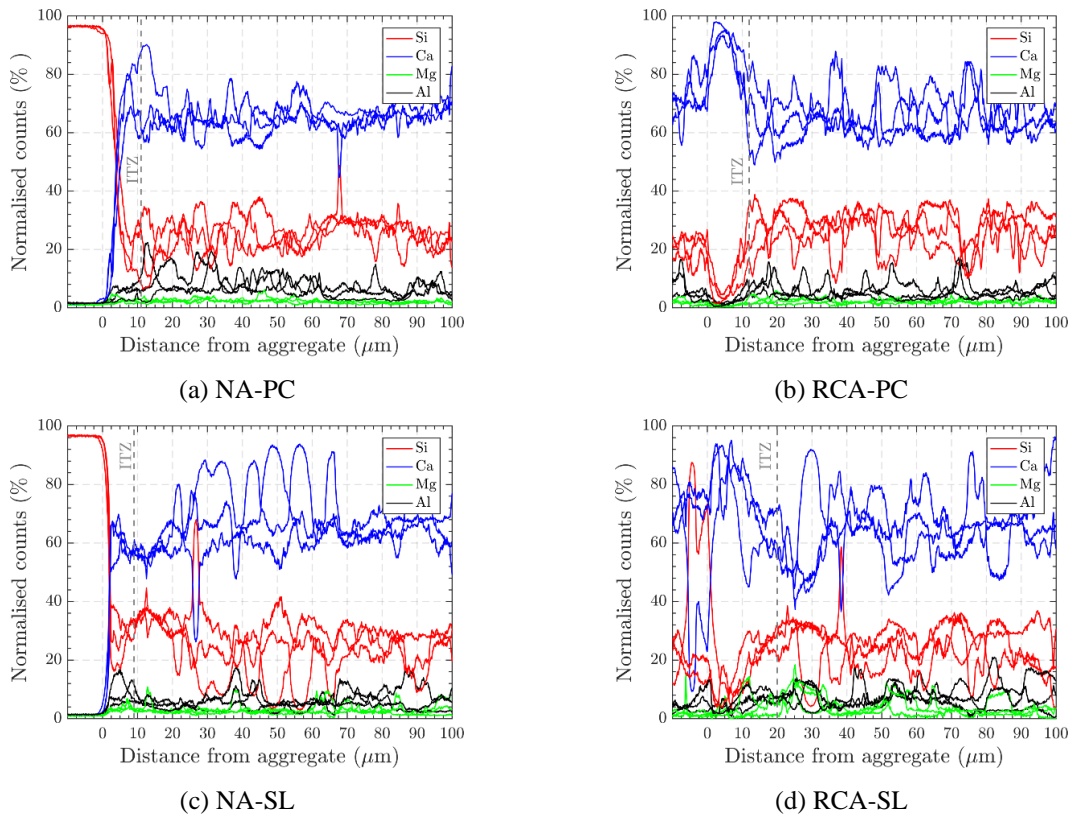
Figure 3: EDX line scans of the ITZ. The 0 in the x-axis indicate the visual interface between the aggregate and the paste

The 3D structure and porosity obtained via XCT are presented in Figure 4. From this analysis, it was possible to identify the 3D spatial distribution of the natural and recycled aggregates, paste, and air voids formed during casting of the samples. Given the limitation of the size of the sample and the resolution, it was not possible to identify the capillary pores in the paste.

XCT void analysis was performed in subvolumes of interest (400 x 400 x 400 voxels = 5.483 mm^3). For each subvolume, the volume percentage of air voids in the paste, the voids in the

aggregate and the cracks were calculated (Table 3). RCA-PC (Figure 4b) showed an increase in the air voids fraction, along with the appearance of cracks, which were not present in NA-PC (Figure 4a). Comparing the NA-SL (Figure 4c) with NA-PC (Figure 4a), it can be seen that there was an increase in voids in the paste and also the appearance of cracks. However, it is noteworthy that the used resolution does not capture the capillary porosity, which is mostly influenced by the presence of ternary systems – as seem in the SEM. As expected, the recycled aggregate showed a higher porosity for both cementitious systems.

Table 3: Voids and cracks from XCT measurements

Type	NA-OPC	RCA-OPC	NA-SL	RCA-SL
Voids in the paste (%)	0.28	0.77	1.12	1.00
Voids in the aggregate (%)	0.12	1.78	0.31	0.69
Cracks (%)	-	0.07	0.14	0.04
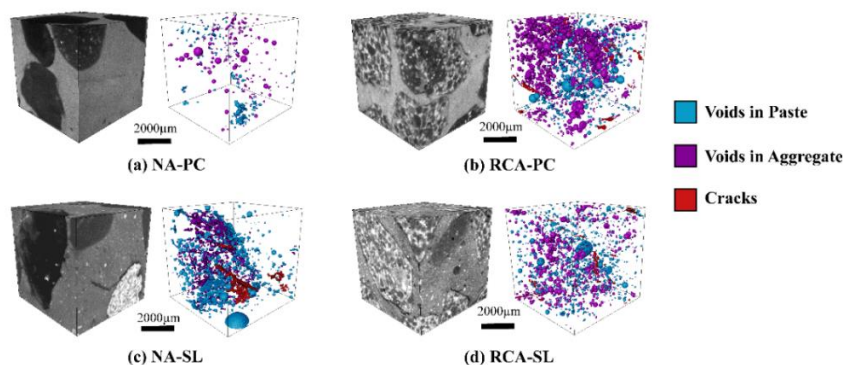
Figure 4: 3D rendering of the porosity from the XCT digital image processing

4. Conclusions

Microscopy techniques were used to identify different features of the ITZ formed using natural aggregates and recycled aggregates in systems made with different types of cement (Portland cement and slag-limestone ternary cement).

SEM revealed that the ITZ of systems made with RCA were more porous than the ones with NA for both cement types. The slag-limestone cement showed a narrower ITZ, but higher porosity, especially when compared to NA-PC. XCT scans identified the 3D distribution of the systems microstructures, providing insights into the 3D distribution of air voids in the cement paste in relation to the aggregates, in the two compared systems. Further work is planned to quantify the ITZ's 2D and 3D spatial distribution in various binders and aggregates to further reveal their effects on porosity, permeability and tortuosity.

Acknowledgements

Infrastructure Materials, University of Leeds, UK, a UKCRIC Research Facility (EP/P017169/1).

References

[1] Luo, Z., Li, W., Wang, K., Castel, A. and Shah, S.P., 'Comparison on the properties of ITZs in fly ash-based geopolymer and Portland cement concretes with equivalent flowability', *Cem. Concr. Res.* **143** (2021) 106392.

[2] Scrivener, K.L., Crumbie, A.K. and Laugesen, P., 'The interfacial transition zone (ITZ) between cement paste and aggregate in concrete', *Interface Sci.* **12** (2004) 411–421.

[3] Alexander, M. and Mindess, S., 'Aggregate in Concrete' (Taylor & Francis, New York, 2010).

[4] Djerbi, A., 'Effect of recycled coarse aggregate on the new interfacial transition zone concrete', *Constr. Build. Mater.* **190** (2018) 1023–1033.

[5] Leite, M.B. and Monteiro, P.J.M., 'Microstructural analysis of recycled concrete using X-ray microtomography', *Cem. Concr. Res.* **81** (2016) 38–48.

[6] BS EN 1097-6, 'Tests for mechanical and physical properties of aggregates. Determination of particle density and water absorption' (BSI, London, 2022).

[7] Sosa, M.E., Carrizo, L.E., Zega, C.J. and Villagrán Zaccardi, Y.A., 'Water absorption of fine recycled aggregates: effective determination by a method based on electrical conductivity', *Mater. Struct. Constr.* **51** (2018).

[8] Li, Z., Liu, J. and Tian, Q., 'Method for controlling the absorbed water content of recycled fine aggregates by centrifugation', *Constr. Build. Mater.* **160** (2018) 316–325.

[9] Evangelista, L. and De Brito, J., 'Concrete with fine recycled aggregates: a review', *Eur. J. Environ. Civ. Eng.* **18** (2014).

[10] Tam, V.W.Y., Soomro, M. and Evangelista, A.C.J., 'Quality improvement of recycled concrete aggregate by removal of residual mortar: A comprehensive review of approaches adopted', *Constr. Build. Mater.* **288** (2021).

[11] Leite, M.B., Figueiredo Filho, J.G.L. and Lima, P.R.L., 'Workability study of concretes made with recycled mortar aggregate', *Mater. Struct. Constr.* **46** (2013) 1765–1778.

[12] Nedeljković, M., Mylonas, A., Wiktor, V., Schlangen, E. and Visser, J., 'Influence of sand drying and mixing sequence on the performance of mortars with fine recycled concrete aggregates', *Constr. Build. Mater.* **315** (2022).

[13] Cuenca-Moyano, G.M., Martín-Morales, M., Valverde-Palacios, I., Valverde-Espinosa, I. and Zamorano, I., 'Influence of pre-soaked recycled fine aggregate on the properties of masonry mortar', *Constr. Build. Mater.* **70** (2014) 71–79.

[14] Wong, H.S., Head, M.K. and Buenfeld, N.R. 'Pore segmentation of cement-based materials from backscattered electron images', *Cem. Concr. Res.* **36** (2006) 1083–1090.

[15] Sosa, M.E., Villagrán Zaccardi, Y.A. and Zega, C.J., 'A critical review of the resulting effective water-to-cement ratio of fine recycled aggregate concrete', *Constr. Build. Mater.* **313** (2021).

[16] Zajac, M., Skocek, J., Adu-Amankwah, S., Black, L. and Ben Haha, M., 'Impact of microstructure on the performance of composite cements: Why higher total porosity can result in higher strength', *Cem. Concr. Compos.* **90** (2018) 178–192.

[17] Dhandapani, Y., Santhanam, M., Kaladharan, G. and Ramanathan, S., 'Towards ternary binders involving limestone additions — A review', *Cem. Concr. Res.* **143** (2021).

RECYCLED AGGREGATE CONCRETE DOSED WITH OPTIMIZED MIXTURES: PROPERTIES IN THE FRESH AND HARDENED STATE

José E. Lima (1), Danilo Barbosa (1), Marcos D. Santos (1), Antonio A. Melo Neto (2), and Arnaldo M. Carneiro (2)

(1) Research Scholar Universidade Federal de Pernambuco [Recife] – Av. Prof. Moraes Rego, 1235 - Cidade Universitária, Recife, Brasil

(2) Professor at the Department of Civil Engineering at UFPE.

Abstract

This study investigated the use of recycled aggregates from construction and demolition waste in concrete performance. To achieve an ideal mix, Excel was employed to simulate natural aggregates with four particle sizes (1.20mm, 6.3mm, 9.5mm, 12.5mm). Two concrete formulations, A and B, were created, each divided into three mix groups (GI, GII, and GIII). GI (reference) with 100% natural aggregates. GII substituted 100% of the 12.5mm natural aggregate with CDWCA, while GIII replaced 100% of the 1.20mm natural aggregate with CDWMS. In A, mortar content (α) was set at 0.5, with a 100 ± 10mm slump, while formulation B maintained a consistent water-to-cement (w/c) ratio and incorporated a superplasticizer. Mechanical strength was assessed at 7, 28, and 90 days. Notably, GIII, without additives and using CDWMS, exhibited superior mechanical strength compared to additive-containing cases. CDWMS's fine texture and adherent clay hindered additive effectiveness, delaying concrete strength development. GIII displayed more significant strength reductions due to increased fine aggregate content. GI and GII exhibited similar strength trends. Overall, higher w/c ratios were associated with reduced mechanical resistance. Optimized mixes favored complete replacement of natural aggregate with recycled aggregate (RA), with additives mitigating RA's high water absorption effects.

1. Introduction

Recycled aggregate concrete (CAR) has characteristics that put it at a disadvantage compared to natural aggregate concrete (CAN) since the former is composed of several elements stuck together, such as mortar residues, ceramics, and other materials that weaken its properties. For example, the fine recycled aggregate (AFR) has high levels of deleterious materials [1]. In general, the (CAR) has a high water absorption rate, high crushing value, and low abrasion resistance, in addition to having residual mortar that increases porosity and microcracks, interfering in the resistance [2]. In the fresh state, the CAR presents a loss of workability due to the increase in cement consumption and high water absorption [3]. In general, concrete needs to be produced in such a way that it can satisfactorily meet the workability, mechanical strength, and durability requirements in the most economical way possible. Considering that the constituent materials of the cementitious compound influence its behavior, the dosage proves to be a fundamental element in the production of concretes that present good performance and are durable. In this sense, the present study investigates recycled aggregate concrete (CAR) properties in the fresh and hardened state of recycled

aggregate concrete (CAR) with optimized mixes of aggregate. Evaluate different compositions of mixes and their influence on the performance of recycled aggregate concrete in its fresh and hardened state; Propose the most suitable mixture for a recycled aggregate concrete that favors its mechanical properties; Evaluate the influence of a superplasticizer additive on the properties of CAR in the fresh and hardened state.

2.   Methodological procedure

2.1   Materials

Was used initial high-strength cement (CP V – ARI), three variations of natural coarse aggregates (NCA2, NCA1, and NCA0), and a fraction of coarse aggregate from construction and demolition waste (CDWCA) of mixed type from a plant located in the city of Recife-PE (Brazil); two variations of natural sands, one of medium granulometry and the other of fine granulometry (NMS, NFA), from deposits located in the cities of Recife-PE and Cabedelo-PB (Brazil), respectively, and a fraction of average sand from construction waste and demolition (CDWMS), of the mixed type. The characterization of the aggregates is presented in Table 1. A visual analysis was conducted, revealing a significant presence of adhering mortar, plaster residue, wood, and plastic. The microstructural and durability assessment of recycled aggregate will be the focus of a separate study, as the current research primarily centers on the material's macroscopic aspects. Additive Clarena HC 5201 is based on polycarboxylates, pH between 4 and 6, a specific 1.08 g/cm³ mass, and solids content between 41.4 and 45.8%.

Tabela 1: Characteristics of the aggregates used in the study

Characteristic	NCA2	NCA1	NCA0	NMS	NFA	CDWCA	CDWMS
Maximum characteristic dimension (mm)	12,5	9,5	6,3	1,2	0,6	19	2,36
Fineness modulus	6,89	6,26	5,59	2,70	1,53	7,26	3,58
Specific gravity (g/cm³)	2,65	2,65	2,65	2,65	2,62	2,47	2,45
Unit mass (kg/m³)	1510	1610	1660	1700	1660	1360	1510
Water absorption (%)	0,61	0,63	0,65	—	—	5,92	10

2.2   Experimental Arrangement

The concretes were dosed using the IPT/EPUSP dosing method [4]. Two dosages (A and B) of concrete were dimensioned. Each dosage was divided into three groups of mixtures (GI, GII, and GIII). GI represented 100% natural aggregates (reference); GII replaced 100% of the 12.5 (NCA2) mm natural aggregate with recycled aggregate (CDWCA); GIII replaced 100% of the 1.20 (NMS) mm natural aggregate with recycled aggregate (CDWMS). In A, the mortar content (α) was set at 0.5 and the slump at 100 ± 10 mm. The w/c ratio was constant in B, and a superplasticizer was used in the mixes. Mechanical resistance was verified at 7, 28 and 90 days. The composition of the traits are shown in Table 2.

Table 2: composition of the mixtures in kg

DOSAGE A

	Mix	Cement	NCA2	NCA1	NCA0	NMS	NFA	CDWCA	CDWMS	SP	Water
	1:3	17,50	9,80	8,05	6,65	10,50	17,50	—	—	—	8,57
GI	1:5	11,67	9,80	8,05	6,65	10,50	23,33	—	—	—	8,34
	1:6	10,00	9,80	8,05	6,65	10,50	25,00	—	—	—	8,12
	1:3	17,50	—	8,05	6,65	10,50	17,00	9,80	—	—	6,42
GII	1:5	11,67	—	8,05	6,65	10,50	23,33	9,80	—	—	7,37
	1:6	10,00	—	8,05	6,65	10,50	25,00	9,80	—	—	7,28
	1:3	17,50	9,80	8,05	6,65	—	17,00	—	10,50	—	7,98
GIII	1:5	11,67	9,80	8,05	6,65	—	23,33	—	10,50	—	7,99
	1:6	10,00	9,80	8,05	6,65	—	25,00	—	10,50	—	7,84

DOSAGE B

	Mix	Cement	NCA2	NCA1	NCA0	NMS	NFA	CDWCA	CDWMS	SP	Water
	1:3	17,50	9,80	8,05	6,65	10,50	17,50	—	—	0,10	6,06
GI	1:5	11,67	9,80	8,05	6,65	10,50	23,33	—	—	0,07	5,94
	1:6	10,00	9,80	8,05	6,65	10,50	25,00	—	—	0,06	6,08
	1:3	17,50	—	8,05	6,65	10,50	17,00	9,80	—	0,10	6,06
GII	1:5	11,67	—	8,05	6,65	10,50	23,33	9,80	—	0,07	5,94
	1:6	10,00	—	8,05	6,65	10,50	25,00	9,80	—	0,06	6,08
	1:3	17,50	9,80	8,05	6,65	—	17,00	—	10,50	0,10	6,42
GIII	1:5	11,67	9,80	8,05	6,65	—	23,33	—	10,50	0,07	7,37
	1:6	10,00	9,80	8,05	6,65	—	25,00	—	10,50	0,06	7,28

2.3   Preparation, molding and curing of specimens

The concrete specimens were molded and cured according to the prescription of NBR 5739 [5]. The reduction was verified according to NBR NM 67 [6]. For each mix of concrete produced, 18 specimens (CPs) were molded, totaling 162 CPs, in metallic cylindrical molds of 10 cm in diameter and 20 cm in height. The process of manual compaction, in 3 layers, was adopted, as provided for in the standard mentioned above, and the specimens were cured in the air for the first 24 hours. After this period, they were demolded and cured, submerged in a water tank until the date of execution of the compressive strength test, at the ages of 7, 28, and 90 days.

3.   Results and discussions

3.1   Analysis of fresh concrete

3.1.   1 Entrained air content e workability

Table 3: Characteristics of concrete in the fresh state

Dosage	Group	Mix	Ratio w/c	Especific mass	Cement consumption (kg/m³)	entrained air content	Slump (mm)
A	GI	1:3	0,49	2.297,08	511,63	0,08	
		1:5	0,55	2.259,32	340,18	2,58	
		1:6	0,80	2.246,70	288,13	2,06	
	GII	1:3	0,48	2.282,44	509,92	0,31	
		1:5	0,63	2.260,88	340,92	1,91	100 ± 10
		1:6	0,80	2.222,92	285,03	2,30	
	GIII	1:3	0,46	2.286,42	512,19	0,57	
		1:5	0,62	2.275,58	343,54	1,57	
		1:6	0,78	2.241,40	287,95	1,89	
B	GI	1:3	0,35	2.345,11	539,54	2,36	136,67
		1:5	0,51	2.290,49	351,91	3,89	93,99
		1:6	0,61	2.246,10	295,23	5,24	48,33
	GII	1:3	0,35	2.347,54	540,10	1,42	21,67
		1:5	0,51	2.246,26	345,11	4,95	111,67
		1:6	0,61	2.252,63	296,09	4,16	18,33
	GIII	1:3	0,35	2.371,07	545,51	1,01	80,00
		1:5	0,51	2.268,91	348,59	4,13	153,33
		1:6	0,61	2.137,03	280,89	9,24	190,00

The analysis of Table 3 shows that the 1:3 mix of all groups of mixtures of the two dosages showed the lowest results of air incorporated in the samples, followed by the 1:5 and 1:6 mixes. Concrete produced with recycled aggregates has a higher water absorption and voids index when compared to conventional concrete, which justifies such behavior. This characteristic occurs due to the increase in the w/c ratio, reduction in specific mass, permeability, and composition of recycled aggregates [7][8][9]. The void ratio increases as cement consumption is reduced. The use of superplasticizers increased cement consumption considerably, mainly when associated with the use of fine recycled aggregate (CDWMS). Fixing the slump in dosage A allowed the mixtures with recycled aggregate to reach w/c values very close to the w/c values of the reference mixtures. Soon, the setting of the slump

seemed to function as a natural controller of the high water absorption of the recycled aggregate, keeping it at apparently adequate levels. As for the analysis of reductions in dosage B, in GI, it is noticed that the richer in cement the mix is, the more significant its reduction will be. In GII, the results presented variations. These variations may be related to the test method (trunk cone), which may hinder the flow of the mixture due to the rougher texture and irregular shape of the recycled aggregate, as already observed in studies by Leite (2001). However, even with this slump variation, the superplasticizer additive seemed to inhibit the high water absorption of the recycled aggregate, allowing the w/c ratio of dosage B to remain at more interesting values than those of dosage A.

3.2 Analysis of the mechanical behavior of concrete

3.2.1 Compressive strength analysis of concrete produced in dosage A

The results of the average resistance to compression of the concrete of dosage A are shown in Table 4. At 7 days, it is observed that only the 1:3 mix from GII presented lower resistance than the reference concrete. This data is likely associated with the aggregate quality used, which brought characteristics of the composite from which it originated. In general, the value was close to the value of concrete with natural aggregate.

Table 4: Results of the compressive strength test for dosages A

Dosage	Group	Mix	Ratio w/c	Compressive strength (MPa)		
				7 days	28 days	90 days
A	GI	1:3	0,49	38,01	41,62	50,08
		1:5	0,55	28,17	32,62	35,23
		1:6	0,80	18,14	22,44	22,07
	GII	1:3	0,48	35,39	46,38	48,38
		1:5	0,63	32,03	32,83	30,28
		1:6	0,80	19,68	22,45	25,78
	GIII	1:3	0,46	43,41	51,46	54,32
		1:5	0,62	31,10	38,83	37,99
		1:6	0,78	20,50	25,67	24,40

At 28 days, the average resistance of GIII was the highest, followed by GII and GI (reference concrete), respectively, in all mixes, Figure 1. At least three aspects justify this:
1. GIII, because it has the highest amount of fine aggregate (natural+recycled), can cause, according to Leite (2001), a greater pozzolanic reactivity of the fine fraction due to the participation of ceramic fraction and clay on the surface and may present higher resistance growth rates between 28 and 91 days.
2. GII, composed of 100% mixed coarse recycled aggregate, has the second highest resistance, as it has unhydrated cement particles on its surface that can hydrate in the new mixture with recycled aggregates, increasing its resistance [10].

3. The greater the amount of recycled coarse aggregate in concrete, the lower its compressive strength when compared to other concrete with 100% recycled fine aggregate [11].

Figure 1 shows the average strength of the A dosage mixes over time, in which G3 remains the group with the highest average compressive strengths and is the group with the lowest w/c ratios, confirming the strong influence of a/c ratio in the compressive strength of concrete, including the CAR.
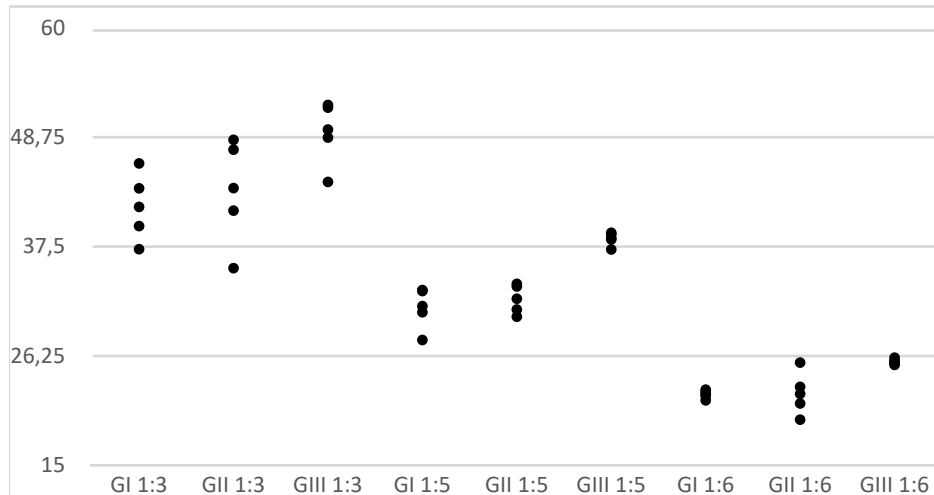
Figure 1: Compressive strength of dosage A to 28 days

3.2.2 Analysis of the compressive strength of concrete produced in dosage B
The compressive strength results are shown in Table 5.

Table 5: Results of the compressive strength test for dosages B

Dosage	Group	Mix	Ratio w/c	Compressive strength (MPa)		
				7 days	28 days	90 days
		1:3	0,35	57,42	68,75	79,70
	GI	1:5	0,51	35,33	43,61	45,41
		1:6	0,61	30,56	34,76	34,38
		1:3	0,35	50,13	57,14	67,64
B	GII	1:5	0,51	34,70	38,83	39,95
		1:6	0,61	28,44	32,26	34,85
		1:3	0,35	79,97	59,97	82,12
	GIII	1:5	0,51	35,97	43,61	47,24
		1:6	0,61	20,37	27,85	31,19

Analyzing the data in Table 5, it can be seen that the higher the w/c ratio, the lower the resistance of the concrete. Among the traits with the lowest w/c ratio, GIII obtained better results, and the other two groups obtained similar resistances. However, for a w/c ratio of 0.61, the GIII presented a more pronounced drop in resistance. Although G3 showed the lowest resistances among the mixes of dosage B, for the mix 1:6, the use of the superplasticizer additive made it possible to maintain a w/c ratio below the w/c ratio of the same blend of dosage A, so values with higher resistances, although with higher abatements. This is justified because the additive inhibits the flocculation of cement particles, favoring hydration and strength gain, as shown. Furthermore, in the w/c 0.61 ratio, GIII presents the highest slump among the three traits, contributing to a lower resistance at the three ages.

3.2.2.1 Analysis of the compressive strength of concrete based on the relationship between the mix and age

At 7 days, the mix 1:3 obtained the lowest resistance with 49.97 Mpa, and at 90 days, it achieved the highest result, 82.12 Mpa, with a strong tendency to grow. The more significant amount of recycled fine aggregate has contributed enormously to the greater increase in the compressive strength of GIII over time due to the fine aggregate's pozzolanic tendency. In traits 1:5 (figure 2), the resistances of GI and GIII showed similar behavior up to 28 days since, at 90 days, the increase in resistance becomes more apparent for GIII.
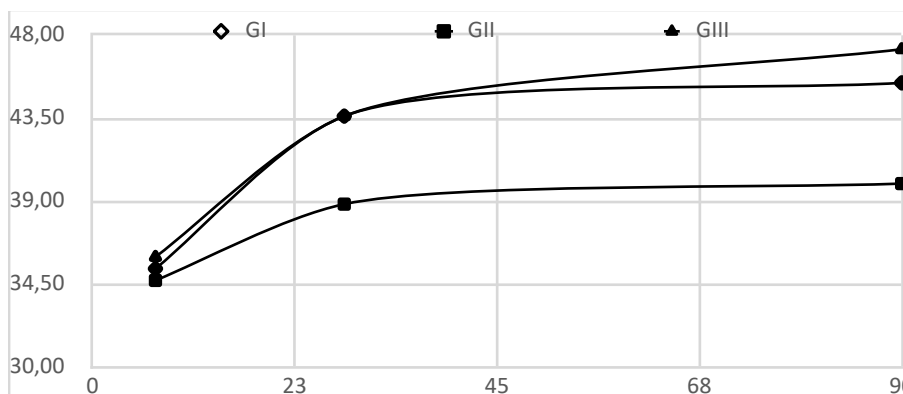
Figure 2: Relationship between compressive strength and time (mix 1:5)

The group GIII presented the lowest resistance values among the studied groups (table 5). GIII, despite having the lowest resistance, was the group that obtained the most significant growth over time in all mixtures> this can be explained by the reaction with the mortar content adhered to the surface of the recycled aggregate and the interaction with the clay contents present more intensely in recycled fine aggregates. The lowest resistances of GIII seem to be related to the highest slump values and the highest values of the w/c ratio in the group.

4.   Conclusions

The fresh and hardened properties of recycled aggregate concrete were investigated in the present study. Based on the experimental results, the following conclusions

can be drawn: 1) Concretes with 1:3 ratios had the lowest levels of incorporated air in all groups of mixtures, among these, however, the recycled aggregate concretes had higher valu 2) es of incorporated air, due to the characteristic of the material;The setting of the slump of the traces of the recycled aggregate concrete allowed w/c values close to those of the reference concrete, minimizing its weaknesses; 3) GIII was the group that obtained the highest reductions, especially when the amount of aggregates was higher in the mixture; 4) GI and GII showed similar trends in mechanical strength; 5) GIII, without additive and with recycled fine aggregate, had the highest compressive strength since the first test; however, when the additive was incorporated into the mixture, there was considerable variation in strength. This is due to the reaction of the additive being more intense in this type of aggregate, as its granulometry is more conducive to containing more clays in the mixture, causing a late growth in strength; 6) In all groups, the higher the w/c ratio, the lower the mechanical resistance. The optimized mixtures favored the total replacement of the natural aggregate by the recycled aggregate (RS), and the additive collaborated by mitigating the consequences of the high water absorption of the AR.

References

[1] Bravo, M., Brito, L., Evangelista, L. and Pacheco, J., 'Superplasticizer's efficiency on the mechanical properties of recycled aggregates concrete: Influence of recycled aggregates composition and incorporation ratio', Construction and Building Materials. 153 (2017) 129-138.

[2] Wang, X., Yang, X., Ren, J., Han, N. And Xing, F., 'A novel treatment method for recycled aggregate and the mechanical properties of recycled aggregate concrete', Journal of material research and Technology. (2021) 1389-1401

[3] Rodrigues, C.R.S. and Fucale, S., 'Experimental mix proportion of concrete made with recycled aggregate from civil construction waste', Ambiente Construído, Porto Alegre, v. 14, n. 1, (2014) p. 99-111

[4] Helene, P. And Terzian, P., Manual de dosagem e controle do concreto. 1nd Edn (PINI, São Paulo, 1993)

[5] ASSOCIAÇÃO BRASILEIRA DE NORMAS TÉCNICAS. NBR 5738: concreto: procedimento para moldagem e cura de corpos-de-prova: especificação. Rio de Janeiro, 2003c.

[6] ASSOCIAÇÃO BRASILEIRA DE NORMAS TÉCNICAS. NM 67: concreto: determinação da consistência pelo abatimento do tronco de cone. Rio de Janeiro, 1998.

[7] Evangelista, B. And Brito, J., 'Mechanical Behaviour of Concrete Made With Fine Recycled Aggregates', Cement and Concrete Composites. 29 (2007) 397-401

[8] Lovato, P.S., 'Verificação dos Parâmetros de Controle de Agregados de Resíduos de Construção e Demolição Para Utilização em Concreto'. (2007) 180

[9] Carrijo, P.M., 'Análise da Influência da Massa Específica de Agregados Graúdos Provenientes de Resíduos da Construção e Demolição no Desempenho Mecânico do Concreto'. (2005) 129

[10] Buttler, A.M., 'Concreto Com Agregado Graúdo Reciclado: influência da idade de reciclagem nas propriedades dos agregados e concretos reciclados'. Dissertação (Mestrado em engenharia civil). USP (2003)

[11] Leite, M.B., 'Avaliação de Propriedades Mecânicas de Concretos Produzidos Com Agregados Reciclados de Resíduos da Construção e Demolição'. Tese (Doutorado em engenharia civil). UFRS

ECOLOGICAL CONCRETE MIX DESIGN USING CARBONATED RECYCLED AGGREGATES AND LOW-CLINKER CEMENT

Paul Dengler[1], *, Mujeebul Rahman Latifi[1], Svenja Vogt[2], Harald Weigand[2] and Rüdiger Kern[1]

(1) Institute for Design and Structure (IKT), THM University of Applied Sciences Gießen, Germany

(2) Competence Centre for Sustainable Engineering and Environmental Systems (ZEuUS), THM University of Applied Sciences Gießen, Germany

* Correspondence: paul.dengler@bau.thm.de

Abstract

Recycling rates need to rise to save resources and landfill space. In Germany, lots of construction and demolition waste (CDW) is used as base-level material for roadways mainly because of lacking alternative high-quality utilization options. On the primary production side, cement clinker production contributes considerably to CO_2 emissions. Here, the issue of high-value CDW utilization combined with CO_2 savings was addressed in the practical application of an infrastructure concrete element. The standard mix was changed using recycled concrete aggregates (cRCA) and fine recycled concrete aggregates (fRCA) as a replacement for coarse crushed natural stone and sand, respectively. Both aggregate types were used in the as-received state and after accelerated carbonation. In addition, a low-clinker cement served to replace ordinary Portland cement in the concrete mix design. To minimize potentially adverse effects of RCA utilization, the water absorption (WA) was determined, and a multi-step mixing technique was used. Tests included workability and compressive strength development. The concrete with 8 vol.-% fRCA together with 30 % cRCA in carbonated state as a replacement for natural aggregates (NA) had a higher 1-day early strength than the initial concrete and showed no further loss in 28-day compressive strength compared to 30 % cRCA only.

1. Introduction

From the 1950s to the early 21st century, concrete developed into the most used material in a multitude of applications, 30 Gt was used worldwide in 2020 [1]. This went along with an increase in the production of cement, which accounts for about 8 % of CO_2 emissions worldwide [2]. As per now, the most effective option to reduce the CO_2 intensity is expected to be reducing clinker content [3, 4].

In terms of resource use, the German concrete industry also processed more than 100 million tons of natural aggregates (NA) in 2018. According to data for 2018 through 2021 gravel had the largest share with 43,1 % followed by sand (36,6 %) and crushed natural stone (20,3 %) [5, 6]. Precast concrete is the second largest product category after transport concrete, making up 20 % or 23 million tons in 2021 [5]. Consequently, precast concrete holds considerable potential for saving resources.

While sand is sufficiently available in Germany in the near future, gravel supply shortage is already of concern and is expected to become more strained [6]. Construction activities are expected to drop, while the generation rate of construction and demolition waste (CDW) is predicted to rise. From this perspective, coarse and especially fine recycled concrete aggregates (cRCA, fRCA) should be used extensively also in view of saving landfill space [7]. This furthermore results in the claim that the minimal substitution rates of NA by RCA should be higher in standard concrete applications and also considered in higher exposition classes [7]. However, with today's recycling methods, the quality of RCA can be unsteady. Adversities like higher water absorption (WA), higher porosity and lower crushing strength challenge high-quality uses [8]. Also, in today's RCA there exist two interfacial transition zones (ITZ), which are the narrow regions between aggregate and cement matrix. These are differentiated between old (adherent mortar to aggregate) and new ITZ (RCA to cement matrix of RAC). One option to upgrade RCA is carbonation – a process by which carbon dioxide is incorporated into RCA as calcium carbonate [9]. Carbonation has been recognized to reduce the porosity and WA of RCA because the CO_2 reacts with Ca-bearing compounds such as $Ca(OH)_2$ and C-S-H [10]. CO_2 treatment also leads to the improvement of the old and new ITZ [11].

It is well known that common low-clinker cements lower the early strength, which can be a critical especially in pre-cast production. This is due to the correlation between the clinker factor and curing speed. Combining the substitution of NA by RCA and the use of a low-clinker cement may even worsen the early strength values. Therefore, alongside the use of low-clinker cement this paper focusses on quantifying the impact of previously accelerated carbonation on the mechanical properties of an optimized concrete mix design.

Since there is no broad consensus on the optimal compilation of a RAC mix design, this study demonstrates a comprehensive approach. For whatever type of RCA is used, the first step is preventing a disturbance of the effective water-cement ratio (w/c). This is only possible by monitoring the WA of the used RCA. The w/c should be kept as low as possible, to ensure higher early strength and durability. In contrast, workability indeed can decrease with RCA incorporation in some cases. A high range water reducing admixture (HRWRA) complementary with the used cement is needed in every respect. Differentiated mixing time in dependence of RCA pre-saturation state is another challenge to prevent de-mixing, as experience has shown, and is described in the following remarks.

2.   Materials and methods

2.1   Concrete specifications

Here we studied a concrete mixture for infrastructure elements in a premanufacturing plant. By specification, the air-entrained concrete had to meet a compressive strength of C35/45 along with exposition classes of XC4, XD3, XF4 and XM1. Flowability should be according to constistency class F3-F4. To maintain the production cycle, an early strength after 20 hours

is required. The initial reference mixture uses a gap grading with crushed natural Diabas (8-16 mm) and natural river sand (0-2 mm). As shown in **Erreur ! Source du renvoi introuvable.Erreur ! Source du renvoi introuvable.**, the used cRCA is sized 2-16 mm and has a content of concrete waste of more than 90 % (designated as Type 1 according to Table 1 of DIN 4226-101 [12]). The fRCA (**Erreur ! Source du renvoi introuvable.**)**Erreur ! Source du renvoi introuvable.** has a grain size ranging from 0 to 2 mm and was produced by concrete waste crushing. CEM III-A 52.5 R "Variodur 40"(Dyckerhoff) was used as a low-clinker cement. It contains 40 % of finely grained granulated furnace slag and 60 % finely ground clinker mixed with cement. Chryso Fluid Optima 145 was used as HRWRA as recommended by the manufacturer. Since a high freeze-thaw resistance is required, Sika LPS V was used as air entrainment admixture.

Figure 1: Dry cRCA (2-16 mm).   Figure 2: Dry fRCA (0-2 mm).

2.2 Carbonation of RCA

The accelerated carbonation of the cRCA (2-16 mm) and fRCA (0-2 mm) was carried out in an axially rotating drum reactor ($V = 75$ L) in batch operation at ambient temperature. 20.66 kg (cRCA) and 15.13 kg (fRCA) were moistened to 5 % and 11.1 % water content and exposed to a pure CO_2 atmosphere for one hour at a rotation rate of 6 and 5 rpm, respectively. Before starting the batch treatments, the reactor was purged with CO_2, followed by CO_2 dosing via a solenoid valve between pressure setpoints of 950 and 1050 hPa. To optimize material mixing a perforated mixing cage was used in the fRCA carbonation experiments. Over the reaction time of one hour the in-vessel pressure was recorded and integrated to quantify the CO_2 uptake, based on dry weight. Table 1 outlines the experimental conditions.

Table 1: Setup of laboratory carbonation process and CO_2 uptake.

	cRCA (> 2-16 mm)	fRCA (≤ 2 mm)
Reactor type	rotating drum	
Loading (solids)	20.66 kg$_{DM}$	15.13 kg$_{DM}$
Water addition	5.0 %	11.1 %
Mixing	axial rotation (6 and 5 rpm)	
Operation mode	batch	
CO_2 dosing	pressure set-points 950 and 1050 hPa	

Duration	1 h	
CO_2 uptake	0.25 wt.-%	1.95 wt.-%

2.3 Water absorption

The WA for fRCA was determined by pycnometry according to DIN EN 1097-6 [13]. The material was stored under water for 24 h, and then spread out on a steel sheet. Even drying was accelerated using a hot air gun with intermittent turning and mixing of the material. Saturated surface dryness (SSD) was determined by filling the material into a steel cone, compressing it lightly with a weight, and lifting the cone up. The SSD was identified with a drying state where the pile maintained its shape to a certain degree, between collapsing completely and staying firm.

The WA by cRCA was determined in accordance with the DAfStb guideline [14]. The material was water flooded for precisely 10 minutes. Then the water not held against gravity (excess water) was filtered through a cloth. After that it was dried with a towel, while the fine fractions additionally with a hairdryer, until the surface appeared visually dry.

2.4 Mixing of concrete

The mixing procedure as shown in Figure 3 was executed with consistent mixing speed and time, using a programmed mixer. The aim was to achieve an optimal ITZ between the RCA and the matrix. A cumulative mixing time of 12 minutes was used to prevent any de-mixing (Table 3). This is also in line with the recommendation by [15]. The WA of cRCA after 10 min, and 24 h for the fRCA is shown in Table 2. To ensure a constant w/c, the amount of additional water absorbed in 10 minutes was added to the concrete mix. [16]. Since oven-dried RCA was used, the three-step procedure suggested by Montero and Laserna [15] was extended to a four-step process including a one-minute prewetting. The higher WA of RCA has the effect, that in concrete it accumulates cement particles around the grains, causing a stronger bond [17]. If complete WA capacity is reached ahead of mixing concrete, this effect is inhibited. In numbers, 50-65 % of the total absorption capacity is considered as optimal initial moisture content of the RCA [18]. Thus, to calculate prewetting, the WA curves of cRCA and fRCA need to be known. In our case, these were estimated based on experience and literature data. Because of the larger grains, the WA of coarse material takes much longer to reach its full capacity than fine materials. The used cRCA reached 75 % of the total WA capacity (WA_{total}) after 10 min, and about 100 % after 24 h. The fRCA approximated WA_{total} after 10 min absorption time

Table 2: Experimental-based WA of native and carbonated RCA.

Material	Size (mm)	$WA_{10\ min}$ (wt.-%)	$WA_{24\ h}$ (wt.-%)	Method/Norm
fRCA	0-2	-	11.50	Pycnometer procedure/ DIN EN 1097-6 2001:01 [13]
fRCA (carbonated)	0-2	-	10.21	
cRCA	2-16	6.74	-	Annex B, DAfStb Guideline

| cRCA (carbonated) | 2-16 | 5.64 | - | "Concrete with recycled aggregates (…)" 2010-09 [14] |
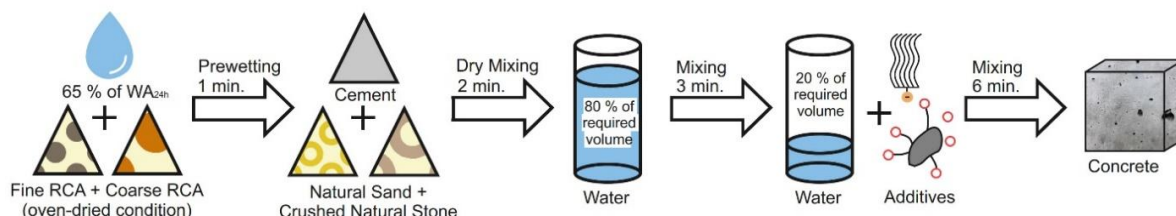
Figure 3: Employed mixing method of RAC manufacturing.

Table 3: Mixing procedure as used for the laboratory manufacturing of RAC.

Mixing step	Time (minutes)	
	Per step	Cumulative
1. Prewetting RCA (65 % of WA$_{total}$)	1	1
2. Dry Mixing of aggregate and cement	2	3
3. 80 % of mixing water including additional water for RCA (minus prewetting)	3	6
4. Additives, remaining water, final mix	6	12

2.5 Mix designs

As shown in Table 3, concrete mixture calculations were made based on 1 m^3 of the final product (fresh concrete). Four mix designs were considered with varied NA, RCA, and carbonated RCA volume fractions. The mixtures were designed depending on the aggregate ratio. The control mixture (C) consisted of NA only. In mix R30, 30 vol.-% of NA was substituted by cRCA. In mix R30S8, 8 vol.-% of natural sand was replaced by fRCA, maintaining a replacement rate for crushed stone of 30 vol.-% cRCA. Mix cR30S8 had the same composition but instead of as-received fRCA and cRCA carbonated RCA fractions were used.

Table 4: RCA content of mixtures as substitute for NA in 1 m^3 fresh concrete.

Material	Unit	C	R30	R30S8	cR30S8
fRCA	(kg/m³)	-	-	115.6	-
fRCA (carbonated)	(kg/m³)	-	-	-	118.4
cRCA	(kg/m³)	-	501.1	501.1	-

Material	Unit	C	R30	R30S8	cR30S8
fRCA	(kg/m³)	-	-	115.6	-
fRCA (carbonated)	(kg/m³)	-	-	-	118.4
cRCA	(kg/m³)	-	501.1	501.1	-
cRCA (carbonated)	(kg/m³)	-	-	-	501.1

3.   Results and discussion

3.1   Fresh properties

All mixes were prepared with a consistent air content of 7.5 ± 0.5 vol.-%. Since HRWRA dosage was kept constant, single flow values fell short of the target range of 420-550 mm. Mix C had the lowest flowability while R30S8 had the highest with values of 390 mm and 500 mm, respectively. When the crushed natural stone was replaced by 30 vol.-% cRCA, the sieve curve shifted to continuous grading and the mixture's workability improved. The flowability of cR30S8 was reduced compared to R30S8. The additional water requirement in cR30S8 was lower due to lower water absorption upon carbonation of the RCA. The reduced flowability may be explained by a lower content of water in the early mixing stage, which possibly reduced the effectiveness of HRWRA. Mixes R30, R30S8 and cR30S8 flowability values translate into the consistency classes F3-F4, and Mix C is classified as F2. No de-mixing was observed under these conditions.

3.2   Compressive strength

Figure 4 shows the compressive strength test results and deviation of the mixes after ageing for 1, 3, 7 and 28 days, based on the mean of three samples prepared for every test. Please note that the 1-day early strength was tested after 20 h to match the production cycle. Early strength was reduced by 4.12 % from C to R30 and decreased by further 5.87 % from R30 to R30S8. However, early strength values clearly exceeded 20 MPa with cR30S8 being the highest. From day 3 to day 7, proportions changed and the cR30S8 compressive strength was lower than R30 but imperceptibly higher than that of the R30S8 mixture. After 28 days compressive strength of C and R30 was 83 MPa and 70 MPa, respectively. The additional substitution of 8 % native sand by fRCA on top of the 30 % cRCA resulted in a further decrease in compressive strength to 63.8 MPa. However, using carbonated RCA, mixture cR30S8's compressive strength drew level with mixture R30. To summarize, mixture C would be classified as C60/75, R30 plus cR30S8 as C50/60 and R30S8 as C45/55.
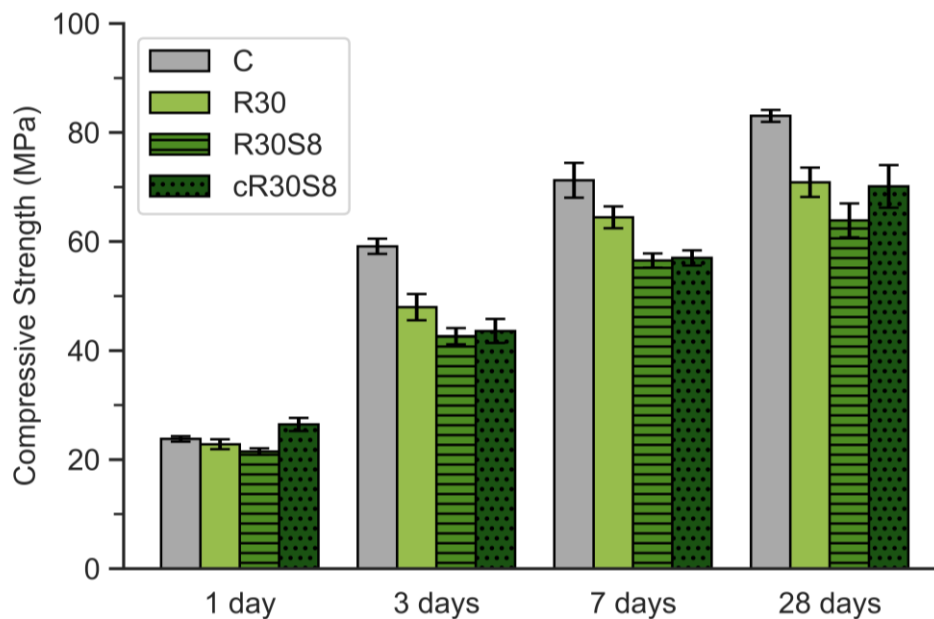
Figure 4: Compressive strength of concrete mixtures.

4. Conclusions

The results of this study demonstrated that:

- The WA of carbonated fRCA decreased by 11.21 % compared to as-received fRCA. The WA of carbonated cRCA decreased by 16.32 % compared to as-received cRCA. This emphasizes moist carbonation process effectiveness in improving RCA's porosity.

- In relation to the substitution rate, the compressive strength decrease of the mix with NA substitution of 8 % fRCA plus 30 % cRCA compared to 30 % cRCA was disproportionally higher than 30 % cRCA to only NA. The reduction of 28-day compressive strength by additional use of 8 % fRCA beyond the 30 % of RCA could be alleviated and the early strength compared to C could be increased by RCA carbonation in the same NA replacement ratio.

- fRCA exhibit higher CO2 uptake potential compared to cRCA. This highlighted their suitability as partial replacement for natural sand in concrete, allowing for enhanced concrete performance and reduced carbon footprint in RAC.

- Further research on fRCA utilization in concrete is recommended because its beneficial effect on early strength. At higher substitution rates, possible workability loss due to the more polygonal shape of fRCA should be in focus.

In summary, the utilization of carbonated RCA and low-clinker cement in ecological concrete mix designs offers significant potential for sustainable concrete production. The results highlight the CO_2 uptake potential of fRCA, improved porosity of carbonated RCA, carbonation's impact on compressive strength, and the importance of w/c in RAC mix design. These results contribute to advancing the understanding and application of ecological concrete processes, promoting resource conservation, and carbon emissions in the construction industry.

Acknowledgements

References

[1] *van Oss, H.:* Minerals Yearbook: Cement. Tech. rep. United States Geological Survey, 2021, usgs.govEd.National Minerals Information Centerhttps://www.usgs.gov/centers/national-minerals-information-center/minerals-yearbook-metals-and-minerals2021.

[2] *Ellis, L.D.; Badel, A.F.; Chiang, M.L. et al.:* Toward electrochemical synthesis of cement-An electrolyzer-based process for decarbonating CaCO3 while producing useful gas streams. *In:* Proceedings of the National Academy of Sciences of the United States of America, Vol. 117 (2020), Iss. 23, pp. 12584-12591. https://doi.org/10.1073/pnas.1821673116.

[3] *Huntzinger, D.N.; Eatmon, T.D.:* A life-cycle assessment of Portland cement manufacturing: comparing the traditional process with alternative technologies. *In:* Journal of Cleaner Production 17 (2009), Journal 7, p.668-675. https://doi.org/10.1016/j.jclepro.2008.04.007.

[4] *Verein Deutscher Zementwerke:* Decarbonisation of cement and concrete – Reduction paths and change strategies. A CO2-roadmap for the german cement industry, 2020, www.vdz-online.de/dekarbonisierung (2020).

[5] *Elsner, H.:* Mining of sand and gravel in germany – Status and challenges. BGR, 2022, bgr.bund.de 13.06.2023https://www.bgr.bund.de/DE/Themen/Min_rohstoffe/Veranstaltungen/Sand_und_Kies_in_Deutschland_2022/1_Vortrag_Elsner_Sand_und_Kies.pdf?__blob=publicationFile&v=32022 Accessed 13.06.2023].

[6] *Elsner, H.; Szurlies, M.:* Gravel - The most important local resource, 2020, bgr.bund.de 13.06.2023Ed.BGRhttps://www.bgr.bund.de/DE/Gemeinsames/Produkte/Downloads/Commodity_Top_News/Rohstoffwirtschaft/62_kies.pdf;jsessionid=76D7FAE4BB876227AD2BF87189DFD678.2_cid321?__blob=publicationFile&v=52020 Accessed 13.06.2023].

[7] *Mostert, C.; Weber, C.; Bringezu, S.:* Modelling and Simulation of Building Material Flows: Assessing the Potential for Concrete Recycling in the German Construction Sector. *In:* Recycling 7 (2022), Journal 2, p.13. https://doi.org/10.3390/recycling7020013.

[8] *Kou, S.; Zhan, B.; Poon, C.-S.:* Use of a CO2 curing step to improve the properties of concrete prepared with recycled aggregates. *In:* Cement and Concrete Composites 45 (2014), p.22-28. https://doi.org/10.1016/j.cemconcomp.2013.09.008.

[9] *Fang, X.; Xuan, D.; Shen, P. et al.:* Fast enhancement of recycled fine aggregates properties by wet carbonation. *In:* Journal of Cleaner Production 313 (2021), 127867. https://doi.org/10.1016/j.jclepro.2021.127867.

[10] *Russo, N.; Lollini, F.:* Effect of carbonated recycled coarse aggregates on the mechanical and durability properties of concrete. *In:* Journal of Building Engineering 51 (2022), 104290. https://doi.org/10.1016/j.jobe.2022.104290.

[11] *Kaliyavaradhan, S.K.; Ling, T.-C.:* Potential of CO 2 sequestration through construction and demolition (C&D) waste—An overview. *In:* Journal of CO2 Utilization 20 (2017), p.234-242. https://doi.org/10.1016/j.jcou.2017.05.014.

[12] DIN 4226-101: Recycled aggregates for concrete in accordance with DIN EN 12620. 08-2017.

[13] DIN EN 1097-6: Tests for mechanical and physical properties of aggregates. 05-2022.

[14] DAfStb-Guideline Concrete according to DIN EN 206-1 and DIN 1045-2 with recycled aggregates based on DIN EN 12620. 09-2010.

[15] *Montero, J.; Laserna, S.:* Influence of effective mixing water in recycled concrete. *In:* Construction and Building Materials 132 (2017), p.343-352. https://doi.org/10.1016/j.conbuildmat.2016.12.006.

[16] *Scheidt, J.:* Determination of the required total water for the production of recycled aggregate concrete with defined w/c ratio. Kaiserslautern, TU Kaiserslautern, Dissertation, 2019 https://kluedo.ub.rptu.de/frontdoor/deliver/index/docId/6028/file/_Dissertation%20Julia%20Scheidt_Ermittlung%20Gesamtwasser%20f%C3%BCr%20R-Beton%20mit%20definiertem%20w_z-Wert.pdf.

[17] *Poon, C.S.; Shui, Z.H.; Lam, L. et al.:* Influence of moisture states of natural and recycled aggregates on the slump and compressive strength of concrete. *In:* Cement and Concrete Research 34 (2004), Journal 1, p.31-36. https://doi.org/10.1016/S0008-8846(03)00186-8.

[18] *Sun, D.; Huang, W.; Liu, K. et al.:* Effect of the Moisture Content of Recycled Aggregate on the Mechanical Performance and Durability of Concrete. *In:* Materials (Basel, Switzerland), Vol. 15 (2022), Iss. 18. https://doi.org/10.3390/ma15186299.

SIMULTANEOUS RECOVERY OF THE FINE AND COARSE FRACTION OF MIXED RECYCLED AGGREGATES IN DESIGNING STRUCTURAL ECO-CONCRETE

Medina, C.[1],*, Urbano, J.[1], Pérez, A.[2], Mateos, J.M.[3], Soriano, M.[4]

(1) Cáceres Polytechnic School, University of Extremadura, Cáceres, Spain.

(2) INGECON Estructuras S.L., Plasencia, Cáceres, Spain

(3) Construcciones ARAPLASA, S.A., Plasencia, Cáceres, Spain

(4) INYGES Consultores S.L., Plasencia, Cáceres, Spain

* cmedinam@unex.es

Abstract

Recovering mixed construction and demolition waste (CDW) is a challenge in the current socio-economic context. Its reuse as a secondary raw material in formulating new recycled concrete will contribute to achieving the concept of green, circular and hypo-carbonic construction.

This research work analyses the feasibility of simultaneously recovering the fine and coarse fraction of mixed CDW incorporating a 10%-15% and 25% -50% percentage, respectively, in designing eco-recycled structural concrete ($f_{ck} \geq 25$ MPa and a/c = 0.55). To evaluate this item, the effect of its incorporation on the fresh (consistency) and hardened (compressive strength, ultrasonic pulse velocity and water impermeability) properties of the new recycled concrete was analysed. The results obtained show that incorporating the mixed coarse and fine fraction of the CDW as a granular skeleton does not translate into significant loss of consistency and mechanical (decreases of less than 19% compared to conventional concrete) performance. Also, all concrete, regardless of the porous mixed recycled aggregate percentage, has a waterproof structure by meeting the established requirements of maximum (≤ 50 mm) and mean (≤ 30 mm) water penetration under pressure required by the Structural Code (CodE).

1. Introduction

The construction industry is one of the greatest consumers of natural resources and contributors to emissions and solid waste. In 2020, it was responsible for emitting 11.7 gigatons of CO_2 and consuming 149 exajoules of energy, equivalent to 37% and 36% of the global totals, respectively [1]. Additionally, the environmental effects of this sector cannot be evaluated only from the perspective of production and construction but also from the perspective of demolition of the aged infrastructure that has completed their service life [2]. The construction and demolition waste (CDW) generates from this activity (new construction, repair, maintenance...) become important and needs to be rigorously considered. CDW constitute 36% of the total waste generated in the EU [3], and every year, around 800 Mt of CDW are generated in Europe [2].

Concrete products are second only to water as the most consumed material in the world by mass, with an estimated yearly consumption approaching 30 billion tonnes, which leads to per capita production greater than that of any other material [4]. This material is mainly made up of aggregates that represent between 60-75% of the volume of a concrete, as well as a smaller percentage of cement (10-15% of the volume of a concrete).

In this context, in recent decades, the scientific community has evaluated the technical feasibility of using recycled aggregates from CDW as an alternative raw material, mainly focusing on the coarse fraction of recycled concrete aggregates that present greater homogeneity and quality than the other fractions and types of recycled aggregates (mixed recycled aggregates and ceramic recycled aggregates).

Mixed recycled aggregates (MRA) represent ~67% of the total CDW in Spain, which has led to a greater quantity of research into the recovery of this type of recycled aggregates in the last decade [5, 6]. However, due to the intrinsic properties of mixed recycled aggregate (MRA), there is currently little knowledge of the feasibility of recovering the recycled mixed coarse and/or fine fraction in the sustainable concrete formulation.

The objective of this research work is the design and classification of environmentally-friendly structural concretes based on the simultaneous recovery of the fine (10% and 15%) and coarse (25% and 50%) fractions of recycled mixed aggregates from CDW. This initial classification entailed determining the consistency in the fresh state, as well as the compressive strength, ultrasonic pulse velocity and maximum and mean water depth with the concrete under pressure in the hardened state.

2. Materials and methodology

2.1 Materials

The recycled aggregates were supplied by the ARAPLASA CDW processing plant located in Plasencia, Cáceres (Extremadura). These aggregates are classified into two granulometric fractions 6/12 mm (Gv-MRA) and 0/6 mm (Ar-MRA). Compositionally, it is a mixed recycled aggregate with a concrete (Rc), unbound aggregate (Ru), ceramic (Rb) and others (X) content of ~28%, ~44%, ~24% and ~4 by weight, respectively. Natural aggregates are siliceous crushed aggregates, presented in two granulometric fractions: natural sand (Ar-NA, 0/6 mm) and natural gravel (Gv-NA, 6/12 mm).

Table 1: Properties of the aggregates.

Property	Gv-MRA	Ar-MRA	Gv-NA	Ar-NA	CodE [7]
Density (kg/m^3)	2.66	2.54	2.78	2.82	-
Water absorption after immersion for 24 h (wt.%)	7.69	7.04	0.88	1.18	≤5
Los Angeles coefficient (wt.%)	40	-	16	-	≤40
Flakiness index (wt.%)	15.48	-	20.36	-	<35
Sand equivalent	-	75	-	73	>70

Table 1 shows the analysed physical and mechanical properties of the aggregates used in this research, as well as the limits required by the Structural Code (CodE) [7] that includes the

requirements for aggregates used for manufacturing structural concrete. It highlights that the new recycled raw materials meet the requirements set forth, except for the water absorption values.

The Portland cement used is a CEM I 42.5 R that meets the physical, chemical and mechanical requirements established in the European EN 197-1 standard [8]. It was supplied by the Lafarge Holcim group plant in Villaluenga de la Sagra, in the Spanish province of Toledo, Spain.

The superplasticiser (SP) used for manufacturing concrete is ViscoCrete®-90 NG, supplied by Sika®.

2.2 Methodology

The experimental program includes the design and manufacture of a total of five mixes: i) reference concrete with natural aggregates (M1); ii) concrete with 10% mixed recycled sand and 25% recycled mixed gravel (M2), iii) concrete with 10% mixed recycled sand and 50% recycled mixed gravel (M3); iv) concrete with 15% mixed recycled sand and 25% recycled mixed gravel (M4); and v) concrete with 15% mixed recycled sand and 50% recycled mixed gravel (M5).

The methodology used to evaluate the formulated eco-concrete was through the classification of its fresh and hardened state. Regarding the fresh state, only workability was studied according to the EN 12350-2 standard [9]. In the hardened state, the following were evaluated: i) compressive strength at 7 and 28 days of curing according to EN 12390-3 [10], determined on a cubic specimen with an edge of 150 mm; ii) ultrasound pulse velocity at 28 days on a 150 mm cubic test tube according to EN 12504-4 [11]; and iii) mean and maximum depth of water under pressure according to EN 12390-8 [12] in cylindrical specimens of Ø150x300 mm. All the test pieces were manufactured according to the EN 12390-1 [13] standard and were cured under water at 20 ± 2ºC according to the EN 12390-2 [14] standard until they were tested.

Table 2: Mix batching.

Component (kg/m^3)	Mixes				
	M1	M2	M3	M4	M5
Natural sand	668.69	601.82	601.82	568.38	568.38
Recycled sand	0.00	59.82	59.82	89.73	89.73
Medium gravel	1017.97	763.48	508.99	763.48	508.99
Recycled medium gravel	0.00	222.39	444.78	222.39	444.78
Cement	313.60	313.60	313.60	313.60	313.60
Water	187.31	203.86	216.64	205.74	218.52
Admixture	2.82	2.82	2.82	2.82	2.82

2.3 Design of the concretes

The different mixes were designed using the Faury dosage method with the aim of obtaining eco-concretes with a characteristic strength (f_{ck}) of 25 MPa and exposure classes X0 and XC.

This method establishes as starting data i) granulometric distribution of the constituent aggregates of the granular skeleton; ii) density and shape of the aggregates; iii) soft concrete consistency (50-90 mm); and iv) cement content (320 kg/m^3).

Table 2 shows the dosing results of all concrete mixes. It shows how the constant effective ratio (a/c) of 0.55 is preserved all the mixes, in order to adequately compare the performance of the manufactured concretes. Corrections were therefore made using the water compensation by absorption of the aggregates method [15].

3. Results

3.1 Consistency

Table 3 shows the consistency results in the Abrams cone of the eco-concretes, observing that all the mixes are within the design objective consistency (50 < S2 < 90 mm). This result shows that the addition of the mixed recycled fine and coarse fraction has no negative effect on this property. This behaviour is in line with what was proposed by Agrela et al. [16] and Medina et al. [17] who proposed strategies to mitigate the negative effect that the greater water absorption of the recycled aggregates has on this property, pre-saturating them before the mixing process or adding the water in the dosage initially absorbed by these recycled aggregates, respectively.

Table 3: Fresh state property in concretes.

Property	Mixes				
	M1	M2	M3	M4	M5
Consistency (mm)	54 ± 3	66 ± 4	52 ± 2	54 ± 2	53 ± 3

3.2 Compressive strength and ultrasonic velocity

Figure 1 shows the evolution of the compressive strength of the different mixes analysed at 7 and 28 days, observing that regardless of the type of concrete: i) the compressive strength increases as the cured age increases, the evolution of which is very similar to that shown by the reference concrete; ii) the relative compressive strength at 7 days is between 86.7%-89.2% of that at 28 days, a percentage that is within the range of values 65-93% recorded by Bravo et al. [18] for concretes that partially incorporate CDW; and iii) the average strength at 28 days is higher than the characteristic design strength of 25 MPa.
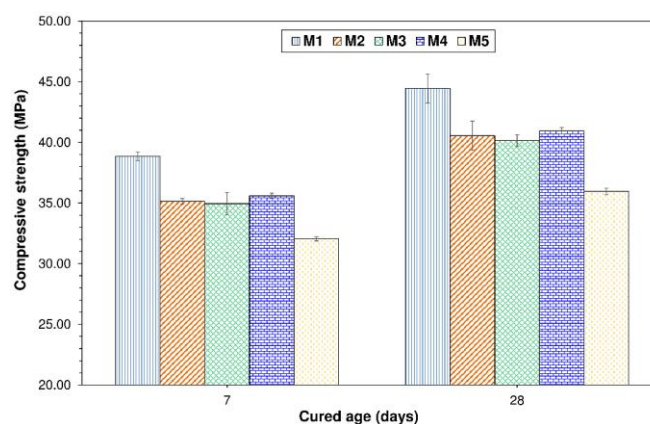

Figure 1: Compressive strength at 7 y 28 days.

Figure 1 also shows that the addition of fine and coarse mixed recycled aggregate causes a performance loss, with decreases between 9.5-17.5% and 8.8-19.1% with respect to M1 at 7 and 28 days respectively. These decreases are less than the addition percentage. The decrease is mainly associated with the intrinsic properties of the recycled aggregate (more porous micro-structure and less resistance to fragmentation) and the presence of a greater number of interphases in the new eco-concretes (M2-M5).

Table 4 shows the ultrasonic pulse velocity results at 28 days of curing. It shows that the addition of the mixed recycled aggregate decreases the speed of passage, mainly due to the greater porosity with respect to the natural aggregate, as previously indicated by Kwan et al. [19]. The minimum and maximum variation corresponds to the M4 and M5 mix by -3.1% and -8.3% with respect to M1, respectively. This variation range is similar to the range (5%-10%) obtained in concretes made with up to 60% of coarse recycled concrete aggregate [20].

Table 4: Ultrasonic pulse velocity (UPV) in concretes.

Property	Mixes				
	M1	M2	M3	M4	M5
Ultrasonic pulse velocity (m/s)	4586 ± 63	4370 ± 137	4349 ± 48	4407 ± 40	4289 ± 29

Finally, according to the results of the UPV [21], it can be considered that concretes with a value higher than 4575 m/s can be considered as excellent quality concretes, and values between 3660 m/s - 4575 m/s as good quality concretes. According to the results presented in table 4, Mix 1 would be of excellent quality and the rest of the mixes (M2-M5) of good quality, these values being very close to the upper limit of this range.

3.3 Penetration depth under pressure

Figure 2 shows the maximum and average depth values of the eco-concretes after 28 days of curing, observing that regardless of the addition percentage, the values are lower than the maximum limit (average depth ≤30 mm and maximum depth ≤50 mm) permitted by the CodE [7]. It can therefore be established that all concretes have a sufficiently impermeable porous structure against water.
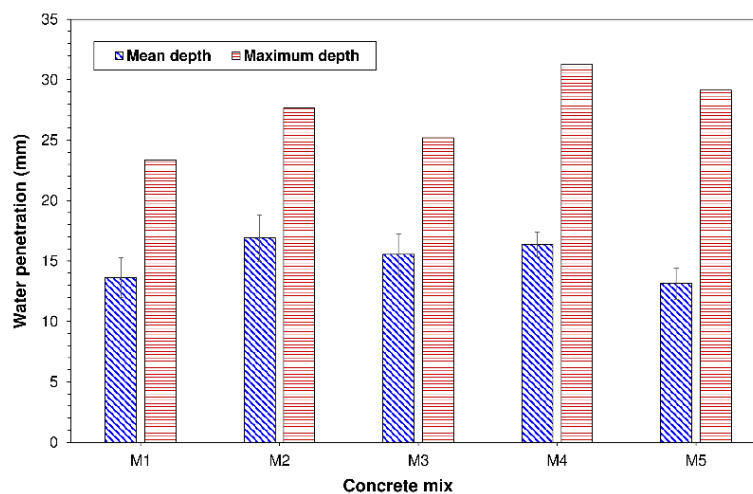

Figure 2: Maximum and mean 28 days depth of water penetration under pressure in concretes.

4. Conclusions

The conclusions obtained from this research work were:

- The addition of mixed recycled aggregate (fine and coarse) does not negatively influence the consistency of the new eco-concretes.

- Eco-concretes have a compressive strength greater than and equal to 25 MPa at 28 days.

- The maximum and average depth of the eco-concretes is less than the maximum value allowed by the CodE.

Finally, the formulated eco-concretes could logically be used as structural concretes for exposure classes X0 and XC, for which their durable properties would need to be evaluated in a second research phase.

5. References

[1] Xing, W., Tam, V., Le, K., Hao, J. and Wang, J. "Life cycle assessment of sustainable concrete with recycled aggregate and supplementary cementitious materials". *Resour. Conserv. Recycl.* **193** (2023), 106947

[2] Ozcelikci, E., Kul, A., Faruk, M., Furkan, B., Yildirim, G., Ashour, A. and Sahmaran, M. "A comprehensive study on the compressive strength, durability – related parameters and microstructure of geopolymer mortars based on mixed construction and demolition waste". *J. Clean Prod.* **396** (2023), 136522

[3] Moschen-Schimek, J., Kasper, T. and Huber-Humer, M. "Critical review of the recovery rates of construction and demolition waste in the European Union – An analysis of influencing factors in selected EU countries". Waste Manage. **167** (2023), 150-164

[4] Griffiths, S., Sovacool, B.K., Furszyfer, D., Foley, A.M., Bazilian, M.D., Kim, J. and Uratani, J.M. "Descarbonizing the cement and concrete industry: a systematic review of socio – technical systems, technological innovations, and policy options". *Renew. Sust. Energ. Rev.*, **180** (2023), 113291

[5] Sáez del Bosque, I.F., Zhu, W., Howind, T., Matías, A., Sánchez de Rojas, M.I. and Medina, C. "Properties of interfacial transition zones (ITZs) in concrete containing recycled mixed aggregate". *Cem. Concr. Comp.* **81** (2017), 25-34

[6] Díaz, M., Plaza, P., Blanco, D., Jordán, M.M., Sáez del Bosque, I.F. and Medina, C. "The design and development of recycled concretes in a circular economy using mixed construction and demolition waste". *Materials* **14** (2021), 4762

[7] Ministry for Transport, Mobility and the Urban Agenda. Structural Code (CodE). Government of Spain, 2022.

[8] European Committee for Standardization, "EN 197-1. Cement - Part 1: Composition, specifications and conformity criteria for common cements", 2011.

[9] European Commission for Standardization, "EN 12350-2. Testing fresh concrete: Part 2: Slump test", 2020.

[10] European Commission for Standardization, "EN 12390-3. Testing hardened concrete: Part 3: Compressive strength of test specimens", 2020

[11] European Commission for Standardization, "EN 12504-4. Testing concrete in structures: Part 4: Determination of ultrasonic pulse velocity", 2022

[12] European Commission for Standardization, "EN 12390-8. Testing hardened concrete: Part 8: Depth of penetration of water pressure", 2020

[13] European Commission for Standardization, "EN 12390-1. Testing hardened concrete: Part 1: Shape, dimensions and other requirements for specimens and moulds", 2022

[14] European Commission for Standardization, "EN 12390-2. Testing hardened concrete: Part 2: Making and curing specimens for strength tests", 2020

[15] Ferreira, L., de Brito, J. and Barra, M. "Influence of the pre-saturation of recycled coarse concrete aggregates on concrete properties". *Mag. Concr. Res.* **63** (2011), 617-627

[16] Agrela, F., Sánchez de Juan, M., Ayuso, J., Geraldes, V.L. and Jiménez, J.R. "Limiting properties in the characterisation of mixed recycled aggregates for use in the manufacture of concrete" *Constr. Build. Mater.* **5** (2011) 3950-3955

[17] Medina, C., Zhu, W., Howind, T., Sánchez de Rojas, M.I. and Frías, M. "Influence of mixed recycled aggregate on the physical and mechanical properties of recycled concrete". *J. Clean Prod.* **68** (2014) 216-225

[18] Bravo, M., de Brito, J., Pontes, J. and Evangelista, L. "Mechanical performance of concrete made with aggregates from construction and demolition waste recycling plants". *J. Clean Prod.* **99** (2015) 59-74

[19] Kwan, W.H., Ramli, M., Kam, K.J. and Sulieman, M.Z. "Influence of the amount of recycled coarse aggregate in concrete design and durability properties". *Constr. Build. Mater.* **26** (2012) 565-573

[20] Cantero, B., Bravo, M., de Brito, J., Sáez del Bosque, I.F. and Medina, C. "Mechanical behaviour of structural concrete with ground recycled concrete cement and mixed recycled aggregate". *J. Clean Prod.* **275** (2020) 122913

[21] Malhotra, V. "Testing hardened concrete: nondestructive methods". Detroit. MI: ACI Monograph, 9 (1976)

OPTIMIZING SELF-COMPACTING MORTAR MIXES WITH RECYCLED WASH-SLUDGE FINES

Yury A. Villagran-Zaccardi (1), Arne Peys (1)

(1) Sustainable Materials, Flemish Institute for Technological Research, Mol, Belgium

yury.villagranzaccardi@vito.be; arne.peys@vito.be

Abstract

The aggregate industry generates massive amounts of sludge, which are typically used in low-value backfilling or landfilled. Given the close relationship between aggregate and concrete industries, using these sludges as a secondary raw material in concrete production makes a great deal of sense. This study examines the use of recycled wash-sludges from crushed granite production as secondary raw materials in self-compacting mortar mixes. Self-compacting mixes require a substantial amount of fines, and using secondary fines reduces the demand for virgin resources. However, the presence of contaminants like clay can affect the mix properties. In this study, slump-flow and V-funnel tests were used to optimise the water-to-powder ratio, filler-to-cement ratio, and superplasticizer content of the mixes. The moderate clay contents in the sludges showed a dual effect by increasing both water demand and cohesion, and the sludge content in the mixes was defined based on such an impact. Our results demonstrate the technical feasibility of this approach, but reducing the impact of clay content further is important for improved performance and cost reduction.

1.   Introduction

The production of crushed gray granite in Norway (Velde site) from excavated material at demolition sites involves a washing step that generates significant amounts of sludges. These sludges are currently used in backfilling with relatively low added value. Therefore, exploring alternative applications as filler for this material in the cement and concrete industry seems valuable.

Initially, the inclusion of filler might be assumed as a simple dilution effect on the performance of the concrete mix, but the impact on the concrete performance is tied to the specific properties of the filler. The dilution effect is not a critical issue for the particular case of self-compacting mixes as the high volume of fines is intended to provide the necessary fluidity and cohesion. However, secondary contributions from the filler could further help reducing the cement content. For instance, using fly ash in self-compacting mixes fills space in the fresh state and develops microstructure through pozzolanic action in the hardened state. Despite these benefits, fly ash does not contribute sufficiently to the cohesion of the mix, requiring the use of viscosity

modifiers that could increase the cost of the self-compacting concrete. Therefore, the assessment is more complex than a simple examination of the dilution effect.

Li et al. [1] assumed null water demand from granite filler when adding it in concrete replacing paste volume (instead of the common approach of replacing cement volume). The use of granite dust as a paste volume replacement to reduce the cement content by up to 25% increased the cube strength of mortar by about 12%. However, the assumption of null water demand proved untrue as the approach increased the superplasticizer dosage to maintain workability.

Results presented in [2] show a similar outcome of increased superplasticizer demand with granite powder, but in this case coupled with a significant dilution effect of performance in hardened state. The granite powder was coarser than the cement and the replacement was made in terms of cement content, leading to expected negative impact on strength.

Contrasting results are presented in [3], where lower superplasticizer demand is reported for fine granite powder inclusion as cement replacement. When granite waste is included unprocessed as a replacement of sand or cement, the coarser fraction of the granite waste introduces significant internal friction that reduces workability. However, as the granite waste was fine enough, no specific demand of superplasticizer by the filler itself was noted. The effect on water demand is different, as it is directly related with the fineness of the material. Mashaly et al. [4] reported greater water demand with higher contents of fine granite powder. For the particular case of excavated material such as the one under study in the present research, more important is the presence of minor constituents, especially clays, as these will significantly affect both the water and superplasticizer demands.

Nepomuceno et al. [5] propose a relatively straightforward application for granite powder as filler for the production of self-compacting concrete. The lack of additional processing for such application is a significant advantage for the valorization strategy, but this becomes arguable if the demand of superplasticizer is increased. When viscosity of the mix is also affected, mixes can no longer be compared based on same water content. An iterative process is then needed to determine the optimal combination of water and superplasticizer contents for adequate self-compactibility. Potential contamination with clays is an important consideration, as these can negatively impact on superplasticizer demand. In a comparison of mortars with the same volume of powder to volume of sand, Nepomuceno et al. [5] found that granite powder was disadvantageous in terms of water and superplasticizer demands when compared to other fillers such as limestone powder or fly ash. Similar results are presented in [6] for production of reactive powder concrete. These results suggest that self-compacting mixes with granite powder would be more expensive than with other type of filler. However, considering the cost, environmental impact, and strength, Asadi Shamsabadi et al. [2] concluded that using granite waste powder as cement replacement could more advantageous if workability loss is compensated by increasing mixing water instead of superplasticizer content. These findings suggest that an appropriate tailored strategy is necessary for the sludges under study.

In terms of compressive strength, Nepomuceno et al. [5] found no significant difference between using granite filler, limestone filler, or fly ash as powder in self-compacting concrete. These may be indirectly affected by the water demand, but if the water-to-cement ratio is maintained constant, the compressive strength remains unaffected, albeit at a high cost. Therefore, the main technical issue for the application of filler derived from the sludges in self-compacting concrete are related to the fresh state.

A comparison of different types of fillers in the production of self-compacting concrete shows that granite filler has advantages over more reactive powders (e.g. silica fume, metakaolin, and even Portland cement) and limestone powder in terms of limited segregation and bleeding [7, 8]. One possibility for explaining this is that the use of granite powder increased viscosity and reduced the dependence on viscosity modifiers for the production of stable self-compacting mixes. Karmegam et al [9] attribute the higher viscosity with granite powder to the particle shape (more angular than fly ash or silica fume); however this does not offer full explanation, as milled clinker and slags are also equally angular but still show high bleeding risks. For the particular sludges under study, the content of clay may as well contribute with increased viscosity in spite of the associated increase in superplasticizer demand. A derived advantage of an increased viscosity is the potential capacity of increasing the maximum aggregate size (usually limited to 12-19 mm) in self-compacting concrete. If a stable mix with a larger maximum aggregate size can be produced, less paste will be needed, and more eco-efficient mixes will be obtained in consequence.

The present study explores the opportunity for the exploitation of sludges derived from gray granite production from excavated material in self-compacting mixes. The complex effects of filler inclusion are connected to the specific properties of the sludges to optimize water and superplasticizer content at paste and mortar level as a preliminary step to assess the economical, environmental, and technical benefits and decide on potential upscaling at concrete level.

2.   Materials and Methods

The used materials were modified polycarboxylic ether-based superplasticizer (MasterGlenium 51®, Master Builders Solutions), cement CEM I 52.5 N, standard CEN sand, and fillers produced with the secondary sludge. The sludge was collected in five sampling campaigns at the production site of Velde (Norway) to assess the variability in properties over different production periods. The sludge was dried out in an oven overnight and disc milled in the laboratory, giving origin to Fillers 1 to 5. The disc mill only grinds the material at low energy to disaggregate the agglomerated material and not to engineer the particle size distribution. Figure 1 depicts the particle size distribution (determined by sieving coupled with laser diffractometry for particles <90 μm) and mineralogical composition (determined by Rietveld analysis of XRD patterns) of the fillers. Due to the limited grinding, the particle size distribution is unchanged from that of the on-site sludge. The size range impedes complete classification as a filler or as a sand. For the purpose of this research, the material was treated as a filler because most of its mass is in that particle size range. The main crystalline phase groups are quartz, feldspars (albite and microcline), and clays (mostly muscovite, but also kaolinite and clinochlore). The average density and loss on ignition at 1050 °C of the filler were (2.64 ± 0.02) g/cm^3 and 1.86 wt%, respectively.

First, the optimal water-to-powder ratio in pastes for each of the five fillers was determined. The mixing was done according to the standard procedure in EN 196-1, except that no sand was used. The flow of each paste was measured using a standard conic mould on a steel plate. The paste was poured into the mould without being compacted, and then the mould was lifted to allow the mix flow freely. Equation 1 was used to convert the final diameter (slump-flow) into the relative slump $\Gamma_{p/m}$, with d_1 and d_2 being the two perpendicular slump-flow values.

$$\Gamma_{p/m} = \left(\frac{0.5 \cdot d_1 + 0.5 \cdot d_2}{100}\right)^2 - 1 \tag{1}$$
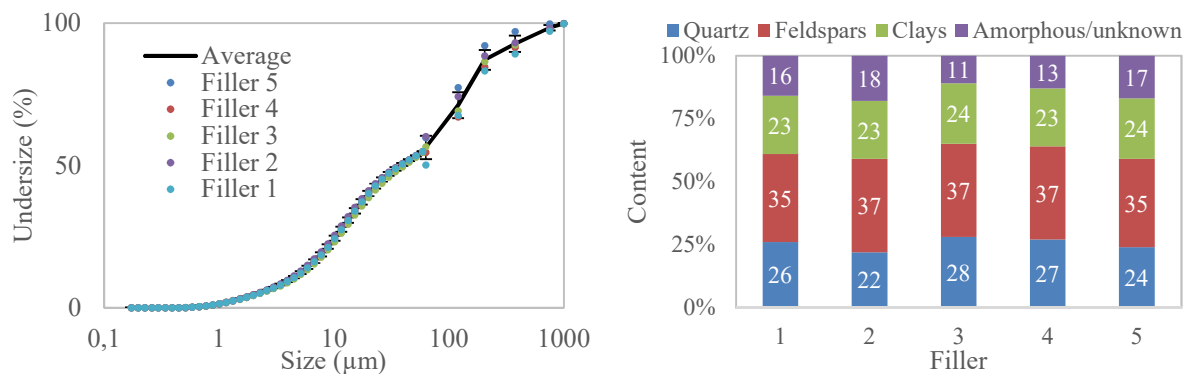
Figure 1: Properties of fillers: left: Particle size distribution; right: mineralogical composition.

Pastes with sludge filler accounting for 30 to 60 wt% of the powder were tested, for water-to-powder volume ratios (W/P) of 1.2, 1.3, and 1.4. Individual relationships for each filler content were constructed in a W/P versus $\Gamma_{p/m}$, and the intersection with the vertical axis was determined as the parameter of interest, βp.

Following that, the superplasticizer content was adjusted in mortar mixes to achieve slump-flow values in the range 240-260 mm (=relative slump-flow $\Gamma_{p/m}$ between 4.76–5.76), reducing the water content to between 85 and 95% of βp so that the targeted V-funnel time (EN 12350-9, adapted for mortar and using an small V-funnel for mortar) was in the range 7-11 s. These mortar mixes were designed with the content of sand representing 50% of the mortar volume and optimized filler content, superplasticizer dose, and W/P (see following section).

For the mortars that met the target slump-flow and V-funnel time, three 40x40x160 mm^3 specimens were cast without any compaction procedure to test hardened properties later: compressive strength, water absorption (EN 1097-6 adapted for vacuum saturation), and porosity.

3.   Results and discussion

Figure 2 depicts the relationships between the relative slump-flow values and the W/P for various filler contents respect to total powder (P30 to P60 for 30 to 60 wt% of filler). Except for P30 with Filler 1, all of the other curves follow a very similar pattern. The precise reasons for the different outcome for P30-Filler 1 are not clear, and it is therefore assumed to be an outlier. The dilution of Portland cement by the filler has no effect on water demand. This result can be attributed to the relatively high content of clays in the sludges. This is considered a disadvantage in terms of costs for the application as filler, as the demand of water will limit the amount of filler that can be incorporated in the mixes to achieve sufficient self-compactability, without affecting the performance in the hardened state.

Based on the results of slump-flow as a function of the W/P, it was decided to define a filler content of 40 wt% of the total powder content. This decision was made as a compromise to maximise the use of the filler while still achieving adequate performance in the hardened state. For filler allowing use ratios of 50 or 60 wt%, it appears that additional treatment of the sludges is required to reduce the content of clay (which may be valorized with a different approach, e.g., as calcined clays). Figure 3 shows the optimization of the superplasticizer content for mortar mixes with Filler 1 (W/P=0.85, 40 wt% filler content). The relative slump-flow appears to be a linear function of superplasticizer content (indicating a range below the saturation point). The targeted slump-flow was achieved for 0.88 wt% of (solid content of) superplasticizer

relative to powder (Fig 3, left). However, the viscosity of the mix was still excessively high, as demostrated with the V-funnel time. The W/P had to be further increased from 0.85 to 0.95 to achieve the required V-funnel time, and to maintain the slump flow value this increase in water content was compensated with a reduction in the superplasticizer from 0.88 to 0.66 wt%.
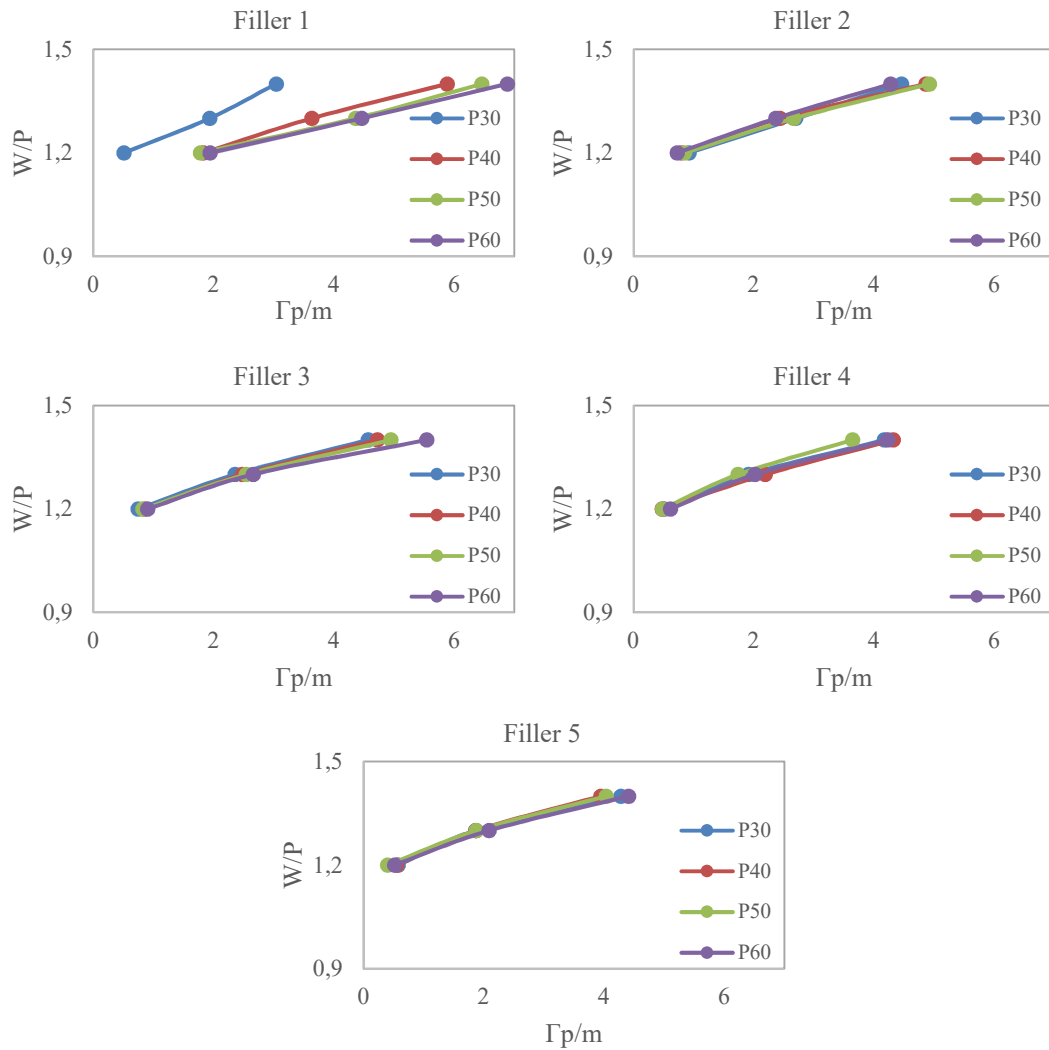

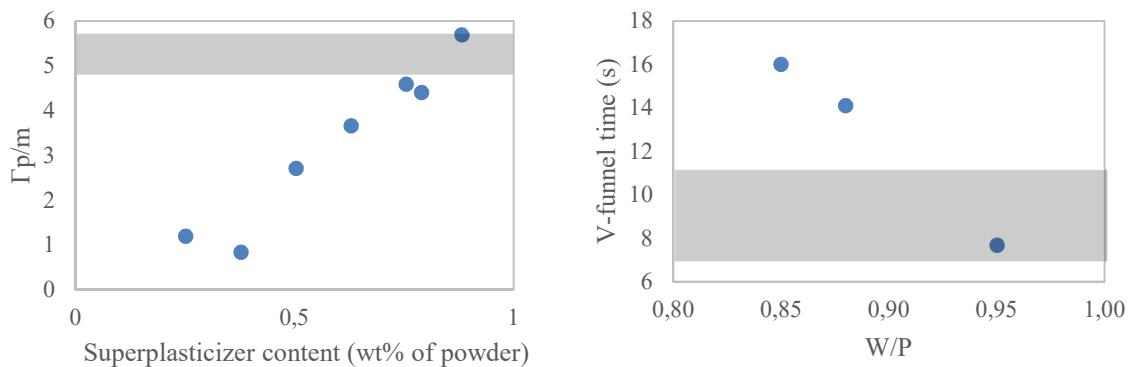Figure 2: Variation of the relative slump-flow with W/P.

Figure 3: Optimization of superplasticizer and water content for target slump-flow (left) and V-funnel time (right), respectively.

The results from fresh mortar mixes show that, even though the filler has a water demand level higher than desired, it also contributes to the viscosity of the mix. This means that these self-compacting mixes have greated cohesion than mixes with other materials used for the same purpose (e.g. limestone, fly ash). In practice, this would mean less segregation and the ability to design self-compacting concrete with a higher coarse aggregate content. Such abilities are to be proven with additional tests at concrete level.

Figure 4 presents the properties of the mortars for the five fillers (filler content = 40 wt%, superplasticizer = 0.66 wt%, W/P = 0.95). The average compressive strength of the mortars is 61.5 MPa, indicating a very promising performance considering that the effective water-to-cement ratio of the mixes was 0.5. The porosity values (calculated from the vaccum saturated water absorption) are also in the expected range for a high performance mix. Overall, these preliminary results at mortar level indicate a promising performance that should be confirmed at concrete level in future research, accounting for relative production costs as well.
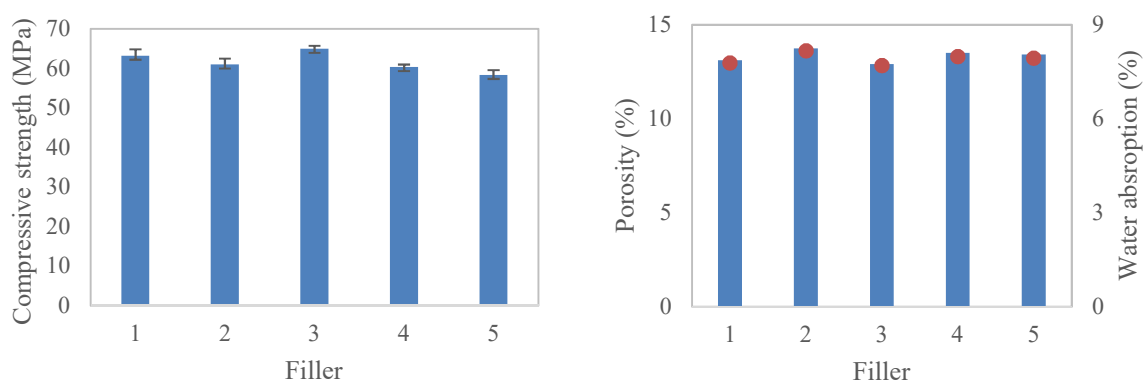
Figure 4: Compressive strength and porosity (bars) (from water absorption capacity, markers), after 28 days of curing.

11.   Conclusions

The variability in composition and properties of the sludges is very limited. This enables to consider the use of the material without additional processing for homogenization. A relatively high content of clays affects the water and superplasticizer demands, which may impact negatively on the production cost of mixes containing these fillers, but it may also contribute to more robust self-compacting mixes with increased cohesion. At this stage, the content of filler seems limited to 40 wt% of the powder. Alternatively, advanced separation techniques may be suitable to reduce the clay content in the sludges, allowing fine-tuned valorization channels to be used as both filler and supplementary cementitious material. The properties of the hardened mortars demonstrate a satisfactory performance, eventually leading to an appropriate strength level and durability of concrete mixes. Such premises are to be confirmed in future research at concrete level.

References

[1] Li, L. G., Wang, Y. M., Tan, Y. P., Kwan, A. K. H., 'Filler technology of adding granite dust to reduce cement content and increase strength of mortar', *Powder Technology* **2019,** *342*, 388-396.

[2] Asadi Shamsabadi, E., Ghalehnovi, M., de Brito, J., Khodabakhshian, A., 'Performance of Concrete with Waste Granite Powder: The Effect of Superplasticizers', *Applied Sciences* **2018,** *8* (10).

[3] Li, H., Huang, F., Cheng, G., Xie, Y., Tan, Y., Li, L., Yi, Z., 'Effect of granite dust on mechanical and some durability properties of manufactured sand concrete', *Construction and Building Materials* **2016,** *109*, 41-46.

[4] Mashaly, A. O., Shalaby, B. N., Rashwan, M. A., 'Performance of mortar and concrete incorporating granite sludge as cement replacement', *Construction and Building Materials* **2018,** *169*, 800-818.

[5] Nepomuceno, M., Oliveira, L., Lopes, S. M. R., 'Methodology for mix design of the mortar phase of self-compacting concrete using different mineral additions in binary blends of powders', *Construction and Building Materials* **2012,** *26* (1), 317-326.

[6] Savadkoohi, M. S., Reisi, M., 'Environmental protection based sustainable development by utilization of granite waste in Reactive Powder Concrete', *Journal of Cleaner Production* **2020,** *266*.

[7] Elyamany, H. E., Abd Elmoaty, A. E. M., Mohamed, B., 'Effect of filler types on physical, mechanical and microstructure of self compacting concrete and Flow-able concrete', *Alexandria Engineering Journal* **2014,** *53* (2), 295-307.

[8] Sadek, D. M., El-Attar, M. M., Ali, H. A., 'Reusing of marble and granite powders in self-compacting concrete for sustainable development', *Journal of Cleaner Production* **2016,** *121*, 19-32.

[9] Karmegam, A., Kalidass, A., Ulaganathan, D., 'Utilization of granite sawing waste in self compacting concrete', *Građevinar* **2014,** *66* (11), 997-1006.

OVERCOMING TECHNICAL AND REGULATORY BARRIERS FOR A BETTER CIRCULAR ECONOMY IN CONSTRUCTION INDUSTRY

Luc Courard, Julien Hubert

Urban and Environmental Engineering, Building Materials, University of Liège

Abstract

The availability of resources for the construction industry is becoming increasingly uncertain, while at the same time the amount of construction waste, but also of industrial and agricultural by-products, is growing. Reconciling needs and secondary resources as well as contributing to reuse is a useful and motivating scientific challenge. But legal and regulatory barriers have to be overcome in order to allow a real circular economy in the construction industry. Working locally and developing an appropriate treatment of Construction and Demolition Wastes is favouring upcycling and valorization of secondary materials for prefabricated and 3D printed concrete. Technical properties of recycled materials are analysed, and proposals are made for increasing the rate of incorporation into concrete prefabricated products. In the same time, minimum requirements are proposed for using recycled sand in 3D mortars. Final properties are compared with classical materials and durability of end products is analysed. Accelerated carbonation process seems to increase recycled sands and aggregates properties (before and/or after manufacturing concrete). But a large and systematic use of recycled materials needs to adapt regulations and requirements for specific applications: this is essential for lowering environmental impact of the construction industry.

1. Introduction

In 2020, the EU-27+UK countries produced a total amount of 2,135 million tonnes (Mt) of wastes (4815 per capita) by all economic activities and households [1]. The construction industry accounts for one third (37.5%) of all the generated wastes and consists of one of the heaviest and most voluminous waste stream in the EU. Construction and demolition wastes (C&DW) represent an amount of about 850 Mt generated every year by the EU-28 or 1.7 tonne produced per year and per EU inhabitant. Moreover, almost two-thirds (64 % or 3.1 tonnes per inhabitant) of the total waste generated in the EU in 2020 was major mineral waste.

On the other side, the annual European demand in aggregates amounted to 2,99 Mt in 2021 (Fig. 1). The European demand represents about 10% of the global demand in aggregates [2].
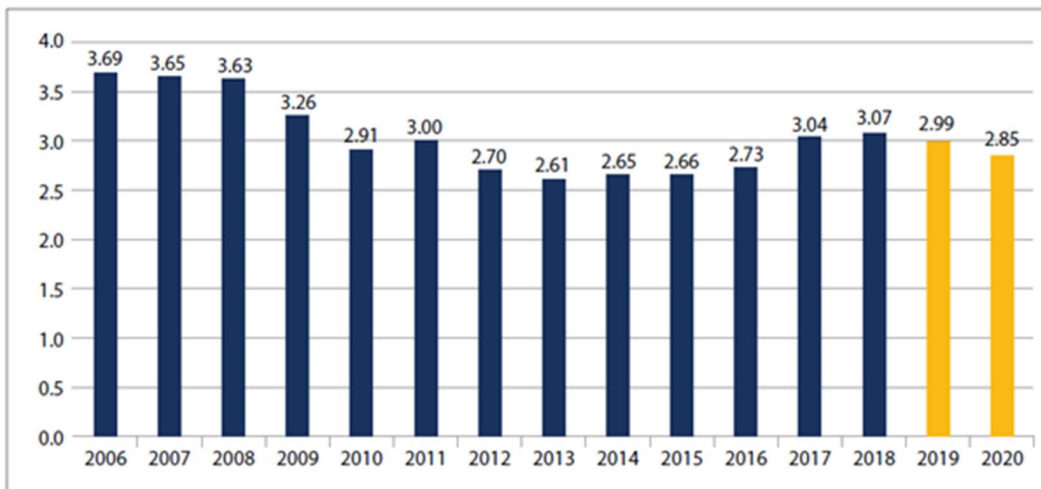
Figure 1: EU+UK+EFTA Trend in Production in Billions of Total Tons (UEPG, 2021) [2]

Aggregate and sand materials are in high demand globally for construction purposes, with an annual growth rate of around 5% while the availability of sand is decreasing. Figure 2 shows the clear increase in sand demands over the previous and coming years. The United States and China show overall the highest yearly demand of sand.
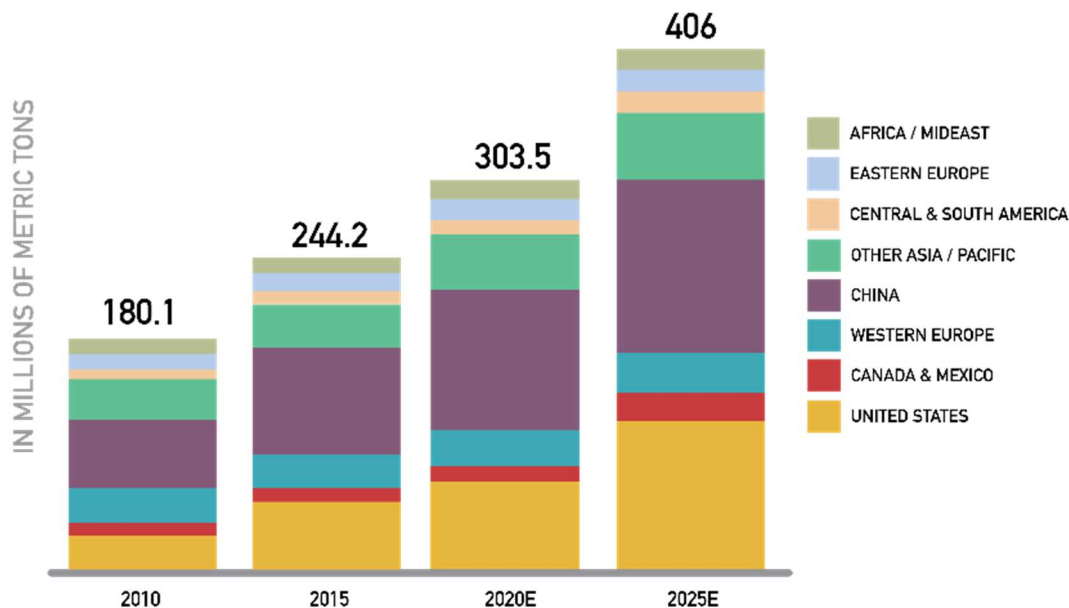
Figure 2: World sand demands in millions of metric tons.
https://iveybusinessreview.ca/6580/lafargeholcim-the-plastic-solution-to-the-global-sand-wars/graphic-2-world-sand-demand/

Figure 3 provides a synopsis of the 2019 national production tonnages categorized by country and aggregate type. Germany emerged as the leading producer, surpassing 500 million tons, followed by Russia, Turkey, France, the UK, and Poland. In contrast, smaller nations such as Malta, Montenegro, Iceland, Luxembourg, and Cyprus exhibited production levels below 5 million tons.
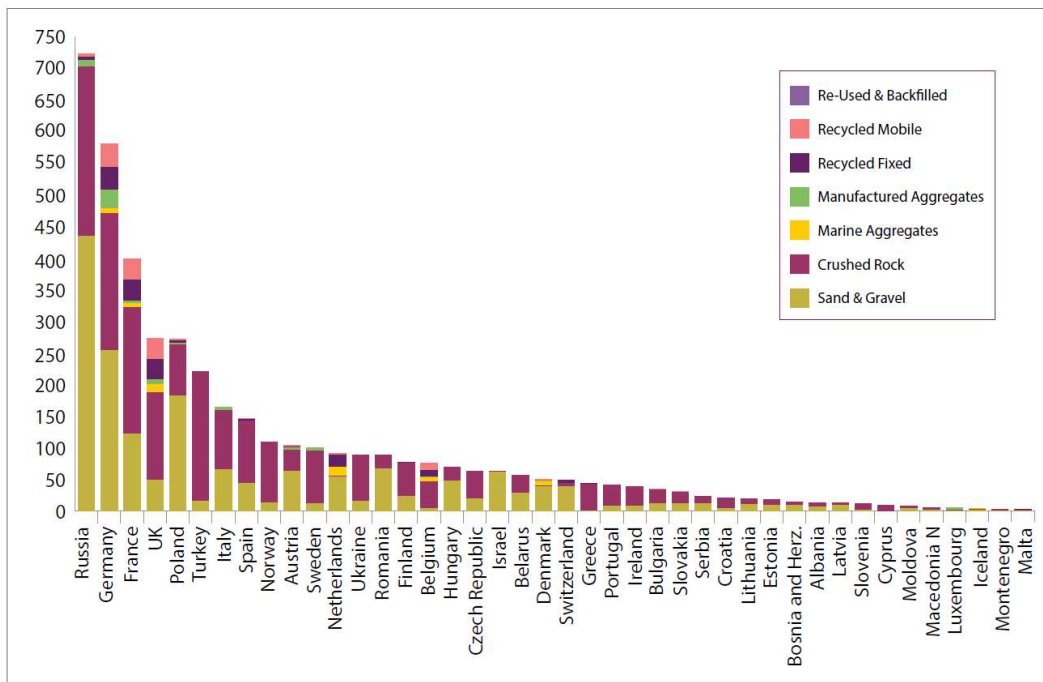
Figure 3: 2019 aggregates production in Europe (UEPG, 2021)

National tonnages depend not only on economic strength, but also on geological availability of and access to deposits, national ambient climate, ruggedness of the terrain and local building traditions.

Figure 4: Aggregate type percentages

The composition of aggregate types (Fig. 4) in the EU27+UK+EFTA countries in 2019 revealed that crushed stone accounted for 46.9% of all production, while sand and gravel constituted

39.7%. Aggregate production from recycled and reused materials contributed 9.3%, with marine and manufactured aggregates comprising the remaining 4%.

2. Market analysis and barriers

The market of recycled sands and aggregates (RS&A) needs to be healthy at country scale to foster member states to reach the target defined in the Waste Framework Directive (2008/98/EC) [3]. The most cited drivers that can boost C&DW recycling are: Green Public Procurement, taxation on C&DW landfilling, taxation on natural sands and aggregates, availability and cost of natural sands and aggregates, quality certification of RS&A, better public perception and increased consumer acceptance and low distance with C&DW recycling plants (e.g. [4]).

A recent study [5] has pointed out the three main key parameters that influence the market of recycled materials: the landfill of inert C&DW, the challenge with primary raw materials and the availability of inert C&DW recycling plants. The market context was investigated in five NWE countries (Belgium, France, Germany, Luxembourg and the Netherlands) towards a quantitative analysis of the generation of C&DW, the production of natural and RS&A, the density of recycling plants, the density of extraction sites for natural materials, and C&DW landfilling legislation.

Results point out that the market of recycled sands and aggregates is more developed and more suitable in the Netherlands and in Flanders (North of Belgium) where all the three investigated key variables are considered as drivers. These regions are characterized by a lack of available local and good quality natural rocky materials, a developed framework of recycling plants for inert C&DW and a favourable legislation that push the waste flux to sorting and recycling. The market in Wallonia (South of Belgium), France, Germany and Luxembourg is challenged by primary raw materials where resources are locally abundant. The French market of recycled materials is furthermore disadvantaged by a lack of incentives that foster sorting and recycling, including landfilling.

A proactive policy of support for the recycling of C&DW therefore implies stopping the disposal of waste in landfills, the setting up of adequate recycling techniques, in particular through the installation of complete sorting centres and the networking of these recycling centres sufficiently dense, so as to reduce the impact of transport. There is a great opportunity for increasing the part recycled products on the NWE market of aggregates. More generally, the following recommendations can be formulated [6]:
- Enhance public procurement through the introduction of mandatory percentages of recycled aggregates in large civil engineering projects;
- Develop reuse/reclaimed products programme of support and promotion (e.g. reuse percentage target);
- Introduce end-of-waste criteria for recycled products;
- Develop standards for recycled materials for various utilization for waste that did not meet end-of-waste criteria;
- Facilitate material content traceability;
- Introduce applications for recycled non-aggregates;
- Encourage the construction products and materials supply chain to have much greater provision for taking back and incorporating recycled materials into new products;
- Deploy financial incentive to use recycled aggregates.

3. Circular economy in construction industry

A survey organized by Tebbat Adams et al. [7] shows (Fig. 5) that the most significant challenge which was highly ranked by all the stakeholders, is the lack of incentive to design for the end-of-life issues for construction products. The low value of products at end-of-life is also an important economic challenge. The construction industry's structure is also viewed to be a significant challenge in the form of a fragmented supply chain [8].
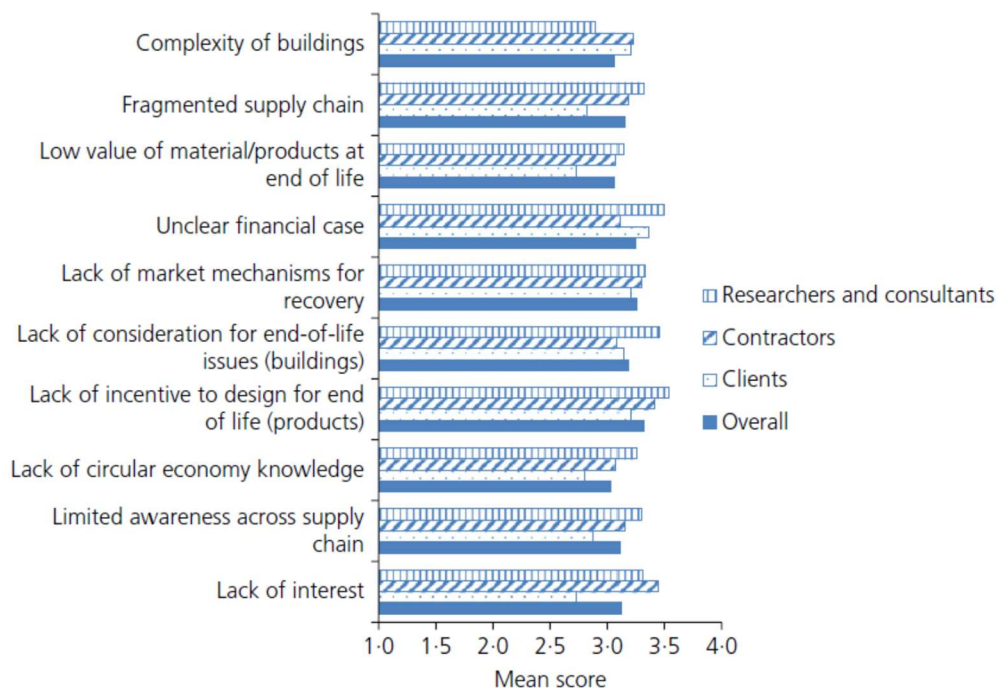
Figure 5: The most significant challenges for implementing circular economy in industrywide [7]

As mentioned in the survey [7], "*a larger obstacle is the existing stock of buildings and infrastructure where circularity principles have not been adopted*". However, many opportunities to advance the circular economy exist. A better recovery of material by means of viable take-back schemes and higher value markets as well as assurance schemes for reused materials are promising (Fig. 6). Cradle to cradle concept is nothing else: waste becomes a nutriment for another product. McDonough et al. [9] promote the idea that biological and mineral cycles have to be separate for favouring reuse and recycling. But also that we must design materials in such a way the end of life and end of use are timely corresponding: because the waste is induce by this discordance of time.

Circular economy in construction industry is clearly a need and a wonderful opportunity [10], regarding the huge amount of C&DW versus the demand of granular materials: compatibility between deposit and market should contribute to change the paradigm and transform the wastes into secondary resources. Coming challenges in this area are longer-lasting materials, repairable products, prefabrication and off-site construction, banks of materials, circular material supply chain, design for adaptation and deconstruction, …
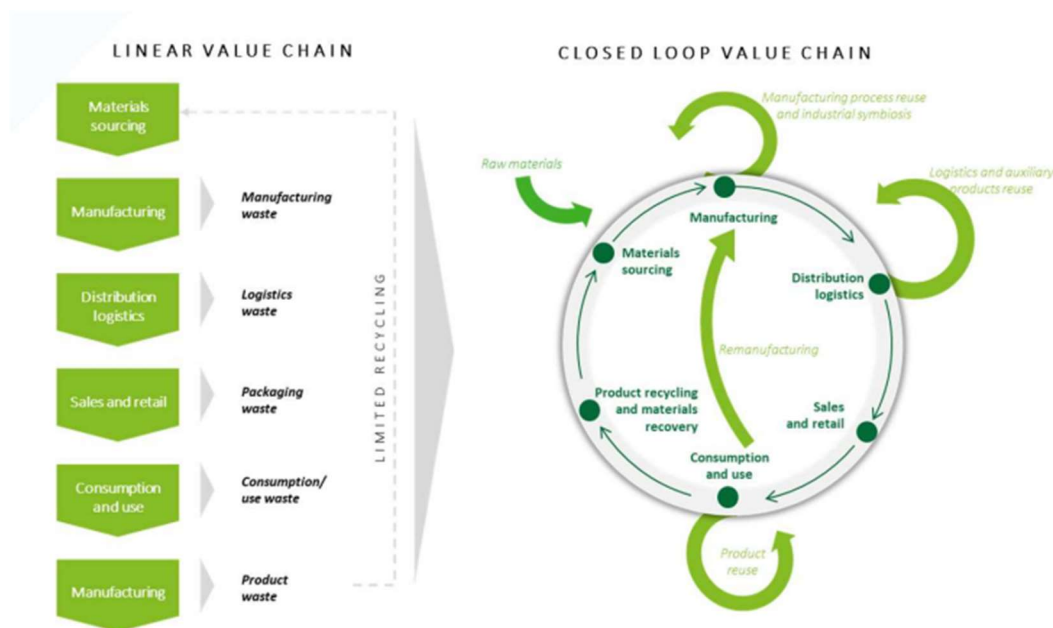
Figure 6: Comparison between linear and circular economy (from [10])

4.   Upcycling of Construction and Demolition Wastes

The needs of civil engineering can be indeed of four main types of materials, namely [11]:

- **Filling materials**, on which there are low requirements and consumed in large quantities, for embankments but transportable over short distances due to costs;
- **Aggregates**, which must meet various specifications depending on the place they will occupy in the structures and the treatment techniques used. The quality requirements can at this level become high, even severe for the surface layers, to lead to finished products of quality identical to that of traditional materials;
- **Binders**, which must meet very precise specifications and whose properties must remain constant over time. Employed in small quantities and competitive with expensive products (cement & bitumen), they may experience pre-employment packaging and bear higher transportation costs;
- **Activators**, which will be used in small quantities, which can cause problems of collection, storage, distribution and regularity.

Specific sorting and grinding process [12], original applications [13], incorporation of production waste into the final product [14], prefabricated products [15] tend to increase needed performances and upcycling of C&DW.

5.   Example: 3D printing with recycled fine aggregates

Concrete 3D printing is an innovative technique allowing for the quick production of easily customizable elements. Yet, it is also facing a lot of criticism targeted in part to its environmental impact. To address it, the entirety of the granular skeleton has been replaced with washed concrete Recycled Fine Aggregates (RFA).

The research [16] investigates the influence of RFA on the mechanical and durability performances of 3D printing mortars. This investigation involves a comparison of mortar samples produced using two types of fine aggregates: virgin fine aggregates and recycled fine aggregates (RFA). The aim is to determine how the incorporation of recycled fine aggregates affects the properties of the mortar. Additionally, the study assesses the impact of the 3D printing process itself on mortar properties. To do this, the performance of mortar samples that were 3D printed are compared with those of samples that were cast using conventional methods.

A battery of tests is conducted to assess various mechanical and durability properties, including compressive strength, tensile strength, flexural strength, porosity, water absorption, and resistance to environmental factors like freeze-thaw cycles. Direct tensile tests have also been used to assess if the cracking pattern followed the interface between two printed layers which would indicate the existence of a structural weak point in the material.

(a) (b)
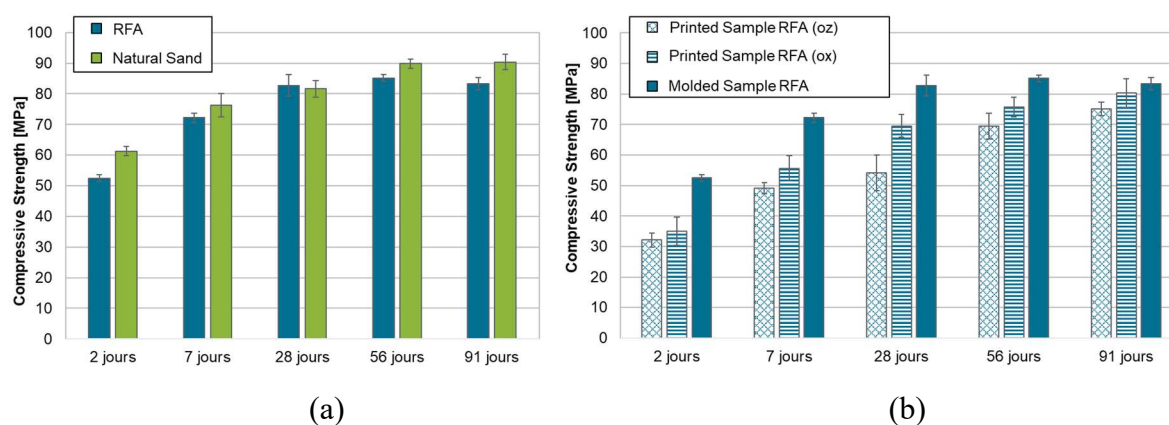
Figure 7: Influence of the use of RFA (a) and of the printing process (b) on the compressive strength of mortars

The research findings indicate that substituting natural sand with RFA does not lead to significant alterations in either the mechanical properties (cf. Figure 1(a)), or the durability aspects, such as resistance to freeze-thaw cycles and carbonation, in the context of 3D printing mortars. However, elements produced through 3D printing exhibit lower mechanical strength compared to samples cast using traditional methods which is assumed to be caused by poor curing conditions during the first 48 hours. Moreover, these 3D-printed samples display anisotropic properties. Specifically, when a load is applied parallel to the printed layers (as shown by "oz" in Figure 1(b)), the resistance is lower compared to when the load is applied perpendicular to the layers (indicated by "ox" in Figure 1(b)). This finding is somewhat counterintuitive because it challenges the assumption that the interface between layers in 3D printing is typically weaker than other parts of the material. These results are supported by the direct tension test, which indicates that the failure plane never corresponds to the interface between two layers. These collective findings suggest that there may not be a pronounced weak point at the interface between layers in 3D-printed mortar elements.

Acknowledgments

References

[1] Eurostat, 2020. Waste statistics. Retrieved from https://ec.europa.eu/eurostat/statistics-explained/index.php?title=Waste_statistics#Total_waste_generation.

[2] UEPG, 2021. European Aggregates Association – Annual Review 2020-2021, Brussels, 30 p.

[3] Construction and demolition waste: challenges and opportunities in circular economy. European Environment Agency, January 2016.

[4] Silva R.V., de Brito J., Dhir R.K., "Availability and processing of recycled aggregates within the construction and demolition supply chain: A review". J Clean Prod 143, 598-614 (2017).

[5] Delvoie S., Courard L., Hubert J., Zhao Z., Michel F., "Construction and Demolition Wastes: specific conditions for recycling in North West Europe". Cement, Lime, Concrete **1** (2020) 3-20

[6] Deloitte, 2015. Screening template for Construction and Demolition Waste management in France.Version 2, September 2015, 55 p.

[7] Tebbat Adams, K., Thorpe T., Osmani M., Thornback J., "Circular economy in construction: current awareness, challenges and enablers". Waste and resources management **170** (1) (2017) 15-24.

[8] Ragossnig A. M., "Construction and demolition waste – Major challenges ahead!" Waste Management & Research **38** (4) (2020) 345–346.

[9] McDonough W., Braungart M. Cradle to cradle: remaking the way we make things. North Point Press. 193p. (2002).

[10] Tomaszewska J, "Construction versus circular economy" 17th International Congress on Polymers in Concrete ICPIC 2023, Sept. 17-20th, Warsaw.

[11] Courard L., Zhao Z., Hubert J. Challenging construction industry with C&DW: opportunities and limits. *IX Congreso Internacional y 23a Reunión Técnica de la AATH "A 73 años de la Primera Conferencia del Hormigón en Argentina*. AATH, Buenos Aires, Argentina (**H59**), 33-45. (https://hdl.handle.net/2268/257024)

[12] Hubert J., Zhao Z., Michel F., Courard L. "Effects of crushing method on the properties of produced recycled concrete aggregates". Buildings **13** (2023) 2217 (https://doi.org//10.3390/buildings13092217).

[13] Grellier A., Bulteel D., Zhao Z., Remond S., Courard L. "Alternative hydraulic binder development based on brick fines: influence of particle size and substitution rate". Journal of Building Engineering (2021) 102263 (https://doi.org/10.1016/j.jobe.2021.102263)(http://hdl.handle.net/2268/252191).

[14] Zhao Z., Courard L., Groslambert S., Jehin Th., Léonard A., Xiao J. "Use of RCA from precast blocks for the production of new concrete building blocks: an industrial scale study". Resources, Conservation & Recycling **157** (2020) 1-13 (https://authors.elsevier.com/a/1ahbs3HVLKiAuJ)(http://hdl.handle.net/2268/246444)

[15] Fanara A., Courard L., Collin F., Hubert J. "Transfer Properties in Recycled Aggregates Concrete: experimental and Numerical Approaches". Construction and Building Materials **326** (2022) 126778 (doi:10.1016/j.conbuildmat.2022.126778) (https://hdl.handle.net/2268/288432).

[16] Hubert J., Muy Y., Courard L. Use of recycled fine aggregates in high added value applications. ICONS23 International Conference on Advances in Engineering and Technology for Sustainable Development. Hanoi University of Civil Engineering, Hanoi, Vietnam, Nov 2-3 (2023).

CHARACTERIZATION OF WASHING SLURRY POWDER AND EXPLOITATION IN CEMENT BLENDS

Jingwen Liu (1), Zeger Sierens (1), Jiaguo He (1), Özlem Cizer (2), Jiabin Li (1), Pieter Rauwoens (1), Brecht Vandevyvere (1)

(1) Department of Civil Engineering, KU Leuven, Campus Bruges, 8200 Bruges, Belgium

(2) Department of Civil Engineering, KU Leuven, Campus Leuven, 3001 Leuven, Belgium

Abstract

Washing slurry powder (WSP) is a fine powder waste (finer than 63µm) generated from the washing process during the production of high-quality recycled concrete aggregate (RCA), which is currently disposed of in landfills. This paper aims to investigate the characteristics and composition of WSP and explore its potential as a substitute for cement. The physical properties, chemical and mineral composition of WSP were characterized by multiple techniques. The impact of WSP on cement hydration was assessed through isothermal calorimetry and quantitative XRD. The fresh and hardened properties of blended cement mortars were thoroughly examined. The results reveal that WSP is a mixture of soil and hydrated cement, with primary mineral phases of calcite and quartz. A small amount of clay minerals, like illite and kaolinite are also detected. Incorporating up to 15% of WSP exhibited negligible negative effects on mortars' performance. Notably, a promoting effect on cement early-age hydration was observed in WSP blended cements. The presence of calcite leads to the formation of hemicarbonate and monocarbonate instead of monosulfate, which is less stable. This research demonstrates the feasibility of recycling WSP as a sustainable cement substitute and disclosing the waste management gap in the green cycle of high-quality recycled concrete aggregate.

Keyword: washing slurry powder (WSP); supplementary cementitious material (SCM); composite cement; low-carbon cementitious products; recycling/upcycling

1. Introduction

Construction and demolition waste (C&DW) is massively generated every year and its eco-disposal has become a big concern. It is reported that around 820 million tonnes C&DW are generated yearly accounting for nearly half of the total solid wastes in EU [1]. In China, it is reported that around 1600 million tonnes of C&DW were produced in only 2016 [2]. The recycling of C&DW after treatment as secondary raw materials in construction is currently the most efficient way to manage this waste stream and represents one of the priorities for achieving circular economy and sustainable development [3]. For instance, the use of recycled aggregates produced by sorting, crushing, cleaning and sieving of C&DW to partially or completely substitute natural aggregate in concrete production has offered a good solution to preserve natural resources and reduce the environmental impact. Particularly, recycled concrete aggregate (RCA) is especially well documented and developed in various countries and regions, given the advantages of its massive amounts, constant quality and less influence on concrete

performance when properly incorporated [3][4][5]. Whilst the reuse of RCA in concrete is often described as the most promising way, its application in concrete still largely depends on its quality. Certain specifications have been proposed in different regions to confine the quality of RAs [6][7][8]. The content of cementitious components and unbound natural aggregate is often considered as the predominating indicator. However, the variability of building methods naturally leads to the fact that RA derived from C&DW will vary in quality and composition. Depending on the origin of C&DW, old concrete, unbound aggregate, brick, asphalt, wood, plastics, soil and other contaminants are often found. The existence of highly porous materials, like adhered mortar, brick, wood and soil, highly relates to the water absorption (WA) of RA and therefore, severely degrades the performance of concrete. Thus, an effective sorting and removing technique is required to reduce the content of those materials [9][10]. Especially, to produce high-quality RCA, a secondary crushing and washing process is normally required to further remove the adhered mortar and fine particles. During this washing process, fraction finer than 4 mm fines is sieved out and the washing slurry is oriented to a sedimentation tank. The very fine powder of this washing slurry is settled down and then pressed into cake, often known as filter cake, which is currently disposed in landfills.

This research investigates the characteristic properties of washing slurry powder collected from a recycling plant in Belgium and evaluates its performance in cement blends. The physical properties, chemical and mineral composition were examined by laser diffraction particle size analyser, XRF and QXRD. Its effect on cement hydration, and the performance of blended cement mortars were also assessed. This research aims to provide some information for understanding and exploring the possibility of using this kind of material in cement and therefore reduce the environmental pressure and economic costs.

2. Materials and research protocols

2.1 Raw materials

The washing slurry powder used in this research was collected from a local recycling plant in Flanders region, Belgium, where a large amount of high-quality recycled concrete aggregate is produced each year. During the last washing process, the floating materials (e.g. plastics, woods) and fine aggregates are washed out. After sieving and sedimentation, fine fraction less than 63µm washing slurry is dewatered and pressed into filter cake. The washing equipment and washing slurry powder after filtering and pressing process are given in Figure 1. In this recycling plant, at present, the annual production of WSP (dry matter) is about 5000-6000 tones, which is currently disposed of in landfilled with a cost of € 30 – 40 per ton.

Figure 1: Aggregate washing equipment (left) and washing slurry powder (WSP) (right)

The collected washing slurry pieces (filter cake) was firstly dried in the lab to reduce the moisture content and milled by means of a ball mill to break the blocks and obtain less than 63 μm fine powder, namely, WSP. A commercial CEM I 52.5 R HES Portland cement and CEN standard sand conforming to EN 197-1 [11] and EN 196-1 [12] were used in this research.

2.2 Characterization of WSP and effects on cement blends

2.2.1 Characterization of raw materials

Particle size distribution of WSP was tested by a Beckman Coulter LS 13 320 laser diffraction particle size analyzer. The chemical composition of WSP was characterized through X-Ray Fluorescence (XRF) using a Bruker S8 TIGER wavelength dispersive spectrometer. The mineral composition was characterized by quantitative X-ray Diffraction (Q-XRD) using Rietveld refinement method. The XRD pattern was obtained through Bruker Advanced D8 Phaser equipped with Cu Kα radiation operated at 40 kV and 20 mA. Samples were scanned between 5º and 65º 2θ with a step size of 0.02° 2θ and a counting time of 2 s. In order to quantify the potential amorphous content, 10% ZnO by mass was added in the sample as internal standard prior to the analysis.

2.2.2 Fresh and mechanical properties of blended mortars

Compressive and flexural strength development of standard mortar prisms was tested according to EN 196-1 [12]. In addition to reference Portland cement mortar, blended mortars in which cement was replaced by 10%, 15% and 25% of WSP by weight, were tested. The water-to-binder ratio was fixed at 0.5 for all mixtures. The fresh mortars were cast in 40x40x160 mm moulds. All samples were demoulded at 24h and further cured in water at 20 °C for 1, 3, 7 and 28 days. All tests were performed in triplicate. The flowability of fresh mortar mixes was tested in accordance with EN 1015-3 [13].

2.2.3 Hydration kinetics and products

Pastes with and without 25% cement replaced by WSP were produced to investigate its effect on cement hydration. WSP and cement were mixed firstly to reach a homogeneous powder. All pastes were mixed with deionized water at water-to-binder ratio of 0.5 by an overhead mixer at 1600 rpm for 2 min. The pastes for hydration products study were cast and sealed in a cylindrical polyethene vessel with a diameter of 21 mm. The samples were cured at 20 °C for 28 days.

Isothermal conduction calorimetry was used to follow the heat release revolution of WSP blended cement and that of the reference cement during the hydration process. An eight-channel TAM Air isothermal calorimeter was used and operated at a controlled temperature of 20 °C. Around 10g paste was cast in the ampoule after mixing.

QXRD was used to identify and quantitatively analyse the hydration products at 28 days. Solvent exchange method as indicated in [14] was adopted for hydration stoppage. Slices were sawn from the middle of the hardened sample. To avoid potential carbonation, 2-3 mm of the edges of the slices were also discarded. The slices were further crushed by a mortar pestle into less than 1 mm. 3 g of the fine samples were immersed in 100 mL isopropanol for 15 min and then vacuum filtered. The filtered residues were dried in a ventilated oven at 40 °C for 8 min. For the XRD test, the dried samples were further milled with 10 % ZnO as internal standard.

3.   Results and discussion

3.1   Characteristics of WSP

As shown in Figure 2, WSP possess a very fine particle size with an upper limit of 60 µm. It has a slightly higher fraction of fine powders than cement, for instance, the d50 value of WSP and cement is 9.15 and 9.47µm. Interestingly, WSP shows a characteristic multimodal particle size distribution. This is ascribed to WSP's intrinsic multi-components. For instance, some hard particles, such as quartz, generally tend to be the coarse fraction.
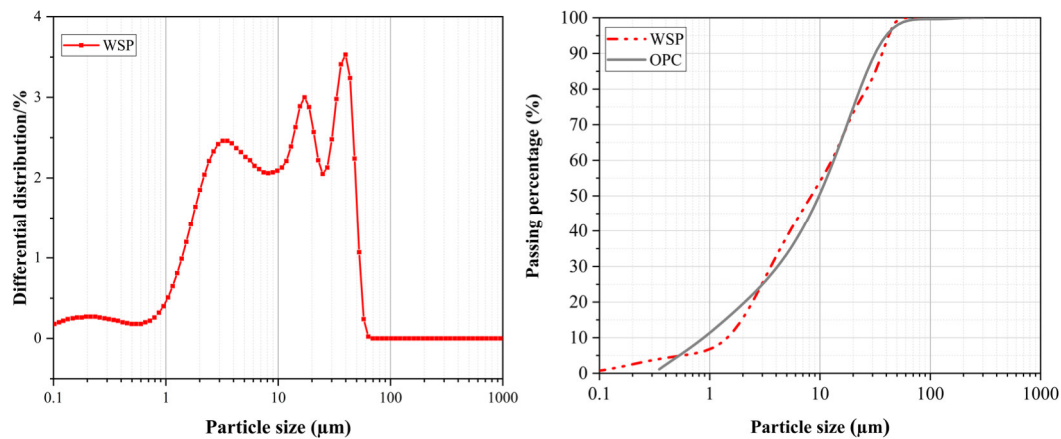
Figure 2: Particle size distribution of washing slurry powder (WSP)

The chemical composition of WSP and OPC are listed in Table 1. As shown in Table 1, WSP is rich in silicon, calcium and aluminium oxides. Given that WSP is originated from old concrete, it could be derived from hydrated cement phases (like calcium silicate hydrate) and the aggregate minerals (quartz and calcite) as well as other potential materials, such as soil.

Table 1: The chemical and mineral composition of washing slurry powder and Portland cement used in this research (results is reported in oxides and by mass ratio (wt.%)

Oxides	WSP	OPC	Minerals	OPC	Minerals	WSP
SiO_2	37.8	18.7	Alite (C3S)	51.8	Quartz	24.1
CaO	27.6	62.8	β-C_2S	14.6	Calcite	31.9
Al_2O_3	4.7	5.7	C_3A	8.0	Vaterite	6.8
Fe_2O_3	3.1	4.2	C_4AF	12.78	Illite	5.8
K_2O	0.9	0.6	Anhydrite	6.29	Kaolinite	1.2
MgO	1.2	1.0	Calcite	3.01	Gypsum	1.4
Na_2O	0.4	0.4			Feldspar	3.8
SO_3	1.6	3.7			Dolomite	3.3
LOI	20.4	3.9			Amorphous	21.7
d50(µm)	9.15	9.47				

The mineral compositions obtained by quantitative XRD analysis are listed in Table 1. WSP is characterized with multiple phases, in which calcium carbonates (calcite and vaterite) and quartz are the dominate minerals. Some minor phases, such as dolomite, feldspar and gypsum were also identified. Those minerals are mainly attributed to the aggregate and mortar portions in RCA. As for gypsum, it could be originated from different components of the raw C&DW, such as plaster boards. Additionally, some clay minerals such as illite and kaolinite was also

detected, which could be resulted from soil. The mineral composition result indicates that WSP is a high mixture of RA powder and soil.

3.2 Fresh and mechanical properties of blended mortars

The influence of replacing cement with different ratios of WSP on the flowability and compressive strength development of blended mortars were tested, and the results are presented in Figure 3 and Figure 4.
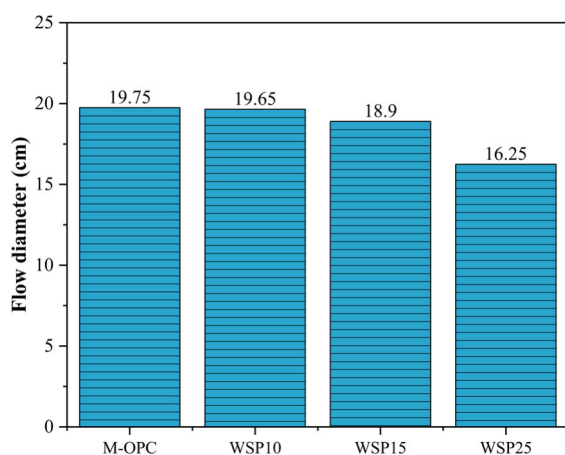

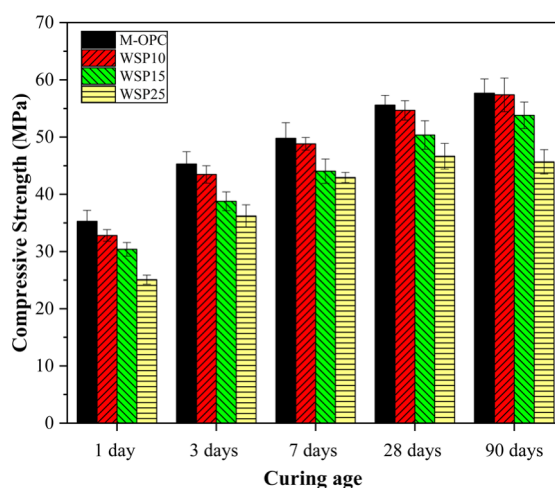Figure 3: Flowability of cement mortars without and with different portion of WSP

Figure 4: Compressive strength of cement mortars with different portions of WSP

The flow table results show a reducing trend on the flowability of mortars with the increase of WSP portions. However, negligible impact can be observed with replacement ratios up to 15%. In spite of that, a noticeable reduction in flowability appears at 25% replacement ratio. The reduction in flowability with increasing replacement ratios with WSP is attributed to its fine particle size and irregular particle shapes considering that it was resulted from the crushed aggregates. The existence of porous materials (e.g. old mortars) and clay minerals, such as illite and kaolinite could be the other reason. Thus, appropriate selection of water reducer or milling process is necessary when incorporating high contents of WSP.

Compared with the reference cement mortar, WSP blended mortars showed obviously lower early-age strength, irrespective of the replacement ratios. However, it is interesting to see that the difference in the compressive strength of the mortar specimens varies with the curing age. At the longer term, however, the difference becomes negligible for 10% and 15% replacement ratios. While for 25% WSP blended cement mortar, an increase of the curing age does not always effectively decrease the strength loss. The lower early age strength (1 day) of WSP blended cement mortar is mainly attributed to the dilution effect. However, up to 15% replacement ratios, the blended cement mortar can catch up the strength of reference mortar at late age. This can be ascribed to the combination of filler effect and potential reaction of WSP in cements, which can therefore offset the dilution effect.

3.3 Hydration kinetics

Figure 5 illustrates the heat flow and cumulative heat release of WSP blended cement hydration versus that of the reference cement. The incorporation of WSP impacts the early-age hydration largely, especially during the first 48h. Higher heat release is observed in WSP blended cement during both the induction period and main hydration peak. The maximal heat flow value for

WSP was observed after 9.4h, while for OPC this was observed after 10.5h. What's more, the induction period is significantly shorter, and the onset of acceleration period is clearly accelerated. As a result, a higher cumulative heat release is transformed. The results indicate that the presence of WSP yields an acceleration of the cement hydration. This is largely due to the "filler effect", which contributes to the cement hydration by providing more water and increased space for cement hydrates to precipitate [16][17][18]. What's more, as previous reported, the presence of calcite in WSP would also promote early-age hydration by promoting C-S-H gel precipitate in the particle surface [19][20]. This result is consistent with the compressive strength results in the last section.
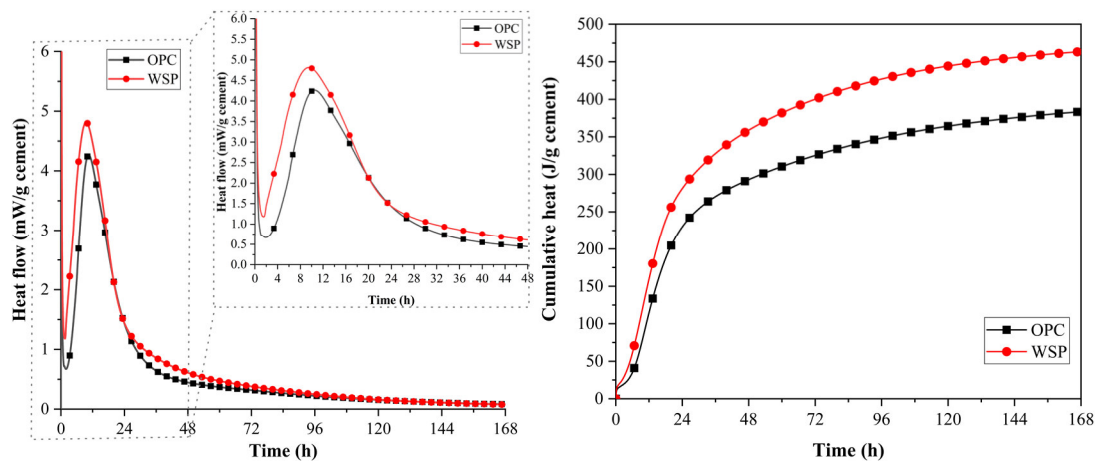
Figure 5: Hydration heat flow and cumulative heat of cement pastes without/with 25% WSP

3.4 Hydration products

As shown in Figure 6, WSP blended paste show similar primary hydrate phases as pure cement paste, such as C-S-H, ettringite and portlandite. The main difference is that both hemicarbonate (Hc) and monocarbonate (Mc) were determined in WSP while only Hc was detected in OPC. The transformation of ettringite to Hc and Mc is related to the presence of calcite. As mentioned above, about 38% Calcium carbonate was determined in WSP. The present results are in good agreement with the previous research that the addition of calcite affects the mineralogical variant of the AFm phase(s) [21].
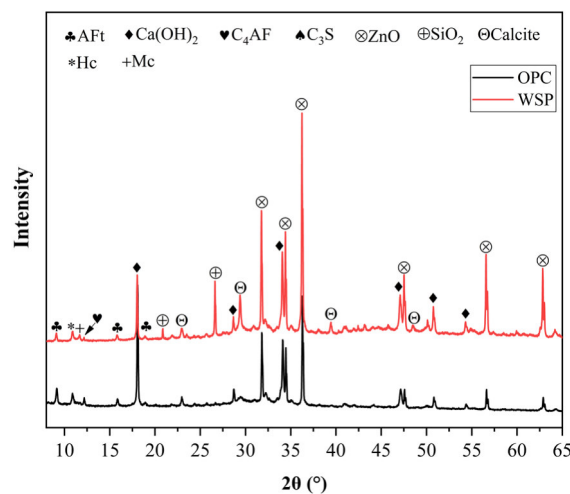
Figure 6: XRD patterns of hydrated cement pastes with 0 and 25% WSP at 28 days

4.   Conclusions

This research investigates the physical properties, chemical and mineral composition of WSP, which is a secondary waste from the production of high-quality RCA, and the potential of using it as a cement substitute for developing low-carbon cementitious composites. The influence of WSP on cement hydration kinetics and products, as well as the performance of blended cement mortars were also studied. Based on the test results, the following conclusions can be drawn:

(1) WSP particles are produced from crushing of old concrete, thus an irregular particle shapes with high angularity and low sphericity are expected, indicating potential negative effect on the flowability of fresh pastes and mortars. A fine particle size with upper limit less than 63 μm is tested.

(2) WSP is rich in Ca, Si and Al. The primary mineral phases are characterized as calcite (vaterite) and quartz. Some minor phases of feldspar, gypsum, dolomite and clay minerals (illite, kaolinite) are also determined.

(3) Incorporating up to 15% of WSP in cement shows negligible effect on the flowability and compressive strength development, while high amount addition would cause a reduction in the performance of the mortar mixtures.

(4) The presence of WSP significantly enhances the early-age hydration of cement. The presence of calcite in WSP affects the mineralogical variant of AFm, leading to both formation of Mc and Hc, which can indirectly stabilize ettringite.

Acknowledgements

References

[1] EU Construction and Demolition Waste, Protocol and guidelines, Available online: https://ec.europa.eu/growth/content/eu-construction-and-demolition-waste-protocol-0_en

[2] J. Xiao, Recycled Aggregate Concrete Structures, Springer, Berlin. (2018)

[3] Silva, R. V., et al. "Properties and Composition of Recycled Aggregates from Construction and Demolition Waste Suitable for Concrete Production." Construction & Building Materials, vol. 65, 2014, pp. 201–17.

[4] Vintimilla, Carla, and Miren Etxeberria. "Limiting the Maximum Fine and Coarse Recycled Aggregates-Type A Used in Structural Concrete." Construction & Building Materials, vol. 380, 2023, p. 131273–.

[5] Pacheco, J., et al. "Experimental Investigation on the Variability of the Main Mechanical Properties of Concrete Produced with Coarse Recycled Concrete Aggregates." Construction & Building Materials, vol. 201, 2019, pp. 110–20.

[6] BS-8500, Concrete-complementary British Standard to BS EN 206-1–Part 2: specification for constituent materials and concrete. UK: British Standards Institution.

[7] CEN, EN 12620: Aggregates for concrete, Brussels.

[8] BCSJ, Proposed standard for the use of recycled aggregate and recycled aggregate concrete, Japan.

[9]   Poon, Chi-Sun, and Dixon Chan. "Effects of Contaminants on the Properties of Concrete Paving Blocks Prepared with Recycled Concrete Aggregates." Construction & Building Materials, vol. 21, no. 1, 2007, pp. 164–75.

[10] Etxeberria, M., et al. "Influence of Amount of Recycled Coarse Aggregates and Production Process on Properties of Recycled Aggregate Concrete." Cement and Concrete Research, vol. 37, no. 5, 2007, pp. 735–42.

[11] CEN, EN 197-1: 2000: Cement–Part 1: Composition, specifications and conformity criteria for common cements, Brussels.

[12] CEN, EN 196-1: 2016: Methods of Testing Cement–Part 1: Determination of Strength, Brussels.

[13] CEN, EN 1015-3: 2014: Methods of test for mortar for masonry-Part 3: Determination of consistence of fresh mortar (by flow table), Brussels.

[14] Snellings, R., Chwast, J., Cizer, Ö. et al. Report of TC 238-SCM: hydration stoppage methods for phase assemblage studies of blended cements—results of a round robin test. Materials and Structures (2018) 51, 111.

[15] ASTM C1897-20: 2020: Standard test methods for measuring the reactivity of supplementary cementitious materials by isothermal calorimetry and bound water. ASTM Int West Conshohocken.

[16] Snellings, R., Horckmans, L., Van Bunderen, C. et al. Flash-calcined dredging sediment blended cements: effect on cement hydration and properties. Materials and Structures 50, 241 (2017).

[17] Berodier, E., and K. Scrivener. "Understanding the Filler Effect on the Nucleation and Growth of C-S-H." Journal of the American Ceramic Society, vol. 97, no. 12, 2014, pp. 3764–73.

[18] Gutteridge, Walter A., and John A. Dalziel. "Filler Cement: The Effect of the Secondary Component on the Hydration of Portland Cement: Part I. A Fine Non-Hydraulic Filler." Cement and Concrete Research, vol. 20, no. 5, 1990, pp. 778–82.

[19] Lothenbach, Barbara, et al. "Influence of Limestone on the Hydration of Portland Cements." Cement and Concrete Research, vol. 38, no. 6, 2008, pp. 848–60.

[20] Stark, Jochen, et al. "Nucleation and Growth of C-S-H Phases on Mineral Admixtures." Advances in Construction Materials 2007.

[21] Matschei, T., et al. "The Role of Calcium Carbonate in Cement Hydration." Cement and Concrete Research, vol. 37, no. 4, 2007.

THE IMPORTANCE OF PHYSICAL AND MECHANICAL CHARACTERIZATION OF EARTH MATERIAL BEFORE ITS REUSE

Maria Idália Gomes (1), Maria Carmo Conde (2) and Catarina Pereira (3)

(1) CERIS, DEC, FCT – UNL, Caparica and DEC, ISEL – IPL, Lisboa, Portugal

(2) DEC, ISEL – IPL, Lisboa, Portugal

(3) Coopérnico, Lisboa, Portugal

Abstract

This article aims to contribute to the paradigm of recycling earth material, in this case the reuse of earth from a rammed earth house demolition in a new building construction.

Earth from excavations corresponds to a considerable percentage of urban waste. Its transport and storage raises a set of challenges that need to be solved. One possible solution is to recycle and reuse earth, transforming it into construction materials with low energy embodied. For this, it is necessary that constructive processes adapt to the existing material.

In this work, the procedure adopted for earth reuse was based on a set of laboratory experimental tests, guided by reference values established in the specialized literature. Indication for earth granulometric correction was followed and new tests were carried out to compare values.

This work points towards the appreciation of earth, from its status of waste to construction material, improving the circular economy.

1.   Introduction

The use we currently make of the planet's natural resources has taken society to a growth level that has become unsustainable. Serious environmental changes indicate that, unless urgent measures are taken, humanity will face considerable difficulties in adapting to new contexts. These environmental alterations influence or imply climate change, the imbalance of ecosystems, shortage of mineral resources, and a decrease in soil fertility. In 2018, the construction sector was responsible for 39 per cent of carbon dioxide (CO_2) emissions from processes and energy, and 36 per cent from end-use energy; of these, 11 per cent resulted from products such as cement, steel, and glass, and from the manufacture of construction materials [1]. Even so, in 2018 and for the second consecutive year, global emissions from buildings increased by 2 per cent, corresponding to 9.7 gigatons of carbon dioxide ($GtCO_2$) released into the atmosphere [1].

Agenda 21 for Sustainable Construction [2] identified the improvement of environmental parameters and the reengineering of the construction process, including sustainable

development, as one of the major challenges for the construction sector. Analysis of these numbers allows us to conclude that the construction sector contributes massively to the degradation of the environment. One example is the cement industry, considered to be among the most polluting, responsible for around 60 per cent of total CO_2 emissions worldwide [3]. By weight, cement is the second most consumed product in the world, second only to water. A building material that is opposed to cement is earth. Earth is non-toxic, ecological, recyclable and has low embodied energy when used for the construction of buildings, offering several advantages [4, 5]. If earth has not been chemically changed or contaminated, its reuse is unlimited, promoting the circular economy. As a way of reducing the carbon footprint in the civil construction sector – largely caused by the extraction of raw materials, processing and transporting them – it becomes advantageous to use local raw materials and to reuse materials, namely from construction and demolition waste.

Earth building construction presumes the use of raw materials from the place (or in a nearby area) where the building will be implemented. In an urban context, this possibility is more conditioned because the amount of earth needed to construct a building is not always available in the area where it will be located. In such situations, the construction of earth buildings would be facilitated by taking advantage of earth from the excavations of other building works, similarly to what is happening in Paris, with the expansion of the public transport network *Grand Paris Express*, for which it is expected that 45 million tons of earth [6] will be excavated by 2026. A public competition of ideas was launched to solve the problem that arose on what to do with the excavated earth from the expansion of the subway network, which resulted in a set of solutions for earth reuse. One of the winning ideas was *Cycle Terre*, a circular economy project aiming to recycle the excavated earth from the works of *Grand Paris Express*, transforming it into earth building materials, namely clay panels, bricks, and plaster [6]. What would have been considered a problem became an opportunity. Solutions like these can contribute to the reduction of landfills and, as mentioned before, may serve as resources to produce natural low-cost building materials, and thus actively participating in the decarbonisation which Europe intends to achieve by 2050.

This article aims to discuss the reuse of an earth material obtained from an old rammed earth house to build a new one. To this end, it was necessary to study the earth and if this would fulfil the reference values described in the specialized literature. Physical and mechanical characterization tests were carried out on the material sample collected from the rammed earth walls of the existing house, which pointed to the existence of a granulometric correction to the original earth.

Results confirmed that it is possible to reuse earth from an old rammed earth house which would have been usually treated as demolition waste, thus benefitting the construction and recycling sectors, and contributing to reduce greenhouse gas emissions.

2.   Materials and methods

This section presents the material and laboratory tests carried out to determine the final composition of the material used to build a new rammed earth building.

To perform all of the laboratory tests, samples were collected from an old rammed earth building. After carrying out preliminary tests on this original earth [7], such as some laboratory testing to characterize soil properties, it was decided to change the sample's granulometric composition in order to meet the specifications and recommendations in the literature for rammed earth construction [8].

Thus, in this paper, the results of laboratory tests in order to obtain the indices of soil properties and the mechanical resistance of the rammed earth will be presented.

2.1 The material

The material used in this study was collected from the walls of an old rammed earth building (Figure 1a), located in Aljezur (south-western Portugal), which we will name "original earth". The new rammed earth building (Figure 1b), was built on the same site as the old rammed earth building, reusing the earth from it. The representativeness of the material, in terms of the proportions and size of particles, was recognized when collecting the material for testing. As can be seen in Figure 1a, walls no longer displayed traces of plaster.

Figure 1: Rammed earth building located in Aljezur, Algarve: (a) old building (July 2021), photograph by Catarina Pereira; (b) new building under construction (December 2021), photograph by Bruno Coutinho

2.2 The laboratory tests

Two samples were used to carry out physical and mechanical characterization tests, the original earth (OE) and corrected earth (CE) in a 2:1 volumetric ratio (original earth:sand) proportion.

Physical characterization was determined through standard laboratory tests that enabled us to determine index properties, earth classification, and characteristics after earth compaction. This included determining the grain size distribution curve, determining the Atterberg limits (i. e., the liquid limit (LL) and plastic limit (PL)), and the modified Proctor compaction test (performed only on corrected earth). Mechanical characterization tests were performed for both earth materials, the original and corrected.

2.2.1 Physical characterization

To complete the grain size distribution curve, two test methodologies were used: (1) sieve analysis for coarse materials of particle size greater than 75 μm, and (2) hydrometer analysis for finest materials with particle size smaller than 75 μm. Sieve and hydrometer analysis were determined in accordance with methods indicated in LNEC Specifications E239 [9] and E196 [10]: respectively, wet sieving of the coarse fraction (pebbles, gravel, and sand), and sedimentation of the fine fraction (silt and clay).

The physical and mechanical behaviour of clayey soil depend on its water content, and it is linked to four different states: solid, semi-solid, plastic, and liquid. Water content is the measure that the soil changes from liquid to plastic state, and from plastic to semi-solid state, and is

defined as liquid limit (LL) and plastic limit (PL). These limits are referred to as Atterberg limits. To classify the original and the corrected earth plasticity, liquid limit (LL), plastic limit (PL), and plasticity index (PI) were obtained in accordance with Portuguese Standard NP 143 [11]. These tests were performed on the soil segment passing through a Nº 40 ASTM sieve (< 0.425 mm). LL was determined by the Casagrande cup method and is defined as the water content, in percentage, at which a groove closure of 10 mm occurs at 25 blows in a liquid limit device. PL is defined as the water content, in percentage, at which the earth crumbles when rolled into a thread of 3 mm in diameter. PI is the range of water content where soil remains plastic, which is calculated by the difference between a soil's liquid limit and plastic limit (PI = LL-LP).

A Proctor compaction test was also performed to determine the compaction characteristics of corrected earth (i.e., the maximum dry density (MDD) and optimum water content (OWC)). As per LNEC Specification E197 [12], the modified Proctor compaction test was carried out in a mould of 102 mm in diameter and 116 mm in height, with the soil being compacted in five layers where each layer received 25 blows from a 4.535 kg rammer falling freely from a height of 475 mm.

2.2.2 Mechanical characterization

To carry out the mechanical characterization, it was necessary to manufacture rammed earth specimens. Six cylinders were prepared: three specimens with original earth; and for the remaining three, corrected earth was used. The cylindrical specimens were compacted in five layers inside a metallic mould with the dimensions of 200 mm in height and 150 mm in diameter. A metallic pestle was used for layers compaction, and when the process was finished specimens were demoulded immediately. The corresponding to OWC measurement was added to all earth specimens. This quantity was determined in the Proctor test (results can be seen in Chapter 3), so as to obtain the MDD (corrected earth values were used). The compressive strength tests were carried out after the specimens had been kept in a room with a temperature of 20 to 22 ºC, and a relative humidity of 55 to 65 per cent (the drying out period consisting of 40 days). Before testing, the six specimens had their top and bottom capped by a layer of gypsum to level the faces of the test pieces. Mechanical characterization was made by compressive strength test which consists of subjecting the specimens to simple compression until complete rupture. For mechanical test, specimens were taken to compression by a press under a load without shock at a constant speed. It was necessary to adjust the equipment manually without impact. Breaking force corresponded to the maximum recorded force. Load was applied under displacement control at a rate of 0.5 mm/min. Compressive strength consists of the individual values average, and it is calculated from the quotient between force and the specimens area on which the force is being transmitted.

3. Results and discussion

3.1 Physical characterization

In rammed earth construction, particle sizes can be distributed over a wide range – well graded, to result in higher mechanical density and greater durability and strength [7]. Original earth presents very high values of clay (particles finer than 0.002 mm) of about 22 per cent; this is above what is referred in the literature, as can be seen from three recommended papers in this field [13, 14, 15] (Figure 2). The literature recognizes that clays become unstable in the presence

of water, so water should be limited in earth building construction. Clay will serve as a binder and must be present in small quantities only [8]. Since the original earth lies outside the recommended limits, it was necessary to proceed with earth correction, in order to reduce its fine level particles, siliceous sand with gravel were added. As the proportion of sand (dimension up to 2 mm) has a value of 60% we will designate, for this mixture, the name of "sand" (curve represented in Figure 2). The granulometric curve of the new mixture, called "corrected earth", presents a volumetric ratio of 2:1 (original earth: sand) (curve also represented in Figure 2). More information about the earth correction can be found in Pereira et al [7]. It is common to add other types of stabilizers, including cement and lime, among others; but one of this study's objectives would be the sustained earth reuse to ensure a circular economy of this fully reusable material. Corrected earth does not respect the lower limit, for particles larger than 0.2 mm, for one of the studied references [15]. However, Keable [15] presents restrictive limits for large particles; nevertheless, corrected earth respects both the upper and lower limits of two other literature references [13, 14].
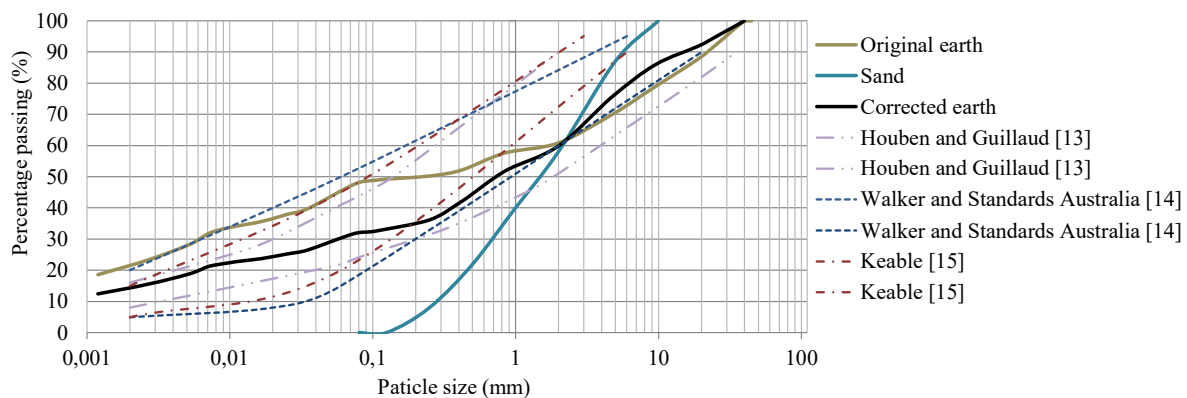
Figure 2: Grain-size distribution curves of the materials analyzed and the recommended values

Table 1 shows test results to determine the Atterberg limits of the original and corrected earth specimens. As expected, corrected earth due to sand addition, shows a decrease in LL and PL values, when compared to those obtained in original earth. Still, PI remained identical because particles of a size below 0.425 mm remain with the same plasticity characteristics (namely clay fraction) of the original earth.

Table 1: Physical properties of materials analysed in this study

Parameters		Original earth	Corrected earth
Atterberg limits	Liquid limit, LL (%)	41	30
	Plastic limit, PL (%)	30	21
	Plasticity index, PI (%)	11	11
Proctor compaction	Maximum dry density, MDD (kg/m^3)	-	2090
	Optimum water content, OWC (%)	-	10

Several studies [8, 14, 16-20] recommend the following range of values for rammed earth construction: LL between 35-45 %; PI between 15-29 %. Values obtained in the present study, when compared with these limits' values, allow us to conclude that only the LL value of original earth is within the indicated recommendations. Table 1 also shows parameters obtained in the Proctor compaction test, where a maximum dry density (MDD) of 2.090 kg/m^3 corresponds to an optimum water content (OWC) of 10 per cent; the compaction curve for the corrected earth can be seen in another paper done by the authors [7]. Despite compaction of rammed earth soils being described as an important feature, Houben and Guillaud [13] are the only authors indicating a range of values between 1.750 kg/m^3 and 2.000 kg/m^3 for MDD and 3.5 to 14 per cent for OWC. Registering a small deviation in dry density, the results obtained show that the analysed material fits in these proposed ranges.

3.2 Mechanical characterization

One essential principle to consider in earthquake-resistant earth construction is the homogeneous distribution of structural elements. Indeed, an adequate geometry is of great importance in construction stability – the more compact the structure and more homogenous the material are, the more stability it will have. Rammed earth constructions work through gravity, so their walls have reasonable, even good, resistance to vertical (compression) stress because of very thick walls, around 0.50 to 0.60 m (on average). Compressive strength results can be seen in Table 2, for original and corrected earth.

Table 2: Results for the compressive strength for the six specimens

Material	Designation	Compressive strength (MPa)		
		Value	Average	Standard deviation
Original earth (OE)	OE$_1$	1.32		
	OE$_2$	1.94	1.75	0.28
	OE$_3$	1.98		
Corrected earth (CE) 2:1 volumetric proportion (original earth:sand)	CE$_1$	2.45		
	CE$_2$	2.81	2.58	0.15
	CE$_3$	2.47		

Average compressive strength was about 1.75 MPa for original earth and 2.58 MPa for corrected earth. Compressive strength of corrected earth achieved values above 50 per cent (on average), which is much higher than the values of original earth. CE values are also more consistent, presenting a standard deviation of 0.15 MPa, while in OE the standard deviation is of 0.28 MPa. The lowest value obtained in OE was 1.32 MPa, meaning that the compressive strength obtained meets the minimum requirements of NZS 4298 [19] for standard grade rammed earth constructions, which indicates values of 1.30 MPa. Therefore, it appears that the values fall within the specifications even for original earth, where the lowest values are found. Walker *et al*. [20] mention values between 0.50 and 4.00 MPa for compressive strength of

unconfined rammed earth and higher values for stabilized rammed earth, of about 10 MPa, after 7 days. Experimental studies carried out in rammed earth buildings in Portugal recorded the following compressive strength values: 0.80 to 2.70 MPa, obtained from buildings in south-western Portugal, in the Barlavento Algarvio region [17]; and 1.26 MPa, an average of five rammed earth specimens with modified soils from the Odemira region [18]. From the values presented (Table 2), it is concluded that all specimens present values higher than the ones recommended, for both original and corrected earth.

4.   Conclusion

This study addressed the characterization of a soil sample collected from old rammed earth building walls, located in Algarve, Portugal. This work aimed to verify whether collected earth can be used in new building constructions, according to specifications and recommendations for this earth building technique; focusing on adding natural materials not to compromise earth reuse.

After a set of tests, it was found that adding sand is necessary to reduce the amount of clay, thus complying with the specifications and recommendations for the granulometric curve, obtaining a corrected earth. Although the tests carried out on corrected earth, LL and PI values were obtained below the range indicated by the reference bibliography, very satisfactory values were obtained for mechanical resistance (values much higher than shown for original earth). This allows us to conclude that corrected earth presents an extensive granulometry where clay fraction functions as a binder.

Corrected earth complies with almost all the recommendations in the documents analysed, similar to those for new rammed earth buildings, without the need to add a mineral binder, such as cement or lime.

Our main conclusion is that results confirmed it possible to reuse earth from old rammed earth housing – which would otherwise be treated as demolition waste – to construct new earth building housing. This benefits the construction and recycling sectors, contributing to the reduction of greenhouse gas emissions and to the circular economy. Moreover, identical processes can be replicated with earth retrieved from construction and demolition waste to renovate and build buildings.

Acknowledgements

References

[1]   IEA and UNEP, 'Global Status Report for Buildings and Construction - Towards a Zero-Emissions, Efficient and Resilient Buildings and Construction Sector', Global Alliance for Building and Construction, (International Energy Agency and United Nations Environment Programme, 2019).

[2]   UN, 'Agenda 21 - Rio Declaration' (United Nations conference on environment & development, Rio de Janeiro, Brazil, 1992).

[3] GCCA, 'Climate ambition statement - Towards Carbon Neutral Concrete' (Global Cement and Concrete Association, Carboneutral, United Kindon, 2020).

[4] Gomes, M. I., Faria P. and Gonçalves, T.D., 'Earth-based mortars for repair and protection of rammed earth walls. Stabilization with mineral binders and fibers'. J Clean Prod. 172 (2018) 2401-2414.

[5] Faria, P., Silva, V., Jamú, N., Dias, I., Gomes, M. I. 'Evaluation of air lime and clayish earth mortars for earthen wall renders', in 'Vernacular Heritage and Earthen Architecture: Contributions for Sustainable Development', Vila Nova de Cerveira, Portugal, October, 2013 (CRC Press/Taylor & Francis Group, London, 2014) 407-413.

[6] Barbier, S. and Paris, J. C., 'Cycle terre - Le fabrique de matériaux em terre crue', Dossier de presse (Direction de la Communication Ville de Sevran, IGC, 2018).

[7] Pereira, C., Conde, M. C. and Gomes, M. I., 'New construction through the reuse of earth. A circular and sustainable economic model', in '18th International Scientific Conference Healthy Houses', Brno, Czech Republic, May, 2022 (Zdravé Domy Healthy Houses, 2022) 33-40.

[8] Gomes, M. I., Gonçalves, T. and Faria, P., 'Unstabilised rammed earth: characterization of material collected from old constructions in south Portugal and comparison to normative requirements', *International Journal of Architectural Heritage,* **8**(2) (2014) 185-212.

[9] Specification 239, National Laboratory for Civil Engineering, 'Soils: Particle size analysis by wet sieving' (in Portuguese), (Lisbon, 1970).

[10] Specification 196, National Laboratory for Civil Engineering, 'Soils: Particle size analysis (by dry sieving and sedimentation)' (in Portuguese), (Lisbon, 1966).

[11] NP 143. IGPAI - Repartição de Normalização, Portuguese Standard, 'Soils. Determination of cohesion limits' (in Portuguese), (Lisbon, 1969).

[12] Specification 197, National Laboratory for Civil Engineering, 'Soils: compaction test' (in Portuguese), (Lisbon, 1966).

[13] Houben, H., and Guillaud, H., 'Traité de construction en terre', 2nd Edn (Editions Parenthèses Marseille, 1995).

[14] Walker, P. and Standards Australia, 'HB 195 - The Australian earth building handbook' (Standards Australia, Sydney, 2001).

[15] Keable, J., 'Rammed earth structure: A code of pratice' (Intermediate Technology Publications, London, 1996).

[16] Doat, P., Hays, A. Houben, H., Matuk, S. and Vitoux, F., 'Construire en Terre'. (CRATerre – Centre de Recherché et d'Application – Terre, École d'Architecture de Grenoble, France, 1979).

[17] Mateus, L., 'Characterization of Coatings used in Rammed Earth Constructions in the Western Algarve (in Portuguese)'. Masters dissertation (Universidade Técnica de Lisboa, Instituto Superior Técnico, Lisboa, 2006).

[18] Silva, R., Oliveira, D., Lourenço, P., Schueremans, L. and Miranda, T., 'Experimental investigation on the repair of rammed earth by means of injection of mud grouts', in 'Vernacular Heritage and Earthen Architecture: Contributions for Sustainable Development', Vila Nova de Cerveira, Portugal, October, 2013 (CRC Press/Taylor & Francis Group, London, 2014) 727–733.

[19] SNZ 4298, 'Materials and Workmanship for Earth Buildings'. Standards New Zealand (NZS, New Zeland, 1998).

[20] Walker, P., Keable, R., Martin, J. and Maniatidis, V., 'Rammed Earth: Design and Construction Guidelines', 1st ed (BRE Bookshop, Watford, 2005).

CONSTRUCTION AND DEMOLITION WASTE AS FINE AGGREGATE IN MORTAR MATRICES: A REVIEW

Ana Antunes[1],*, Hugo Costa[2], Ricardo Carmo[2], and Eduardo Júlio[1]

(1) University of Lisbon, Lisbon, Portugal and CERIS, IST, Portugal

(2) Coimbra Polytechnic – ISEC, Portugal and CERIS, IST, Portugal

* email(s) of the corresponding author(s)

Abstract

Construction and demolition waste (CDW) represents more than a third of waste generated in Europe Union economic activities and households. Its valorisation as a raw material is urgent to achieve sustainability in the construction sector, reducing its deposit in landfills and the extraction of natural raw materials, promoting the circular economy.

This work intends to compile several studies carried out in recent years, focusing on the recycling of CDW and its incorporation as fine recycled aggregate in mortar matrices. Several formulations of mortars produced with the replacement of different percentages of sand by CDW of concrete, brick and mix are presented. For the different mixtures considered, the mechanical properties and durability are analysed, a comparison is made with reference mixtures produced only with natural aggregates, and the collected results are discussed.

It is concluded that the various analysed solutions have favourable characteristics for the use of this type of waste as a construction material and are viable options for use in current construction works. Produced mortars replacing natural aggregates (NA) by recycled aggregates (RA) is certainly viable for constructive purposes.

1.   Introduction

In 2007, the world's population became, for the first time, more urban than rural, and it is estimated that by 2050, 68% of the total population will live in urban centres (1). This population growth in urban regions, and the degradation of its buildings, has been a concern all over the world. (1,2).

The accelerated pace of urbanization and urban renewal has intensified construction and demolition activities, which in turn has led to increased use of non-renewable resources, and increased CDW production (3–6). Currently, these correspond to about 37% of waste generated in economic and domestic activities in the European Union, representing one of the heaviest and most voluminous flows (7). This factor influences aspects of sustainable development with regard to environmental, economic and social concerns (8). In several countries, CDW is a growing problem for the construction sector, due to the rapid pace of infrastructure development and construction (9).

The valorisation of CDW is economically viable and essential to reduce dependence on finite natural resources, such as geological and energy reserves, and to promote a sustainable environment (8–10). But as most countries do not have a specific processing plan for CDW, these are generally sent to landfills instead of being reused and recycled in new constructions (11), which in addition to causing environmental problems is also a waste of resources (12). In order to maximize its use, the forms of treatment must be changed to methods that maximize resource efficiency (13). It is particularly important to try to reintroduce CDW, through reuse or recycling, in new construction, thus helping to close the material loop and reduce the environmental impact (14). The valorisation of CDW as recycled aggregates (RA) decrease the excessive use of natural aggregates (NA) and, consequently, reduce the environmental impact associated with the extraction of raw materials and with the deposit of CDW in landfills (12). The recycling of aggregates must be done through an optimized process to achieve sustainability in construction and to reduce resource consumption and other environmental impacts in the approaching years (15). The proper use of recycled materials can generate financial and environmental benefits, by reducing the volume of natural resources used and the waste volume sent to landfills (16). In addition to the environmental and economic gains in the use of RA, it was found that they have potential for use as RA to replace NA (17–20).

The present study intends to analyse different mortars produced by several authors, with RA of CDW, in terms of mechanical properties, compressive and flexural strength. This analysis has as main objective to validate the replacement of NA by RA in the production of mortars, grouts and screeds.

2.   Mortars Composition

In the present study, several types of mortars produced with RA of concrete CDW (European Waste Code - EWC 170101), bricks CDW (EWC 170102), and mixture CDW (EWC 170107), with different binders and with several ratios (Binder/aggregate - B/A), by different authors, are analysed (Table 1 to Table 3).

Table 1 – Compositions of mortars with RA of CDW concrete (Co-Concrete; Br-Bricks; Mix-Mixture; M-Mortar; C-Cement; HL-Hydraulic Lime; LF-Limestone Filler; F-Filler)

Code	(B/A)	RA	Binder	Ref.	Code	(B/A)	RA	Binder	Ref.
1/3coC1	1/3	Co	C	(21)	1/5coCL1	1/5	Co	C+HL	(22)
1/3coC2	1/3	Co	C	(21)	1/5coCF1	1/5	Co	C+LF	(22)
1/3coC3	1/3	Co	C	(23)	1/5coC1	1/5	Co	C	(24)
1/4coC1	1/4	Co	C	(25)	1/5coC2	1/5	Co	C	(26)
1/4coC2	1/4	Co	C	(27)	1/5coC3	1/5	Co	C	(26)
1/4coC3	1/4	Co	C	(21)	1/5coC4	1/5	Co	C	(26)
1/4coC4	1/4	Co	C	(21)	1/6coC1	1/6	Co	C	(24)
1/4coC5	1/4	Co	C	(28)	1/7coC1	1/7	Co	C	(29)
1/4coC6	1/4	Co	C	(24)	1/10coC1	1/10	Co	C	(30)

Table 2 – Compositions of mortars with RA of CDW Bricks (Co-Concrete; Br-Bricks; Mix-Mixture; M-Mortar; C-Cement; HL-Hydraulic Lime; LF-Limestone Filler; F-Filler)

Code	(B/A)	RA	Binder	Ref.	Code	(B/A)	RA	Binder	Ref.
1/3brC1	1/3	Br	C	(23)	1/4brC4	1/4	Br	C	(21)
1/3brC2	1/3	Br	C	(21)	1/4brC5	1/4	Br	C	(31)
1/3brC3	1/3	Br	C	(21)	1/5brC1	1/5	Br	C+HL	(22)
1/3brC4	1/3	Br	C	(32)	1/5brC2	1/5	Br	C+LF	(22)
1/3brC5	1/3	Br	C	(32)	1/5brC3	1/5	Br	C	(33)
1/3brL1	1/3	Br	HL	(32)	1/5brmC1	1/5	Br+M	C	(29)
1/3brL2	1/3	Br	HL	(32)	1/5brcoC1	1/5	Br+Co	C	(34)
1/3brcoC1	1/3	Br+Co	C	(35)	1/6brC1	1/6	Br	C	(33)
1/4brC1	1/4	Br	C	(36)	1/7brC1	1/7	Br	C	(37)
1/4brC2	1/4	Br	C	(36)	1/7,5brcoC1	1/7,5	Br+Co	C	(34)
1/4brC3	1/4	Br	C	(21)					

Table 3 – Compositions of mortars with RA of CDW mix (Co-Concrete; Br-Bricks; Mix-Mixture; M-Mortar; C-Cement; HL-Hydraulic Lime; LF-Limestone Filler; F-Filler)

Code	(B/A)	RA	Binder	Ref.	Code	(B/A)	RA	Binder	Ref.
1/3mixC1	1/3	Mix	C	(21)	1/4mixCF1	1/4	Mix	C+F	(38)
1/3mixC2	1/3	Mix	C	(21)	1/4mixCF2	1/4	Mix	C+F	(38)
1/3mixC3	1/3	Mix	C	(39)	1/5mixC1	1/5	Mix	C	(24)
1/3mixL1	1/3	Mix	HL	(39)	1/5mixC2	1/5	Mix	C	(40)
1/3mixC4	1/3	Mix	C	(23)	1/6mixC1	1/6	Mix	C	(24)
1/3mixC5	1/3	Mix	C	(41)	1/6mixCL1	1/6	Mix	C+HL	(42)
1/4mixC1	1/4	Mix	C	(21)	1/6mixCLf1	1/6	Mix	C+HL	(42)
1/4mixC2	1/4	Mix	C	(21)	1/6mixCL2	1/6	Mix	C+HL	(43)
1/4mixC3	1/4	Mix	C	(44)	1/7mixC1	1/7	Mix	C	(44)
1/4mixC4	1/4	Mix	C	(31)	1/8mixC1	1/8	Mix	C	(45)
1/4mixC5	1/4	Mix	C	(28)	1/8mixC2	1/8	Mix	C	(45)
1/4mixC6	1/4	Mix	C	(24)	1/8mixC3	1/8	Mix	C	(45)

3. Mechanical Properties

3.1 Compressive Strength

The compressive strength values of the different identified mortars incorporating RA of CDW studied by the aforementioned authors are presented. Figure 3.1 shows the compressive strength variation graphs depending on the type and percentage of RA used, the type of binder and the proportion B/A; graph (a) shows the values of mortars in which part or all of the NA was replaced by RA of concrete CDW; graph (b) shows the values referring to samples where NA was replaced by RA of brick CDW, including mixtures of brick and concrete (1/3brcoC1;1/5brcoC1; 1/7,5brcoC1) and brick and mortar (1/5brmC1); graph (c) presents the data referring to the samples where the NA was replaced by RA of CDW mix. In most mixtures it is possible to observe a decrease in compressive strength with the increase in the replacement percentage of NA by RA, except for the mortars produced with concrete CDW in a 1:5 ratio, where there is an increase in compressive strength. For mortars with reduced paste strength, when a decrease in strength is observed with the increase in the percentage of replacement of NA by RA, it is often insignificant or negligible, resulting in a reduction of the influence of RA.
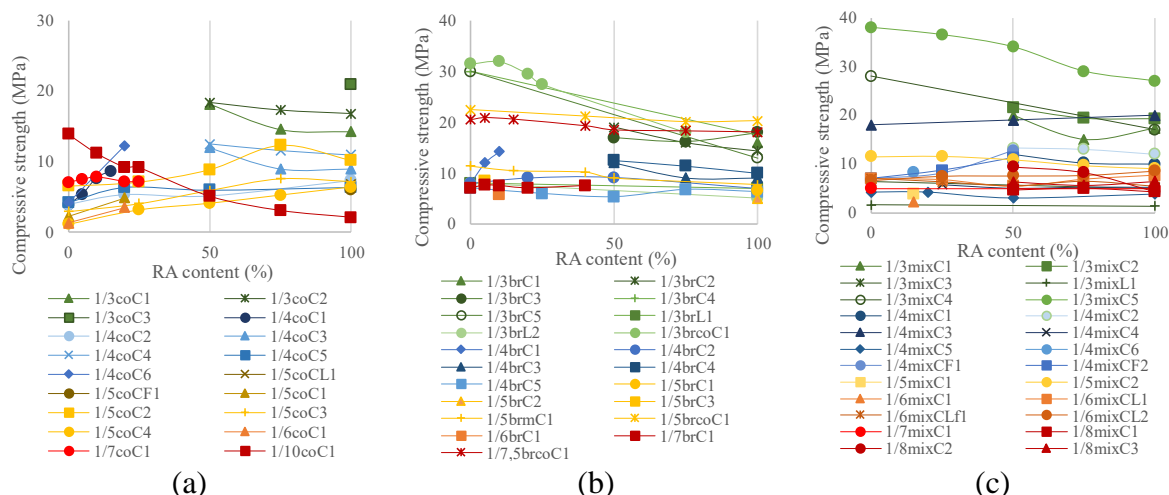

Figure 3.1 - Compressive strength – (a) mortars with RA of concrete CDW; (b) mortars with RA of bricks CDW; (c) mortars with RA of mix CDW.

3.2 Flexural Strength

The flexural strength values of the different mortars incorporating RA studied by the aforementioned authors is presented in Figure 3.2, where the graphs show the flexural strength variation depending on the type and percentage of used RA, on the type of binder and on the ratio binder/aggregate: graph (a) shows the values of mortars with RA of concrete CDW; graph (b) shows the values of samples with RA of brick CDW including mixtures of brick and concrete (1/3brcoC1;1/5brcoC1; 1/7,5brcoC1) and brick and mortar (1/5brmC1); graph (c) presents the data of samples with RA of CDW mix. In terms of flexural strength, the influence of RA is identical to that regarding compressive strength, generally observing a decrease in strength with the replacement increase of NA by RA, excepting for mortars produced with concrete CDW at a ratio of 1:5, where there is an increase in strength. Despite some decreases in strength with increasing replacement of NA by RA, this is almost imperceptible in most mixtures where the matrix has low strength, due to the low influence of the RA in these cases.
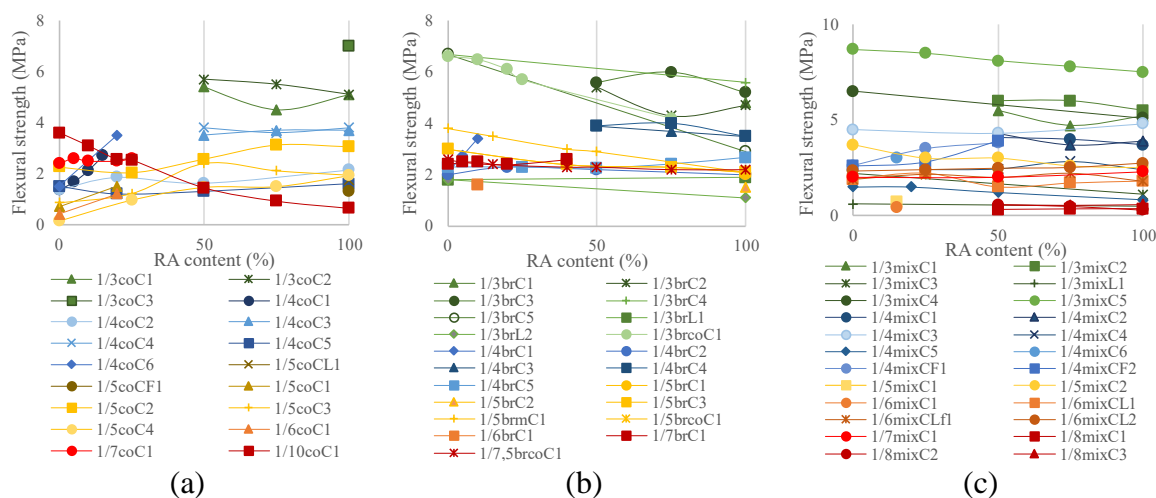
Figure 3.2 - Flexural strength – (a) mortars with RA of concrete CDW; (b) mortars with RA of bricks CDW; (c) mortars with RA of mix CDW.

4. Discussion and Final Considerations

The type, volume, and properties of the incorporated aggregates influence the behaviour of the mortars in different ways, as noted by several authors (28,46–49). Well-distributed granulometry ensures good particle packing and good performance in cementitious mixtures (48). Similarly, the irregular shape of the particles and the increase in the proportion of finer material contribute to the increase in inter-particle friction and consequently the viscosity of the paste (46). If the particle size curve of recycled aggregates is determined based on that of the original aggregate, the mortar can achieve better compressive and tensile strength values (49). It is conclusive that, in some mixtures, the replacement of NA by RA result in an increase in mechanical strength, which is most probably related to the high quality of RA and to water absorption that may reduce w/c effective ratio.

For all types of mortar, the mixtures with the highest cement content (1:3) are those with the highest mechanical performance, both in terms of flexural strength and compressive strength. The mixture 1/3mixC5, made with RA of CDW mix and single used cement as binder, presents the highest values. Although this mortar was produced with CDW mix (EWC 170107), it is important to highlight that the CDW used was composed of 80% concrete, 10% stone, 7% masonry and 3% other; the high proportion of RA in the concrete improves the mechanical performance.

In addition, mortars made with binder matrices that initially have high values of compressive and flexural strength do not change significantly when NA is replaced by RA, regardless of the type of used CDW. In the future, a more detailed analysis will be carried out to study and assess the strength gradients associated with the incorporation of different types of CDW. In general, there is a slight decrease in strength proportional to the increase in the replacement of NA by RA, as previously stated by Marinkovic *et al.* (50), with the exception of RA of CDW concrete, where it is verified that some mixtures present an increase in mechanical strength with the replacement of NA by RA. This tendency may be related to a possible deviation of the absorption water, eventually reducing the effective w/c ratio; the mechanical performance tends to be maintained or improved with a lower w/c ratio, as noted by Silva *et al.* (51).

With the replacement of NA by RA, of up to 30%, the loss of strength is residual, as already mentioned by Evangelista *et al.* (18) and Llanes *et al.* (34), mainly in the RA of CDW concrete. The exception is for mortars made with higher proportions of aggregate, such as the case of the 1/10coC1 mixture, where there is a significant loss, around 30%, both in compressive and flexural strengths.

The quality of the RA affects the mechanical properties, as mentioned by Kim (12); however, RA have a high potential to replace NA in the production of mortars in terms of mechanical strength, and their use in the production of mortars is undoubtedly viable for construction purposes, as concluded by Silva *et al.* (51).

Acknowledgements

References

1. United Nations, Department of Economic and Social Affairs PD (2019). World Urbanization Prospects: The 2018 Revision (ST/ESA/SER.A/420) [Internet]. United Nations, editor. United Nations, Department of Economic and Social Affairs, Population Division (2019). New York; 2018. Available from: https://population.un.org/wup/Publications/Files/WUP2018-Report.pdf

2. Ornelas C, Miranda Guedes J, Sousa F, Breda-Vázquez I. Supporting Residential Built Heritage Rehabilitation through an Integrated Assessment. Int J Archit Herit [Internet]. 2020;00(00):1–14. Available from: https://doi.org/10.1080/15583058.2020.1712496

3. Akhtar A, Sarmah AK. Construction and demolition waste generation and properties of recycled aggregate concrete: A global perspective. J Clean Prod [Internet]. 2018;186:262–81. Available from: https://doi.org/10.1016/j.jclepro.2018.03.085

4. Jin R, Li B, Zhou T, Wanatowski D, Piroozfar P. An empirical study of perceptions towards construction and demolition waste recycling and reuse in China. Resour Conserv Recycl. 2017;126(July):86–98.

5. Zhao W, Leeftink RB, Rotter VS. Evaluation of the economic feasibility for the recycling of construction and demolition waste in China-The case of Chongqing. Resour Conserv Recycl. 2010;54(6):377–89.

6. Wu H, Wang J, Duan H, Ouyang L, Huang W, Zuo J. An innovative approach to managing demolition waste via GIS (geographic information system): A case study in Shenzhen city, China. J Clean Prod [Internet]. 2016;112:494–503. Available from: http://dx.doi.org/10.1016/j.jclepro.2015.08.096

7. Eurostat. Waste statistics [Internet]. European Union. 2020. p. 1–12. Available from: https://ec.europa.eu/eurostat/statistics-explained/index.php/Municipal_waste_statistics

8. Marzouk M, Azab S. Environmental and economic impact assessment of construction and demolition waste disposal using system dynamics. Resour Conserv Recycl [Internet]. 2014;82:41–9. Available from: http://dx.doi.org/10.1016/j.resconrec.2013.10.015

9. Ahmad OA. the Usefulness of Construction and Destruction Waste As Recycled Aggregates in Concrete. Int J GEOMATE. 2020;19(75):8–18.

10.   Zanni S, Simion IM, Gavrilescu M, Bonoli A. Life Cycle Assessment Applied to Circular Designed Construction Materials. Procedia CIRP [Internet]. 2018;69(May 2018):154–9. Available from: http://dx.doi.org/10.1016/j.procir.2017.11.040

11.   Silva R V., De Brito J, Dhir RK. Properties and composition of recycled aggregates from construction and demolition waste suitable for concrete production. Constr Build Mater [Internet].   2014;65:201–17.   Available   from: http://dx.doi.org/10.1016/j.conbuildmat.2014.04.117

12.   Kim J. Influence of quality of recycled aggregates on the mechanical properties of recycled aggregate concretes: An overview. Constr Build Mater [Internet]. 2022;328(September 2021):127071. Available from: https://doi.org/10.1016/j.conbuildmat.2022.127071

13.   Zhang Y, Luo W, Wang J, Wang Y, Xu Y, Xiao J. A review of life cycle assessment of recycled aggregate concrete. Constr Build Mater [Internet]. 2019;209:115–25. Available from: https://doi.org/10.1016/j.conbuildmat.2019.03.078

14.   Coelho A, De Brito J. Influence of construction and demolition waste management on the environmental impact of buildings. Waste Manag. 2012;32(3):532–41.

15.   Estanqueiro B, Dinis Silvestre J, de Brito J, Duarte Pinheiro M. Environmental life cycle assessment of coarse natural and recycled aggregates for concrete. Eur J Environ Civ Eng [Internet].   2018;22(4):429–49.   Available   from: http://dx.doi.org/10.1080/19648189.2016.1197161

16.   Silva R V., de Brito J, Dhir RK. Use of recycled aggregates arising from construction and demolition waste in new construction applications. J Clean Prod [Internet]. 2019;236:117629. Available from: https://doi.org/10.1016/j.jclepro.2019.117629

17.   Poon CS, Chan D. The use of recycled aggregate in concrete in Hong Kong. Resour Conserv Recycl. 2007;50(3):293–305.

18.   Evangelista L, de Brito J. Mechanical behaviour of concrete made with fine recycled concrete aggregates. Cem Concr Compos. 2007;29(5):397–401.

19.   Kou SC, Poon CS, Agrela F. Comparisons of natural and recycled aggregate concretes prepared with the addition of different mineral admixtures. Cem Concr Compos [Internet]. 2011;33(8):788–95. Available from: http://dx.doi.org/10.1016/j.cemconcomp.2011.05.009

20.   Kurad R, Silvestre JD, de Brito J, Ahmed H. Effect of incorporation of high volume of recycled concrete aggregates and fly ash on the strength and global warming potential of concrete. J Clean Prod. 2017;166:485–502.

21.   Saiz Martínez P, González Cortina M, Fernández Martínez F, Rodríguez Sánchez A. Comparative study of three types of fine recycled aggregates from construction and demolition waste (CDW), and their use in masonry mortar fabrication. J Clean Prod. 2016;118:162–9.

22.   Martínez I, Etxeberria M, Pavón E, Díaz N. Influence of Demolition Waste Fine Particles on the Properties of Recycled Aggregate Masonry Mortar. Int J Civ Eng [Internet]. 2018;16(9):1213–26. Available from: http://dx.doi.org/10.1007/s40999-017-0280-x

23.   Corinaldesi V, Moriconi G. Behaviour of cementitious mortars containing different kinds of recycled aggregate. Constr Build Mater [Internet]. 2009;23(1):289–94. Available from: http://dx.doi.org/10.1016/j.conbuildmat.2007.12.006

24.   Jesus S, Pederneiras CM, Farinha CB, de Brito J, Veiga R. Reduction of the cement content by incorporation of fine recycled aggregates from construction and demolition waste in rendering mortars. Infrastructures. 2021;6(1):1–16.

25.   Braga M, De Brito J, Veiga R. Incorporation of fine concrete aggregates in mortars. Constr Build

Mater [Internet]. 2012;36:960–8. Available from: http://dx.doi.org/10.1016/j.conbuildmat.2012.06.031

26. Kaplan G, Turkoglu M, Bodur B, Bayraktar OY. Usage of recycled fine aggregates obtained from concretes with low w/c ratio in the production of masonry plaster and mortar. Environ Dev Sustain [Internet]. 2022;24(2):2685–714. Available from: https://doi.org/10.1007/s10668-021-01551-5

27. Neno C, Brito J De, Veiga R. Using Fine Recycled Concrete Aggregate for Mortar Production 2 . Literature Review 3 . Sequence of Testing. Mater Res. 2014;17(1):168–77.

28. Roque S, Maia Pederneiras C, Brazão Farinha C, de Brito J, Veiga R. Concrete-Based and Mixed Waste Aggregates in Rendering Mortars. Materials (Basel) [Internet]. 2020 Apr 23;13(8):1976. Available from: https://www.mdpi.com/1996-1944/13/8/1976

29. Ledesma EF, Jiménez JR, Fernández JM, Galvín AP, Agrela F, Barbudo A. Properties of masonry mortars manufactured with fine recycled concrete aggregates. Comput Chem Eng [Internet]. 2014;71:289–98. Available from: http://dx.doi.org/10.1016/j.conbuildmat.2014.08.080

30. Vegas I, Azkarate I, Juarrero A, Frías M. Diseño y prestaciones de morteros de albañilería elaborados con áridos reciclados procedentes de escombro de hormigón. Mater Constr. 2009;59(295):5–18.

31. de Oliveira Andrade JJ, Possan E, Squiavon JZ, Ortolan TLP. Evaluation of mechanical properties and carbonation of mortars produced with construction and demolition waste. Constr Build Mater. 2018;161:70–83.

32. Corinaldesi V. Environmentally-friendly bedding mortars for repair of historical buildings. Constr Build Mater [Internet]. 2012;35:778–84. Available from: http://dx.doi.org/10.1016/j.conbuildmat.2012.04.131

33. Silva J, De Brito J, Veiga R. Fine ceramics replacing cement in mortars partial replacement of cement with fine ceramics in rendering mortars. Mater Struct Constr. 2008;41(8):1333–44.

34. Llanes MC, Pérez MR, González MJG, Raya JPB. Construction and demolition waste as recycled aggregate for environmentally friendly concrete paving. Environ Sci Pollut Res [Internet]. 2022;29:9826–40. Available from: https://doi.org/10.1007/s11356-021-15849-4

35. Raini I, Jabrane R, Mesrar L, Akdim M. Evaluation of mortar properties by combining concrete and brick wastes as fine aggregate. Case Stud Constr Mater [Internet]. 2020;13:e00434. Available from: https://doi.org/10.1016/j.cscm.2020.e00434

36. Silva J, Brito J de, Veiga R. Incorporation of fine ceramics in mortars. Constr Build Mater. 2009;23(1):556–64.

37. Jiménez JR, Ayuso J, López M, Fernández JM, De Brito J. Use of fine recycled aggregates from ceramic waste in masonry mortar manufacturing. Constr Build Mater. 2013;40:679–90.

38. Cuenca-Moyano GM, Martín-Morales M, Valverde-Palacios I, Valverde-Espinosa I, Zamorano M. Influence of pre-soaked recycled fine aggregate on the properties of masonry mortar. Constr Build Mater [Internet]. 2014;70:71–9. Available from: http://dx.doi.org/10.1016/j.conbuildmat.2014.07.098

39. Corinaldesi V. Mechanical behavior of masonry assemblages manufactured with recycled-aggregate mortars. Cem Concr Compos [Internet]. 2009;31(7):505–10. Available from: http://dx.doi.org/10.1016/j.cemconcomp.2009.05.003

40. Fernández-Ledesma E, Jiménez JR, Ayuso J, Corinaldesi V, Iglesias-Godino FJ. A proposal for the maximum use of recycled concrete sand in masonry mortar design. Mater Construcción

[Internet]. 2016 Mar 30;66(321):e075. Available from: http://materconstrucc.revistas.csic.es/index.php/materconstrucc/article/view/1976/2411

41. Poon CS, Kou SC. Properties of cementitious rendering mortar prepared with recycled fine aggregates. J Wuhan Univ Technol Mater Sci Ed. 2010;25(6):1053–6.

42. Ferreira RLS, Anjos MAS, Nóbrega AKC, Pereira JES, Ledesma EF. The role of powder content of the recycled aggregates of CDW in the behaviour of rendering mortars. Constr Build Mater [Internet]. 2019;208:601–12. Available from: https://doi.org/10.1016/j.conbuildmat.2019.03.058

43. Ferreira RLS, Anjos MAS, Ledesma EF, Pereira JES, Nóbrega AKC. Evaluation of the physical-mechanical properties of cement-lime based masonry mortars produced with mixed recycled aggregates. Mater Constr. 2020;70(337):1–14.

44. Ledesma EF, Torres Gómez AI, López M, Ayuso J, Jiménez JR. Effect of powdered mixed recycled aggregates on bedding mortar properties. Eur J Environ Civ Eng [Internet]. 2016;20:s1–17. Available from: http://dx.doi.org/10.1080/19648189.2016.1246689

45. Miranda LFR, Constantino CS, Monich CR, de M. Neto AA. Use of Recycled Sand Produced at Construction Sites in Bedding Mortars. J Mater Civ Eng. 2013;25(2):236–42.

46. Westerholm M, Lagerblad B, Silfwerbrand J, Forssberg E. Influence of fine aggregate characteristics on the rheological properties of mortars. Cem Concr Compos. 2008;30(4):274–82.

47. Gismera S, Alonso MDM, Palacios M, Puertas F. Rheology of alkali-activated mortars: Influence of particle size and nature of aggregates. Minerals. 2020;10(8):1–15.

48. Haddad LD de O, Neves RR, Oliveira PV de, Santos WJ dos, Carvalho Junior AN de. Influence of particle shape and size distribution on coating mortar properties. J Mater Res Technol [Internet]. 2020;9(4):9299–314. Available from: https://doi.org/10.1016/j.jmrt.2020.06.068

49. Jang H, Kim J, Sicakova A. Effect of aggregate size on recycled aggregate concrete under equivalent mortar volume mix design. Appl Sci. 2021;11(23).

50. Marinković S, Radonjanin V, Malešev M, Ignjatović I. Comparative environmental assessment of natural and recycled aggregate concrete. Waste Manag [Internet]. 2010 Nov;30(11):2255–64. Available from: https://linkinghub.elsevier.com/retrieve/pii/S0956053X10002217

51. Silva R V., De Brito J, Dhir RK. Performance of cementitious renderings and masonry mortars containing recycled aggregates from construction and demolition wastes. Constr Build Mater [Internet]. 2016;105:400–15. Available from: http://dx.doi.org/10.1016/j.conbuildmat.2015.12.171

RESEARCH APPROACHES FOR RECYCLING CALCIUM SULFATE FLOWING SCREEDS

Andreas Hecker[1],*, Alexander Schnell[1] and Horst-Michael Ludwig [1]

(1) Bauhaus-Universität Weimar, F.A. Finger-Institut für Baustoffkunde (FIB), Germany

* *andreas.hecker@uni-weimar.de*

Abstract

Gypsum is used in interior building construction. In addition, building materials containing calcium sulfate are used as gypsum board, gypsum wallboard and also as screeds for floors and on wall and ceiling surfaces as plaster. Around 60% of the demand for raw gypsum in Germany is still covered by flue gas desulfurization gypsum (FGD gypsum). About 40 % is supplied by mining natural gypsum. The supply of FGD gypsum as a by-product of coal-fired power plants will decline very sharply generation. Recycling of gypsum building materials will become an important contribution to effective resource utilization. Currently, gypsum board is the main supply source for gypsum recycling. A second source could be calcium sulfate screeds. This resource is not recycled until now. In a joint research project, companies and universities are engaged in evaluating various calcium sulfate resources and investigating them in terms of application. Initial results on the processing and reuse of calcium sulfate screeds are presented. The objective was to process (crush, screen) and calcine calcium sulfate screeds on the basis of different calcium sulfate binders and aggregates. The focus was on achieving the highest possible strength contribution from the recycled thermal anhydrite to fit application requirements.

1.   Introduction

Around 60% of the demand for raw gypsum in Germany is covered by flue gas desulfurization gypsum (FGD gypsum). About 40 % is supplied by mining natural gypsum [1]. With the environmentally necessary phase-out of coal-fired power generation, this valuable secondary raw material will disappear and new sources of calcium sulfate building materials must be found. According to an estimate by Altmann et.al. [2], [3], 75 million m² of calcium sulfate flowing screed and 75 million m² of screed were installed in East Germany from 1976 to 1989. This corresponds to a total of about 6 million m³ with an assumed installation thickness of 4 cm. In 1989, calcium sulfate screed accounted for only 9% of the total screed market in the former West Germany and 3% of the flowing screed market. After 1990, however, the share rose very sharply. Today, calcium sulfate screeds have a screed market share of just under 50% in Germany, with an annual volume of 1.3 million m³ [4]. The average service life of floating screeds is estimated at 40 to 80 years, and up to 80 years for composite and separating layer screeds [5]. In the future, therefore, considerable quantities of calcium sulfate screeds will

accumulate during the refurbishment or demolition of buildings, and depending on the type of installation (floating screed, separating layer), they can also be separated from the floor slabs and covering layer relatively easily and without leaving residues. This provides a good starting point for potential recycling.

2.   Own tests

From commercially available calcium sulfate flowing screeds, factory dry mortars and calcium sulfate binder compounds for factory fresh mortar flowing screed, screed slabs with a thickness of 4 cm were produced. Based on the existing technology in the lab scale processing at Bauhaus-Universität Weimar (jaw crusher, roller mill, screens), two crushing and separation stages were carried out to achieve maximum utilization as a recycling binder (recycled thermoanhydrite RTA). The achieved degrees of separation of binder and aggregate (sulfate content) and particle distribution were controlled. First, the screeds were crushed and dried at 40°C. Dried coarse material was fed to a jaw crusher and particles smaller than 1mm were separated by screening. The particles larger than 1mm were fed to a roller mill and separated into the fractions <1mm, 1- 2 mm and 2 - 4 mm. There were 2 recycled (RC) screed fractions 0 - 1 mm available (1st crushing stage jaw crusher, 2nd crushing stage roller mill), which were fired for 4 hours at 500°C in a lab scale chamber furnace.

2.1   Calcium sulfate flow screed

The variation for the tests was according to the type of calcium sulfate binder (alpha hemihydrate, synthetic anhydrite, natural anhydrite and thermo-anhydrite) and the aggregate (natural anhydrite or natural sand). The screeds were mechanically crushed and the recycled aggregate was fractionated. Table 1 shows the water of crystallization and dihydrate contents of the recycled aggregate 0-1 mm of the calcium sulfate flowing screeds. The calcium sulfate dihydrate content (DH) between 39 % and 48 % of the recycled fraction 0-1 mm indicates the recyclable gypsum content.

Table 1: Chemically bound water (water of crystallization) - and dihydrate content (DH) of the recycled grain (RC) 0-1mm of the calcium sulfate flowing screeds.

	binder	aggregate	free moisture	crystal water	gypsum content
			(40 °C)	(350 °C)	(Dihydrate %)
			%	%	%
RC1	35% synth. anhydrite	65% quartz sand 0-2mm	0,1	8,3	38,9
RC2	Natural anhydrite + Alpha HH	natural anhydrite grain size 0-2mm	0,1	9,5	44,6
RC3	Natural anhydrite + Alpha HH	natural sand 0-2mm	0,1	10,2	48,1
RC4	Alpha HH	natural sand 0-4mm	0,1	9,8	45,8

2.2 Recycling thermo-anhydrite

The recycled aggregate (RC) smaller than 1 mm was fired in a chamber furnace for 4 hours at 500 °C to form a recycled thermo-anhydrite (RTA) (Ex: RC1 to RTA1). RTA contains about 30% to 40% gypsum content (calcium sulfate phases), depending on the CSFE. Wet-chemical gypsum phase analysis (table 2) detects a proportion of poorly soluble anhydrite (AIIs) of 10% (RTA2) to 25% (RTA4). Without aggregate, this corresponds to about 25% AIIs (RTA2) and 60% AIIs (RTA4). Calcium sulfate hemihydrate and AIII are present in small amounts.

Table 2: Determined gypsum phases of the RTA fraction 0 - 1 mm, wet chemical analysis

gypsum phase		RTA 1	RTA 2	RTA 3	RTA 4
AIII	%	0,1	0,8	1,3	1,0
HH (1h)	%	4,3	3,0	4,3	6,4
AIIs (72h)	%	12,4	9,5	16,5	24,5
crystal water (350°C)	%	0,4	0,2	0,4	0,5

The RTA was subsequently mixed with a basic and acidic accelerator, 3 % white hydrated lime CL 90 and 0.6 % potassium sulfate, in order to accelerate the hydration (hardening). The influence of different superplasticizers on processing time, slump and strength was also tested.

2.2.1 Hydration, hardening up to 24 hours

The hardening process of the activated recycled thermo-anhydrite (RTA) is shown in figure 1. The ultrasonic velocity was measured over a period of 24 hours. All four recycling thermo-anhydrites show a similar hardening process in the first 10 hours with a slower increase up to 20 hours.
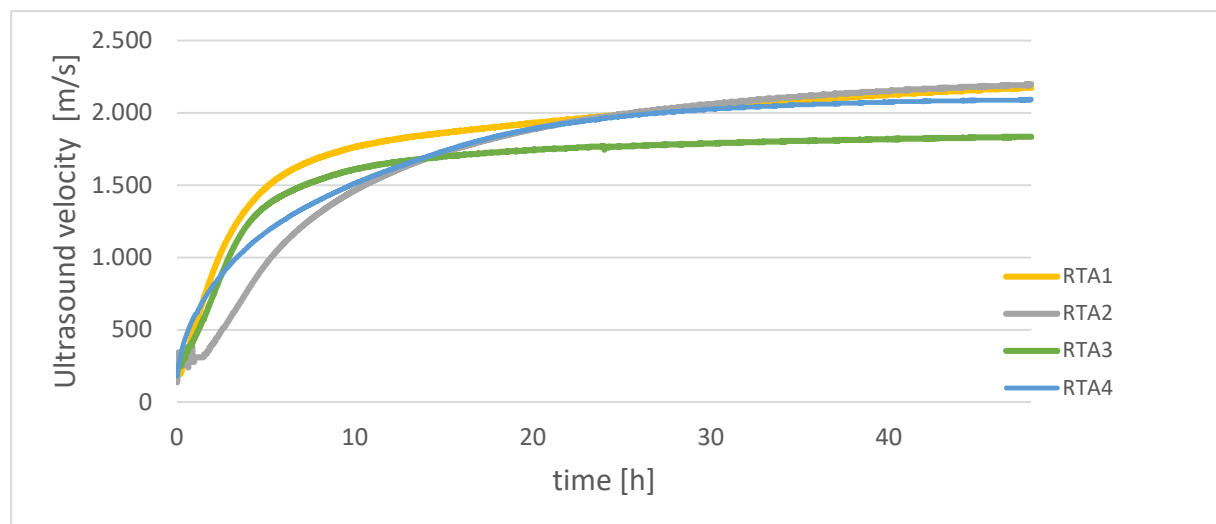

Figure 1 Ultrasonic speed up to 24 h, activated RTA with white hydrated lime and potassium sulfate as accelerator.

The hardening times were measured according to DIN EN 13279-2 (Vicat cone method) (Table 2). The water solids value was set to 0.4 (exception RTA1 0.35) and the consistency was determined by the spreading flow factor. The onset of hardening was measured to be 60 min for all RTAs, except 150 min for RTA 2 (Table 3).

Table 3: Water solids value (W/F value), flow spread value acc. to DIN EN 1015-3 and hardening start acc. to DIN EN 13279-2

	w/s value	Spread [cm]	Start hardening (VB) [min]
RTA1	0,35	203	60
RTA2	0,4	205	150
RTA3	0,4	170	60
RTA4	0,4	202	60

Figure 2 shows the ultrasonic velocity of the RTAs of the first 5 hours. Also marked is the onset of cure (VB), which shows that VB corresponds to an ultrasonic velocity of about 500 m/s. Compared to all other RTA`s, RTA 2 has a significantly slower hardening course.
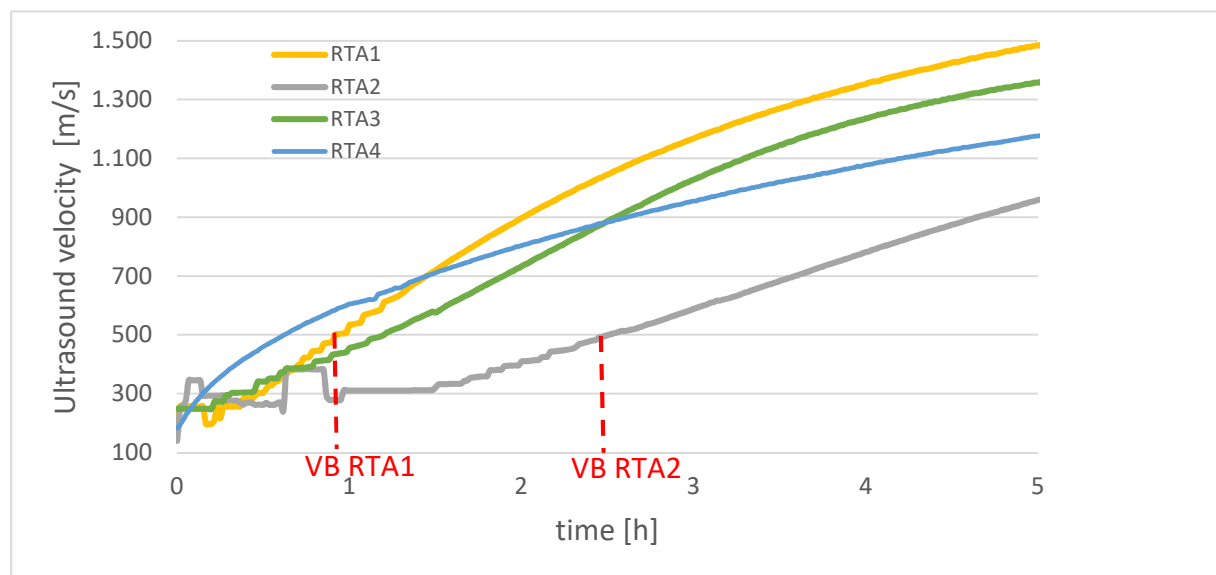

Figure 2: Ultrasonic velocity up to 5 h, for RTA1 and RTA2 the onset of cure (VB) according to DIN EN 13279-2 (Vicat cone method) plotted.

2.2.2 Influence of superplasticizer on processing time

Superplasticizers are a very important additive for the mortar calcium sulfate flowing screed. The stability of the flowable consistency determines the processing properties. Based on DIN EN 13454-2 (calcium sulfate binder, calcium sulfate composite binder and calcium sulfate ready-mixed mortar for screeds), the processing time (consistency retention) was determined. The working time is the time in which the original flowability of the mortar is reduced by 20 %. For flowable mortar, the flow dimension must not fall below 190 mm, and for highly plastic

mortar, the spread dimension must not fall below 130 mm [6]. The initial consistency in all tests was about 210 mm for the slump and 270 mm for the spread. Four different superplasticizers (F1, F2, F3, F4) were tested with a dosage of 0.1 wt.% in the activated recycled thermo-anhydrites, partly in combination with retarders (V1, V2) (Figure 3). The superplasticizer base for F1 is a spray-dried powder based on melamine sulfonate and for F2, F3, F4 spray-dried powders based on modified polycarboxylate ethers (PCE). The flow measurement is marked [FM] in Figure 3 as a consistency measurement. The unmarked values are results of the spreading measure. RTA1 has a processing time of 40 min to 55 min for all 4 superplasticizers. In contrast, RTA2 only achieved a processing time of 18 min with F2 superplasticizer. RTA3 and RTA4 were mixed with a retarder and are therefore not comparable with RTA1 and RTA2. RTA3 was provided with a retarder V1 based on a phosphonate mixture. Superplasticizer F3 resulted in the longest processing time of 85 min in this system. RTA4 was provided with a retarder V2 (modified amino acid). Nevertheless, only very short processing times (20 min to 30 min) were achieved with all four superplasticizers.
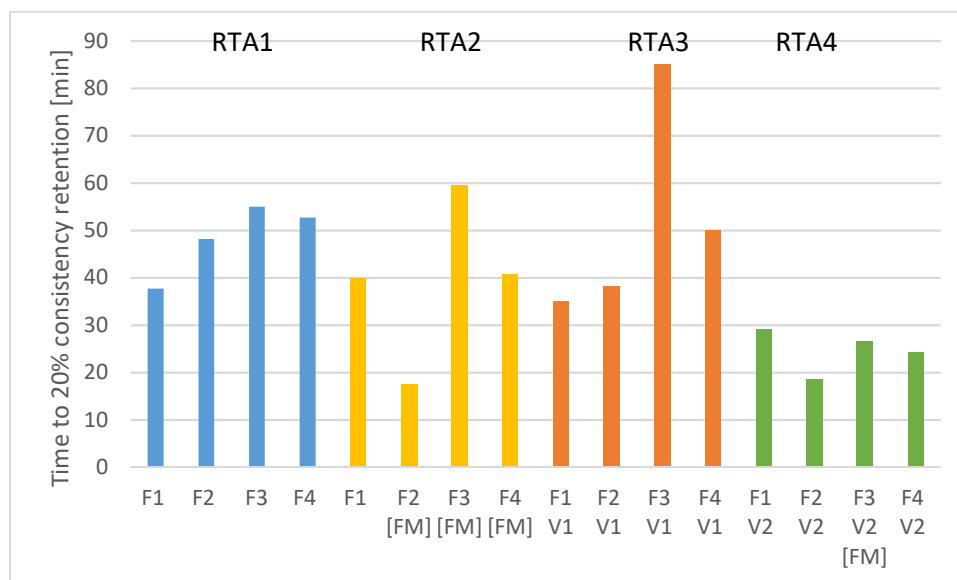

Figure 3: Measurement of consistency retention following DIN EN 13454-2, time at 20 % decrease of spreading value or slump flow, superplasticizer (F1, F2, F3, F4) partly in combination with retarder (V1, V2) [7].

2.2.3 Strengths RTA

For floating screeds, the flexural strength is relevant, the activated recycled thermo-anhydrites RTA1, RTA2 and RTA4 reach 2.5 MPa to 3 MPa (RTA2). For a calcium sulfate flowing screed of strength class CAF-C25-F5, this would be a 50% contribution of the flexural strength. For separating layer or bonded screed, the compressive strength is decisive, RTA 1 reaches 6 MPa, RTA2 8.5 MPa, which corresponds to a 30% contribution in the compressive strength of a CAF-C25-F5.
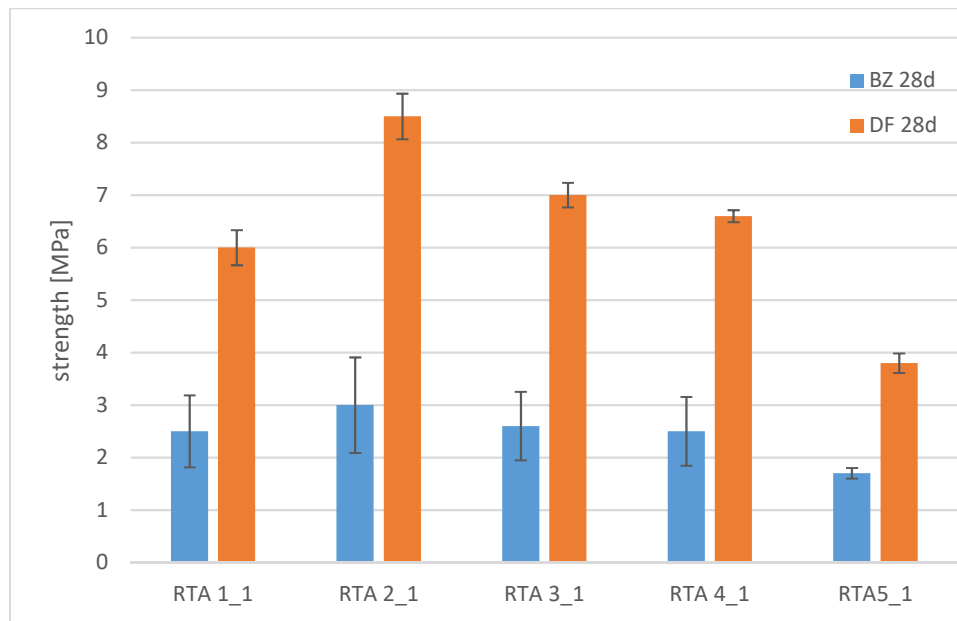
Figure 4: Activated RTA, flexural tensile strength (BZ) and compressive strength (DF) after 28 days of storage.

3.   Conclusions

Recycled thermo-anhydrite from screeds containing calcium sulfate makes an appreciable contribution to the strength of a calcium sulfate flowing screed. Further processing in factory dry or factory fresh mortars by a proportional addition to calcium sulfate flowing screeds is very promising according to the current results. In addition to the water-binder value and the flowability, superplasticizers also influence the processing time (consistency retention) of recycled thermo-anhydrite and calcium sulfate flow screeds. The chamber furnace used in lab scale is not a typically used in industrial scale. Further investigations are needed for the scale up and for optimization of mechanical and thermal processing of the calcium sulfate flowing screeds.

Acknowledgements

4.   References

[1] M. Buchert, J. Sutter, H. Alwast, N. Schütz, *Ökobilanzielle Betrachtung des Recyclings von Gipskartonplatten*, TEXTE 33/2017, Forschungskennzahl 3715 343200, Umweltforschungsplan des Bundesministeriums für Umwelt, Naturschutz, Bau und Reaktorsicherheit

[2] Christian Herrmann; Ursula Lindel; Heinz-Dieter Altmann; *Aspekte bei der Behandlung von Fließanhydrit- Fußböden*; EstrichTechnik, 1/92, S.7-9

[3] Heinz-Dieter Altmann; *Stand der Technik*; floors walls 16/ Juni 2008; S.38- S.40

[4] Marktdaten: B+L / Destatis / MIS Statistik, f=Prognose, Stand 09/2020

[5] Lebensdauer von Bauteilen und Baustoffen (Bundesverband Altbauerneuerung e. V.), BAKA Liste, Ausgabe 2021

[6] DIN EN 13454-2, Calciumsulfat-Binder, Calciumsulfat-Compositbinder und Calciumsulfat-Werkmörtel für Estriche, Teil 2: Prüfverfahren; Deutsche Fassung EN 13454-2:2003+A1:2007

[7] Tobias Gaedtke, Einflüsse von Additiven auf das Recycling von Calciumsulfatfließestrich, Bachelorarbeit Reg.Nr. B/B/2021/6, 2021, S.32

FROM RECYCLING TO CIRCULARITY - HOW A CIRCULAR DESIGN APPROACH CAN MAKE OUR BUIDLINGS BETTER FOR THE ENVIRONMENT AND ITS INHABITANTS

Maria Hirnsperger[1]*, Angie Müller-Puch[2]*, Erik Hegre[3]

(1) Behnisch Architekten, München, mhi@behnisch.com

(2) Behnisch Architekten, Weimar, am@behnisch.com

(3) Behnisch Architekten, Boston, eh@behnisch.com

Abstract

Finite resources, climate change and high carbon emissions are the main challenges facing the contemporary building industry. As a result, the industry tends to design energy efficient buildings through the implementation of technical systems and highly insulated building envelopes.

Efficient in operation, but intense in grey emissions and material consumption - a look at the 55,4% of construction and demolition waste in Germany 2020[1] shows that this cannot be the only strategy to make the building sector carbon neutral.

A holistic approach that considers the entire lifespan of our buildings is needed to reduce carbon emissions as well as resource consumption. This starts with precise programming, flexible floorplans, a focus on pre-use and post-use of materials, and the possibility to adapt entire buildings to future needs and climate change.

This research, based on a real building project, provides an overview on how reuse and recycling can become part of a fluid design process through parametric modelling. It illustrates how to create buildings that are easy to repair and adapt and how this enhances user acceptance. It shows how secondary materials can be used and reused with low energy input to transform the so called "Urban mine"[2] into a circular environment.

1.0   Introduction

For the last decades, the predominant thinking around sustainable design and construction has been driven by the ambition to make buildings more energy-efficient, in particular during the operational period of their lifecycle. In response, the construction market has focused on developing efficient technical building equipment, while designers strive to create buildings that require less energy to operate - a compelling strategy because it simultaneously reduces energy consumption and minimizes the costs of operation. To increase energy efficiency, the standards for technical equipment and building envelopes were continuously raised which led to a significant increase of new building material used in construction and renovation.

Thus, reduced carbon emissions during operation, led to an increase in grey emissions during construction which should pay off over the buildings' lifespan.

"However, as buildings become more energy efficient, the embodied environmental impacts stemming from production, construction, maintenance and disposal of building materials represent an increasing share of a buildings' total environmental burden" according to Leonora Charlotte Malabi Eberhardt.[3]

The 2022 UN Global Status Report for Buildings and Construction states "(…) the observed emissions and energy consumption have continued to increase in 2021 even beyond pre-pandemic levels, indicating the decarbonization of building stock is "not on track" to reach the Goals of the Paris Agreement".[4] Furthermore, the building sector is facing a significant resource and waste problem. Minerals and waste are traded and shipped around the world.[5] Besides the important environmental impact, the resulting social injustice caused is apparent. Therefore, a holistic approach for the future of building is needed, which takes into account not only the operational energy, but also the embodied energy over the whole lifespan of our buildings and beyond.

As a reaction to this, the building industry has to change its approach towards sustainability and seek to develop circular construction strategies which focus on the Pre-Use as well as the Post-Use-Potential of materials. This fosters the implementation of reused, recycled and renewable materials as well as the creation of adapted construction methods and design strategies. Throughout the industry two major approaches to this topic can be observed.

One concept is based on the current predominant linear planning process. First the orientation, shape, functional organization and appearance of a building are developed. After that, materials are selected, produced and delivered on site in a timely manner. Where possible conventional materials are replaced by recycled ones, adapted to the specific project. This enables a large-scale applicability with minimal effect on planning and design what makes this an interesting approach for big scale developments. But the overall environmental impact can be subject to discussion.

The second approach reverses the above-mentioned linear process. In this case the projects' start is characterised by harvesting the buildings components, either through professional reuse-material-sellers or a selected host building that can be deconstructed and reassembled into a new project. The resulting design is based on the re-assembly of the previously found objects. Attractive in terms of carbon efficiency, because of its high capacity to implement existing materials, this approach is impacted by the missing knowledge about our building stock and the lack of warranty regulations for circular materials.[6] The dependency on material availability and the guarantee risk result in the predominant application of this concept in small scale projects.

As a result, "wide-scale adoption is still lacking, and the current development and implementation of circular economy building design and construction strategies is fragmented."[3]

The following research based on a real housing project in Hamburg Wilhelmsburg pushes the boundaries of circularity through an integrated circular design process which is sustainable and scalable. The project is embedded into Hamburg's Circuit – Horizon 2020 research project which aims to improve the practical applicability of secondary materials in the building sector.

2.   Sustainable and scalable – An integrative approach

Dealing with the availability and existing properties of materials and their possible places of implementation must be considered right from the start. Therefore, the design process needs to be transformed from a linear into an interlaced, holistic process. (Figure 1) This design research project in Hamburg Wilhelmsburg, will illustrate how design decisions in different project stages and scales can enhance a diverse and extensive implementation of circular materials in building construction. It shows how a holistic approach effects all design stages from how much (Reduce) and how we build (Reuse / Recycle / Renewable), how our buildings can evolve over time (Repair) and adapt to future needs (Super-Use).
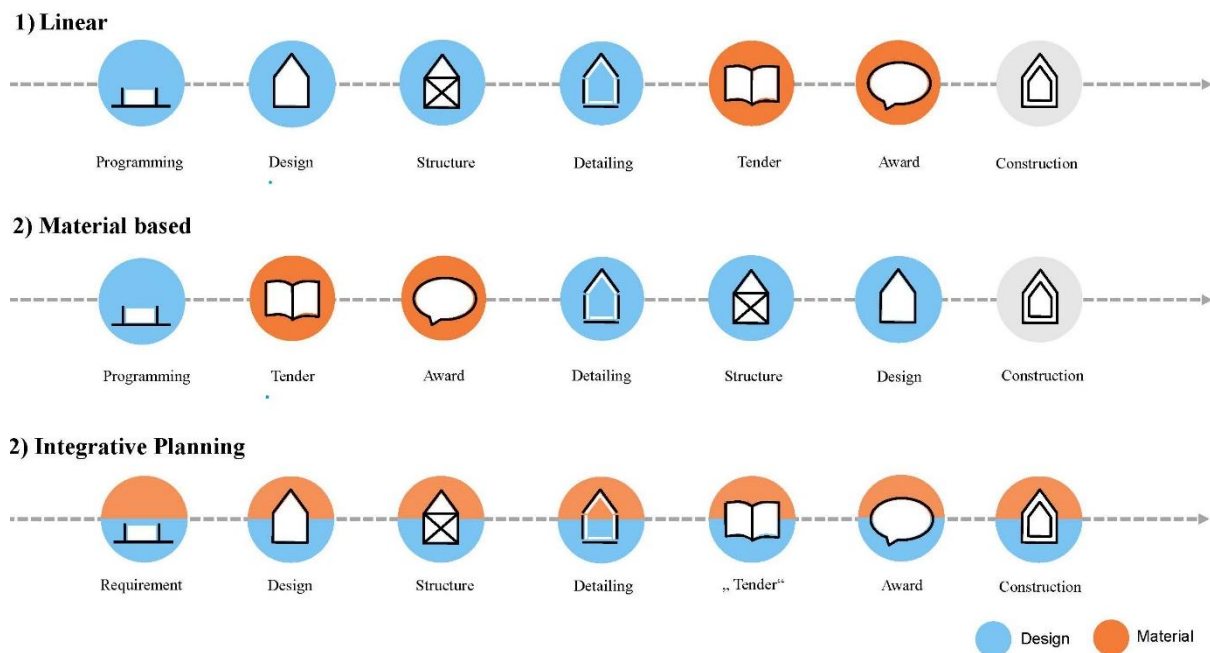

Figure 1: Circular design methods

2.1   Reduce and Super-Use: Designed to be circular

The existing building codes, especially fire and thermal regulations (in Germany), can limit the use of circular materials. To enhance the implementation of those materials, special attention to the buildings' fire classification is needed. According to current norms, a high-rise building classification can result in various limiting regulations. For example, structural elements as well as ceiling and façade constructions are required to be non-combustible and must be technically proven to achieve certain fire resistance through standardized testing, which can be either cost prohibitive or unfeasible when utilizing reused or recycled materials. In timber construction, this leads in most cases to a complete encapsulation of the wooden structure or the installation of a sprinkler system. In the present project in Hamburg Wilhelmsburg, the cities masterplan proposed an 8-story building, which is considered as a high-rise-building by only one floor. In this case the design team, including the client, decided against this additional rental area in order to avoid the high-rise classification in favour of a circular design, which provided more flexibility in the choice of materials and special systems requirements.

Moreover, this project promotes the creation of spaces with lower requirements in terms of thermal regulations which allow the implementation of reused façade elements with outdated U-values. Loggias are transformable into thermal buffer zones, which help the building to adapt to seasons and future climate change, through a secondary layer of reused windows. Outside, weather-protected outdoor staircases enable reduced fire regulations and the use of reused facade elements whilst becoming a social gathering space for the residents.
In addition, the buildings' functional organization plays a major role for the future lifecycle. Flexible floorplans, shared spaces and apartments that can easily be adapted over time help to transform the building into a vivid organism with a maximized lifespan (Super-Use).

These examples show that circularity is far more than the implementation of recycled materials. Sustainable urban structures which can adapt to user needs and climate change as well as constructions that allow the reuse of building materials can promote circularity and lead to new, surprising design results.

2.2   Reuse, Recycle, Renewable: Circular material parameters

Following the above-mentioned holistic approach, it is important to develop the buildings' construction elements based on their global warming potential (GWP) and material consumption as well as their re-use potential, flexibility and space requirements. Thus, in a first step construction elements with a significant influence on the buildings' environmental performance are identified. Secondly the impact of different material choices on the overall building design is evaluated.

Concerning the carbon footprint, the buildings' primary structure, the ceiling and the façade elements have a major influence, as they represent a significant portion of the building mass.[7] Therefore, early design decisions on these elements have an irreparable impact on the buildings' carbon footprint.
Efficient in primary resource consumption and carbon footprint, the implementation of reused construction elements can be an interesting option due to the missing production process. Only transport distances and de- and reconstruction influence the GWP.[6] Thus, the most carbon efficient way of building with secondary materials is either to keep them installed or store them on site until subsequent reuse is possible. Besides the low climate impact, the choice reuse components can provide a solution for the crucial construction waste problem. But looking at e.g. the City of Hamburg's construction waste management plan, the challenge of this option becomes clear, though more than 80% of the available stock are crushed mineral materials such as soil, stone, concrete, brick,[8] which can be recycled but not reused.
Dealing with recycled (RC) construction components, particular focus needs to be set on the GWP of the recycling process. For instance, the simple replacement of "traditional" concrete with a RC alternative reduces on the one hand primary resource consumption, such as gravel, but it increases on the other hand the carbon emissions.[9] Concerning RC concrete, more sustainable formulas are in development. RC-steel for example can be already manufactured with renewable energies. If recycled components are chosen special attentions should be paid on their installation to enable future reuse of these elements.
Another alternative is the use of renewable construction materials such as wood. The material itself has a negative carbon footprint, but in this case the fabrication process is also crucial, though load-bearing applications often require industrial wood such as GLT (glued laminated timber) or CLT (cross-laminated timber) though construction wood would lead to increased

material dimensions. This has an impact on the GWP and limits their fabrications to specialized companies what mostly results in large transportation distances.

This comparison between reuse, recycling and renewable construction elements highlights that besides the GWP of the material itself, various parameters have to be coordinated to create a structure with the lowest possible emissions and the highest possible recyclability, Pre- and Post-Use.

Figure 2: Circular material parameters

In the present design research project in Wilhelmsburg, the major construction elements were analysed based on material characteristics as well as their overall impact on the buildings' sustainability. Developing the primary structure reused steel, recycled concrete and wood were compared with the result that a skeleton structure based on wooden columns (GLT 36x36) and recycling steel supports (HEB 280) were selected.

Due to its anisotropic behaviour, wood has very different properties in terms of compressive and tensile strength, depending on the direction of the grain. The characteristic compressive strength in the grain direction is between 17 and 32 N/mm² and therefore comparable to concrete C25/30, which has a characteristic compressive strength of 30 N/mm². This means that wood is just as suitable as concrete for the use of pressure-loaded components such as columns.

If subject to bending or tensile loads, as required for ceiling beams, wood is significantly less effective compared to e.g. steel (tensile strength of wood 10-36 N/mm² compared to steel 235-500 N/mm²). As a consequence, a wooden beam compared to steel would increase material consumption by twenty times and through that raise the construction height of each floor by 35 centimetres. This would result in a major increase in carbon emission in construction and operation of the building due to an increased column and façade height and heated volume. (Figure 3) Following the Urban Mining Index[9] standard steel profiles are considered as largely reusable if attention is paid to detachable joints. In this project standard steel profile dimensions promote the implementation of reuse steel beams. If no reuse components can be found RC-steel fabricated with renewable energies will be installed.
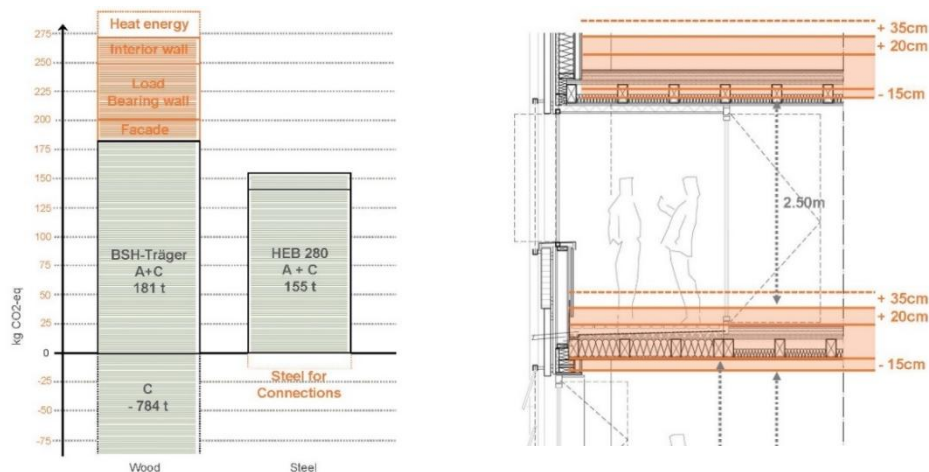
Figure 3: Wood vs. RC-Steel, overall environmental impact

The secondary structure such as ceiling components were designed as removable wooden elements with a focus on reuse and easy regional fabrication. Depending on the fire protection and load requirements, they are planed either as stacked planks or as wooden beam ceilings without any glue. With a span of 6.2 m, material-efficient cross-sections can be used for both timber constructions.

Similar to the ceiling construction, the facade construction consists of prefabricated wooden frame elements filled with reused or biobased insulation. Compared to a solid wooden wall, the frame construction saves up to 75% of wood. By placing the façade elements between the floor slabs steel components and joints can be reduced. The facade cladding is designed to be reused one-to-one in the next building in the event of demolition. In order to always maintain the same detail for suspension, frames form the basis of the elements. They can be filled with different reuse materials (clinker, wood, metal facades, etc.) and are suspended from the wooden substructure using the principle of wedge lathing/ battens. This gives the ability to react to changing future material stock.

All connections are designed to be disassembled. Furthermore, it is elementary for the design that all materials and components, regardless of whether they were created from new building materials or from reuse materials, can be fed back into a post-use later.
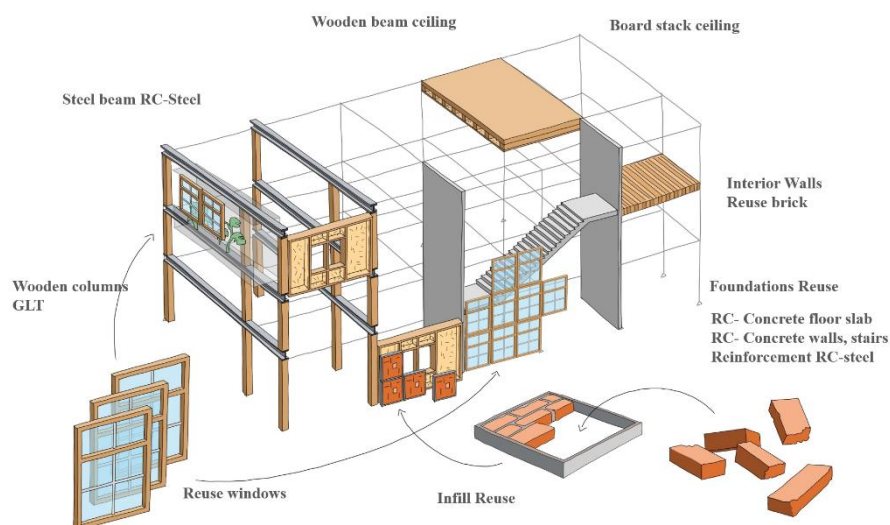

Figure 4: Selected circular construction components

2.3 Consideration processes and benefits of the advance in technology (BIM)

In the course of the analysis and development of the "Circuit Wilhelmsburg" project, a large number of parameters arose which had an impact on the final outcome. It turned out that it was not always easy to predict from the beginning on which part of the project a single parameter would have an influence. A representative example is the decision-making process for the system of beams described in chapter 2.2. This decision affects the flexibility of the building, the height of the building and consequently the building class and height of the facade and interior walls. Some of these parameters imply a functional impact on the building, while others are reflected in higher CO_2e or the inability to disassemble.

In the research project, the effects were calculated individually at the beginning and the decision-making process was supported, for example, in the form of spider charts. In order to be able to profit from the results obtained in the future and to optimize decision-making processes, the critical parameters were summarized in a script based on the example of the facade. The choice of program was Grasshopper in Rhino, in order to also visually illustrate the geometric effects. In the further project it is planned to extend the script to all relevant fields of the building.
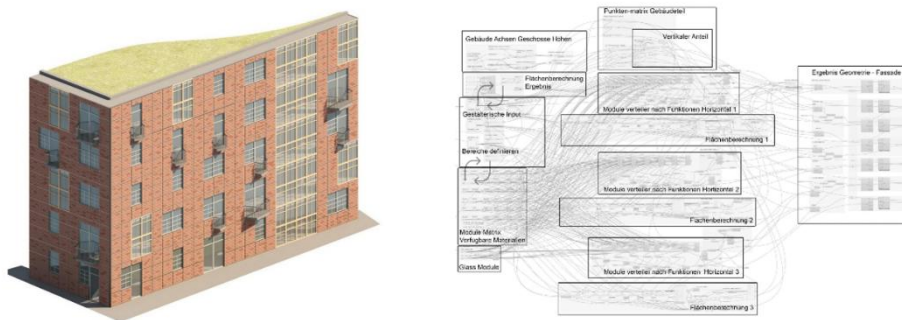

Figure 5: Decision making process based on parametric modelling

3. From Recycling to Circularity

At the beginning of the project "Wilhelmsburger Rathausviertel" the design team was tempted to take a small-scale, boutique approach to circular construction. According to the theme, "one building is deconstructed and the next one arises from it." Ideally, with exactly the materials that were envisioned in the design process of the building. The analysis of the data of the waste management plan of Hamburg and the statement of the study injected by the TU Hamburg about buildings available for demolition in the future show, that in the next few years mainly mineral recyclates will be available, and in a form that is difficult to "harvest". Two things can be deduced from this for this purpose. First, it is easiest to make circular use of the existing building stock if old concrete structures are not demolished, but the primary structures are retained as a basis for rebuilding. Second, if the building cannot be preserved, it must be used to create building components that can be easily reused when it is deconstructed again. The intent is to shift the act of recycling into one of reuse.

The calculation of the life cycle shows that the use of recycled and renewable raw materials saves a high proportion of the CO_2 equivalent, if the construction and the future deconstruction of the building are factored in. It should be noted that the improvement depends on many parameters, which means that the most obvious solution does not always automatically have the most positive effect. A holistic approach is therefore preferable

compared to an individual consideration of the relevant problems. The interconnection of the individual parameters is thereby not always recognizable at first sight or simple to calculate. Computer scripts can help to absorb the amount of data and to validate different scenarios faster. When trying to show the impact of a building on our environment, one is confronted on the one hand with different calculation and presentation models, such as life cycle calculations, material loop or different certification programs. On the other hand, there are supporters of the statements that buildings are particularly sustainable if they are perceived as "beautiful" by their environment and thus remain longer or if they are particularly flexible. In our eyes, these approaches should not contradict each other. There should not be either ecological or flexible or aesthetic architecture, but always a combination of all of these approaches. This is the only way we can master the challenges of the future together.

Figure 6: Visualization of the final project

4. References

[1] https://www.umweltbundesamt.de/daten/ressourcen-abfall/abfallaufkommen#deutschlands-abfall, (Accessed 2023/06/15)

[2] Heisel, F., Hebel, D., 'Urban Mining und kreislaufgerechtes Bauen: Die Stadt als Rohstofflager', (Fraunhofer IRB Verlag, Stuttgart, 2021)

[3] Eberhardt, L. & Birkved, M., Birgisdottir, H., 'Building design and construction strategies for a circular economy', (Architectural Engineering and Design Management, 2020)

[4] https://www.unep.org/resources/publication/2022-global-status-report-buildings-and-construction, (Accessed 2023/06/15)

[5] Choppin D., Delon N., 'Matière grise – Matériaux, réemploi, architecture', (Editions du Pavillon de l'Arsenal, Paris, 2014)

[6] Stricker E., Brandi G., Sonderegger A., Angst M., Buser B., Massmünster M., 'Bauteile wieder-verwenden - Ein Kompendium zum zirkulären Bauen', (Park Books, Zürich, 2021)

[7] Jusselme T., 'Research at the Service of Building Design`, in Rey E., Andersen M. 'Exploring, Research Driven Building Design', (Park Books, Zürich, 2019)

[8] Freie und Hansestadt Hamburg / Behörde für Umwelt und Energie, Gemeinsamer Abfallwirt-schaftsplan für Bau- und Abbruchabfälle von Hamburg und Schleswig-Holstein (Hamburg, 2020)

[9] Hillebrandt, A., Riegler-Floors, P., Rosen, A., Seggewies, J., 'Atlas Recycling: Gebäude als Materialressource, (Edition DETAIL, München, 2021)

DEVELOPMENT OF CALCIUM CARBONATE CONCRETE FOR PERMANENT RESOURCE RECYCLING AND CARBON NEUTRALITY

Takafumi Noguchi (1), Manabu Kanematsu (2), Masaki Tamura (3), Ippei Maruyama (1), Ryoma Kitagaki (4), Satoshi Fujimoto (5), Masato Tsujino (6), Hikotsugu Hyodou (7), Hiroshi Hirao (7), Haruo Nakazawa (6), Yasuhiro Kuroda (6) and Takayoshi Masuo (8)

(1) Department of Architecture, The University of Tokyo, Japan

(2) Department of Architecture, Tokyo University of Science, Japan

(3) Department of Architecture, Kogakuin University, Japan

(4) Division of Architecture, Hokkaido University, Japan

(5) Department of Architecture and Urban Design, Utsunomiya University, Japan

(6) Institute of Technology, Shimizu Corporation, Japan

(7) Central Research Laboratory, Taiheiyo Cement, Japan

(8) Masuo Recycle, Japan

Abstract

Cement concrete is an indispensable construction material, but its production uses a large amount of limestone and emits a large amount of CO_2. To fundamentally solve these problems, Ca in cement concrete is regarded as a potential unused resource capable of capturing CO_2. By developing a technology to regenerate cement concrete demolition waste and CO_2 in the air as calcium carbonate concrete (CCC), a new resource recycling system called "C^4S", Calcium Carbonate Circulation System for Construction will be realized. An efficient crushing method and an efficient CO_2 capture and storage method for concrete waste were developed. After crushing, the powders were used to produce calcium bicarbonate solution and the large particles were densely packed with pressure in a container as aggregate. Calcium bicarbonate solution was flowed or impregnated between the aggregate particles, and calcium carbonate crystals were precipitated and bonded the aggregate particles to form CCC. In addition, various studies were conducted to implement C^4S in society, including studies on structural design, optimum recycling scenario, and analysis of $LCCO_2$ reduction effect. Through these series of research and development, CO_2 in the atmosphere is expected to be efficiently captured and stored, and the energy required for manufacturing does not matter.

1.   Introduction

Cement concrete is an indispensable construction material for social capital development, but its production uses a large amount of limestone, which is by no means an unlimited natural resource, and emits a large amount of CO_2, which is a global warming substance. It is estimated that Japan's total limestone reserves are roughly 24 gigatons. Assuming that about 60% of the reserves is a recoverable resource, 14 through 15 gigatons of limestone can be utilized in the future. On the other hand, 150 megatons of limestone are consumed annually in Japan, including use in cement production. If this consumption continues, limestone will be depleted in 100 years. To solve these problems fundamentally, C^4S (Calcium Carbonate Circulation System in Construction) moonshot project started in the autumn of 2020 with a 10-year plan with financial support from the Japanese government. In the project, Ca in cement concrete accumulated as construction is regarded as a potential unused resource capable of absorbing CO_2, and the calcium carbonate made from Ca absorbing CO_2 is expected to bind aggregates to create hardened concrete, which can be recycled many times. Technologies are being developed to regenerate cement concrete waste, which is generated by construction demolition, and CO_2 in the atmosphere as calcium carbonate concrete (CCC) which will be put into practical use as a main construction material to replace conventional cement concrete. As a result, a new resource recycling system will be realized.

As shown in Figure 1, the project is developing technology to produce rapidly carbonated CCC raw materials from demolished concrete waste, technology to produce structural CCC using the raw materials, and technology and systems to implement CCC in buildings. Through these series of research and development, most of the CO_2 released by calcination of limestone is recovered and fixed as CCC, and CCC will be recycled as a main construction material many times with low energy. As a result, the environmental impact caused by utilization of cement concrete after the Anthropocene will
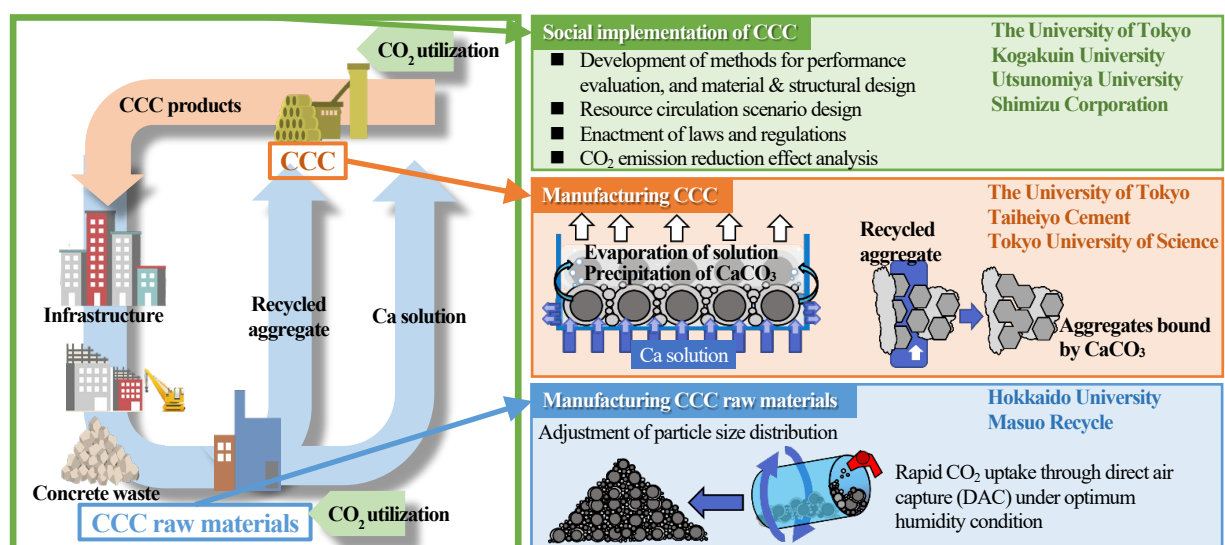

Figure 1: Overview and organization of CCC development

be restored, and the amount of CO_2 generated by the material loop of cement concrete will gradually approach zero. Consequently, it is expected that global warming will be greatly suppressed, and the global environment will be regenerated.

2.   Manufacturing of CCC raw materials

2.1   Production of carbonated raw materials

In general, high humidity conditions (>80% relative humidity) accelerate carbonation of cement paste powder (CPW). On the other hand, carbonation of coarse CPW with a certain particle size (e.g., 0.6 to 1.18 mm), assuming crushed concrete waste from demolition, partially progresses in the initial stage but is suppressed after a few days due to the improved gas barrier properties caused by the formation of calcium carbonate. Therefore, for practical application of CO_2 absorption into concrete waste, it is essential to develop technology for direct air capture (DAC) acceleration into coarse hardened cement paste powder, assuming crushed concrete waste. To improve the gas permeability of concrete waste, basic experiments on DAC acceleration technology are underway, focusing on a wet-heat cycle using natural ventilation. Comparing the RH60% and RH80% constant humidity and RH60-80% cycle conditions shown in Table 1, Figure 2 shows that carbonation of coarse CPW can be accelerated when exposed to RH60-80% cycle humidity, rather than RH60% or RH80% constant humidity conditions. Larger scale studies are currently being conducted to implement these techniques.

Table 1. Experimental conditions

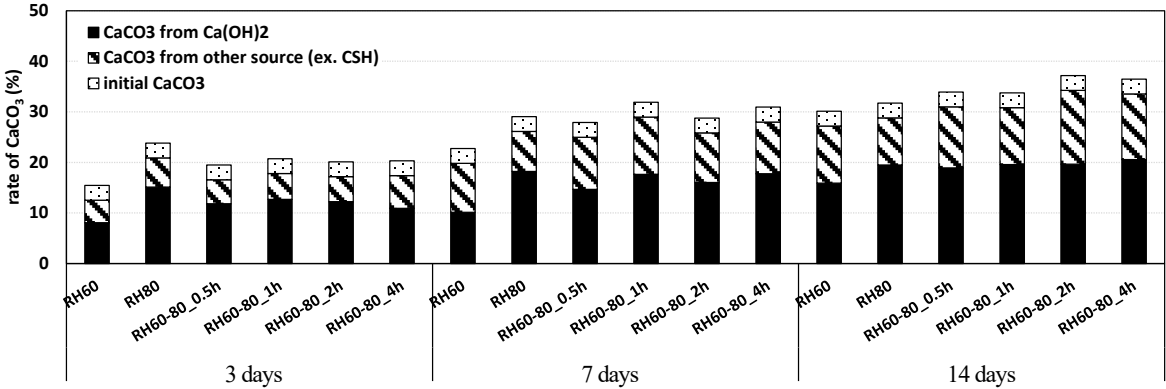| Relative humidity	RH 60%	RH 80%	RH 60-80%
Cycles	-	-	0.5 h, 1 h, 2 h, 4 h
Temperature	20°C		
CO_2 concentration	0.03% (concentration in the atmosphere)		
Particle size of CPW	0.6 - 1.18 mm		
Periods	3 days, 7 days, 14 days		

Figure 2: Calcium carbonate production rate by each source of calcium

2.2   Production of bicarbonate solution

Calcium bicarbonate solution for CCC manufacturing can be produced by blowing carbon dioxide into water in which calcium hydroxide or calcium carbonate has been added. In general, the Ca solubility in calcium bicarbonate solution is highly dependent on temperature [1], and the rate of increase in Ca solubility is affected by the particle size of solid particles containing Ca. Therefore, calcium bicarbonate solutions were produced using carbonated cement paste and carbonated mortar simulating powders and grains obtained from concrete waste, and the changes in Ca^{2+} concentration and pH at 5°C and room temperature (20°C) were measured. In the experiments, ion-exchanged water was placed in a container, cooled to a predetermined temperature, and stirred while CO_2 gas of a predetermined concentration was blown into the container for 18 hours, after which the carbonated cement paste and mortar were added and the changes in Ca^{2+} concentration and pH were measured over time. The results are shown in Figures 3. As expected, Ca solubility was higher at 5°C than at 20°C. The smaller the grain size, the greater the dissolution rate of Ca and the higher the Ca solubility.
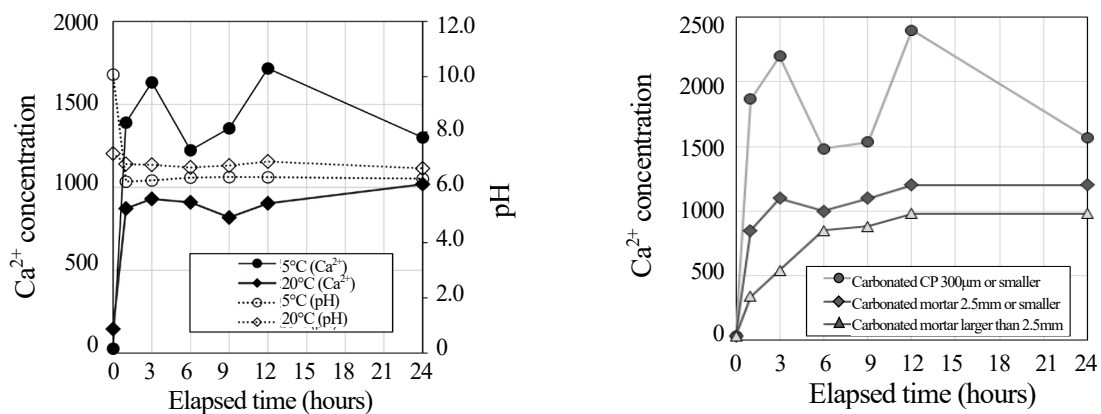
Figure 3: Effects of temperature and particle size on Ca solution

3.   Manufacturing of CCC

3.1   Precipitation method

The carbonated concrete waste particles and the powder portion that remains after the calcium has been extracted are packed into a container, and the calcium bicarbonate solution is poured between the particles/powder and the container is heated. Since the solubility of calcium carbonate decreases with increasing temperature, calcium carbonate precipitates when the container is heated. This precipitation forms a cross-linked structure between the particles/powder, which gives strength to the CCC. When calcium carbonate is precipitated from calcium bicarbonate solution, CO_2 is generated again. To capture and utilize this CO_2 efficiently, it is desirable that some of the filled particles/powders have hydrates with uncarbonated calcium that contribute to further carbonation. Therefore, even if the concrete waste is not fully carbonated, the process of wet carbonation can efficiently carbonate the calcium in the concrete waste. Since the production process currently under development involves heating, the dominant precipitating phase of calcium carbonate is aragonite in needle-like crystals [2],

as shown in Figure 4. This differs from naturally occurring concretions. Previous studies have shown that the precipitation of aragonite is useful in the development of CCC strength [3].

3.2 Pre-loading method

Another method of manufacturing CCC is to apply pre-loading to concrete waste particles packed in a mold. Figure 5 shows an overview of this production method. CCC raw material, carbonated mortar powder of 0.6 mm or less, is mixed with water (10-15% of the powder's mass), packed in a mold, and loaded at 10 MPa. The mold is removed, and the specimen is immersed in a calcium bicarbonate solution with a calcium ion concentration of 0.5 g/L and total carbonate concentration of 1.3 g/L for 2 hours, and then dried for at least 12 hours to form a CCC hardened body. Up to now, compressive strength of up to 56 MPa has been obtained with a specimen of φ10 x 20 mm. It has been confirmed that the addition of magnesium sulfate or seawater during immersion in the calcium bicarbonate solution can further increase the strength of the material. Currently, optimization of the manufacturing process is underway with the aim of increasing the size of CCC hardened specimens.
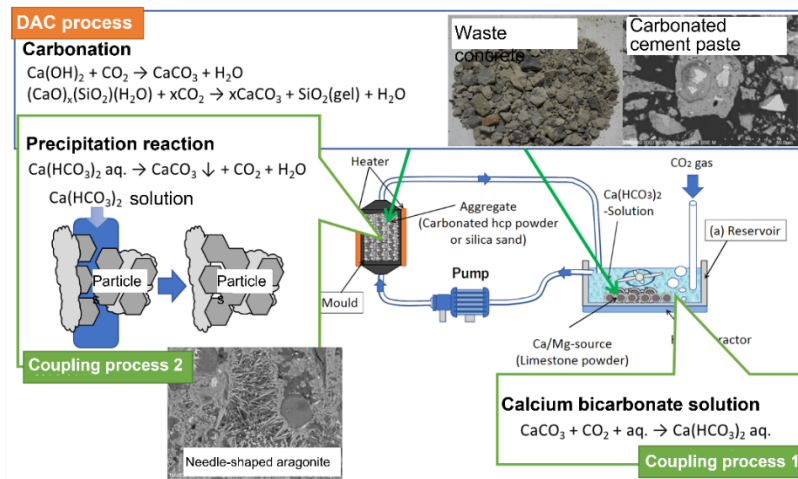

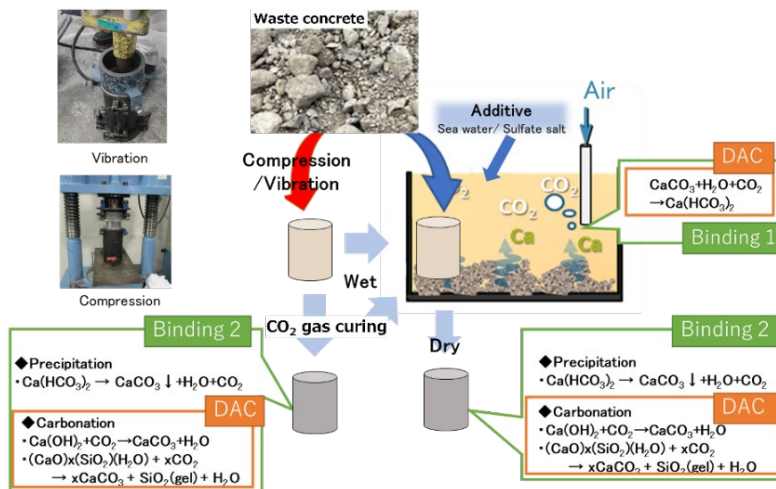Figure 4: Precipitation method for CCC manufacturing

Figure 5: Pre-loading method for CCC manufacturing

4. CCC structural members

A possible structural form of CCC is to manufacture unit members filled with CCC in a thin-walled steel tube and connect them by tensioning materials, as shown in Figure 6. As a fundamental study for the realization of this structural form, compression tests were conducted on simulated members filled with low-strength concrete in thin-walled steel tubes. The relationship between the restrained steel ratio and strength is shown in Figure 7. Even when the strength of concrete was about 5 MPa, the thin-walled steel pipe provided a confining effect, resulting in a strength of 10 MPa or higher, and the relationship between the strength of the member and the restrained steel ratio was linear. Therefore, the strength of CCC member can be estimated from the strength of CCC and the specifications of steel tube for structural design.
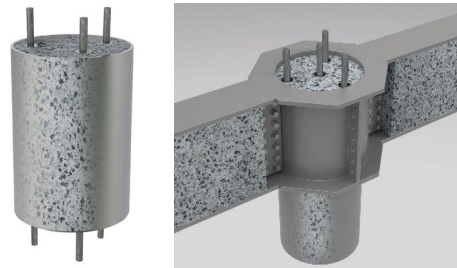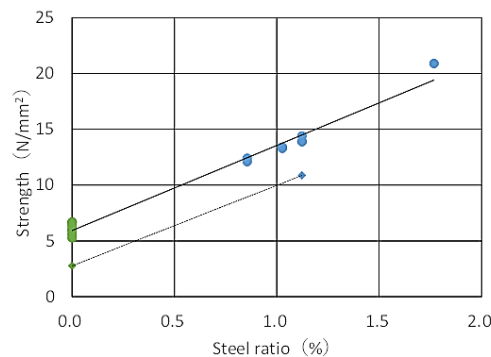
Figure 6: An example of a CCC structural form

Figure 7: Confining effect of steel tube on strength

5. Social implementation of CCC structures

5.1 Resource circulation

To stably manufacture CCC in the future, a stable supply of concrete waste generated by demolition of structures is needed. Therefore, based on various statistical information, the amount of concrete waste generated by building demolition in Japan from 2018 to 2050 was estimated. The results are shown in Figure 8. It is also known that the amount of concrete waste generated from civil engineering structures is about 80% of that from buildings. Taking this into account, the total amount of concrete waste generated in Japan by 2050 is expected to be about 6.9 gigatons, which can be effectively used as raw material for CCC.

If CCC completely replaces conventional cement and concrete in the future, the material flow related to concrete is expected to be as shown in Figure 9. In other words, concrete waste generated every year from the demolition of structures will become a source of CO_2 absorption, and by using all concrete waste as raw materials to produce CCC, 20.4 megatons of CO_2 will be absorbed every year in Japan. And all CO_2 released into the atmosphere to date from calcination of limestone during cement production, i.e., about 2 gigatons in Japan and 55 gigatons worldwide, will be recovered and fixed as CCC. CCC is then recycled repeatedly with energy savings.
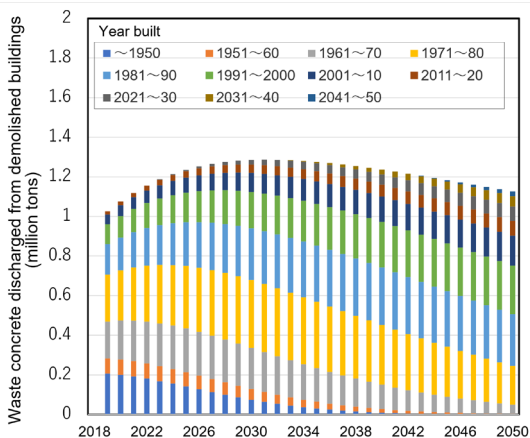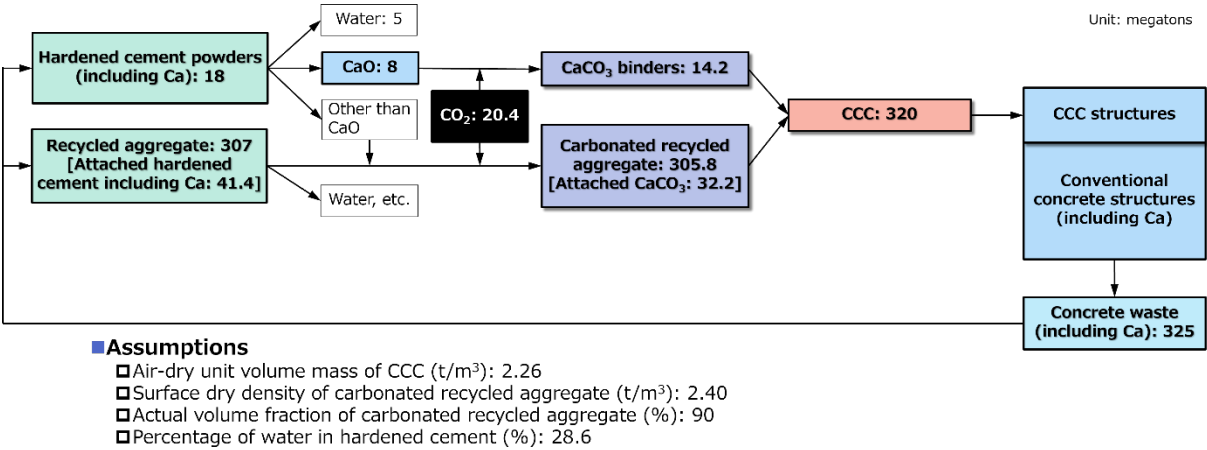

Figure 8: Concrete waste generation

■Assumptions
  ☐Air-dry unit volume mass of CCC (t/m³): 2.26
  ☐Surface dry density of carbonated recycled aggregate (t/m³): 2.40
  ☐Actual volume fraction of carbonated recycled aggregate (%): 90
  ☐Percentage of water in hardened cement (%): 28.6

Figure 9: Concrete related material flow in Japan after replacing with CCC

5.2   CO₂ emission and sequestration

In manufacturing CCC raw materials and CCC, CO_2 is generated in crushing of concrete waste, rapid carbonation by wet and dry cycles, pressure molding, and cooling and heating of calcium bicarbonate solutions. On the other hand, crushed concrete waste sequestrates a large amount of CO_2. Ideally, the sum of these should be carbon negative. The balance of CO_2 emissions and absorption in manufacturing CCC raw materials and CCC at laboratory level to date and in actual plants in the future is shown in Figure 10. In the future, carbon negative CCC can be achieved by increasing the scale of

CCC, improving the efficiency of CCC production, reducing CO_2 emissions using waste heat energy, and increasing the carbonation rate of the CCC raw material.
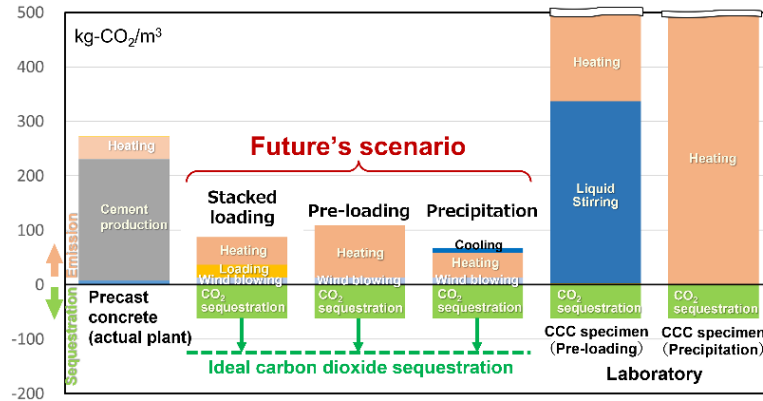

Figure 10: CO_2 emission and sequestration in CCC

6.　Conclusions

Since CCC is a structural material that is completely different from conventional concrete, it is necessary to establish guidelines and standard specifications for CCC manufacturing methods, as well as design, construction, and maintenance methods for CCC structures, to promote CCC widely in the world. Furthermore, if CCC is to be applied to the main structural components of buildings, it will be essential to investigate the legalization of CCC. CCC turns back the clock on the environmental impact caused by cement and concrete since the Anthropocene, and concrete has since been converted to a carbon-neutral construction material. In ancient times, hundreds of millions of years ago, CO_2 was fixed in the process of raising the Himalayas and the Alps, creating a cool earth where living organisms could live. There are great expectations for C^4S project, which is a grand attempt to reproduce this event in modern civilized society and save the earth again.

Acknowledgements

References

[1] Kojima, Y. et al., 'Control of Crystal Shape and Modification of Calcium Carbonate Prepared by Precipitation from Calcium Hydrogencarbonate Solution', *Journal of Ceramic Society of Japan*, 100(1165): 1145-1153, 1992

[2] Tai, C.Y. and Chen, F.B., 'Polymorphism of $CaCO_3$, precipitated in a constant-composition environment', *AIChE Journal*, 44: 1790-1798, 1998

[3] Maryama, I. et al., 'A New Concept of Calcium Carbonate Concrete using Demolished Concrete and CO_2', *Journal of Advanced Concrete Technology*, 19(10): 1052-1060, 2021

THERMALLY REACTIVATED CEMENTS AND THEIR HYDRATION ABILITY

Neshable Noel[1,*], Tommy Mielke[1], Gustave Semugaza[1] and Doru C. Lupascu[1]

(1) Institute for Materials Science and Center for Nanointegration Duisburg-Essen (CENIDE), Faculty of Engineering, University of Duisburg-Essen, Universitätsstraße 15, 45141 Essen – Germany

*neshable.noel@uni-due.de

Abstract

Concerning the role of ordinary Portland cement (OPC) production towards carbon emissions, the cement and concrete sectors are forced to implement eco-efficient solutions. An innovative approach relies on the recycling of cement from waste concrete. Various researchers have made efforts to recover the cementitious part of waste concrete through thermal treatment and thus highlighted the recycling possibility of cement. This research intends to better understand the recovery of the cementitious mineral phases through a thermal treatment approach. Different batches of 28-day-hydrated waste cement paste powders (WCPPs) are prepared using source material, OPC (CEM 1, 52.5R). WCPPs are then thermally treated at temperatures 600°C, 650°C, 700°C, 750°C and 800°C to prepare reactivated cements (RCs). RCs are again re-hydrated for 28 days. Furthermore, RCs and their re-hydration ability are studied using X-ray diffraction (XRD) supported by scanning electron microscopy (SEM). The results show the reformation of calcium silicate clinker phases in the RCs in the tested temperature range which is much lower than the actual sintering temperature of 1450°C used at the industrial scale. The re-hydration of RCs reproduces typical cementitious hydration mineral phases.

Keywords: Carbon Emissions; Waste Concrete; Thermal Reactivation; Recycled Cement; Analytical Techniques

1.   Introduction

Industrially produced ordinary Portland cement (OPC) is a vital building material. It majorly consists of reactive tri-calcium silicate ($C_3S = 3CaO.SiO_2$) and di-calcium silicate ($C_2S = 2CaO.SiO_2$) clinker phases which are responsible for the hydraulic reactions and thus the development of mechanical properties [1, 2]. The main step in the formation of these calcium silicate phases is the decarbonation of the primary raw material, limestone ($CaCO_3$). Only this step is responsible for almost 60% of total carbon emissions related to cement production. As a result, cement production contributes about 5-8% of global CO_2 emissions [3, 4]. Therefore, researchers and the cement and concrete sectors are forced to introduce sustainable and eco-friendly solutions [5]. One of the eco-friendly solutions is concrete recycling. This technique

has been investigated for many years but the main idea was to use the waste or old concrete as a replacement for natural aggregates [6] or the waste concrete fines as a filler for partial cement replacement [7]. Recently, several researchers have made efforts to recover the cementitious part of the waste concrete through thermal treatment at the laboratory scale. They subjected hydrated cement paste (HCP) to different temperature steps and have seen the inversion phenomenon of cement hydration which leads to the reformation of anhydrous compounds with similar physiochemical characteristics as the original clinker phases [8–10]. Thus, they have highlighted the recycling possibility of cement.

Hydrated cement paste (HCP) mainly consists of hydration products such as ettringite (Aft = $3CaO \cdot Al_2O_3 \cdot 3CaSO_4 \cdot 32H_2O$), portlandite (CH = Ca $(OH)_2$), calcium silicate hydrates (CSH = $CaO.SiO_2.H_2O$), and calcite (CC = $CaCO_3$). These hydration products start to decompose when HCP is exposed to elevated temperatures. It has been reported in various works that the decomposition range of ettringite (AFt) is 80°C - 120°C. Portlandite (CH) decomposes between 450°C – 550°C and the calcium silicate hydrates (CSH) decompose or depolymerized in the temperature range of 120°C to 450°C. In the end, calcite decomposes at 600°C to 900°C, to free lime (C = CaO) in the system liberating CO_2 [5, 8, 10]. The decomposition or in other words the de-polymerization of calcium silicate hydrates (CSH) is very important in the whole dehydration process as its onset promotes the formation of new nesosilicates with similar stoichiometry as dicalcium silicate phase (C_2S) [5]. According to Real et. al [8] and Serpell et. al [11], there is a direct de-polymerization of calcium silicate hydrates (CSH) into the alpha$^/$ polymorphic form ($\alpha^/$- C_2S) of the dicalcium silicate mineral. The $\alpha^/$-C_2S can be characterized as alpha-low dicalcium silicate ($\alpha_L^/$-C_2S) or alpha-high dicalcium silicate ($\alpha_H^/$-C_2S) depending upon the phase transition temperature of dicalcium silicate [2]. In case of thermally treated recycled cements, such $\alpha^/$-C_2S polymorphs form at a lower temperature range of 600°C – 800°C and represent higher reactivity because of their higher surface area and lower crystallite sizes. Above 800°C, the $\alpha^/$-C_2S polymorphs start to transform into the beta polymorphic form (β-C_2S) of dicalcium silicate which is known as a less reactive product [8, 11]. Due to the high reactivity of $\alpha^/$-C_2S in the 600°C – 800°C, various authors have linked the better physical performance of recycled cement to this polymorphic form [4, 10–12].

This paper aims to contribute to a better understanding of the chemical transformations during the laboratory-scale preparation of thermally reactivated cements and their re-hydration. Various authors [4, 5, 8] agree on the optimum temperature range. Thus, the reactivated cements are prepared at 600°C, 650°C, 700°C, 750°C and 800°C. Furthermore, the phase transformations of these reactivated cements and their re-hydration ability are studied using X-ray diffraction (XRD) supported by scanning electron microscopy (SEM).

2. Materials and characterization

2.1 Preparation of reactivated cements (RCs) and re-hydrated cement pastes (RCPs)

Ordinary Portland cement (OPC) type CEM I 52.5R from Wittekind (Hugo Miebach Söhne KG) was used as source material. The OPC was mixed with water (water-to-cement ratio = 0.5) for 4 minutes as per EN DIN 196-1 to produce hydrated cement paste (HCP) specimens. These specimens were stored for 1 day at laboratory conditions (20 ± 5°C & 60 ± 5% relative humidity) and cured underwater (100% relative humidity) for 27 days. After a total of 28 days of hydration, the specimens were firstly crushed using a jaw crusher and then grounded to

powder in a disc mill for 1 minute. Afterwards, the milled powder was sieved to a particle size < 250µm. Different batches of milled powders (< 250µm) were prepared and labelled as waste cement paste powders (WCPPs). The thermal reactivation of WCPPs was carried out in a muffle furnace (Nabertherm AG, Germany) by heating at 5°C/min up to the desired treatment temperature. Different temperature steps: 600°C, 650°C, 700°C, 750°C and 800°C were selected. A constant holding time of 1 hour for every treatment temperature was maintained. The powders treated at the corresponding reactivation temperatures were allowed to cool down to room temperature inside the furnace. The dehydrated powders thus obtained were called reactivated cements (RCs) and labelled as RC 600°C to RC 800°C referring to the reactivation temperatures. The entire process for the laboratory scale preparation of RCs is represented in Figure 1.
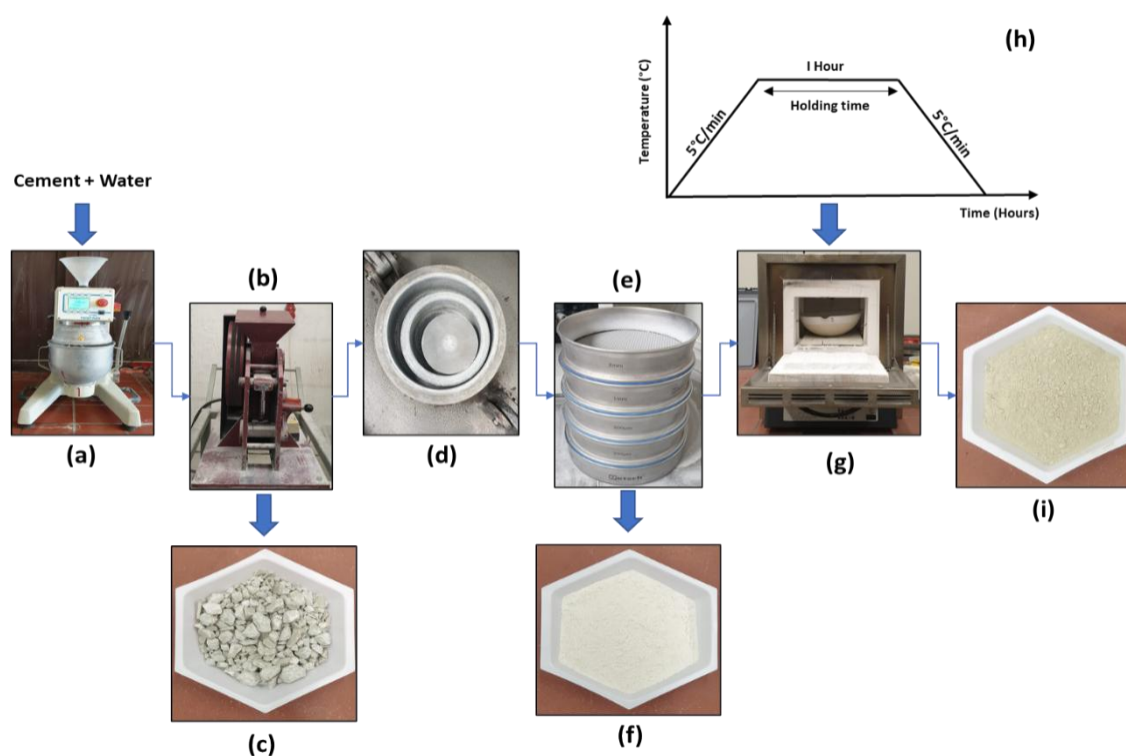

Figure 1: Process for reactivated cements (RCs) preparation: (a) Mixing; (b) Crushing; (c) Material after crushing; (d) Milling; (e) Sieving; (f) Waste cement paste powder (WCPP); (g) Furnace heating; (h) Heating regime; (i) Reactivated cement (RC 800°C)

Thermally produced reactivated cements are known for their higher reactivity and water demand [8]. Therefore, to ensure maximum workability, a water-to-cement ratio of 0.75 was chosen for all RCs 600°C – 800°C. RCs were mixed with water for the standard 4 minutes of mixing (EN DIN 196-1) and the re-hydrated cement paste (RCP) specimens were produced. The RCP specimens were cured for 1 day at laboratory conditions (20 ± 5°C & 60 ± 5% relative humidity) and a further 27 days underwater (100% relative humidity). After 28 days of total hydration, the RCP specimens were named RCP 600°C to RCP 800°C. To compare the hydration ability of the RCs to OPC, a reference 28 days hydrated cement paste (HCP-0.75) was also produced at a similar water-to-cement ratio, mixing, and curing procedures as RCPs.

2.2   X-ray diffraction (XRD) and scanning electron microscopy (SEM) analysis

- **Characterization of OPC and RCs**

The mineral phases in OPC and the RCs were analyzed qualitatively using an Empyrean powder diffractometer (Panalytical) with CuK_a radiation source. Powder samples of OPC and RCs (<250μm) were scanned in the 2θ range of 5°- 90° with a step size of 0.013° and scanning speed of 0.018°/s.

- **Characterization of HCP-0.75 and RCPs**

Before characterizing (HCP – 0.75) and RCPs, the hydration phenomenon was stopped after 28 days of hydration using the solvent exchange method [13]. The hardened paste specimens of size 1 – 2 cm were immersed in isopropanol for 24 hours to remove the free water followed by 24 hours of oven drying at 40°C. After that, the specimens of HCP-0.75 and RCPs were stored in a desiccator under a vacuum (200 mbar) until studied. For XRD analysis, the specimens were gently grounded to a powder (< 250 μm) using a mortar and pestle. For SEM analysis, the hardened specimens (1-2 cm in size) were made surface conductive by being coated with gold-palladium alloy (Au80Pd20) using a sputtering device (Sputter Coater Cressing-ton MTM 10) before the morphological studies.

3. Results and discussion

3.1 Characterization of the RCs

Figure 2 represents the qualitative XRD analysis of OPC, WCPP, and RCs 600°C – 800°C. The diffraction pattern of OPC (Figure 2a) indicates the presence of traditional clinker phases: tri-calcium silicate ($C_3S = 3CaO.SiO_2$), dicalcium silicate ($\beta\text{-}C_2S = 2CaO.SiO_2$), aluminate ($C_3A = 3CaO.Al_2O_3$), brownmillerite ($C_2AF = 2CaO.Al_2O_3.Fe_2O_3$) and gypsum ($C\bar{S} = CaSO_4$) [1]. The diffractogram of WCPP (Figure 2b) indicates the presence of hydration mineral phases: ettringite (Aft), portlandite (CH), calcite (CC), and calcium silicate hydrates (CSH).

For RC 600°C (Figure 2c) the presence of an intense peak of portlandite (CH) roughly at an angle of 18.06° can be observed. The dehydroxylation of portlandite ($Ca(OH)_2 \rightarrow CaO + CO_2$) would be expected to occur below 600°C but the presence of portlandite highlights its re-crystallization ability while cooling down the heated powders to room temperature in the furnace and such behavior has also been reported by other authors [5, 11]. The peak intensity of portlandite almost disappeared for RC 800°C (Figure 2g), indicating its complete decomposition into free lime (C) [8]. Similarly, the calcite (CC) peak that appeared at a diffraction angle of 29.38° is more intense for RC 600°C (Figure 2c) but it becomes less intense with increasing temperature and completely varnishes for RC 800°C. This supports the decarbonation of calcite ($CaCO_3 \rightarrow CaO + CO_2$) and thus RC 800°C (Figure 2g) contains sharp peaks of free lime (CaO) at angles 2θ = 37.33°C and 53.84° approximately [10, 11]. In the case of RCs 600°C – 800°C, the hump region between angle 2θ = 32°- 34° is interesting to study as the formation and phase transition of calcium silicate mineral phases can be observed in this region. For all RCs, the peak position at angle 33.18° matches with the diffraction pattern of the high-temperature polymorphic form of di-calcium silicate: alpha low dicalcium silicate ($\alpha_L'\text{-}C_2S$). The formation of this reactive polymorph is related to the de-polymerization of calcium silicate hydrates (CSH) and is in line with the literature [8, 11]. For RC 600°C (Figure 2c), $\alpha_L'\text{-}C_2S$ represents the less intense peak and this peak becomes highly intensive and well-defined in the case of RC 750°C (Figure 2f) indicating its higher crystallinity level.

This shows the dominance of α'_L-C$_2$S in the temperature range between 600°C – 750°C in the RCs system.
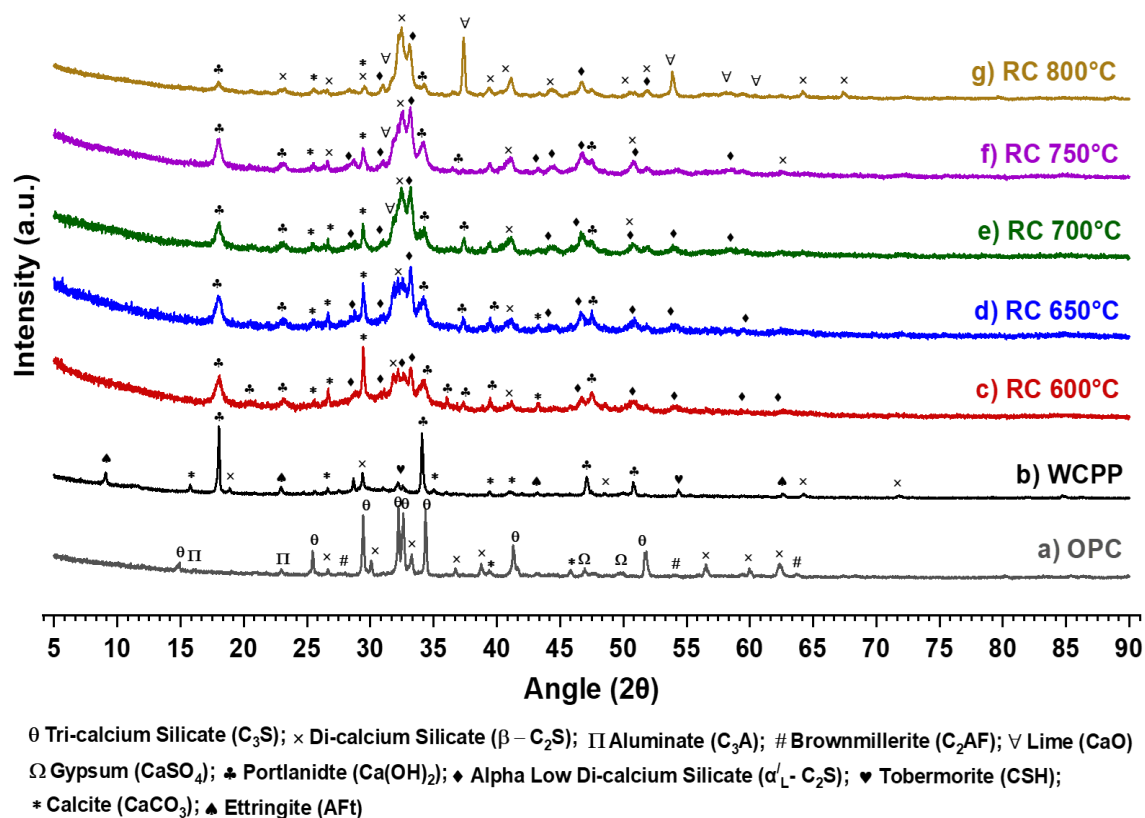

Figure 2: Qualitative XRD analysis of OPC and RCs 600°C – 800°C

Parallelly, the presence of beta-dicalcium silicate (β-C$_2$S) polymorphic form is also identified at an angle roughly 32.45° for RCs 600°C – 800°C and its peak intensity also increases with increasing temperature but still, it is less intense than the α'_L-C$_2$S up to RC 750°C (Figure 2f). In the case of RC 800°C (figure 2g), the peak intensity and thus the crystallinity of β-C$_2$S is higher than α'_L-C$_2$S and represents the dominance of the poorly reactive polymorph for RC 800°C. This phenomenon is related to the transformation of highly reactive α'_L-C$_2$S into less reactive β-C$_2$S above 750°C [8, 11].

3.2 Characterization of the RCPs

Figure 3 represents the XRD analysis for the hydrated cement paste (HCP-0.75) and re-hydrated cement pastes (RCPs 600°C – 800°C) after 28 days of hydration. By comparing the diffractogram of RCPs (Figure 3 b-f) with HCP (Figure 3a), it can be noticed that the RCPs consist of similar hydration products as HCP-0.75 [4, 8]. The reformation of the hydration products such as ettringite (Aft), portlandite (CH), and calcium silicate hydrates (CSH) can be confirmed roughly at diffraction angles 9.05°, 18.01°, and 49.45°, respectively. The reformation of cementitious hydration mineral phases highlights the re-hydration capability of thermally reactivated cements. Furthermore, as discussed in section 3.1, the reactivated cements (RCs) consist of two polymorphic forms of di-calcium silicate: α'_L-C$_2$S and β-C$_2$S. Only the less reactive polymorph β-C$_2$S is still present in RCPs. It can be estimated that the

$\alpha_L^/$-C$_2$S polymorph has almost completely reacted with water due to its higher surface area and smaller crystalline size, providing portlandite (CH) and calcium silicate hydrates (CSH) to the system [8, 11]. Therefore, the performance of reactivated cements (RCs) is largely related to this reactive mineral phase [5, 8].

♣ Portlanidte (Ca(OH)$_2$); ♥ Tobermorite (CSH); ▲ Ettringite (AFt); × Di-calcium silicate ($\beta - C_2S$); ✳ Calcite (CaCO$_3$); ∀ Hemicarbonate (AFm)
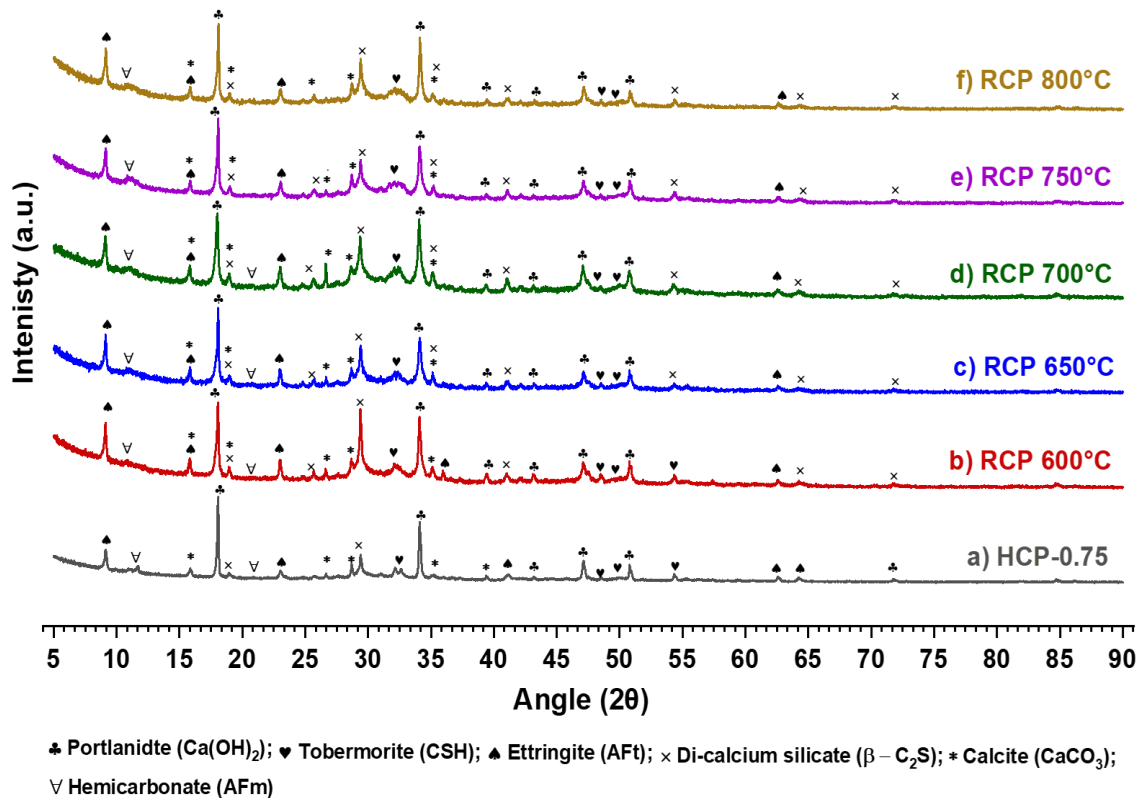
Figure 3: Qualitative XRD analysis of HCP-0.75 and RCPs 600°C – 800°C

Figure 4 shows the SEM analysis for the HCP-0.75 and RCPs 600°C – 800°C. The presence of typical mineral phase-containing structures: needle-like ettringite (AFt), plate-like portlandite (CH), and gel-like calcium silicate hydrates (CSH) can be seen for HCP-0.75 (Figure 4a). In the case of RCP 600°C, the prominent dominance of needle-like ettringite can be seen (Figure 4b). These structures become short-length ordered and reduced in quantity with increasing treatment temperatures (Figure 4c-f) [4, 8]. But, in general, the SEM images for re-hydrated cement pastes (RCPs) confirm the reformation of similar hydration products as hydrated cement paste (HCP-0.75).

Figure 4: SEM Images – (a) HCP-0.75; (b) RCP 600°C; (c) RCP 650°C; (d) RCP 700°C; (e) RCP 750°C; (f) RCP 800°C

4. Conclusion

The research study aimed to investigate the chemical transformations during the preparation of thermally reactivated cements (RCs) and their re-hydration phenomena using analytical methods: X-ray diffraction (XRD) and scanning electron microscopy (SEM). The min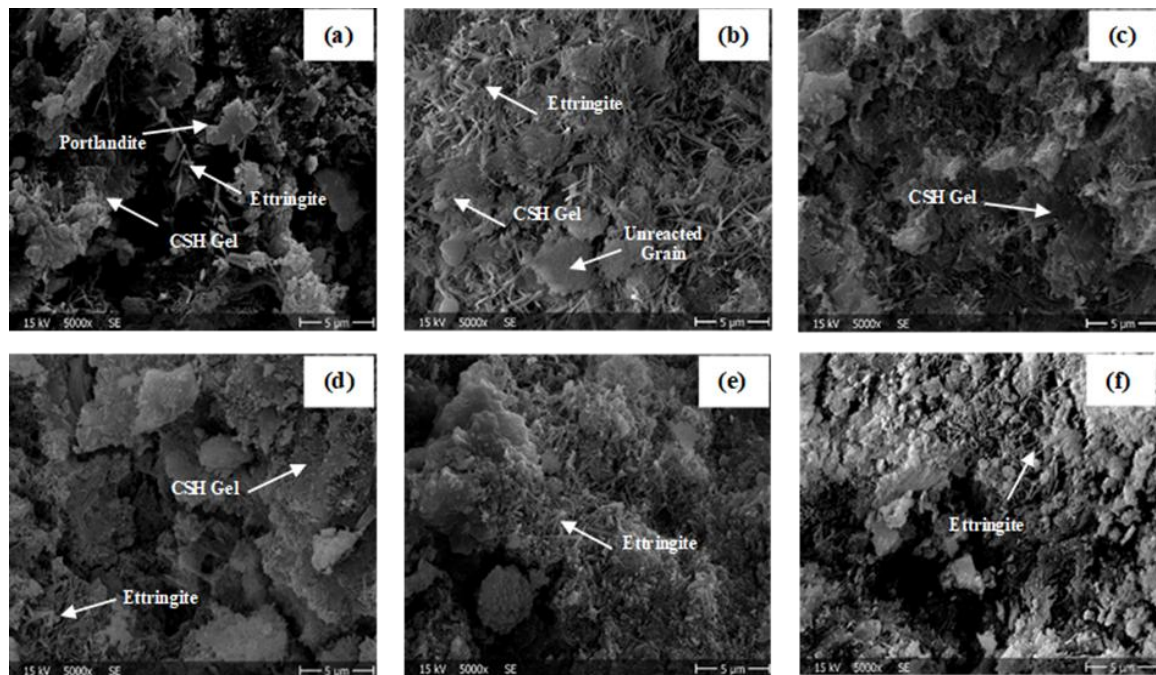eral phase development in RCs was compared with the reference OPC (CEM I, 52.5R). Similarly, the re-hydration capability of the RCs was compared with hydrated cement paste (HCP-0.75). From the results, the following conclusions can be drawn:

- The XRD qualitative analysis shows that the OPC mainly consisted of tri-calcium silicate (C_3S) and di-calcium silicate (C_2S) mineral phases. In the case of reactivated cements (RCs), only the di-calcium silicate mineral phase is present in two polymorphic forms: highly reactive alpha-low dicalcium silicate (α_L'-C_2S) and less reactive beta-dicalcium silicate (β-C_2S). The reactive α_L'-C_2S form dominates up to RC 750°C and the dominance of β-C_2S is observed in the case of RC 800°C. Also, at RC 800°C, the intensive lime (C) was generated mainly by the complete decomposition of portlandite (CH) and calcite (CC), thus releasing bound CO_2 into the atmosphere. This phenomenon is unfavorable as it contributes negatively to the CO_2 emission control concept. Therefore, according to this study, the optimum temperature range for reactivated cements (RCs) is between 600°C – 750°C which is half of the sintering temperature of 1450°C required for cement production at an industrial scale.

- The XRD qualitative analysis of re-hydrated cement pastes (RCPs) supports the reformation of similar hydration products as hydrated cement paste (HCP-0.75) for 28 days of the hydration period. The SEM images of RCPs again confirm the rehydration ability of RCs and represent the development of the same hydrated mineral structure as HCP-0.75.

References

[1] M. Liska, F. M. Lea, and P. C. Hewlett, Lea's Chemistry of Cement and Concrete, 5th ed.: Butterworth-Heinemann, 2019.

[2] H. F. W. Taylor, Cement chemistry, 2nd ed. London: Telford, 2004.

[3] Z. He, X. Zhu, J. Wang, M. Mu, and Y. Wang, "Comparison of CO_2 emissions from OPC and recycled cement production," Construction and Building Materials, vol. 211, pp. 965–973, 2019, doi: 10.1016/j.conbuildmat.2019.03.289.

[4] G. Semugaza, T. Mielke, M. E. Castillo, A. Z. Gierth, J. X. Tam, S. Nawrath, and Doru C. Lupascu, "Reactivation of hydrated cement powder by thermal treatment for partial replacement of ordinary portland cement," Mater Struct, vol. 56, no. 3, 2023, doi: 10.1617/s11527-023-02133-9.

[5] J. A. Bogas, A. Carriço, and S. Real, Sustainability of Concrete with Synthetic and Recycled Aggregates: Thermoactivated Recycled Cement, May 4th, 2022.

[6] I. Nováková, and K. Mikulica, "Properties of Concrete with Partial Replacement of Natural Aggregate by Recycled Concrete Aggregates from Precast Production," Procedia Engineering, vol. 151, pp. 360–367, 2016, doi: 10.1016/j.proeng.2016.07.387.

[7] A. Bordy, A. Younsi, S. Aggoun, and B. Fiorio, "Cement substitution by a recycled cement paste fine: Role of the residual anhydrous clinker," Construction and Building Materials, vol. 132, pp. 1–8, 2017, doi: 10.1016/j.conbuildmat.2016.11.080.

[8] S. Real, A. Carriço, J. A. Bogas, and M. Guedes, "Influence of the Treatment Temperature on the Microstructure and Hydration Behavior of Thermoactivated Recycled Cement," Materials (Basel, Switzerland), vol. 13, no. 18, 2020, doi: 10.3390/ma13183937.

[9] Z. Shui, D. Xuan, W. Chen, R. Yu, and R. Zhang, "Cementitious characteristics of hydrated cement paste subjected to various dehydration temperatures," Construction and Building Materials, vol. 23, no. 1, pp. 531–537, 2009, doi: 10.1016/j.conbuildmat.2007.10.016.

[10] C. Alonso, and L. Fernandez, "Dehydration and rehydration processes of cement paste exposed to high temperature environments," Journal of Materials Science, vol. 39, no. 9, pp. 3015–3024, 2004, doi: 10.1023/B: JMSC.0000025827.65956.18.

[11] R. Serpell, and M. Lopez, "Properties of mortars produced with reactivated cementitious materials," Cement and Concrete Composites, vol. 64, pp. 16–26, 2015, doi: 10.1016/j.cemconcomp.2015.08.003.

[12] M. Vyšvařil, P. Bayer, M. Chromá, and P. Rovnaníková, "Physico-mechanical and microstructural properties of rehydrated blended cement pastes," Construction and Building Materials, vol. 54, pp. 413–420, 2014, doi: 10.1016/j.conbuildmat.2013.12.021.

[13] K. Scrivener, R. Snellings, and B. Lothenbach, A Practical Guide to Microstructural Analysis of Cementitious Materials: CRC Press, 2018.

SODIUM SILICATE FROM WASTE GLASS CULLET AS AN ACTIVATOR FOR CEMENT-LESS CONCRETE

Daniel W. McCloskey[1], *, Marios. Soutsos[1]

(1) School of Natural & Built Environment, Queen's University Belfast, Northern Ireland

* Corresponding author - dmccloskey12@qub.ac.uk

Abstract

Waste glass is a significant problem with almost 200,000 tonnes of glass from construction sites in the UK alone sent to landfill in 2018. Furthermore, proper recycling of all building glass waste could avoid 925,000 tonnes of landfilled waste every year and save around 1.23 million tonnes of primary raw materials annually. This study was undertaken to find an alternative use of waste glass cullet as an activator for alkali activated materials. Not only will this make use of waste glass otherwise destined for landfill, but alkali activated materials have shown a possible reduction of 30% - 80% of global warming compared to Portland cement concrete. The study used a mixture of waste domestic glass and flat glass from a local refuse collector. The waste glass was milled to a powder and combined with sodium hydroxide to form a crude glass-derived sodium silicate activator. This activator was successfully used for the activation of blended precursors containing Ground Granulated Blast Furnace Slag (GGBS) and Fly Ash (FA) that performed similarly in terms of compressive strength to the same precursors activated with commercial activators. Furthermore, the activator was used for the casting of normal density concrete building blocks that reached an impressive strength of 15.6 MPa.

1.   Introduction

Within the first 3 months of 2023, over 500 million tonnes of solid waste has been generated [1]. Globally the construction and demolition industry is the largest contributor of solid wastes, accounting for 36% [2]. Within the construction industry, waste glass is a significant issue with almost 200,000 tonnes of glass from construction sites in the UK alone sent to landfill in 2018 [3]. Furthermore, proper recycling of all building glass waste could avoid 925,000 tonnes of landfilled waste every year and save around 1.23 million tonnes of primary raw materials annually [4]. This high amount of unrecycled glass within the UK is due to the significant imbalance in the amount of green glass collected for recycling and the amount used in container manufacture. UK container glass production focuses on clear glass and currently, a significant amount of green cullet is used in secondary applications such as aggregates or is disposed to landfill due to a low demand for manufacturing green glass bottles.

Not only is the construction industry the largest contributor of solid waste but the production of Portland cement (PC) contributes to between 6% - 8% of CO_2 emissions on a global scale [5]. The amount of CO_2 released is mainly due to the calcination of calcium carbonate ($CaCO_3$) which is used to form calcium oxide (CaO) whilst releasing CO_2 and also indirectly through the energy required to heat the kilns to between 1400°C – 1450°C for the calcination process [5].

Alkali activated materials (AAMs) are emerging as a promising alternative to PC because they have the potential to consume considerable amounts of waste materials and significantly reduce the carbon footprint of the concrete industry [5]. AAMs are usually derived from the reaction between a chemical activator, typically sodium silicate and sodium hydroxide [5, 6], and an aluminosilicate based precursor material which is typically waste derived. Geopolymer is a sub group of AAMs and is defined as aluminosilicate polymers which consist of amorphous and three dimensional structures formed from the geopolymerisation of aluminosilicate monomers in alkaline solutions [7].

However, there are drawbacks with AAMs and these drawbacks are associated with the reliance on chemical activators that are normally used in the chemical industry, therefore the cost of AAMs can be more than 15% compared PC based binders. Furthermore, the production of activators such as sodium silicate are energy intensive. With the most widely used method being direct fusion which requires the melting of soda ash (Na_2CO_3) and a source of silica, typically quartz sand (SiO_2) above 1100-1200 °C in a suitable oil, gas or electrically fired furnace [8]. This process is not overly different to the calcination of calcium carbonate for the production of Portland cement and therefore current research has begun to look into the synthesis of sodium silicate from silica rich waste streams for the use in AAMs.

This study was undertaken to find an alternative use of waste domestic glass and flat glass by synthesising an activator at much lower temperatures, i.e. 160 °C instead of > 1100 °C which can be used for the activation of AAMs. This activator was then used for the activation of blended mixes containing GGBS and FA for the use in building mortars and normal density concrete building blocks.

2.   Experimental Programme

The materials used for the research will firstly be described, followed by the methodology used for the synthesis of the sodium silicate from waste glass and the mix proportions used for the casting of mortar specimens and concrete building blocks. Mixing and sample preparation will then be described, followed by the presentation of testing procedures.

2.1 Materials

Glass cullet was supplied by a local recycler in Northern Ireland, which contained a mixture of different coloured bottle glass and plate glass from car windscreens and windows. The glass cullet was milled to a powder with a mean particle size (D50) < 32 µm using a Retsch planetary ball mill PM400. The chemical composition of the glass powder was analysed through X-Ray fluorescence (XRF) and is shown in Table 1. Commercial grade sodium hydroxide (Atznatron caustic soda from AkzoNobel, Germany) in microprills with a purity greater than 99% was used for the reaction with the glass powder. For control samples a commercially available sodium hydroxide solution (30% by mass) supplied by William Clements Chemicals Ltd and a commercially available sodium silicate solution, Betol 52 T (produced by Woellner Group, with the composition: 15% Na_2O, 30% SiO_2) were used.

FA conforming to BS EN 450–1:2012 was supplied by Kilroot power station, Northern Ireland. Kilroot powder station is a coal fired power station, with significant production of fly ash. In addition significant amounts of FA are stored within a lagoon and research has begun in order to extract, process and use lagoon ash [9]. The GGBS conformed to BS EN 15167-1:2006 and was supplied by ECOCEM, Ireland. The major oxides for each of the precursor materials were determined through XRF and are shown in Table 1 below. The fine aggregate used for the mortar mixes was a siliceous lake sand with abundance in quartz, sourced locally in Northern Ireland. It had an oven dried particle density of 2700 kg/m^3 and water absorption of 0.9 % at 24-hours. Both density and water absorption were determined according to BS 812-2:1995. The aggregates used for the normal density concrete building blocks were supplied by T&J recycling in Dungannon and consisted of 10mm round stone, crushed quarry dust and quartz sands.

Table 1: Oxide compositions and loss on ignition (LOI) of glass, fly ash FA and GGBS

Oxide	SiO_2	TiO_2	Al_2O_3	Fe_2O_3	MnO	MgO	CaO	Na_2O	K_2O	SO_3	LOI
Glass	69.9	0.087	1.37	0.61	0.042	3.33	9.5	13.2	0.44	0.148	1.34
FA	46.78	1.05	22.52	9.15	0.05	1.33	2.24	0.89	4.09	0.9	3.57
GGBS	29.38	1.05	11.23	0.36	0.51	6.94	43.72	1.05	0.93	1.76	2.4

2.2 Synthesis of Sodium Silicate

For the synthesis of sodium silicate the waste glass cullet was ground to a fine powder and then mixed with sodium hydroxide and only sufficient water to form a paste, following the process proposed by R. Vinai [10]. A ratio of 11 parts glass, 10 parts sodium hydroxide and 3 parts water were used to form the paste. This allowed for the creation of a Sodium Metasilicate where the ratio of Na_2O and SiO_2 was 1 and therefore there was no need for extra sodium hydroxide to be added during the mixing stage to reach satisfactory compressive strengths. The glass/sodium hydroxide paste was prepared in batches of approximately 400 g and placed within an electric muffle furnace (Nabertherm LT 15/13/P330) for 2 hours at 160 °C. Following heating the resulting material was ground to a powder using a mortar and pedestal and the resulting powder became the glass-derived sodium silicate that could then be used as an activator for cement free building products.

2.3 Mix Proportions

The mix design was carried out following the guidelines presented by A. Rafeet [11] and for the mortar mixes the paste percentage was kept constant at 50 % for comparison purposes. Two different mortar mixes were investigated, firstly a geopolymer with a precursor consisting of 100 % FA and an alkali activated blend consisting of 70 % GGGBS + 30 % FA. These mixes are represented by C100, M100 and C70, M70 respectively. Where the "C" represents the control mix created with commercially available sodium silicate and sodium hydroxide and M represents the mixes with the glass-derived activator. The concrete mixes for the alkali-activated blocks are shown as "AAB1" and "AAB2". AAB1 contained a mixture of 70% GGBS and 30% FA while AAB2 contained a mixture of 50% GGBS and 50% FA. The glass-derived sodium silicate activator was used to activate all the mixes and therefore the alkali modulus (Na_2O/SiO_2) was constant at 1.0 while the alkali dosage (M+) varied from 7.5 for the blended mortar mix (M70) and 10 for the 100% FA mix (M100). Both AAB1 and AAB2 had an alkali dosage (M+) of 9.0. The water to solid ratio was 0.39 and 0.44 for the 100% FA mix (M100) and the blended mix (M70) respectively while the water to solid ratio of the blocks was constant at 0.40.

2.4 Procedure for mixing, casting and curing

Mortar samples were prepared using a 10 L capacity planar-action high shear mixer. While the concrete mixes for the normal density building blocks were prepared using a 25 L capacity forced action pan mixer. For mortar samples, the aggregates and precursors were placed in the bowl and mixed by hand, the activator and water were then added. The mortar was mixed for 2 minutes at slow speed, 2 minutes at high speed and finally 1 minute at slow speed. For concrete samples, the aggregates and half the water were added and allowed to mix for 1 minute. The precursors were then added and mixed for 3 minutes subsequently the activator was added and allowed to mix for 1 minute. Finally, the remaining water was added and mixing continued for 4 minutes. The workability for the mortar mixes was tested by measuring the jolted spread in accordance with ASTM C 1437: 2020.

Following mixing, the mortar samples were cast in two layers into 50 mm three-gang plastic moulds and compacted using a vibrating table. The samples were wrapped in plastic wrap and placed into the appropriate curing conditions, where the 100 % FA samples were oven cured for 24 hours at 70 °C and then stored in the constant temperature room at Queen's University Belfast (QUB) where the temperature remained at 20 °C ± 1 °C with a relative humidity greater than 90 %. While the blended mixes were stored in the constant temperature room following casting and until compressive strength testing.

Following concrete mixing, a "squeeze" test was carried out to check the workability, then 10 kg of fresh concrete was placed into steel moulds and compacted to a height of 220 mm (half the height of commercial blocks) using a vibro-compaction rig, which was used to simulate the compaction used during the casting of normal density blocks in the factory. The steel moulds were then placed within the constant temperature room at QUB until the relevant testing age was reached. Both mortar and concrete samples were demoulded after 24 hours and returned to the constant temperature room.

2.5 Testing procedure

Compressive strength testing of the mortar cubes was carried out at 1, 7 and 28-days and was determined by crushing three 50×50×50 mm cubes each time at a constant loading rate of 0.83 kN/sec and determining the average.

Compressive strength testing of the normal density concrete building blocks was carried out at 7, and 28-days. The average compressive strength was determined by testing at least six samples (using a continuous loading rate of 50 kN/min). The loading surfaces were protected with soft board to reduce the effect of unevenness.

3. Results and Discussion

3.1 Compressive strength of mortar samples

Two mixes were investigated to determine if the glass-derived activator could be successfully used for the activation of a geopolymer containing 100% FA see Figure 1(a) and for the activation of a blended GGBS/FA mix see Figure 1(b). The compressive strength results of both mixes are shown in Figure 1 below.
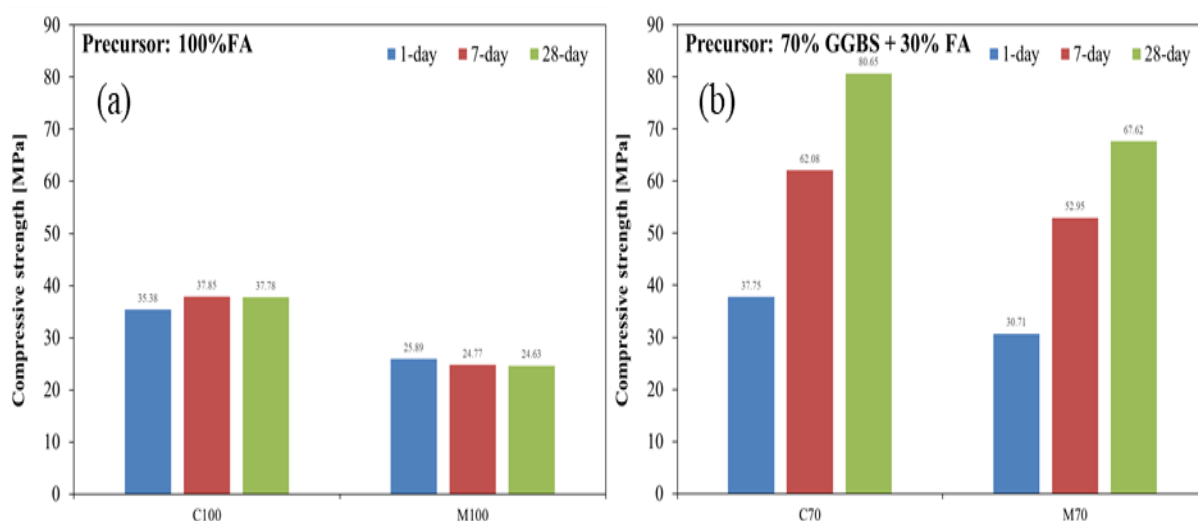

Figure 1: Compressive strength results of mortar specimens (a) containing 100% FA (b) containing 70% GGBS and 30% FA.

From Figure 1 it is clear that the glass-derived activator can successfully be used for the activation of both 100% FA and a blended mix containing 70% GGBS + 30% FA. While there is a negligible difference of only 10% between C70 and M70, there was, however, a 35% reduction in the compressive strength between C100 and M100.

3.2 Normal density concrete building blocks

Laboratory mixes were carried out prior to the factory trials. Several mixes were carried out to achieve the desired workability and surface finish on the cast blocks, and these resulted in the initial mix "AAB1". The average compressive strength at 7 days was determined to be 15.8 MPa. This mix was then optimised to find a balance between compressive strength and cost, which resulted in mix "AAB2" which had an average compressive strength at 7 days of 11.5 MPa whilst providing a saving of 8%. Mix AAB2 was then selected for upscaling in the T&J factory in Dungannon. The main facilities utilised for the trials were the mixing tower, the block machine loader and the block compacting machine.

The concrete was batched in volumes of 1 m^3 which allowed for approximately 110 full sized building blocks (440 x 220 x 100 mm) to be cast per batch. The precursor materials and glass-derived activator were weighted and batched in buckets and carried to the mixing tower while the aggregates and water were pre-stored in silos and added by the automatic system within the mixing tower. The aggregates were pre-wet and mixed together before the precursor materials, activator powder and remaining water were added. The process followed for the factory trial is shown in Figure 2.

Figure 2: factory trials for the production of alkali activated blocks (a) "clumps" of glass-derived activator (b) squeeze test for workability (c) block making machine (d) cast blocks.

During batching it was observed that the glass-derived activator contained large clumps of activator and it was thought that this activator would break down during mixing. Following casting of the first batch, "clumps" of activator were visible in the cast blocks and during the later compressive strength testing "clumps" of activator were also observed, see Figure 3. This clearly implied that the activator clumps were too large and they were not dissolving during mixing. This resulted in an activator solution with a lower pH, with the undissolved clumps acting as a type of weak aggregate in the blocks and this is believed to be the reason for the significant reduction in compressive strength compared to the laboratory trials. For this reason, the activator powder was broken down and a second batch was cast.

During the second batch, due to fears of flash setting, the added water was reduced and an issue in dispensing the concrete into the block loader resulted in a significant delay to the casting of the blocks.
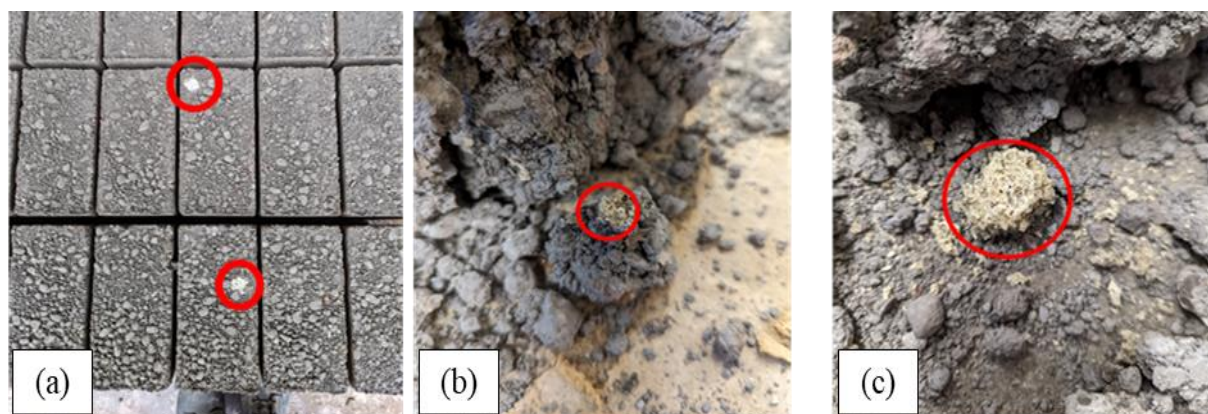

Figure 3: (a) Visible clumps of glass-derived activator in the cast blocks and (b & c) visible clumps of glass-derived activator in the core of blocks following compressive strength testing.

It is believed that the reduction in added water, the activator clumps not dissolving properly and the technical difficulties encountered during casting were responsible for the reduced compressive strength of batch 2.

This became clear when the actual water to solid ratio was calculated for the factory trials and compared with the laboratory trial. The calculated water to solid ratio at the factory was 0.346 whereas the water to solid ratio used for the laboratory trial was 0.40. This reduced water content affected the proper dispersion of the activator solution and therefore reduced the ions released from the precursor materials which in turn affected the system's ability to form the reaction products leading to the hardened matrix. The average compressive strengths are shown in Figure 4 below.
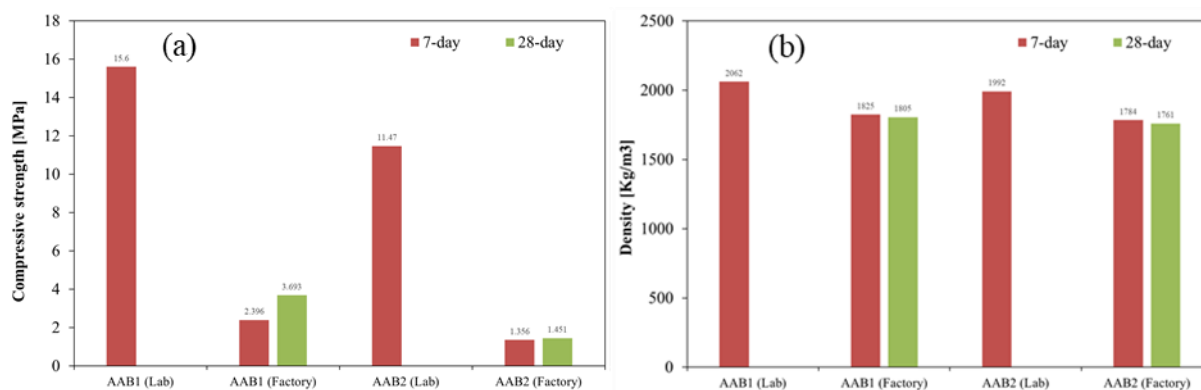

Figure 4: (a) Average compressive strength (b) density Note: 28-days testing not completed for lab blocks.

4.   Conclusions

This paper has described the experience gained from the creation of a sodium silicate activator from waste glass and its application as an activator. The upscale of the laboratory process confirmed that AAMs can be used for the manufacture of concrete building blocks with the smooth transition from the laboratory to the lab emphasising that the technology is easily transferrable. Furthermore, this research has proven that waste glass can be utilised for the synthesis of sodium silicate, which can be used as an activator for cement-less concrete products. The main conclusions from this research are presented below:

1. This new process for the synthesis of sodium silicate from waste glass, regardless of colour or source, has been successfully implemented using significantly lower temperatures compared to the commercial approach of melting soda ash and silica sand at 1100-1200 °C. Using waste glass and sodium hydroxide at 160 °C is much less energy intensive and demanding.
2. The glass-derived activator can be successfully used for alkali activation of both, 100% FA mixes and blended mixes containing 70% GGBS + 30% FA.
3. At laboratory scale, normal density concrete building blocks have successfully been cast and significantly exceeded the target compressive strength of 7 MPa, which is required for building blocks within the UK.
4. The water content and particle size of the glass-derived activator is critical. Large particle size can be difficult to dissolve and results in lower compressive strength. In addition, providing enough added water is critical for the activation process and without

the necessary water, the alkali solution will be less effective at breaking down the structure of the precursors leading to lower compressive strengths.

5. Based on the findings, further trials should be carried out and more care should be taken to ensure the water to solid ratio is correct. Furthermore, trials to reduce the paste content should also be carried out to reduce the cost of the finished building blocks.

5.   References

1.   Counts, T.W. *Global Challenges - Waste*. 2023   [cited 2023 28/03/2023]; Available from: https://www.theworldcounts.com/challenges/waste/global-waste-problem.

2.   Ferdous, W., et al., *Recycling of landfill wastes (tyres, plastics and glass) in construction – A review on global waste generation, performance, application and future opportunities.* Resources, Conservation and Recycling, 2021. **173**: p. 105745.

3.   Speyer, T., *Glass from Glass* in *Building Glass into a Circular Economy*. 2018: UK Green Building Council p. 6.

4.   Graeme, D.E., Babic,, *Re-thinking the life-cycle of architectural glass*. 2018, ARUP.COM: ARUP.

5.   Luukkonen, T., et al., *One-part alkali-activated materials: A review.* Cement and Concrete Research, 2018. **103**: p. 21-34.

6.   Samarakoon, M.H., et al., *Properties of one-part fly ash/slag-based binders activated by thermally-treated waste glass/NaOH blends: A comparative study.* Cement and Concrete Composites, 2020. **112**: p. 103679.

7.   Davidovits, J., *Geopolymers and geopolymeric materials.* Journal of thermal analysis, 1989. **35**(2): p. 429-441.

8.   Thompson, R., *The modern inorganic chemicals industry : the proceedings of a symposium organised by the Inorganic Chemicals Group of the Industrial Division of the Chemical Society*. Special publication (Chemical Society (Great Britain)), ed. R. Thompson. 1977, London: Royal Society of Chemistry. 466.

9.   McCarthy, M., et al., *Characterising long-term wet-stored fly ash following carbon and particle size separation.* Fuel, 2013. **111**: p. 430–441.

10.   Vinai, R. and M. Soutsos, *Production of sodium silicate powder from waste glass cullet for alkali activation of alternative binders.* Cement and Concrete Research, 2019. **116**: p. 45-56.

11.   Rafeet, A., et al., *Guidelines for mix proportioning of fly ash/GGBS based alkali activated concretes.* Construction and Building Materials, 2017. **147**: p. 130-142.

CDW AS SOURCES OF CO$_2$ ABSORPTION

Catarina Brazão Farinha (1)(2)(3), Cinthia Maia Pederneiras (1)(2)(3), David Bastos (1)(2), Ricardo Infante Gomes (1)(2), Rosário Veiga (2), António Santos Silva (2), Isabel Martins (2)

(1) c^{5}Lab – Sustainable Construction Materials Association, Linda-a-Velha, Portugal

(2) LNEC – National Laboratory for Civil Engineering, Lisbon, Portugal

(3) CERIS – Civil Engineering Research and Innovation for Sustainability, University of Lisbon, Lisbon, Portugal

Abstract

Cementitious materials have a considerable global warming footprint. This is due mainly to the cement incorporated. For a tonne of cement produced other 800 kg of CO$_2$ [1] are released into the atmosphere.

According to the European Sustainable Development Goals, cement industry should become carbon neutral by 2050. To meet this goal, the European Cement Association (Cembureau) developed a Roadmap with specific guidelines by 2050 based on five approaches (5C). The first four are focused on improvements in clinker production, cement formulation, construction processes and concrete formulations. The last 5C is re-carbonation of the cementitious materials.

This research investigates the CO$_2$ absorption capability of recycled aggregates (RA) from construction and demolition wastes (CDW), when submitted to a forced carbonation. It is known that CDW still have some potential to CO$_2$ capture, which is a long-term and secure carbon storage. For that purpose, several CDW were collected from recycling plants, from selective demolitions and from concrete plants.

It was concluded that RA when submitted to forced carbonation absorb between 47 to 315 kg of CO$_2$ per tonne of cement paste, which has a potential to meet the re-carbonation targets established by the roadmaps to carbon neutrality.

Introduction

The concentration of atmospheric CO$_2$ is at its highest level ever. Cement industry, among others, is responsible for considerable CO$_2$ emissions to atmosphere.

Cement plants need to achieve carbon neutrality by 2050, in accordance with the 13th United Nations Sustainable Development Goals. In order to meet this goal, the European Cement Association (Cembureau) developed a Carbon Neutrality Roadmap 2050 [2]. This roadmap is divided on 5 approaches ("5C") to reduce the CO$_2$ emissions due to the cement production.

These 5C focus improvements on: Clinker, Cement, Concrete, Construction and Carbonation. 5C approaches include the use of alternative decarbonated materials as fuels in kilns, the reduction of clinker in cement production, the reduction of cement used on cementitious materials and a more efficient design for constructions. Besides these strategies acting directly in clinker, cement, concrete and constructions, it is necessary to account the amount of CO_2 re-absorbed through carbonation to achieve the carbon neutrality.

Cementitious materials, such as mortars and concretes, can re-absorb part of the CO_2 emitted in their production. This occurs because these materials contain portlandite ($Ca(OH)_2$), ettringite (AFt) and calcium silicate hydrate (CSH), which under certain conditions react with atmospheric CO_2. This carbonation reaction depends on the type of material, type and content of cement, porosity of cement paste, temperature, moisture, and exposure to CO_2 conditions (Bastos et al. [3] [4]). Cementitious materials absorb CO_2 in two difference phases: during their life cycle in building environment and after demolition [5]. After demolition, these materials have higher surface area promoting the carbonation reaction more easily.

In this research, the forced carbonation of cementitious materials after the demolition phase is investigated. These materials are recycled aggregates (RA) from construction and demolition wastes (CDW). The RA already absorbed CO_2 during building environment and during demolition and storage, however even after these phases it still have some potential to CO_2 capture through forced carbonation Nedunuri et al. [6], Ivanica et al. [7], Ueno et al. [8] and Ho et al. [9]. Therefore, RA forced carbonation comes as an additional source of CO_2 absorption, since natural carbonation process may be hindered by the accumulation of the RA in stockpiles at recycling plants and do not reach their full carbonation potential.

Materials and methods

In this research recycled aggregates (RA) were collected from three different sources: RA from recycling plants (RP), collected in-situ (IS) and from industrial wastes (IW) generated in a concrete plant. Three mixed recycled aggregates (MRA-RP) and two recycled concrete aggregates (RCA-RP) were collected from recycling plants and one RA was collected from a specific demolition site (RCA-IS) of the concrete structure from an old plant of prefabricated concrete. It was also collected a RCA in a concrete plant (RCA-IW), that came from testing samples of commercial concrete (cubic specimens) for quality control. Due to its source, the latter RCA is a low carbonated aggregate.

The constitution of each recycled aggregate was determined according to EN 933-11 [10] and it is summed up in Table 1. Only the constituents that are included in Rc (concrete products, mortar and concrete masonry units) have cementitious paste and contribute for CO_2 absorption. It was estimated that only 11%-16% (in weight) of Rc is cement paste, meaning that the RA have between 5.0% to 12.2% (in weight) of cement paste in its composition (Table 1).

The CDW analysed in this research were crushed, and only particles smaller than 2 mm were used since their future application should be for rendering mortars.

RA were submitted to forced carbonation in a climatic chamber (ARALAB Fitoclima 300 EP) at 23 ºC, 60% RH and 25% [CO_2]. For MRA the exposure time was defined by 5 hours and the RCA was submitted to forced carbonation for 12 hours based on previous testing to evaluate the time needed for maximum CO_2 capture (Bastos et al. [3] [4]).

Table 1: Recycled aggregates constitution (wt.%)
Adapted from Bastos et al. [3] [4] and Gomes et al. [11]

Recycled aggregates	Rc (%)	Ru (%)	Rb (%)	Ra (%)	Rg (%)	X (%)	Fl (%)	Cement paste (%)
MRA-RP1	42.5	27.5	21.7	9.6	0.2	0.8	Fl5-	5.7
MRA-RP2	61.5	26.7	9.2	0.2	0.0	2.4	Fl5-	8.3
MRA-RP3	37.4	16.3	26.6	6.2	6.9	6.7	Fl5-	5.0
RCA-IS	62.1	18.0	18.4	0.0	0.1	0.5	Fl5-	8.4
RCA-RP1	57.8	28.4	12.4	0.0	0.2	0.4	Fl5-	7.8
RCA-RP2	89.0	10.6	0.4	0.0	0.0	0.0	Fl5-	12.0
RCA-IW	90.4	9.6	0.0	0.0	0.0	0.0	Fl5-	12.2

Classification: Rc - concrete, concrete products, mortar and concrete masonry units; Ru - unbound aggregates, natural stone and hydraulically bound aggregates; Rb - clay masonry units; Ra - bituminous materials; Rg - glass; X - other materials, including cohesive, metals, plastic, rubber, non-floating wood and gypsum plaster.

To quantify the CO_2 capture of these aggregates the thermogravimetric analysis (TGA) technique was used. TGA measurements were performed with a simultaneous TGA-DTA thermal analyser manufactured by SETARAM. The samples were ground with mortar and pestle until all materials passed a 106 μm sieve. Then, a sample from the sieved material was placed in a Pt-Rh crucible and introduced into TGA-DTA instrument where it was heated from 25 to 1000 °C at a uniform rate of 10 °C min^{-1}, with an argon atmosphere (3 L/h).

Results and discussion

TGA measurements were carried out on RA samples before and after forced carbonation. In Figure 3 and Figure 4 the DTG curves are illustrated before and after carbonation of a MRA and a RCA, respectively.

In MRA-RP2 sample the main difference between the DTG curves (pre and post carbonation) is the peak formed between 500-900 °C that is greater after carbonation. This peak corresponds to the carbonates decomposition indicating that the sample absorbed CO_2 during forced carbonation. From the mass loss between 500-900 °C, the amount of CO_2 present in the samples is obtained.

In RCA-RP1 sample some differences can be noticed between the DTG curves before and after forced carbonation. The first difference are the 2 peaks formed between 80 ° and 200 °C, which decreased with carbonation. These peaks correspond to the dehydration of ettringite (Aft) and calcium silicate hydrate (C-S-H) (Bastos et al. [3] [4]), meaning that those compounds reacted with CO_2 during forced carbonation. At 400-500 °C it as also noticed that the peak that was present before carbonation disappeared after carbonation. This peak is related to the presence of portlandite ($Ca(OH)_2$) that reacted with CO_2 forming $CaCO_3$. Thus, it is possible to conclude that there was CO_2 capture during forced carbonatation.
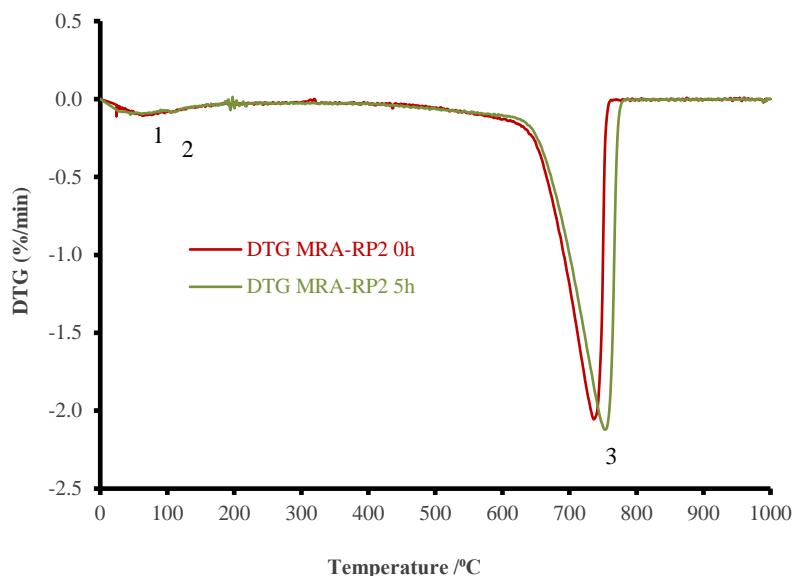
Legend: 1-Dehydration of ettringite; 2-Dehydration of C-S-H; 3-Decarbonation of calcium carbonate

Figure 1: DTG curves of MRA-RP2 before (0 h) and after 5 h of forced carbonation
(Adapted from Bastos et al. [3] [4])
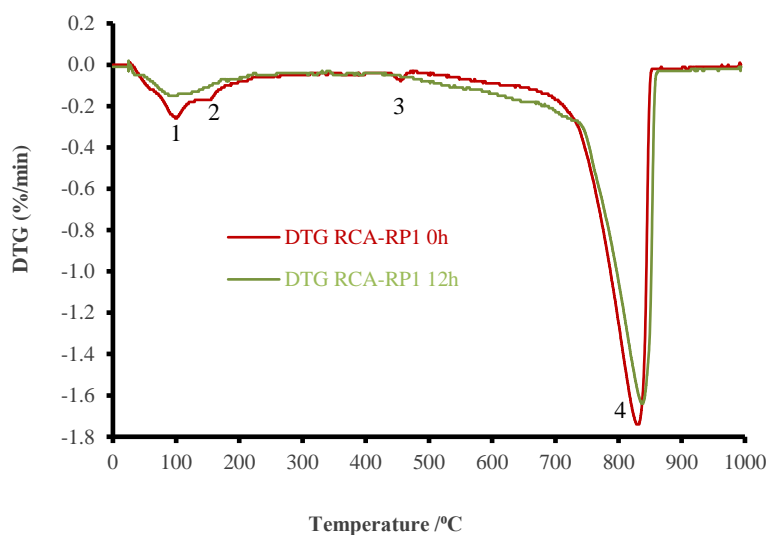
Legend: 1-Dehydration of ettringite; 2-Dehydration of C-S-H; 3-Dihydroxylation of portlandite; 4-Decarbonation of calcium carbonate

Figure 2: DTG curves of RCA-RP1 before (0 h) and after 12 h of forced carbonation
(Adapted from Bastos et al. [3] [4])

By TGA it was possible to conclude that mixed recycled aggregates capture between 0.6% to 1.8% of CO_2 per tonne of aggregate (Figure 3), while RCA capture between 0.6% to 4.1%

(Figure 4), when exposed to forced carbonation [3] [4]. The values are low because the cement paste present in the RA is limited to 5.0 wt.% to 12.2 wt.% (Table 1).
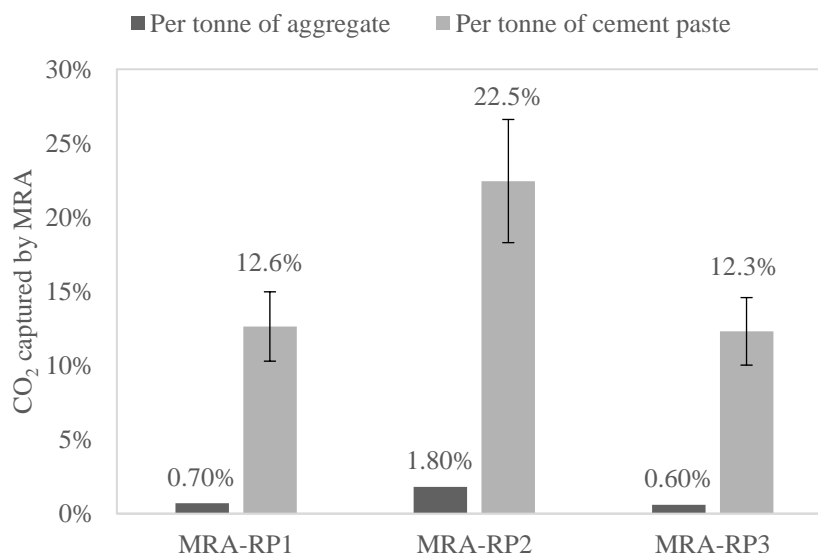

Figure 3: CO_2 capture by tonne of aggregate and by tonne of cement paste in MRA

The cement paste is the RA's constituent that contributes the most for CO_2 emissions. However, it is also able to re-absorb CO_2 not only during its life cycle in the built environment but also after demolition during storage and with forced carbonation. Per tonne of cement paste, it is possible to re-absorb between 5.2% to 34.8% of CO_2 (Figure 3 and Figure 4). The amount of CO_2 re-absorbed by RA depends on its initial carbonation level. RCA-RP2 was the RA that less CO_2 re-absorbed with forced carbonation. It probably absorbed more CO_2 in other phases, such as during its life cycle or during demolition and storage. On the other hand, RCA-IW was the RA that re-absorbed the highest amount of CO_2 per cement paste. This is explained by its low degree of carbonation before being exposed to forced carbonation. The remaining five RA re-absorbed between 11.1% to 22.5% of CO_2 in this stage.

The significant difference between the CO_2 uptake of MRA and RCA is due to their composition and their pre-carbonation state, which are very variable. In particular, the RCA-IW, being a concrete based RA includes a higher amount of cement paste compared to MRA and additionally it is a concrete not much exposed to natural carbonation, which also contributes to a higher CO_2 capture. In general, RCA can capture higher amounts of CO_2 by tonne of aggregate compared with MRA. However, as MRA present much lower cement paste contents, the captures by tonne of cement paste are similar and may in some cases be higher than in the case of RCA.

According to the roadmaps to carbon neutrality [2] [12] construction sector may re-absorb 51 kg of CO_2 per tonne of cement paste by 2050. This re-absorption includes the phases in building environment and after demolition. With forced carbonation, it was concluded that RA re-absorbed from 52 to 348 kg of CO_2 per tonne of cement paste (Figure 5). All RA just with forced carbonation may meet the goals stablished, independently the building environment and demolition phases. This means that RA have a great potential to re-absorb CO_2 emissions produced by cement industry, being sources of CO_2 absorption and storage.
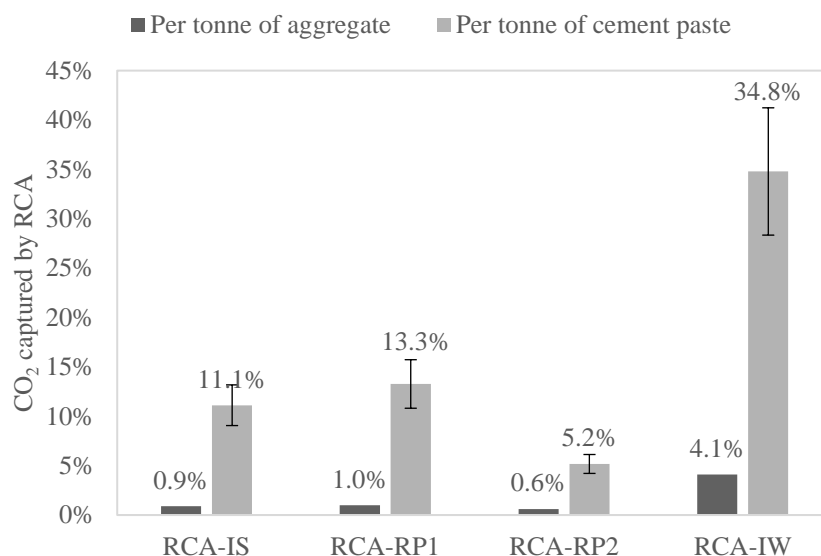
Figure 4: CO_2 capture by tonne of aggregate and by tonne of cement paste in RCA
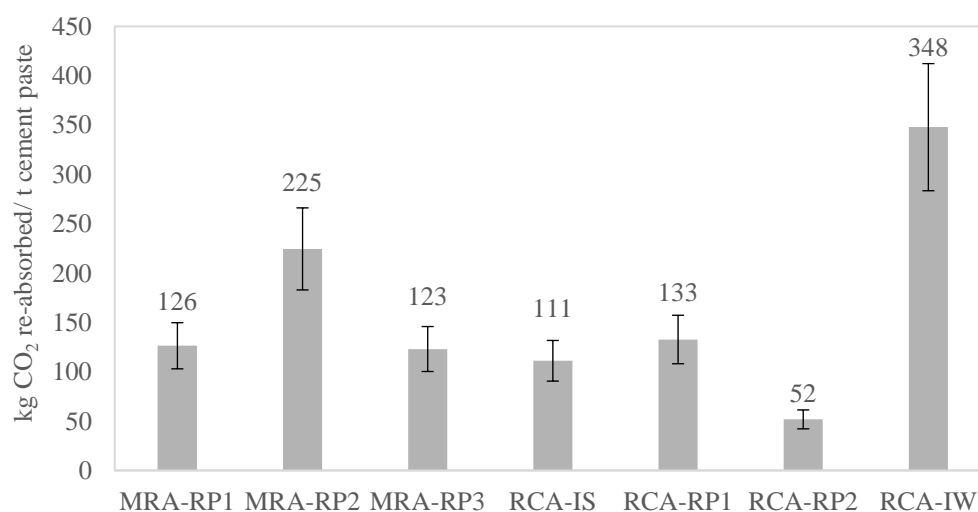
Figure 5: kg of CO_2 re-absorbed per tonne of cement paste

Conclusions

In this research the forced carbonation of recycled aggregates from construction and demolition wastes was investigated. These materials have carbonated during their lifetime in a building environment and then immediately after when they were demolished and stored. In this research an additional CO_2 capture by forced carbonation in a climatic chamber with higher concentrations of CO_2 was investigated. From this research it was concluded that:

- Recycled aggregates have potential to absorb CO_2 by forced carbonation, even after the building environment and demolition carbonation phases;

- Mixed recycled aggregates can absorb between 0.6% to 1.8% of CO_2 per tonne of aggregate while recycled concrete aggregates capture between 0.6% to 4.1%;
- Considering only the cement paste, it was concluded that RA can re-absorb between 5.2% to 34.8% of CO_2, that corresponds to 52 to 348 kg of CO_2 per tonne of cement paste;
- The roadmaps to carbon neutrality goals aim the construction to re-absorb 51 kg of CO_2 per tonne of cement produced by 2050. It was concluded that forced carbonation, independently of the building environment and demolition carbonation phases, has a potential to meet the goals stablished.

Therefore, CDW come as source to CO_2 capture, re-absorbing part of the CO_2 emitted in the production of cement.

Acknowledgements

References

[1]   European Cement association (CEMBUREAU), 'Environmental Product Declaration (EPD)', (2020).

[2]   European Cement association (CEMBUREAU), '2050 Carbon Neutrality Roadmap', (2020).

[3]   Bastos, D., Brazão Farinha, C., Maia Pederneiras, C., Santos Silva, A., Bogas, A., Veiga, R., Infante Gomes, R., 'CO2 uptake by recycled aggregates obtained from construction and demolition waste', Submitted, (2023).

[4]   Bastos, D., Brazão Farinha, C., Maia Pederneiras, C., Infante Gomes, R., Santos Silva, A., Veiga, R., '1st Report: Characterization and CO2 capture by construction and demolition recycled aggregates'. c5Lab - Sustainable Construction Materials Association (2023).

[5]   Pederneiras, C. M., Brazão Farinha, C., Veiga, R., 'Carbonation Potential of Cementitious Structures in Service and Post-Demolition: A Review', CivilEng (2022) 211–223.

[6]   Nedunuri, A.; Mohammed, A.; Muhammad, S. 'Carbonation potential of concrete debris fines and its valorisation through mineral carbonation', Construction and Building Materials (2021) 310, 125162.

[7]   Ivanica, R.; Risse, M.; Weber-Blaschke, G.; Richter, K. 'Development of a life cycle inventory database and life cycle impact assessment of the building demolition stage: A case study in Germany', Journal of Cleaner Production (2022), 338, 130631.

[8]   Ueno, A.; Kawai, K.; Kobayashi, K.; Tanaka, S. 'Evaluation of visual methods for CO_2 uptake by demolished concrete'. Construction and Building Materials (2014)67, 393–398.

[9]   Ho, H.J.; Iizuka, A.; Shibata, E.; Tomita, H.; Takano, K.; Endo, T. 'Utilization of CO_2 in direct aqueous carbonation of concrete fines generated from aggregate recycling: Influences of the solid–liquid ratio and CO_2 concentration', Journal of Cleaner Production (2021), 312, 127832.

[10]   EN 933-11, 'Tests for geometrical properties of aggregates. Part 11: Classification test for the constituents of coarse recycled aggregate', (2009).

[11]   Infante Gomes, R., Bastos, D., Brazão Farinha, C., Maia Pederneiras, C., Veiga, R. de Brito, J., Faria, P., Santos Silva, S., 'Mortars with CDW recycled aggregates submitted to high levels of CO_2', Infrastructures 6 (11) (2021).

[12]   ATIC - Associação técnica da Indústria do Cimento, 'Roadmap to Carbon Neutrality 2050. For a sustainable future (In Portuguese)', (2021).

EVALUATION OF THE USE OF RECYCLED CONCRETE POWDER (RCP) IN THE WORKABILITY AND COMPRESSIVE STRENGTH OF PORTLAND CEMENT PASTES

Joaquin H. A. Rocha (1), Nahúm G. C. Chileno (2), Matheus P. Tinoco (1) and Romildo D. Toledo Filho (1)

(1) Civil Engineering Program, Federal University of Rio de Janeiro, Brazil

(2) Federal University of Lavras, Brazil

Abstract

Construction is one of the industries with the greatest environmental impact in the world, highlighting the emission of CO2 and the generation of waste. In this sense, reducing, reusing, and recycling materials is a sustainable alternative to mitigate this problem. This study aims to evaluate the use of Recycled Concrete Powder (RCP) as a substitute for Portland cement, considering two sources of RCP: demolition and laboratory waste. Cement pastes containing 10, 20, and 30% RCP from both sources were prepared. Workability was evaluated through the mini-slump test. Compressive strength was determined for 7 and 28 days. The modulus of elasticity and microstructure were analyzed after 28 days. With increasing substitution of Portland cement by RCP, there is a downward trend in the properties evaluated, regardless of source. However, the compressive strength of 10% RCP and reference was statistically similar, indicating that the use of lower proportions is feasible. Using a scanning electron microscope (SEM), various hydration products, such as ettringite (AFt), calcium hydroxide (CH), and calcium silicate hydrates (C-S-H) were observed in all pastes containing RCP. The source of RCP does not affect the properties evaluated, and its use can be indistinct.

1. Introduction

Cement-based materials are the most widely used in the construction industry and their demand is growing every year [1,2]. Therefore, ways to improve the performance of these materials are being investigated, both technically and in regards to reducing their environmental impact, which is mainly associated with the production of Portland cement [3]. It is estimated that Portland cement requires 125 kW/h of electricity and emits 800 kg of CO_2 during its production [4]. As such, recent investigations have investigated recycled concrete powder (RCP) as a supplementary cementitious material (SCM) [5-7].

The RCP comes from the production of recycled concrete aggregate (RCA), considering particles smaller than 150 μm [8]. However, it is recommended that the particle size of the RCP be close to the granulometry of Portland cement, in order to improve its reactivity [6,9]. Therefore, it is suggested that RCP be finely ground to obtain adequate performance in cement-

based materials [10]. Various studies have shown the potential of using RCP as a sustainable SCM within a construction and demolition waste (CDW). Rangel et al. [11] suggest that due to its physical and chemical characteristics, RCP can be used as an auxiliary material in cement. He et al. [12] found that up to 30% replacement of Portland cement with ultrafine RCP (D50=2.3µm) could equal or even improve the mechanical strength of the reference paste. Kim and Jang [13] point out that the use of 10% RCP reaches 95% of the reference mechanical strength, and 20% RCP can achieve the target strength. Oliveira et al. [14] recommend that a replacement of up to 25% can be viable in mortars and concretes without affecting their mechanical properties, considering it a sustainable material.

Although RCP can be used to replace Portland cement, substitution rates are low and RCP sources, e.g., demolition [8,10,12] and laboratory [4,14,15], have not been compared. The objective of this study is to compare two sources of RCP (demolition and laboratory) in the mechanical properties of cement pastes. For this, Portland cement was substituted in percentages of 10, 20, and 30% by RCP. The workability of the pastes was studied by means of the mini-slump test; the modulus of elasticity was evaluated at 28 days; compressive strength was analyzed at 7 and 28 days, and the microstructure of the pastes was analyzed at 28 days.

2.   Materials and methods

The cement used was a CP II-F32 from Lafarge Holcim, classified as ASTM type II according to ASTM C150 [16]. Two sources of RCP were used: a) demolition of a hospital in Rio de Janeiro (RCP-D) and residues of concrete samples tested in the laboratory (RCP-LAB). The RCP went through a sieving process and the material that passed the #100 sieve, maximum size of 150 µm, was selected. Subsequently, in order to achieve a granulometry close to Portland cement, a metal ball mill was used for 30 minutes.

By means of X-ray fluorescence (Shimadzu EDX-720 spectrometer) the chemical composition of the materials was established. The loss on ignition (LOI) was calculated using the procedures of NBR NM 18 [17]. The density of the materials was quantified using a helium pycnometer. The particle size was established through laser diffraction and the specific surface area (SSA) was calculated following ASTM C204 [18] standard.

The pastes were molded with a water-cement ratio of 0.4. Portland cement was replaced in three percentages by RCP (by weight): 10, 20, and 30%, in addition to the reference. Table 1 presents the mixtures analyzed and the proportions of the materials.

Workability was measured using the mini-slump test, considering the average of four measurements per mixture. The compressive strength was established at the age of 7 and 28 days using a Shimadzu UH-F (100 kN), with four specimens per mixture. The modulus of elasticity was determined at 28 days, according to ASTM C469 [19], in which the longitudinal displacement was measured using electrical transducers (LVDT). Finally, the microstructure of the pastes at 28 days was analyzed using a scanning electron microscope (Hitachi TM3000).

The results were statistically evaluated by an analysis of variance (ANOVA) and Tukey test for a significance of 0.05.

3. Results and discussion

3.1 Materials properties

The chemical composition of the materials is detailed in Figure 1. The largest component of Portland cement is CaO, followed by SiO_2 and Fe_2O_3. Regarding the loss on ignition (LOI), this was 11.78%, which is within the recommendations for the type of cement (CP II - F), according to NBR 16697 [20]. The RCP has a lower content of CaO and a higher content of SiO2, Fe2O3 and Al2O3, in relation to cement; however, the sum of these components does not reach 70% and the LOI is greater than 4.5% to comply with ASTM C618 [21] to be within the pozzolanic material classification.

Table 1: Proportion of materials (by weight)

Mixture	Cement Porland	RCP-D	RCP-LAB
CP	100	-	-
D10	90	10	-
D20	80	20	-
D30	70	30	-
LAB10	90	-	10
LAB20	80	-	20
LAB30	70	-	30
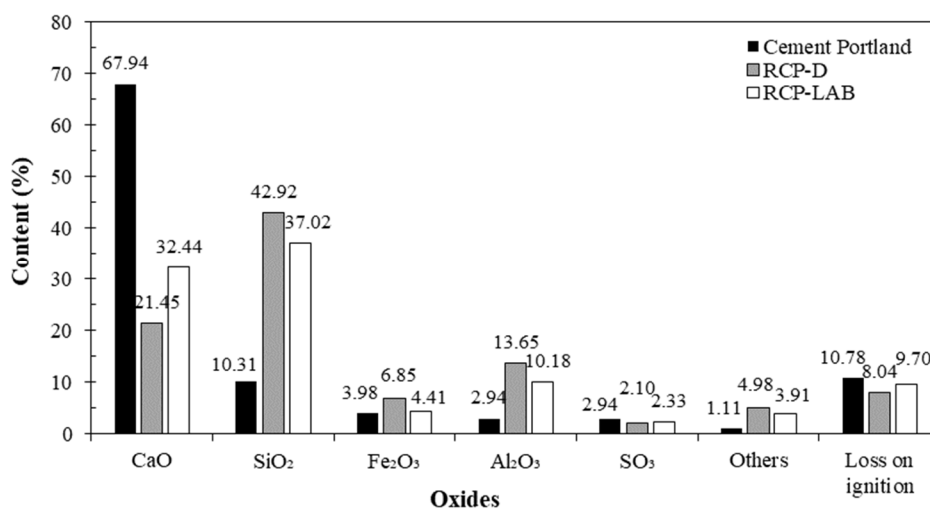
Figure 1: Chemical composition of materials

The physical properties of the materials are described in Table 2. The grinding time was adequate to achieve a particle size close to that of Portland cement (D50). The RCP (D and LAB) have D10 and D90 values lower and higher than those of Portland cement, respectively. Regarding density, Portland cement has the highest density, followed by RCP-D and RCP-LAB. The specific surface is higher for RCP-D and RCP-LAB, in that order.

The morphology of the RCP-D and RCP-LAB particles is presented in Figures 2a and 2b, respectively. In both, crystalline particles can be observed, referring to the quartz present in the RCP, as well as hydration products, the latter both separately and adhered to larger particles.

Table 2: Physical properties of materials

Parameter	Cement Portland	RCP-D	RCP-LAB
D10 (μm)	2.06	1.77	1.71
D50 (μm)	14.14	13.19	13.82
D90 (μm)	47.79	57.23	62.49
Specific gravity (g/cm³)	3.05	2.66	2.61
Specific surface area (cm^2/g)	3762.77	8614.72	7988.73
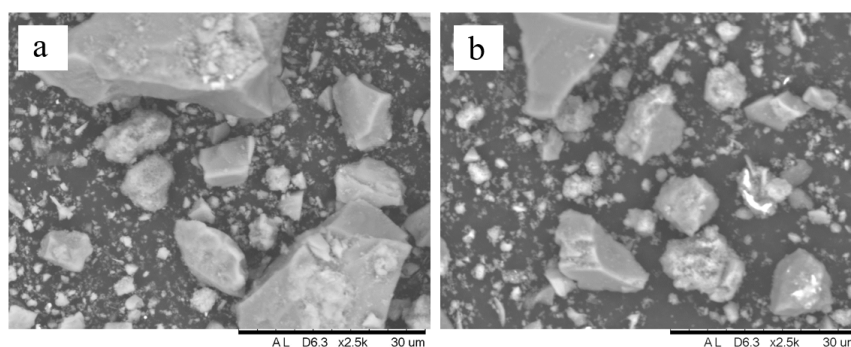
Figure 2: Morphology of the particles of a) RCP-D and b) RCP-LAB

3.2 Workability

The workability was expressed in spreading area (Figure 3). The results show that the greater the replacement of Portland cement by RCP, the workability decreases. The smallest reduction occurs for 10% of RCP, 20.38 and 22.76% for RCP-D and RCP-LAB, respectively. The maximum reduction occurs for pastes with 30% RCP, 43.10 and 48.42% for RCP-D and RCP-LAB, respectively. This negative trend is due to the morphology of the RCP particles (Figure 2) and their SSA (Table 2), increasing water requirement [7].

Figure 3: Spreading area

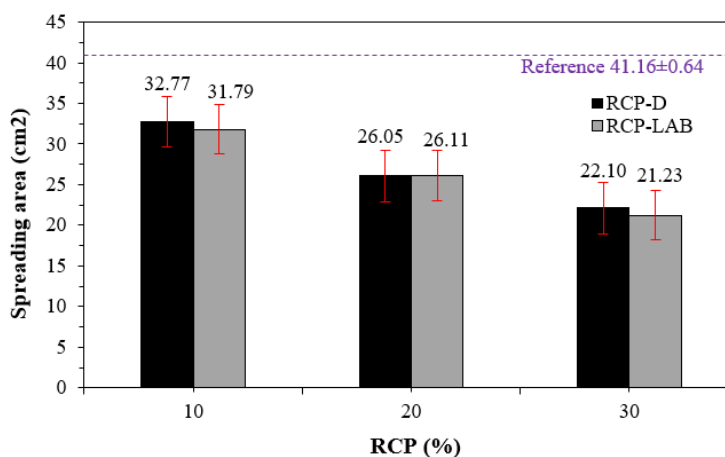Through an ANOVA, it can be concluded that there are significant differences between the means of the mixtures (p value<0.05). The Tukey test established that the reference had greater workability than all the mixtures with RCP, regardless of the source. These results indicate that even 10% RCP had a significant negative influence on this property.

When the results between the two sources of RCP are compared by substitution percentage, it can be established that the results are statistically similar (p value>0.05). The p value for D10-LAB10, D20-LAB20 and D30-LAB30 were 0.615, 0.928 and 0.999, respectively. Therefore, the loss of workability is influenced by the substitution percentage and not by the RCP source. As observed in Figure 2, the morphology of the particles from both RCP sources was similar, in addition to their physical characteristics (Table 2); therefore, it can be expected that their influence on workability is the same, indicating a predominant physical effect of the RCP.

3.3 Compressive strength

The compressive strength of the pastes with RCP-D and RCP-LAB are presented in Figures 4a and 4b, respectively. For both sources, a negative trend is observed as Portland cement is replaced by RCP. In the case of RCP-D, for a substitution of 10%, the reduction is 5.13% and 3.11% for the ages of 7 and 28 days, respectively. The greatest reduction occurs for the substitution of 30%, with 31.40% and 20.76% for the ages of 7 and 28 days, respectively. The same behavior occurs for RCP-LAB; for a 10% substitution, the reduction is 2.25% and 3.56% for 7 and 28 days, respectively. For the case of 30% RCP, the decrease is 30.27% and 23.96% for 7 and 28 days, respectively. The negative effect on compressive strength is due to dilution effect of Portland cement and the low reactivity of the RCP particles [5,13].
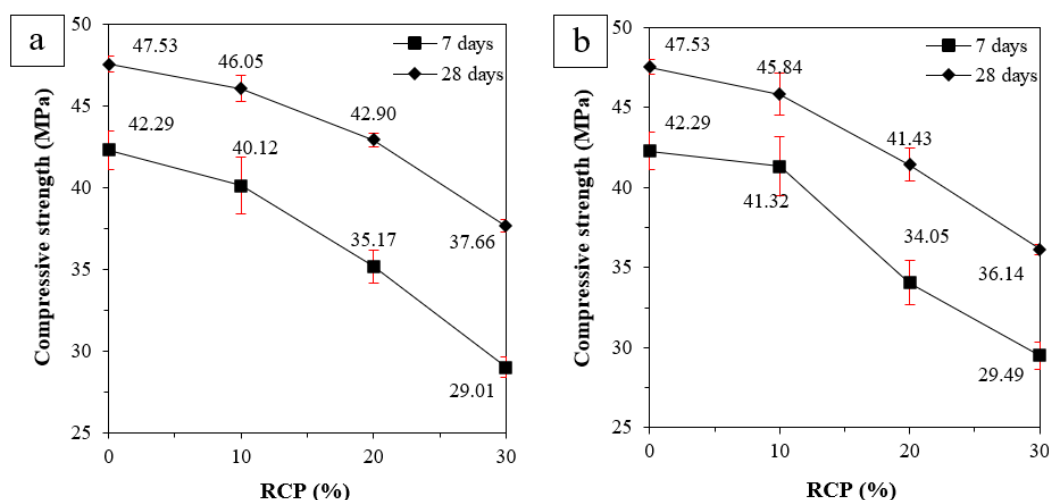
Figure 4: Compressive strength for a) RCP-D and b) RCP-LAB

By ANOVA and Tukey test it is concluded that there are differences between the mixtures (p value<0.05). As previously mentioned, there are small differences between the reference and 10% RCP, regardless of the source, being similar for 7 days and 28 days. The results indicate that up to 10% replacement of Portland cement by RCP has no influence on this property. In the comparison between the results of RCP-C and RCP-LAB, it is observed that the results are similar, with a p value>0.05 for both ages and all substitution percentages. The p value for 7 days of the D10-LAB10, D20-LAB20 and D30-LAB30 mixtures was 0.844, 0.879 and 0.998, respectively. While, for 28 days, the p value of D10-LAB10, D20-LAB20 and D30-LAB30 was 0.999, 0.144 and 0.121, respectively. Therefore, the RCP source does not have a direct influence

on this property, although they differ in their chemical composition; the results show that most of the RCP components are inert, demonstrating predominantly a physical rather than a chemical effect.

3.4 Modulus of elasticity

Figure 5 presents the values of the modulus of elasticity of the pastes. As with the compression strength, a tendency to decrease is observed with the increase in the content of RCP-C and RCP-LAB. It has been established that there are significant differences between the tested samples (p value<0.05). According to the Tukey test, the modulus of elasticity of the mixtures with 10% RCP, regardless of the source, is equal to the reference (p value>0.05), indicating that this percentage does not affect the modulus of elasticity. The decrease in the modulus of elasticity for high percentages (20 and 30%) The decrease in the modulus of elasticity for high percentages (20 and 30%) can be attributed to the lower hardness and rigidity of the RCP particles and to the dilution effect [14].
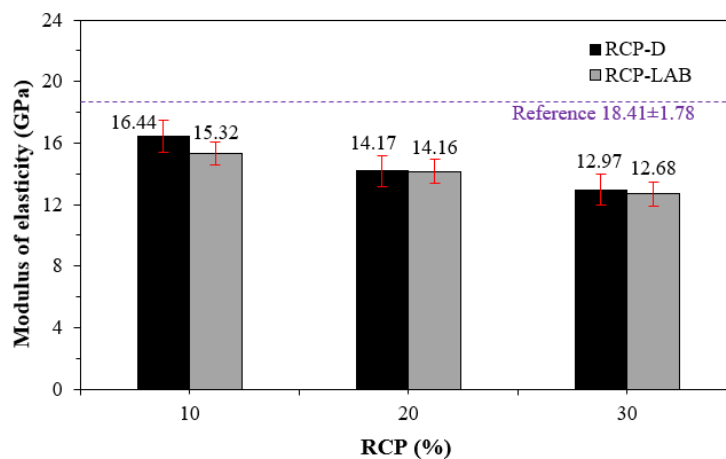
Figure 5: Modulus of elasticity

When comparing the results between both sources of RCP, it can be established that there are no differences in the modulus of elasticity, corroborating the results of the previously analyzed properties. The p value for D10-LAB10, D20-LAB20, and D30-LAB30 were 0.961, 1, and 0.999, respectively.

3.5 Microstructure

Figures 6 shows the microstructure of the pastes with 10, 20 and 30% RCP. It is observed that in all the pastes, hydration products were generated: hydrated calcium silicate (C-S-H), ettringite (AFt) and calcium hydroxide (CH), attributing that the RCP does not influence the formation of the different types of hydration products, but reduces the quantity.
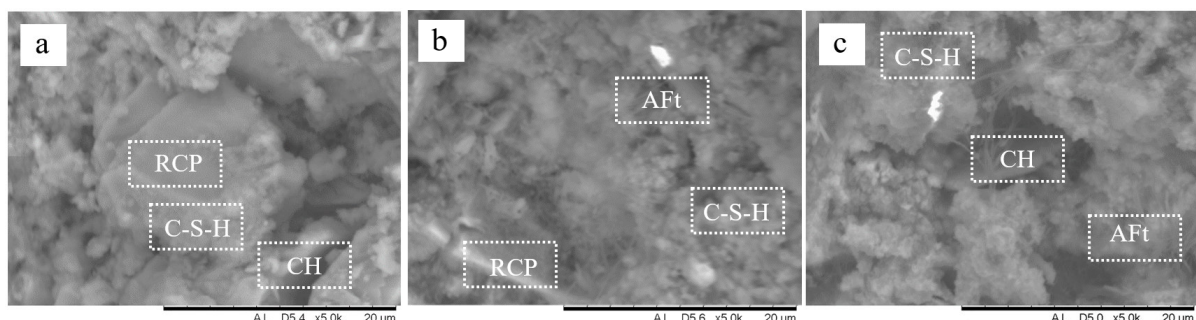
Figure 6: Microstructure of a) D10, b) D20 c) D30, d) LAB10, e) LAB20, and f) LAB30

For 10% RCP pastes, there is the formation of traditional products with a relatively dense microstructure. Additionally, the presence of RCP covered by hydration products is observed, indicating a nucleation and filling effect in the cement matrix, characteristics that maintained the mecha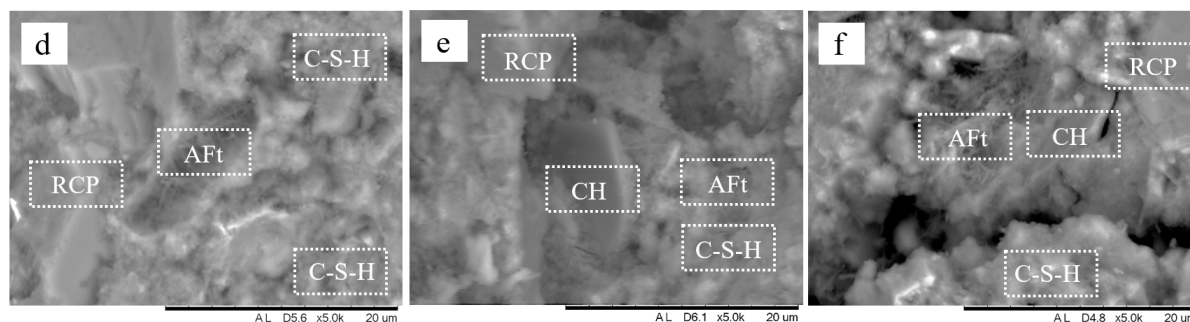nical strength (Figure 4). In the case of pastes with 20 and 30% RCP, a loose microstructure is observed, especially for 30% RCP, explaining the significant reduction in compressive strength and modulus of elasticity.

4.   Conclusions

An experimental investigation was conducted to assess the use of two sources of RCP: demolition and laboratory. Cement pastes were made with RCP as a replacement of Portland cement, leading to the following conclusions:

The RCP, regardless of the source, yielded the same results in the evaluated properties, indicating that, although this material can be considered heterogeneous due to its physical and chemical characteristics, it is composed of inert material, acting more like a filler. The morphology and SSA of the RCP particles reduce the workability (increase in water requirement), indicating a negative trend with increasing RCP.

The compressive strength was compromised with the inclusion of RCP, particularly at high percentages (30%), which can be attributed to the formation of fewer hydration products (dilution effect); however, 10% RCP did not significantly affect this property. The modulus of elasticity also exhibited similar behavior, with a non-significant reduction for 10% of RCP, indicating that the use of RCP would be feasible up to this percentage. The microstructure revealed the formation of hydration products in the pastes with RCP: C-S-H, CH, and AFt; however, a loose microstructure may become evident as the RCP content increases.

References

[1] Boudali, S., Abdulsalam, B., Rafiean, A. H., Poncet, S., Soliman, A. and ElSafty, A., 'Influence of fine recycled concrete powder on the compressive strength of self-compacting concrete (SCC) using artificial neural network', *Sustainability* **13** (6) (2021) 3111.

[2] Habert, G., Miller, S.A., John, V.M., Provis, J.L., Favier, A., Horvath, A. and Scrivener, K.L., 'Environmental impacts and decarbonization strategies in the cement and concrete industries', *Nat. Rev. Earth Environ.* **1** (11) (2020) 559-573.

[3] de Brito, J. and Kurda, R., 'The past and future of sustainable concrete: A critical review and new strategies on cement-based materials', *J. Clean. Prod.* **281** (2021) 123558.

[4] Cantero, B., Bravo, M., de Brito, J., Sáez del Bosque, I.F. and Medina, C., 'Thermal performance of concrete with recycled concrete powder as partial cement replacement and recycled CDW aggregate', *Appl. Sci.* **10** (13) (2020) 4540.

[5] Liu, X., Liu, L., Lyu, K., Li, T., Zhao, P., Liu, R., Zuo, J., Fu, F. and Shah, S.P., 'Enhanced early hydration and mechanical properties of cement-based materials with recycled concrete powder modified by nanosilica', *J. Build. Eng.* **50** (2022) 104175.

[6] Tang, Q., Ma, Z., Wu, H. and Wang, W., 'The utilization of eco-friendly recycled powder from concrete and brick waste in new concrete: A critical review', *Cem. Concr. Compos.* **114** (2020) 103807.

[7] Cantero, B., Bravo, M., De Brito, J., del Bosque, I.S. and Medina, C., 'Mechanical behaviour of structural concrete with ground recycled concrete cement and mixed recycled aggregate', *J. Clean. Prod.* **275** (2020) 122913.

[8] Xiao, J., Ma, Z., Sui, T., Akbarnezhad, A. and Duan, Z., 'Mechanical properties of concrete mixed with recycled powder produced from construction and demolition waste', *J. Clean. Prod.* **188** (2018) 720-731.

[9] Kim, Y.J. and Choi, Y.W. 'Utilization of waste concrete powder as a substitution material for cement', *Constr. Build. Mater.* **30** (2012) 500-504.

[10] Horsakulthai, V., 'Effect of recycled concrete powder on strength, electrical resistivity, and water absorption of self-compacting mortars', *Case Stud. Constr. Mater.* **15** (2021) e00725.

[11] Rangel, C.S., Toledo Filho, R.D., Amario, M., Pepe, M., de Castro Polisseni, G. and de Andrade, G.P., 'Generalized quality control parameter for heterogenous recycled concrete aggregates: A pilot scale case study', *J. Clean. Prod.* **208** (2019) 589-601.

[12] He, X., Zheng, Z., Yang, J., Su, Y., Wang, T. and Strnadel, B., 'Feasibility of incorporating autoclaved aerated concrete waste for cement replacement in sustainable building materials', *J. Clean. Prod.* **250** (2020) 119455.

[13] Kim, J. and Jang, H., 'Closed-loop recycling of C&D waste: Mechanical properties of concrete with the repeatedly recycled C&D powder as partial cement replacement', *J. Clean. Prod.* **343** (2022) 130977.

[14] Oliveira, T.C., Dezen, B.G. and Possan, E., 'Use of concrete fine fraction waste as a replacement of Portland cement', *J. Clean. Prod.* **273** (2020) 123126.

[15] Ma, Z., Yao, P., Yang, D. and Shen, J., 'Effects of fire-damaged concrete waste on the properties of its preparing recycled aggregate, recycled powder and newmade concrete', *J. Mater. Res. Technol.* **15** (2021) 1030-1045.

[16] ASTM, 'ASTM C150/C150M-22: Standard Specification for Portland Cement', ASTM (West Conshohocken, 2022).

[17] ABNT, 'NBR NM18: Cimento Portland - Análise química - Determinação de perda ao fogo', ABNT (Rio de Janeiro, 2012).

[18] ASTM, 'ASTM C204: Standard Test Methods for Fineness of Hydraulic Cement by Air-Permeability Apparatus', ASTM (West Conshohocken, 2019).

[19] ASTM, 'ASTM C469/C469M-22: Standard Test Method for Static Modulus of Elasticity and Poisson's Ratio of Concrete in Compression', ASTM (West Conshohocken, 2022).

[20] ABNT, 'NBR 16697 - Cimento Portland Requisitos', ABNT (Rio de Janeiro, 2018).

[21] ASTM, 'ASTM C618-22: Standard Specification for Coal Fly Ash and Raw or Calcined Natural Pozzolan for Use in Concrete', ASTM (West Conshohocken, 2022).

ZERO-EMISSION CIRCULAR CONCRETE

Peter Stemmermann (1), Krassimir Garbev (1), Angela Ullrich (1), Günter Beuchle (1)

(1) Institute for Technical Chemistry (ITC), Karlsruhe Institute of Technology, Germany

Abstract

The project Zero Emission Circular Concrete develops a CO_2-neutral, high-quality, and resource-efficient concrete cycle starting with end-of-life concrete. A cement clinker with a reduced CO_2 footprint is processed from waste concrete fines at a strongly reduced temperature of approximately 1000°C. The main clinker mineral is belite, Ca_2SiO_4. The residual CO_2 is released in concentrated form and used for the technical carbonation of either waste concrete fines as supplementary cementitious material or of coarse crushed waste concrete. The coarse fraction is treated in a new process based on a pressurized autoclave, where hardening by carbonation improves the properties of the recycled aggregate. Both carbonation options are investigated on a laboratory scale.

Recycling cement is developed from belite cement clinker, Portland cement clinker, and other substitutes in a joint project with the industry. A 30% substitution rate of Portland cement clinker compared to European cement standards is targeted. Subsequently, formulations for recycling concrete will be developed from recycled cement and recycled aggregate. The processing of concrete products and precast concrete elements will be tested in plant trials.

A pilot plant for belite cement clinker is currently under construction to bring its technology readiness level to four.

1.   Introduction

The production of concrete is responsible for about 6 to 9 % of all man-made CO_2 emissions, whereby these emissions are almost exclusively linked to the upstream production of Portland cement clinker (PCC). CO_2 from the clinkering process originates to about 60% from the calcination of limestone (process emissions) and about 40% from fuels.

Waste concrete, on the other hand, could capture up to 80% of the process emissions generated during cement manufacture by recarbonation. During service life, demolition, and subsequent crushing, a value of about 5% is observed [1].

Today's standard procedure for the recycling of concrete waste neither includes its use for carbon sequestration nor for the production of cement clinker. Waste concrete is usually processed into crushed aggregate as a substitute for natural aggregate in road construction. Therefore, an excess of crushed concrete fines remains, which is hardly usable. In Germany,

the economic value of the recycled product is currently about 1/3 of fresh concrete, which is why it's called downcycling. In the considered case, downcycling reduces the demand for natural raw materials but does not contribute to reducing CO_2 emissions in the cement industry.

In principle, it is possible to use waste concrete fines in particular as a raw meal component for cement clinker production in existing cement plants, whereby CO_2 emissions could be slightly reduced. Economically, however, the transport of concrete waste is limited to a distance of about 20 km, so at best a very small proportion of concrete waste could be used. The situation will become even worse in the future, when the need to implement carbon capture, use, and storage (CCUS) will require investments in expensive infrastructure for the transport of CO_2, which, according to the current state of the art, is only economical for very large plants. A technical solution for high-quality closed-loop recycling of waste concrete with an average transport distance of 20 km of secondary raw materials is missing.

2. Zero Emission Circular Concrete at KIT

The KIT project for the production of zero-emission circular concrete is therefore aiming at technologies that are designed for stand-alone plants with a cement clinker capacity of about 50,000 t/a, far smaller than existing cement plants. The objective of the project is to reduce CO_2 emissions from clinker production by using crushed concrete fines as a second component besides limestone in the production of cement clinker (figure 1). The unavoidably released CO_2 is then to be fixed as completely as possible in other mineral wastes, preferably in crushed aggregate from old concrete. This is done by crystallizing carbonates in a hydrothermal process. Infrastructure e.g. pipelines for CO_2 transport thus become obsolete. The structural properties of the aggregate are even improved due to pore closure induced by the growth of carbonates. Carbonated crushed aggregate shall be used together with recycled cement clinker for the production of recycled concrete without the need for an increased cement content compared to standard concrete formulations.
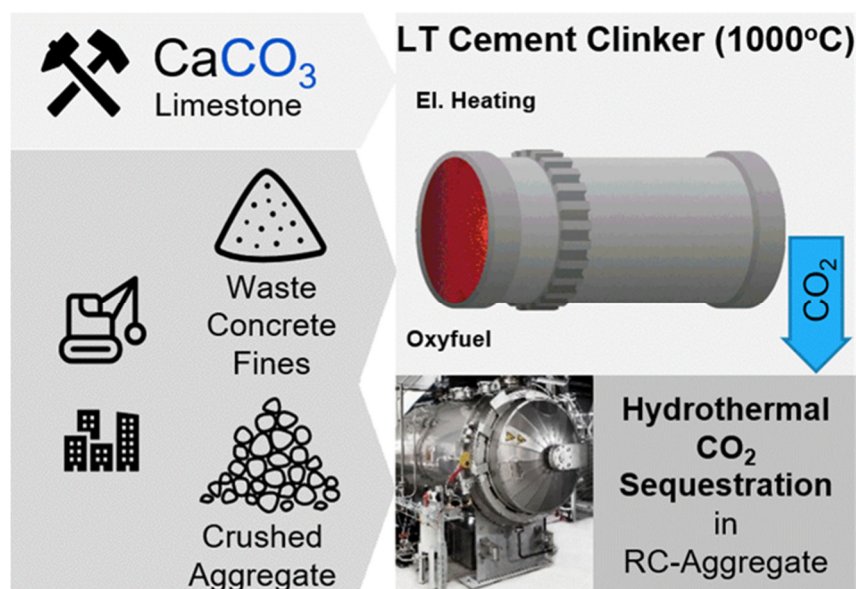

Figure 1: Combined low-temperature processing of belite cement clinker and carbonated recycled aggregate from waste concrete and limestone aiming at zero CO_2 emission.

3. Low-temperature belite cement clinker (LT-BCC) from waste concrete

To process belite cement clinker at low temperatures, a new cement raw meal characterized by a lower lime content and the addition of mineralizing agents as well as new process conditions were investigated [2]. The technology consists of a rotary kiln with a maximum process temperature of $1000^{\circ}C$, preferably operated electrically or with oxyfuel combustion in an almost pure CO_2 atmosphere. The combined presence of CO_2 and selected mineralizing agents, e.g. $CaCl_2$ or Na_2CO_3, results in the formation of a carbonate-rich melt at temperatures below $700^{\circ}C$, which allows extremely fast clinkering. Concrete-damaging components such as sulfate and chloride are bound in dedicated and insoluble reservoir minerals [3].

In the raw meal, limestone is partially replaced by the hardened cement paste contained in the crushed concrete fines. A further reduction of the limestone content compared to PCC is achieved by the low molar CaO/SiO_2 ratio of 2, which overall cuts the process emissions by about 30%.

The LT-BCC produced consists to a large extent (>60 wt.%) of the calcium silicate belite (Ca_2SiO_4) present in both polymorphs: β-C_2S and $\alpha`_H$ C_2S. The most common clinker mineral of today's PCC, alite (Ca_3SiO_5) is not present. LT-BCC is intended to at least partially replace PCC in accordance with cement standards. The initial target in the research project URBAN [4] is a substitution rate of 30 wt.%. High sulfate contents in the waste fines may result in the formation of ternesite or ellestadite if $CaCl_2$ is used as mineralizing agent. Besides clinker, highly concentrated CO_2 exits the kiln (90-95 wt.%).

LT-BCC processing has been successfully tested using different wastes e.g. post demolition autoclaved aerated concrete (AAC) [5] and has been demonstrated on a 1.5-ton scale using waste concrete fines. The replacement of 25 wt.% Portland cement by LT-BCC in the production of AAC has been demonstrated on a technical scale [6]. The total reduction of emissions depends in particular on the available electricity mix. If only electricity from renewable sources is used, 400 kg CO_2 per t LT-BCC was calculated [7].

A pilot plant with a capacity of 10kg/h is currently being built at KIT funded by the Ministry of the Environment Baden-Württemberg [8]. The closing of the concrete cycle is being optimized in the URBAN project [4] together with several industrial companies (cement manufacturers, construction chemicals companies, and manufacturers of precast concrete parts). As part of the Innopool project EuK [9], a superstructure approach is being developed in collaboration with the Jülich Research Centre [10] to identify scenarios under which the production can become economically and ecologically viable.

4. Hydrothermal carbonatization of recycled aggregate from waste concrete

The mechanical processing of waste concrete leads preferentially to fractures in the hardened cement paste. Therefore, about 50% of the cement content of waste concrete is found in the crushed fine fraction, although it represents only about 30% of its total mass. The other half of the cement remains in the recycled aggregate and increases both, its specific surface area and porosity, which degrades its properties compared to natural aggregate. In the production of RC concrete, this is usually compensated for by increasing the cement content.

One possibility to close the porosity of hardened cement paste is carbonation, which causes an increase in volume. However, under standard conditions, turnover and reaction rate are very limited. Freshly precipitated calcium carbonate closes pores and cracks near the surface thus preventing the further transport of carbonate ions into the interior of the grain.

One approach to increase the carbonation yield is to further increase the specific surface area by crushing. However, the material can then no longer be used as concrete aggregate, but only as a substitute for sand or as supplementary cementitious material (SCM). The use as SCM is pursued in the Marie Skłodowska-Curie Doctoral Network CO2Valorize funded by the European Commission.

The aim of the approach pursued in the zero-emission circular concrete project is to reduce clogging using suitable reaction control in a technical autoclave, similar to that used for AAC production. The effectiveness of the approach has been demonstrated on a laboratory scale. For carbonation, the concentrated CO_2 from the clinker kiln is used. A conversion of $> 80\%$ of the sequestration capacity within a treatment period of 6h is aimed at. The autoclave is heated by the waste heat of the clinker kiln.

11. Conclusions

High quantities of cementitious mineral wastes such as waste concrete, post-demolition autoclaved aerated concrete (AAC), and others on the one hand, and decreasing quantities of landfill capacities for mineral residues on the other hand require higher recycling rates in Germany. The approach of zero emission circular concrete developed at KIT combines high-quality closed-loop recycling with the sequestration of released CO_2 into the generated products. The concept is primarily designed for small, decentralized plants with an output of about 50,000 t/a cement clinker, which corresponds according to own calculations to the waste concrete fines generated annually in an urban area of about 1 to 1.5 million inhabitants, and within an average transport distance of 20 km.

The zero-emission circular concrete plant consists of a clinker line for LT-belite cement clinker, which is coupled with an autoclave line for the carbonation of the aggregates. Both modules could also be operated independently. An LT-BCC line at the site of an existing cement plant would be possible.

The variable composition of secondary raw materials derived from wastes and the potential contamination with constituents harmful to concrete requires, on the one hand, an elaborate and as yet not established analytical routine and mixing technology. On the other hand, cement standards may have to be adapted if the concept of insoluble reservoir minerals presented is to be used for general applications.

References

[1] Achternbosch, M. and Stemmermann, P., "The carbon uptake by carbonation of concrete structures – some remarks by perspective of TA," 1000131215, 2021, doi:<u>10.5445/IR/1000131215</u>.

[2] Hunsinger, H., Beuchle, G., Stemmermann, P., Schweike, U. et al., "Verfahren zur Herstellung von Dicalciumsilikat," WO 2014/019656 A1.

[3] Ullrich, A., Garbev, K., Schweike, U., Köhler, M. et al., "CaCl$_2$ as a Mineralizing Agent in Low-Temperature Recycling of Autoclaved Aerated Concrete: Cl-Immobilization by Formation of Chlorellestadite," *Minerals*, 2022, doi:<u>10.5445/IR/1000150781</u>.

[4] "Verbundvorhaben URBAN - CO$_2$-reduzierter Beton durch Upcycling von Reststoffen aus der Betonaufbereitung und CCU," FKZ 03EE5130A BMWK, 7. Energieforschungsprogramm, 2022 bis 2025.

[5] "ReziProK - Verbundvorhaben REPOST - Recycling-Cluster Porenbeton: · Optimierung von Rückbau und Sortierung von Altporenbeton und Erarbeitung neuer Optionen für die Kreislaufführung von Porenbeton - TP 4: Dicalciumsilikat aus Porenbetonresten aus Abbruchmaßnahmen,"(FKZ 033R249D), 2019-2022.

[6] Stemmermann, P., Ullrich, A., Beuchle, G., Garbev, K. et al., "Belite cement clinker from autoclaved aerated concrete waste – A contribution towards CO$_2$ -reduced circular building materials," in *CE/Papers 2022 – 2022 Xella International Colloquium*:17–26.

[7] Stemmermann, P., Volk, R., Steins, J.J., and Beuchle, G., "Recycling belite cement clinker from post-demolition autoclaved aerated concrete – assessing a new process," *submitted to Journal of Industrial Ecology*, 2023.

[8] "R-Zement: CO$_2$-arme Herstellung des Klinkerminerals Dicalciumsilikat aus Recycling - Baustoffen,"(L7521115), 2021-2024.

[9] "Innopool Projekt Energiewende und Kreislaufwirtschaft (EuK): Dekarbonisierung und Flexibilisierung energieintensiver Recycling-Prozesse," 1/2021-12/2023.

[10] Paredes, A.Y.O., Sandaka, G., Beuchle, G., Stemmermann, P. et al., "Superstructure optimization for a novel cement production process utilizing secondary raw materials," *Abstracts*, Helmholtz Energy Conference, Koblenz, 12. - 13.6., 2023.

CLOSER - A PROJECT FOR IMPLEMENTING PRE-DEMOLITION AUDITS IN PORTUGAL

Martins, I.[1,*]

(1) Laboratório Nacional de Engenharia Civil, Portugal

imartins@lnec.pt

Abstract

The construction industry is one of the largest sectors in Europe and, on average, construction and demolition waste (CDW) accounts for one-third of the total waste generated. The recovery rate of these wastes surpasses the 70% target defined in the Waste Framework Directive 2008/98/EC. Nevertheless, this fact does not ensure that the sector is moving towards a transition from a linear to a circular economy at the end-of-life phase of buildings.

In Portugal, a recovery rate of 95% of non-hazardous CDW prepared to reuse, recycling or other recovery operations is reported, although more than half of these residues are used as material for backfilling, therefore it does not represent a true circular transition due to downcycling.

The project CLOSER, aiming to promote the application of circular economy principles by reducing material use and waste production, assessed the actual Portuguese practice for the management of CDW and evaluated the benefits of performing a pre-demolition audit in a pilot study. This project highlighted the crucial relevance of investing in training to improve green and digital skills. In what concerns building materials/elements reuse and recycling, changes to national policies were proposed.

1.   Introduction

The alteration of resource growth trend as a way to achieve ecological and economic stability was pointed up in *The Limits of Growth* [1]. Over 50 years later, the increase in resource depletion calls more than ever for efficient actions that counterbalance the increased consumption of natural raw materials. This aspect is of utmost relevance for the construction sector, which accounts for 40% of all materials used in urban areas and for one-third of the total waste generated [2].

Different strategies along the whole life cycle have been proposed to decrease the high environmental impacts related to the construction sector and to boost the transition to a low-carbon built environment. Examples of such strategies include material choice in the design phase, prefabrication and modularity in the construction phase, and deconstruction and recovery of construction and demolition waste (CDW) at the end-of-life.

Focusing on end-of-life, the enforcement of a 70% target for CDW recovery in Europe [3] has proven to be insufficient to tackle issues such as the proper sorting of this waste stream or the routing of the recovered resources to the application that adds the most value to it. In Portugal, although a recovery rate of 95% of non-hazardous CDW prepared to reuse, recycling or other recovery operations is reported by Eurostat, more than half of these residues are used as material for backfilling and the largest part is mainly made up of mixed waste (17 01 07 and 17 09 04) [4].

The circular material use rate of 2.2 in 2020 and the OCDE review of Portugal's environmental performance highlight that major challenges remain concerning sustainable consumption and production patterns (SDG 12) and new strategies must be implemented to ensure a circular transition to close the loop of the resources [5].

The project CLOSER – Close to Resources Recovery was developed to assist in the minimization of CDW production and in enhancing material reuse during total or partial demolition of buildings by performing Pre-Demolition Audits (PDA). This was a 1-year project promoted by the National Civil Engineering Laboratory (LNEC), the Portuguese Environment Agency (APA) and the Institute of Public Markets, Real Estate, and Construction (IMPIC), which have national-level competencies in the areas of civil engineering works, environment and building regulations, respectively. The project assessed the use of PDA in European countries, sent a questionnaire to construction companies about their practices concerning the demolition of buildings, prepared a Portuguese Guide for Pre-Demolition Audits, evaluated the benefits of performing PDA in a pilot study and proposed the relevant legislative amendments.

2. Methods and results

2.1 The questionnaire

The questionnaire outcomes were supported by 680 valid responses, for an approximate population of 40000 construction companies, and for a confidence level of 98%, the margin of error of the answers is estimated below 5%. For the analysis of responses to the open-ended questions the Yake Natural Language Processing (NLP) program, which uses artificial intelligence (AI), was used to collect the important keywords repeated among the participants' answers as well as analysing patterns of 2- and 3-word sets.

The questionnaire carried out showed that 90% of the companies engaged in construction activities are micro and small enterprises, performing demolition and rehabilitation for several years, not committed to waste management, as evidenced by the low investment of their budget in waste management, the lack of knowledge of the applicable legislation and little practise on preventing the production of CDW or to sort these residues. On the other hand, medium and large enterprises easily spread the culture of proper waste management.

The destination for materials arising from the resources retrieved during building demolitions is shown in Fig. 1. It is important to draw attention to some features: there is a high elimination percentage of mineral-based materials like concrete or bricks that are not justifiable; the quite similar destinations for single streams and mixtures of streams may indicate a downgrading of the first; the reuse practise is overlooked to recycling; the metals are the material with the highest recycling rate.

Another very important aspect to be emphasized in the data of Figure 1, is the lack of understanding that hazardous substances or materials containing hazardous substances,

specifically asbestos, have to be eliminated when removed. The two bottom bars of the chart highlight the practice of reuse, recycling or other recovery operations for resources containing dangerous substances, for up to 25% of these resources. This practice would favour the continuity of these substances in the loop contaminating other materials

The data in Figure 1, reveals that there is scope to improve the potential of the retrieved materials/elements/waste for future uses, mainly if a pre-demolition audit is implemented. Additionally, the upskilling of workers towards understanding how to manage resources at end-of-life is urgent, especially for dangerous substances.
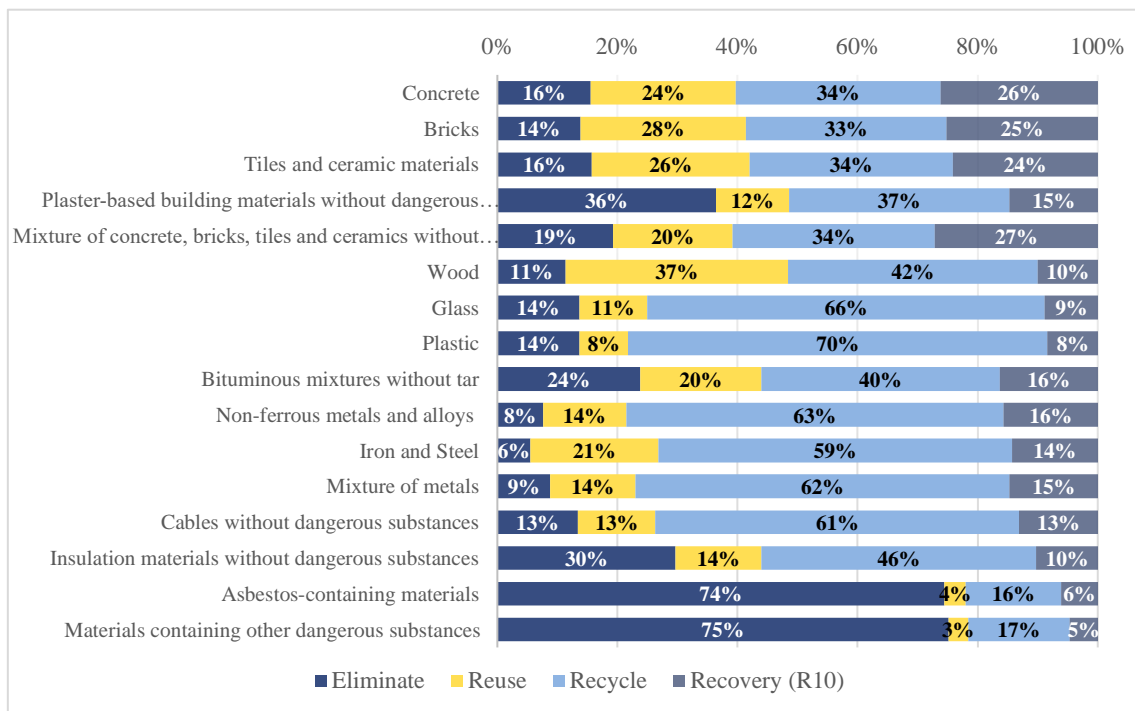

Figure 1: Destination of retrieved materials

The survey also identified that workers' training is not geared towards providing skills in the field of circularity. Only about a quarter of respondents answered positively regarding specific training on deconstruction and demolition and it was found that even the basic concepts of reuse and recycling have not been internalised. Traditionally, the construction sector is reluctant to make major changes but raising awareness and improving the competencies of the labour force is essential and is a priority to drive the transition to a circular economy model. This is a barrier to minimising CDW generation and increasing reuse during building demolition.

2.2 Portuguese guide for pre-demolition audit

The European pre-demolition assessment guidelines and the Level(s) framework regarding the sustainability of buildings were used as support documents for the development of the Portuguese guide for pre-demolition audit of buildings to be demolished or rehabilitated [6,7].

The pre-demolition audit encompasses a desk study complemented by an *in-situ* study for elaborating an inventory of materials/constructive elements and wastes (Fig.2), and proposals for their potential destinations so that these resources re-enter the economy.

Material	LoW Code	Nature of waste	Quantity	Unit	Conversion factor	Estimated quantity (kg)	Quality (Condition)	Floor	Location(s) of material in building / building site	Preferred destination	Precautions to take	Additional information	Photos
concrete	17 01 01	Inert/Non dangerous	12.00	m3	2300	27600	Very good – Negligible anomalies	1	Interior walls	Recycled aggregates			
tiles	17 01 03	Inert/Non dangerous	25.00	kg	2.4	60.0	Good – Aesthetic anomalies	3	Roof covering inclined	Reuse element/material on site	Handle with caution		
wood	17 02 01	Dangerous	4.00	m3	700	2800.0	Medium – Anomalies could hinder reuse	3	Roof structure	Landfill for dangerous waste	Personal protective equipment	Positive test	

Resources Inventory — Materials/ Elements & CDW

Figure 2: Inventory

Particular attention has been given to dangerous substances to decrease their presence in future building materials. Within this context, the Portuguese guide comprises a list of potential groups of dangerous substances and their common location within the buildings. A set of factsheets for the most usual resources collected during demolition and their feasibility of being reused or recycled was also included in the guide.

In practice, the implementation of a PDA should be supplemented with a deconstruction of the building to lead to maximum environmental and economic benefits. To this end, the contractor must ensure that workers have adequate skills.

2.3 Pilot case

To quantify the improvements in the recovery of resources with and without the application of the Portuguese guide for PDA, more than 200 construction companies have been contacted to know about the feasibility of having one or more buildings to be demolished at the time of the CLOSER case study task.

The case study was carried out at Cais da Malveira (Fig. 3). This is a building used only for the storage of products in a railway station. Although this is not the usual type of building to be demolished, it was the only one that was made available for carrying out the pre-demolition audit followed by deconstruction.

Figure 3: Cais da Malveira (East view)

An analysis of the impacts of end-of-life practices was carried out. Based on the map of quantities of recovered CDW and reused material/elements the economic and environmental

impacts were estimated using a tool developed within another research project aimed at improving the transition to a circular economy. Considering that the tool used only covers a restricted set of construction elements and materials, the impacts of the whole of the materials/elements removed during deconstruction were not surveyed. Other constraints due to the used tool were assessed in the project. Therefore, the approach used only estimated the difference between the impacts of the materials that were reused and those impacts if these materials were recycled.

The tool used is based on the Waste Reduction Model (WARM) [8], developed by the USA Environmental Protection Agency (EPA), which provides estimates of the potential GHG emissions, energy savings and economic impacts of baseline and alternative waste management practices. According to the WARM methodology, the impacts of reuse correspond to the emissions avoided from the use of a new product, therefore a negative value is assigned to the impacts of production. On the other hand, the impacts of recycling, include all the impacts associated with the collection, transportation, processing, and manufacturing of the recycled material into a new product for use. The benefit associated with the avoided production of the same quantity of product from virgin materials is also calculated. This benefit is the difference between the impacts of producing material from 100% input of recycled raw materials (considering material losses) and the impacts of producing an equivalent quantity of material from 100% input of virgin raw materials.

The original plan of waste management for the demolition of this building did not address the reuse of the existing materials/elements. After performing the PDA, it was identified that 49.73 tonnes of materials were to be reused on-site and off-site. The remaining, 96,42 tonnes, were classified as CDW. There was a decrease of 34% in generated CDW due to the feasible reuse of resources identified in the pre-demolition audit. As regards dangerous substances, 1.5 tonnes of materials containing asbestos fibres were identified and removed by a certified company for elimination. An assessment of the possible contamination of timber beams that rely near the panels with asbestos was carried out by SEM analysis with negative results.

The results in Table 1 showed that in terms of environmental impacts, the recycling option is better for the elements in question because it leads to a larger quantity of avoided CO_2- eq emissions.

The analysis of these results highlights that in the case of the steel doors, the fact that steel is a mixture of virgin and recycled material (steel is rarely produced with 100% virgin raw material input) could be assigned to reuse being less beneficial than recycling because the amount of virgin raw material avoided in recycling is less than the amount in the material reused.

In what concerns to clay roof tiles, there is no specific recycling destination for this product. It was assumed that it is possible to recycle broken or damaged roof tiles when mixed with other construction and demolition waste. The WARM methodology used in the tool does not consider recycling for clay, it only considers reuse and landfill. However, the tool did consider the benefits associated with recycling mixed CDW, based on the literature. There is therefore a level of uncertainty associated with the use of different sources of information and calculation methodologies that could be assigned to have better environmental impacts for recycling.

It should be emphasized that the tool used is to carry out a preliminary analysis of the impacts of end-of-life practices. More reliable data demands for collecting and implementing product-specific data and interpreting results of environmental impacts in a building project, preferably including contacting a life cycle assessment (LCA) consultant.

From the perspective of economic impacts, they are frankly more positive in the case of reuse.

Table 1: Environmental and economic impacts

Construction elements	Environmental impacts (kg CO_2.eq)		Economic impacts (€)	
	Reuse	Recycling	Reuse	Recycling
Wood	-93	-59	- 236,916	897
Clay roof tiles	-67	-84	- 33,246	5,867
Steel doors	-147	-222	- 201,836	13,037
TOTAL	-307	-365	- 471,998	19,801

It is noteworthy that only collecting and implementing product-specific data would allow an accurate assessment of the impacts associated with this second life of the reused materials, namely the negative impact of transporting the ceramic roofing tiles to the building where they will be laid and the benefit of avoiding the production of new tiles. Additionally, performing a life cycle analysis (LCA) would assess several environmental impacts and all life cycle stages giving an in-depth analysis, and allowing more informed decisions about reuse and recycling alternatives. It is also relevant to mention that other impacts, like the dismantling process or the excessive use of resources for preparing constructive elements to reuse, can overlap the environmental benefits in general assigned to reuse.

2.4   Legislative amendments

The Portuguese Decree-Law no. 46/2008, which created legal conditions for the correct management of CDW favouring the prevention of production and hazardous materials, resulted from a national initiative and, unlike other waste streams, the European Union did not issue specific legislation for CDW.

Currently, the CDW management is under the Decree-Law no. 102D/2020 and within the activities of the CLOSER project the following major amendements were proposed: i) the producers of CDW must take the necessary measures to ensure the selective collection of waste at source and in case of demolition or renovation of buildings when the area to be demolished or rehabilitated is larger than 100 m2, promote the pre-demolition audit; ii) the owner of the building is responsible for appointing an auditor, or team of auditors, who shall prepare an inventory identifying and quantifying the materials and building elements to be reused and the construction and demolition waste, as well as a preliminary plan for their disposal; iii) the auditor or the team of auditors must be a qualified expert, or integrate qualified experts as appropriate, with appropriate knowledge of current and past building materials (including hazardous materials), current and past construction techniques and construction history; they must also be familiar with demolition techniques, waste treatment and processing, and (local) markets; iv) the model for the inventory of materials will be published on the Portuguese Environmental Agency.

3.   Conclusions

For a long time, CDW has been looked at as an inevitable stream. The increasing efforts developed toward the recyclability and the reusability of CDW/building elements/materials at the end-of-life have evolved at different paces in the various Member States.

The project's CLOSER objectives aimed at having better control of quantities of resources generated during the demolition and rehabilitation of buildings, providing possible destinations for these resources, and minimizing the content of dangerous substances for secondary uses. To this end, a Portuguese guide for pre-demolition audits was elaborated.

The efficacy of the PDA was assessed in a pilot study and a preliminary approach to the environmental and economic benefits was performed. More reliable impacts of reuse and recycling must be provided through LCA analysis. The reuse of resources recovered during the demolition decreased the generation of CDW. The recovery of the existent resources has privileged the uptake of reuse as the main operation for materials arising from the demolition.

The amendments to the Portuguese CDW legislation have not yet been reached. although it is expected that the transition to a circular economy model in the construction sector may favour its implementation.

4.   Acknowledgements

The author acknowledges the partners APA and IMPIC, for the successful development of the CLOSER project, and Infraestruturas de Portugal which enabled the pilot study to be carried out.

5.   References

[1] Meadows, D.H., Meadows, D.L., Randers, J., Behrens Ill, W.W., "The Limits of Growth: Report for the Club of Rome´s Project on the predicament of mankind", (Universe Books, New York 1972).

[2] Olubukola O.T., Rodgers, G., Waschl, B., Salter, J., Ashraf, M., "Harmonising life cycle sustainability thinking in material substitution for buildings". Resources, Conservation and Recycling, Volume 185, 2022.

[3] Directive 2008/98/EC of the European Parliament and of the Council of 19 November 2008 on waste and repealing certain Directives (Text with EEA relevance). OJ L 312, 22.11.2008, p. 3-30.

[4] Eurostat. Treatment of waste, by waste category, hazardousness, and waste management operations (online data code: ENV_WASTRT), 2020.

[5] OECD. Environmental Performance Reviews: Portugal 2023 [online] https://read.oecd-ilibrary.org/environment/oecd-environmental-performance-reviews-portugal-2023_d9783cbf-en#page11

[6] European Commission. Guidelines for the waste audits before demolition and renovation works of buildings. GROW.DDG1.C.4, 2018.

[7] Donatello S., Dodd N. & Cordella M., 2021. Level(s) indicator 2.2: Construction and Demolition waste and materials user manual: introductory briefing, instructions and guidance (Publication version 1.1), 2021.

[8] EPA, Waste Reduction Model (WARM). https://www.epa.gov/warm/basic-information-about-waste-reduction-model-warm, 2023.

CONSTRUCTION AND DEMOLITION WASTES RECYCLING IN BRAZIL: EVOLUTION AND CHALLENGES

Leonardo C. Machado[1], Lidiane S. Oliveira[1], Levi Torres[2], Sérgio C. Angulo[1],*

(1) University of São Paulo, Escola Politécnica - Brazil

(2) Brazilian Association for Construction and Demolition Waste Recycling (ABRECON) - Brazil

* email(s) of the corresponding author(s): *sergio.angulo@lme.pcc.usp.br*

Abstract

In 2000, the resolution 307 was implemented by the Brazilian environmental council (CONAMA) establishing procedures to properly manage construction and demolition waste (CDW), and CDW recycling started to increase after it. In 2010, the Brazilian Association for CDW Recycling (ABRECON) was founded. The association has worked for the last 10 years in the structuration of the CDW recycling private sector and produced periodically national reports about the evolution of CDW recycling in Brazil. The objective of this manuscript is to present some results of the last reports (2020, 2022) organized by the authors. The number of Brazilian recycling plants over time was presented herein; 334 operational CDW recycling plants in 2022, most of it fixed and operated by private sector. The recycling plants can recycle 50% of CDW produced in Brazil and the actual CDW recycling rate in the country is 33%. Discussions about regional differences in the country, territorial occupation and size of municipalities, infrastructure and logistic scenario, and public policies were done to face the challenges to implement a high recycling rate.

1.   Introduction

In 2015, the recycling rate of construction and demolition waste (CDW) worldwide was around 30%, by mass [1]. Most of the CDW has been landfilled despite the long effort to promote CDW recycling. Countries like the Netherlands, Germany and Japan has achieved recycling rates of 90-100% in the last decades [2]. Other countries as France, Spain, Portugal, United States and China have increased the recycling rates to 60%. Therefore, there are challenges to advance CDW recycling particularly in populous developing countries such as India, Brazil, Russia, Indonesia, Pakistan, Bangladesh, and Mexico, once the higher the population, the higher the CDW generation [3,4] (**Table 1**).

Nowadays, Brazil has a population of over 203 million inhabitants[1]. Previous studies about CDW generation in Brazil have pointed to a median CDW generation per capita of 0.5 ton/

---

[1] https://cidades.ibge.gov.br/

inhabitant-year [5,6]; therefore, we assume herein that around 100 million of tons of CDW are generated in Brazil.

In 2000, Brazilian environmental council approved a specific resolution CONAMA 307 establishing procedures for the CDW management [7]. The disposal of CDW in sanitary landfills was prohibited by CONAMA 307 since then, and the resolution promoted the implementation of CDW sorting and recycling units to avoid illegal dumping at the cities. A public management network has been provided to collect the small-scale CDW generator; typically, citizens who self-construct houses and undertake housing renovations, as well as a private CDW management network to attend construction and demolition companies, regulated by public sector in terms of operating concessions. The informal sector plays an important role in developing countries (around 50% of CDW generation in Brazil) [5] and the CDW public management has progressed slower than that of private sector operated by companies. Since 2000, CDW recycling plants have been implemented progressively [8].

Table 1 – Population, CDW generation and a relation with the Gross Domestic Product (GDP) per capita.

Country	Population (inhabitants)	CDW Generation (in tons)	CDW per capita[1] (tons/inhab.year)	GDP per capita (US$ / inhab)
United States	334 million	700 million	2.1	80,000
European Union (27 countries)	448 million	800 million	1.8	39,940
China	1.4 billion	2.3 billion	1.6	13,721
India	1.4 billion	1 billion	0.7	2,601
Brazil	203 million	107 million	0.53	9,672

[1] CDW generation excludes soils.

In 2010, the Brazilian Association for CDW Recycling (ABRECON[2]) was founded. This action was motivated by the publication of a Brazilian law that implemented the political guidelines to manage the solid wastes [9]. In this document, an integrated solid waste management was proposed considering the integration of federal, states and municipalities plans. The CDW managing plan should take part of it. ABRECON has acted in the last 10 years structuring the private CDW recycling sector and periodically published national reports on CDW recycling. In the last edition, the authors of this manuscript have worked with this association producing the newest versions (2020 and 2022). The 2020 CDW report was published in Portuguese, and it can be freely downloaded [10].

1.1   Objective

The objective of this manuscript is to discuss the evolution on CDW recycling in Brazil bringing herein some results of the latest reports (2020, 2022) [10] and point the challenges for the

---

[2] https://abrecon.org.br/

progress of the CDW recycling in Brazil. We believe that the lessons learned may help other developing countries to improve CDW recycling scenarios and enhance the circularity of such important waste stream in society.

2.   Methodology

Since 2010, the association (ABRECON) registers the CDW operators as sorting-recycling plants and inert landfills. To consider a company operational, the criteria used by secretary were: i. a regular e-mail contact with the producer, ii. Google image showing the real operation in the informed place, among others. This list has been updated in every CDW report produced (2013, 2015, 2018, 2020). The 2022 report is currently in progress.

In the 2020 CDW report, questionnaires developed by ABRECON using Google Forms tool were applied [10]. One of those was applied to the owners of either CDW sorting/recycling plants, or CDW inert landfills. In the analysis, duplicate data entries, responses that deviated significantly from the expected pattern indicating a lack of understanding of the question, typing errors, or blank fields were not considered. After the data selection, we obtained valid results from 113 CDW recycling plants/landfills owners between years of 2019 and 2020. The 2022 valid answers corresponded to 20% of the total number of plants catalogued and operating in the country; therefore, data has representativeness.

The questionnaire contained 48 questions including open-ended questions and multiple-choice questions. The questions covered topics such as: company/plant's profile, information about the city in which it was established, monthly reception and production volumes, control systems, equipment used, characterization of the material received, market challenges, among others. The analysis was conducted based on their responses, with the application of certain extrapolation factors.

To estimate the CDW generation value, the factor of 0.5 ton per inhabitant per year was applied [6]. Based on the recycling capacity, the quantity of CDW received, and Recycled Aggregates (RA) production, we extrapolated the data considering the catalogued quantity of CDW plants, or those where operation is confirmed.

3.   Results

Erro! Fonte de referência não encontrada. shows the quantity of operational CDW sorting-recycling plants or inert CDW landfills catalogued in Brazil in the last 30 years. After 2002 and the publication of CONAMA resolution 307, Brazil experienced a substantial increase in the quantity of CDW plants per year. The quantity of CDW plants per year reduced after 2015, which may be related to the financial crisis started after that.

In 2023, 334 operational CDW plants in the country. 2/3 of it (near 200 plants) are fixed plants which have a larger processing capacity. 1/3 of it (near 100 plants) are mobile plants and started to operate after 2008 mainly near demolition sites or construction sites dedicated to large infrastructure projects, such as stadiums of the Olympic games, sanitary and transportation networks near large cities. 2/3 of these plants are operated by the private sector.

Mobile plants do not yet constitute the majority of CDW plants in the country as it is the case in Germany [11] or other countries where demolition waste plays the major role. In Brazil, demolition waste demolition is not large, usually less than 25% of CDW volume. Construction

and renovation waste usually represents 75% of the total volume [12]; particularly in medium to low-size cities where live around 70% of Brazilian population. We believe that the market for mobile plants will grow significantly in the next decades to recycle concrete roads, infrastructure construction sites and old multi-storey buildings located in large cities, mostly of those constructed after the Brazilian construction boom lived on the 1970s.
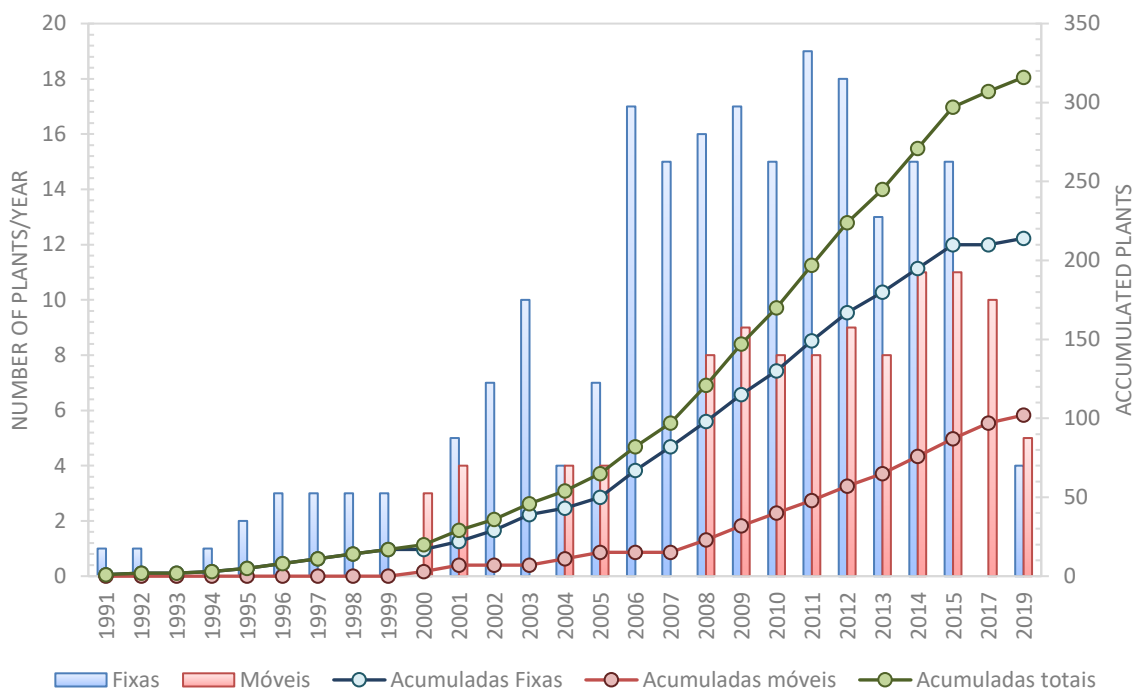

Figure 1 – Quantity of CDW recycling plants in Brazil over time. Data from Miranda, Angulo [8] **joined with data from the CDW reports.**

Although the number of Brazilian CDW plants have been increasing over the time, the recycling rates is not as high as other countries such as Germany, Netherlands, Portugal, Spain (**Table 2**).

Table 2 – Recycling rates and processing units of different countries

Country	Recycling rate, without landfilling (%)	Recycling rate, with landfilling and incineration (%)	Number of construction and demolition waste (CDW) processing units
Netherlands	97	97	-
Germany	80	90	12,000
France	60	70	-
Spain	60	70	4,000
Portugal	45	95	500
Brazil	23	33	575 units: 230 fixed plants, 100 mobile plants 113 inert landfills 118 sorting areas

The distribution of the CDW plants is not uniform in Brazil. The Southeastern and Southern regions are responsible for the largest quantity of the CDW plants (near 80% of the total),

notably in the state of São Paulo (near 54% of the total). These regions present the best management and recycling scenario for solid wastes, where sanitary landfills exhaustion exist, CDW illegal dumping near cities are frequent, and environmental state agencies are very active. Due to the high demand for aggregates near the large and medium size cities, CDW aggregates can be offered by reduced prices compared with those of natural aggregates. In some regions near the metropolitan regions of São Paulo and Rio de Janeiro, there is a scarcity of natural sand and restrictions for mining sand. Crushed rock (alternative, industrially processed) sand has been commonly used over decades, and CDW aggregates can contribute as an alternative source. Crushed coarse aggregates are usually transported over 50 km where CDW recycling and logistic optimization in CDW management and recycling become more attractive and economically feasible [13].

In the 2020 CDW report [10], we estimated aproximatelly 105 Mton/year of CDW in Brazil. Therefore, the Brazilian recycling plants had the capacity to recycle about 50% of the waste volume. In fact, only 23% was recycled (Figure 2). The recycling rate can be calculated dividing the CDW received at the plants by the CDW generated. The authors believe that it is more accurate way to calculate instead of using CDW recycled aggregate production divided by the CDW generated. Soils, wood, gypsum, among other sorted materials in the recycling plants are also directly reused as landfilling material, or recycled. After processing, there is also a reduction of the effective volume due to better accommodation of the crushed material.

The CDW recycling scenario suffered a drop in the 2018 economic crisis, as well as due to the pandemic period of COVID-2019. The 2022 CDW report is in progress and will be published soon. The preliminary results of 2022 show that the recycling rate in Brazil increased to 31%, the best scenario observed and close to the rate of 2015 (a period of economic prosperity in Brazil). 70% of CDW is not recycled, and a higher part of CDW is being disposed in improper operated public landfills or illegally dumped in streets or in informal large urban areas. As a result, geotehcnical accidents have occurred in large cities involving many deaths. The monitoring of geological and risk areas in cities has been usually done to avoid similar disasters, and it is necessary to improve the life conditions of urban less favorable populations.
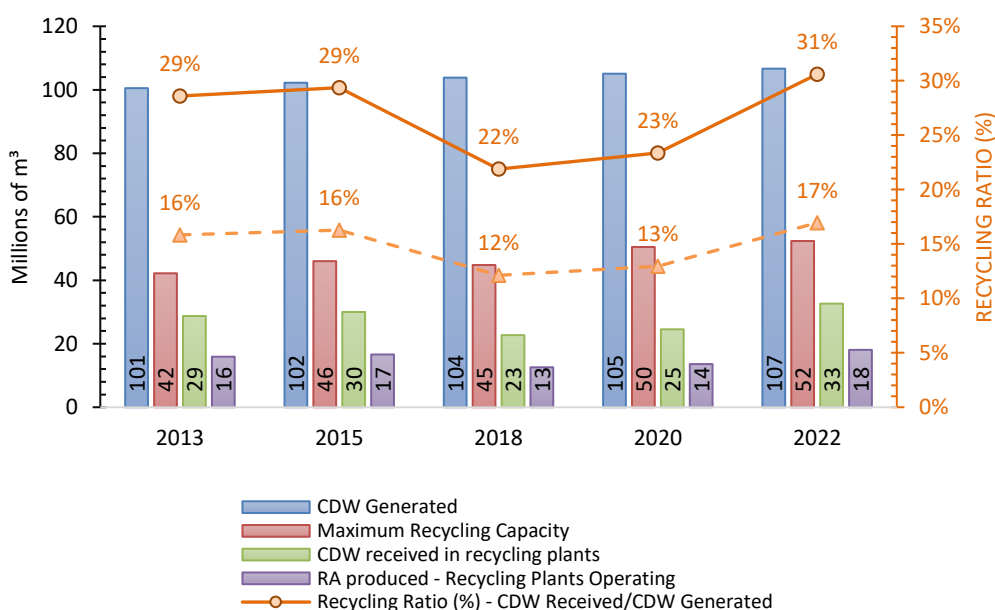

Figure 2 – CDW generation and recycling in Brazil.

Some public policies have been implemented over the years to combat this scenario, but the results are still far from reaching the ideal goals. So, initiatives to monitor illegal CDW or waste disposals in the cities have been done by ABRECON together with the Brazilian companies' association for solid wastes collection and treating (ABRELPE) targeting the elimination of this practice and assisting better public sector action.

Brazil is a continental-sized country with diverse economic, geographical, and environmental characteristics, which ultimately impacts how waste is managed and recycled. The **Figure 3** illustrates the regional disparities in CDW generation, recycling capacity, and actual recycled aggregate (RA) production in 2020.
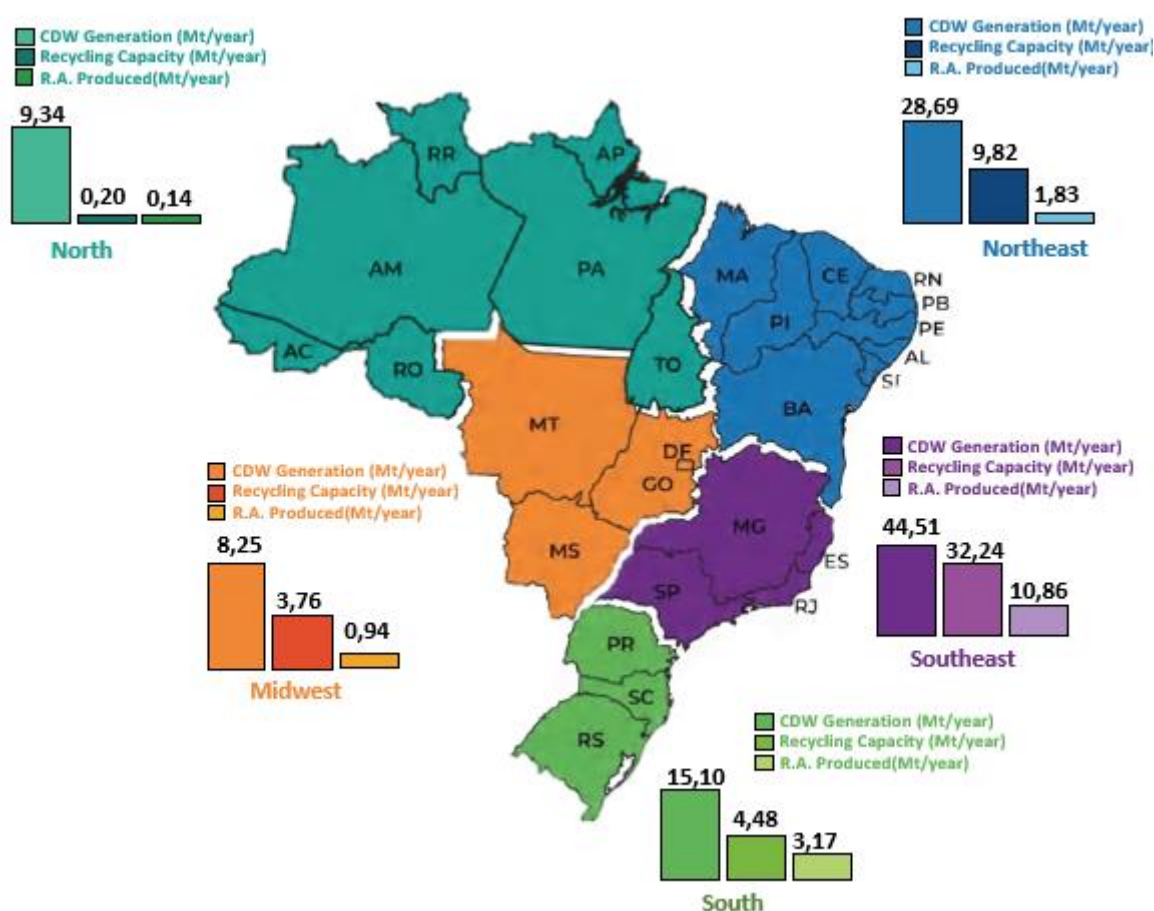

Figure 3 – Scenario of CDW generation and recycling for Brazilian regions in 2020 [10].

Considering the vast territorial dimensions of Brazil, and that half of the population lives near the coast in large and medium-size cities (more than 50,000 inhabitants), a logistical challenge exists. Half of the population lives spread in 5,000 small municipalities (less than 50,000 inhabitants) of a total of 5,500 municipalities, spread across the largest area of the country. In the countryside region, there is no adequate infrastructure, particularly in terms of road conditions. The Northern and Midwest regions are regions where there is the largest lack of infrastructure. The Northern region has recurrent flooding of cities and roads during year. The

logistical obstacles make it challenging to meet the demands. In small cities, recycling is not economically feasible, and the solid waste management scenario is not properly implemented due to high costs involved in the implementation of sanitary landfills. Despite we have policies to increase recycling targets, there is no clear policy to zero landfills or circular economy strategy. The investment to obtain sanitary landfills has dictate the municipality actions over last decades without success; there is an absence of public agents able to deal with financial system, and a lack of specialists in public sector to deal with waste and environmental issues.

When comparing the selling price of natural coarse aggregate (NA) with that of recycled coarse aggregate (RA), in 2022, a significant difference is evident (**Figure 4**). Furthermore, the preliminary results of the 2022 CDW report show that this difference increased after the COVID-19 pandemic. This discrepancy can be attributed to two main factors: i. Many recycling plants in Brazil began operations without proper physical space planning, leaving little space for stockpiles, and improper operating conditions (focus on CDW crushing instead of sorting, its efficiency). The focus has been only in fees charge to receive CDW at the plant. Many facilities developed a habit of either donating or selling recycled aggregates at a very low price to clear their inventories and make space for new CDW receiving. ii. Brazil still lacks a culture of purchasing recycled aggregates among public authorities and builders. Without a proper product codification, the material cannot be large offered in public selling systems. A perception held by many is that recycled aggregates have lower quality and there is a lack of knowledge on how to properly apply them. As a result, recycled aggregate prices are often reduced to keep a minimum attractiveness on the market.
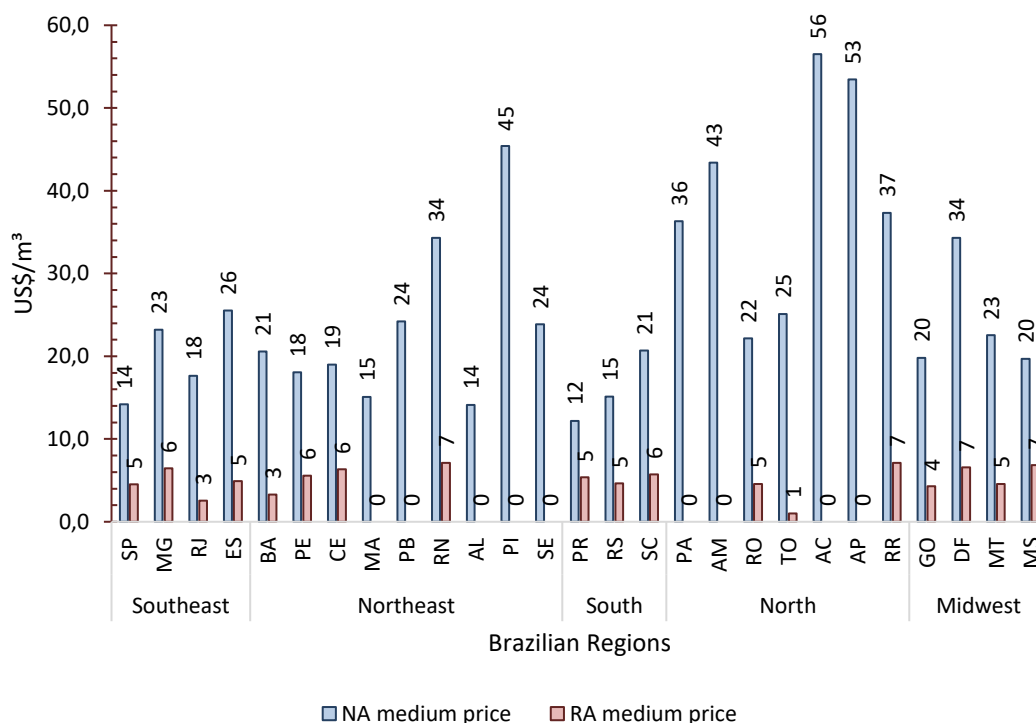

Figure 4 – Natural and Recycled aggregates selling prices at different Brazilian states in 2022 [10]

4.   Conclusions

This study presented the evolution of the CDW management and recycling in Brazil over recent decades. Brazil is a continental country with regional disparities. Although some significant progress has been made, there is a long way to achieve high recycling ratios. Challenges associated with irregular CDW disposals, logistical and infrastructure problems, implementation of more effective public policies, the lack of culture of purchasing recycling aggregates are factors, among others, which need to be faced to achieve highest indicators. There is space to increase the number of recycling plants, including the mobile ones. Sorting seems to be an important topic to improve CDW aggregate quality.

5.   Acknowledgements

6.   References

[1] W. Haas, F. Krausmann, D. Wiedenhofer, M. Heinz, How Circular is the Global Economy?: An Assessment of Material Flows, Waste Production, and Recycling in the European Union and the World in 2005, Journal of Industrial Ecology. 19 (2015) 765–777. https://doi.org/10.1111/jiec.12244.

[2] V. Monier, S. Mugdal, M. Hestin, M. Trarieux, S. Mimid, Service contract on management of construction and demolition waste, Bio Intelligence Service S.A.S., Paris, 2011.

[3] H. Wu, J. Zuo, G. Zillante, J. Wang, H. Yuan, Status quo and future directions of construction and demolition waste research: A critical review, Journal of Cleaner Production. 240 (2019) 118163. https://doi.org/10.1016/j.jclepro.2019.118163.

[4] K. Chen, J. Wang, B. Yu, H. Wu, J. Zhang, Critical evaluation of construction and demolition waste and associated environmental impacts: A scientometric analysis, Journal of Cleaner Production. 287 (2021) 125071. https://doi.org/10.1016/j.jclepro.2020.125071.

[5] T.P. Pinto, J.L.R. Gonzáles, Manejo e gestão de resíduos da construção civil: como implantar um sistema de manejo e gestão nos municípios, Ministério das Cidades, Ministério do Meio Ambiente e Caixa Econômica Federal, CAIXA, Brasília, 2005.

[6] T.P. Pinto, Metodologia para a gestão diferenciada de resíduos sólidos da construção urbana, Tese (Doutorado), Universidade de São Paulo, 1999. http://www.ietsp.com.br/Documentos/textos-t%C3%A9cnicos/disserta%C3%A7%C3%B5es-e-teses/.

[7] Conselho Nacional do Meio Ambiente (CONAMA), Resolução nº 307: estabelece diretrizes, critérios e procedimentos para a gestão dos resíduos da construção civil, Brasília, 2002.

[8] L.F.R. Miranda, S.C. Angulo, É.D. Careli, A reciclagem de resíduos de construção e demolição no Brasil: 1986-2008, Ambiente Construído. 9 (2009) 57–71.

[9] BRASIL, Lei 12.305: Lei de Resíduos Sólidos, Brasília, 2010.

[10] S.C. Angulo, L.S. Oliveira, L.C. Machado, Pesquisa setorial ABRECON 2020: a reciclagem de resíduos de construção e demolição no Brasil, EPUSP, São Paulo, 2021.